ROYAUME DU MAROC

UNIVERSITE CADI AYYAD
MARRAKECH

جامعة القاضي عياض
مراكش

Faculté des Sciences Semlalia

كلية العلوم السملالية

N° d'ordre

RHOMAD HANANE

HYDRODYNAMICAL AND ECOLOGICAL MODELING OF THE MOROCCAN ATLANTIC COAST

Année Initiale du dpt (P, C, B, G, I, M)

N° d'ordre :

THÈSE

présentée à l'Ecole Supérieure de Technologie d'ESSAOUIRA

pour obtenir le grade de :

Docteur

CED : Sciences et Techniques et Sciences Médicales

Spécialité : Modélisation en sciences de l'environnement

HYDRODYNAMICAL AND ECOLOGICAL MODELING OF THE MOROCCAN ATLANTIC COAST

par :

RHOMAD HANANE

(Master: Écologie et gestion des écosystèmes aquatiques continentaux)

soutenue le 16 Mai 2022 devant la commission d'examen :

Président	**: B. BOUGADIR**	PES	ESTE, UCA, Maroc,
Examinateurs	**: K. W. WIRTZ**	PES	HZG, Geesthacht, Allemagne,
	K. HILMI	DR	INRH, Casablanca, Maroc,
	O. ETTAHIRI	DR	INRH, Casablanca, Maroc
	M. MAAROUF	PES	FST, Marrakech, Maroc
	K. KHALIL	PES	ESTE, UCA, Maroc
	K. ELKALAY	PES	ESTE, UCA, Maroc

FOREWORD

• **Author:** RHOMAD Hanane

• **Thesis title:** Hydrodynamical and ecological modeling of the Moroccan Atlantic coast.

• **Supervisor:**

- **Full name and grade:** ELKALAY Khalid, PES

- **Laboratory and institution:** Laboratory of Applied Sciences for the Environment and Sustainable Development, High School of Technology of Essaouira, Essaouira Aljadida, Morocco.

- **Co-supervisor:**

• **Full name and grade:** KHALIL Karima, PES

• **Laboratory and institution:** Laboratory of Applied Sciences for the Environment and Sustainable Development, Morocco. High School of Technology of Essaouira, Essaouira Aljadida, Morocco.

- **Laboratories where the research work was carried out:**

• MARETEC, Instituto Superior Técnico, Universidade de Lisboa, Lisbon, Portugal

• CESAM, Departamento de Física, Universidade de Aveiro, Aveiro, Portugal

- **Period of realization of the thesis work:** January 2017-December 2021

• **Reporters other than the supervisor :**

- **Belaïd Bougadir**, PES ESTE, UCA, Maroc

- **Kai W. Wirtz**, PES, HZG, Geesthacht, Allemagne

- **Karim Hilmi**, DR, INRH, Casablanca, Maroc

- **Omar Ettahiri**, DR, INRH, Casablanca, Maroc

- **Abdelmalek Maarouf**, PES, FST, Marrakech, Maroc

- **Frameworks for cooperation (or support):**

• The research has been financially supported by CNRST (project PPR, Prog 308/2017, Morocco).

• Grant for the Mare Nostrum project, Erasmus+ 2017/2018.

• Instituto Superior Técnico (project IMAR, Nº 294300139/2019, Portugal).

• FCT/MCTES (CESAM, UIDP/50017/2020+UIDB/50017/2020, Portugal).

This work has led to the following results (Publications, Communications and Award):

Publications

• **H. Rhomad,** K. Khalil, R. Neves, B. Bougadir, AND K. Elkalay, Modeling investigation of the nutrients and phytoplankton dynamics in the Moroccan Atlantic coast: A case study of Agadir coast. *Ecological Modelling*, 447,(2021), 109510. DOI:https://doi.org/10.1016/j.ecolmodel.2021.109510.

• Z. Damsiri, K. Khalil, G. Derhy, **H. Rhomad,** T. Adebola, A. Elkalay, B. Bougadir, AND K. Elkalay, An Ecopath model for fisheries management in the Mogador marine protected area (Moroccan, Atlantic). *Community Ecology*, (2022) DOI:https://doi.org/10.1007/s42974-021-00069-0.

• **H. Rhomad,** K. Khalil, R. Neves, J. Sobrinho, M. Dias, B. Bougadir, AND K. Elkalay, Three-dimensional hydrodynamic modelling of the Moroccan Atlantic coast: A case study of Agadir Bay. *Journal of sea research* (Accepted).

• **H. Rhomad,** K. Khalil, Z. Damsiri, B. Bougadir AND K. Elkalay, Trends and hotspots of coastal science in Moroccan Atlantic coast: A bibliometric analysis. *Science of the Total Environment* (Submitted).

• **H. Rhomad,** K. Khalil, AND K. Elkalay, Water quality modelling: Review and science mapping, 1981–2021. *Environmental Nanotechnology, Monitoring and Management* (Submitted).

Conference paper/chapter

• K. Khalil, **H. Rhomad,** W. Belokda, H. Ahdour, Z. Damsiri, AND K. Elkalay, Modelling Approach of the Biogeochemical Cycle on the Moroccan Shallow Reservoir. *In book: Recent Advances in Environmental Science from the Euro-Mediterranean and Surrounding Regions* (2nd Edition), (2019, October), pp. 529-533. Springer, Cham. DOI:10.1007/978-3-030-51210-1_84.

• K. Elkalay, **H. Rhomad,** Z. Damsiri, H. Essekhyr, G. Derhy, AND K. Khalil, Moroccan Atlantic Marine Research State of the Art: A Review Analysis.*In book: Recent Advances in Environmental Science from the Euro-Mediterranean and Surrounding Regions* (2nd Edition), (2019, October), pp. 2129-2133. Springer, Cham. DOI:10.1007/978-3-030-51210-1_333.

• K. Elkalay, I. Zafzafi, **H. Rhomad,** Z. Damsiri, AND K. Khalil, An Ecopath Model For the Management of Moroccan Fisheries. *In book: Recent Advances in Environmental Science from the Euro-Mediterranean and Surrounding Regions* (2nd Edition), (2017, November), pp. 1655-1656. Springer, Cham. DOI:10.1007/978-3-319-70548-4_480.

• **H. Rhomad,** K. Khalil, A. Egdadi, AND K. Elkalay, Preliminary Analysis of the Nador Lagoon (NE Morocco): Trophic Network with the Ecopath Model. *In book: Recent Advances in Environmental Science from the Euro-Mediterranean and Surrounding Regions*.(2017, November), pp. 1653-1654. Springer, Cham. DOI:10.1007/978-3-319-70548-4_479.

Posters

• **H. Rhomad,** K. Khalil, R. Neves, J. Sobrinho, J. Dias, AND K. Elkalay, Hydrodynamic and biogeochemical functioning of the Agadir Bay (Moroccan Atlantic coast): a numerical modeling approach. International conference: *The 52nd Ocean Liege colloquium*, May 17-21 2021, Liege, Belgium.

• **H. Rhomad,** K. Khalil, R. Neves, J. Sobrinho, M. Mateus, L. Pinto, E. Hbid, O. Ettahiri, AND K. Elkalay, Water quality modeling of the Moroccan Atlantic Coast, a case study of Agadir Bay. National Workshop. *Protection et valorisation des espaces littoraux et marins - Quelle vision et quelles actions pour une gestion intégrée et durable?*, June 27 2018, Rabat, Morocco.

• K. Elkalay, I. Zafzafi, **H. Rhomad,** Z. Damsiri, AND K. Khalil, Management of Moroccan fisheries with the Ecopath model. International conference: *Euro-Mediterranean Conference for Environmental Integration, EMCEI*, November 22-25 2017, Sousse, Tunisia.

Video Communication

• **H. Rhomad,** K. Khalil, Z. Damsiri, B. Bougadir, AND K. Khalil, Spatial and seasonal variability in temperature, chlorophyll and macronutrients in the Agadir coast (Moroccan Atlantic coast): A 3D hydrodynamic–biogeochemical modeling study. *The 2nd Workshop Les Mathématiques: Modélisation et Applications en gestion de pêcheries*, March 25-26 2021, Larache, Morocco. https://www.facebook.com/encg.tanger.uae/videos/270514411215825/?app=fbl

Doctoriales

• Participation in the 1st to 4th edition of Doctoriales, Essaouira, Morocco.

Awards

• Award for Best Student Presentation of the 4th edition of Doctoriales, *Maroc Recherche interdisciplinaire et innovation: quelles opportunités en temps de crise ?* December 18-19, 2020, Essaouira, Morocco.

Acknowledgements

I would like first to thank God, for always being there for me. This dissertation could not also have completed without the grat support that I have received from so many peaple.
I am grateful to Prof. Khalid Elkalay and Prof. Karima Khalil for their unconditional support throughout this process. I am forever grateful for their wisdom, advice, encouragement, and patience; without it my thesis would not have been possible.

I would like to thank Prof. Ramiro Neves for providing me the opportunity to join his team (MARETEC). He taught me a lot about life and modelling; It was a pleasure and honor to work with him.

I acknowledge my gratitude Mr. Belaïd Bougadir for giving me the access to the SAEDD laboratory and for agreeing to chair the jury for the defense of my thesis.

My very sincere thanks to Prof. Kai W. Wirtz , Prof. Karim Hilmi and Prof. Omar Ettahiri for their interest in this work by agreeing to report on this manuscript.

I also thank Prof. Abdelmalek Maarouf who accepted to be examiner in my thesis jury.

I would like to thank Dr. João Sobrinho for his expertise, suggestions and guidance.

I would like to thank Prof. Marcos Mateus, Prof. Ligia pinto, Jorge Palma, Hilda de Pablo, Dr. Francisco Campuzano and the other members of the Maretec team.

I thank Prof. João Miguel Dias from CESAM, Universidade de Aveiro, Aveiro, Portugal and Diego Macias from Instituto de Ciencias Marinas de Andalucía, Spain for their assistance with the hydrodynamic and biogeochemical models, respectively.

I would like to express my sincere thanks to Elmansouri family for the warm hospitality.

I would also like to thank my friends; Marta López, Dr. Hassan Essekhyr, Youssef Elkabdani, Prof. Lamia Zaid, Prof. Fatima-ezzahra Amatoul, Aicha Elmansouri for their valuable help, support and friendliness.

Finally, thank you Sara and Aicha for your continuous encouragement and moral support; Much love.

ABSTRACT

Coastal systems are amongst the most productive ecosystems of the land-ocean aquatic continuum, but they are also under high climate and anthropic pressures. Too sparse observations have hindered the understanding of complex interactions between water quality, coastal hydrodynamics and biogeochemical transformations. Despite the advances in coastal modeling, few of such simulation models are seen related to the subtropical North-East Atlantic. As the first step toward our final goal to provide a decision support tool for coastal management of North-West Africa (Moroccan Atlantic coast), this study implemented a three-dimensional (3D) hydrodynamic-biogeochemical model of Agadir coast. The hydrodynamic model was externally derived by meteorological data, tidal oceanic forcing and boundary conditions of Agadir coast. It was used to calculate the sea surface level, harmonic tidal constituents and physical factors, especially water temperature and salinity. The model was included with the injected mass of tracers using Lagrangian transport model and used to calculate the local residence time (RT) and estimate the possible pathway of passive tracers. The pre-computed scalar transport and boundary conditions from the hydrodynamic solution were then used to conduct biogeochemical calculations in an offline coupled model. The model was used to explore the spatial and seasonal patterns in the dynamics of physico-chemical parameters and nutrient limitation on phytoplankton growth. The model was calibrated and validated using a combination of available in-situ measurements, satellite products, climatology and ARGO floats data. Despite some discrepancies, the findings revealed a good match between simulations and observations, which underlines the feasibility of the model in simulation the main dynamic features of the Agadir coast. Overall results suggest that the interaction between bathymetry and westerly and northwesterly prevailing winds, a baroclinic double-gyre circulation, dominating the general circulation affect physico-chemical parameters and nutrient distributions. Nitrate appears as the key factor controlling phytoplankton dynamics. Nitrate depletion occurs faster driving the area towards nitrogen limitation. The flagellate (dominated total Chl-a) bloom coincident with warming water temperatures, higher salinities, intense stratification and lower nutrient concentrations. This has major repercussions for the flow of carbon in the area, as flagellates contribute to low carbon export to deeper waters compared to diatoms.

Key–Words : Water quality, Nutrients, Phytoplankton, Nitrogen limitation, Biogeochemical modeling, Hydrodynamic modeling, Lagrangian model, Performance evaluation, Moroccan Atlantic coast, Agadir coast. .

RÉSUMÉ

Les systèmes côtiers comptent parmi les écosystèmes les plus productifs du continuum aquatique terre-océan, mais ils sont également soumis à de fortes pressions climatiques et anthropiques. Des observations trop rares ont empêché la compréhension des interactions complexes entre la qualité de l'eau, l'hydrodynamique côtière et les transformations biogéochimiques. Malgré les progrès réalisés dans la modélisation côtière, peu de ces modèles de simulation sont vus en relation avec l'Atlantique Nord-Est subtropical. Comme première étape vers notre objectif final de fournir un outil d'aide à la décision pour la gestion côtière de l'Afrique du Nord-Ouest (Côte Atlantique Marocaine), cette étude a mis en œuvre un 3D modèle hydrodynamique-biogéochimique (MOHID) de la côte d'Agadir. Le modèle hydrodynamique a été forcé de l'extérieur par les données météorologiques, le forçage océanique de marée et les conditions aux limites de la côte d'Agadir. Il a été utilisé pour calculer le niveau de la surface de la mer, les constituants harmoniques de la marée et les facteurs physiques, notamment la température et la salinité de l'eau. Le modèle a été inclus avec la masse injectée des traceurs en utilisant le modèle de transport lagrangien qui a été utilisé pour calculer le temps de résidence local (RT) et estimer le chemin possible des traceurs passifs. Le transport scalaire pré-calculé et les conditions aux limites de la solution hydrodynamique ont ensuite été utilisés pour effectuer des calculs biogéochimiques dans un model couplé hors ligne. Le modèle a été utilisé pour explorer les modèles spatiaux et saisonniers de la dynamique des paramètres physico-chimiques et de la limitation des nutriments sur la croissance du phytoplancton. Le modèle a été calibré et validé en utilisant une combinaison de mesures in-situ disponibles, de produits satellitaires, de climatologie et de données de flotteurs ARGO. Malgré quelques divergences, les résultats ont révélé une bonne correspondance entre les simulations et les observations, ce qui souligne la faisabilité du modèle dans la simulation des principales caractéristiques dynamiques de la côte d'Agadir. Les résultats globaux suggèrent que l'interaction entre la bathymétrie et les vents dominants d'ouest et de nord-ouest, une circulation barocline à double gorge, dominant la circulation générale affectent la distribution des paramètres physico-chimiques et des nutriments. Le nitrate apparaît comme le facteur clé contrôlant la dynamique du phytoplancton. L'épuisement du nitrate se produit plus rapidement, entraînant la zone vers une limitation de l'azote. L'efflorescence des flagellés (domine la Chl-a totale) coïncide avec le réchauffement des températures de l'eau, des salinités plus élevées, une stratification intense et des concentrations de nutriments plus faibles. Cela a des répercussions importantes sur le flux de carbone dans la zone d'étude, car les flagellés contribuent à une faible exportation de carbone vers les eaux plus profondes par rapport aux diatomées.

Mots-clés : Qualité de l'eau, Nutriments, Phytoplancton, Limitation en azote, Modélisation biogéochimique, Modélisation hydrodynamique, MOHID, Modèle Lagrangien, Évaluation des performances, Côte Atlantique Marocaine, La côte d'Agadir.

Table of Contents

List of Tables

Table **Page**

List of Figures

Figure **Page**

List of Abbreviations

- **3D :** Three-dimensional
- **ACMS :** Agadir Coast Model System
- **ADE :** Advection–dispersion equation
- **ADI :** Alternating direction implicit
- **BIAS :** Difference of mean values
- **BSi :** Biogenic silica
- **CBEG :** Coastal Blue Economy Growth
- **Chl-a :** Chlorophyll-a
- **CMEMS :** Copernicus Marine Environment Monitoring Service
- **CSTR :** Continually stirred tank reactor in series
- **DO :** Dissolved oxygen
- **DONnr :** Dissolved non-refractory organic nitrogen
- **DONr :** Refractory dissolved organic nitrogen
- **DOPnr :** Non-refractory dissolved organic phosphorus
- **DOPr :** Refractory dissolved organic phosphorus
- **DPSIR :** The Driver Pressure State Impact Response
- **DSi :** Dissolved silica
- **FES2012 :** Finite Element Solution, global tidal model version 2012
- **GIS :** Geographic information system
- **GOTM :** General Ocean Turbulence Model
- ***H* :** Humidity
- ***I* :** Wind intensity
- **ICZM :** Integrated Coastal Zone Management
- **IF :** Impact factor of journals
- **JCR :** Journal Citation Reports
- **KM :** Knowledge management
- **MACOMS :** Atlantic Coast Operational Model System
- **MODIS :** Moderate Resolution Imaging Spectroradiometer

- **MSS :** Model Skill Score
- **N :** Nitrogen
- **N_2 :** Nitrogen gas
- **NB :** Number of publications
- **NH :** Ammonia
- **NO_2 :** Nitrite
- **NO :** Nitrate
- **NOAA :** National Oceanic and Atmospheric Administration
- **OBC :** Open boundary conditions
- **ODEs :** Ordinary differential equations.
- **P :** Phosphorus
- ***P :*** Atmospheric pressure
- **PO :** Inorganic phosphorus PON: Particulate organic nitrogen
- **POP :** Particulate organic phosphorus
- **r :** Correlation coefficient
- **RMSE :** Root mean squared error
- **RT :** Residence time
- **SD :** Standard deviation
- **SDGs :** Sustainable Development Goals
- **SJR :** SCImago Journal and Country Rank
- **Si :** Silica
- **SSL :** Sea surface level
- **SSS :** Surface seawater salinity
- **SST :** Seawater temperature
- ***T :*** Temperature
- **US EPA :** United States Environmental Protection Agency's
- **USDA-ARS:** U.S. Department of Agriculture- Agricultural Research Service
- **WOA :** World Ocean Atlas
- **WRF :** Weather Research and Forecasting

Chapter 1

Introduction

1.1 General context

WThe ecosystems Water plays a crucial role in human well-being, socio-economic development, and ecosystem sustainability [454]. Water is considered to be the most valuable and universal resource, it contains nutrients and is regarded as a carrier of energy thus, water systems intersect with different aspects of society, industry and the natural environment [433]. The increased stress on limited water resources has reached a tipping point in recent years, resulting in reduced water availability as well as jeopardized water quality [402]. The ecosystems cannot function well without adequate water supplies of appropriate quality, making water scarcity a critical stressor in major aquatic ecosystems [463]. Simultaneously, the seriousness of the problem has risen in frequency and magnitude at a global scale [76, 205] due to the combination of climate change and increasing world population [342, 409, 424].

Over the past years, climate change has become a major threat to coastal systems [93]. Sea level rise, modifications in precipitation and wind patterns as well as extreme events, such as cold waves, heat and storms are being caused by global warming [93]. These alterations are expected to continue throughout the twenty-first century affecting the dynamics of coastal ecosystems (e.g., [382]). Climate projections for the end of the twenty-first century show an increase air temperature and global mean sea level [93]. These changes will have an direct impact on the temperature, and salinity as well as depths of the water column in ecosystems [404], thus influencing nutrient fluxes in the sediment-water column and consequently the phytoplankton dynamics [70, 356], among others. According to the Framework Convention on Climate Change, climate change is directly or indirectly linked with anthropogenic activities [2]. Nevertheless, increasing world population has produced growing demand and consumption of water over the past half century [3]. Scenarios of global population are expected to increase to 9.2 billion by 2050 with a peak at 9.3 billion in 2062 [71], leading to a predicted increase in global water demand of 55% by 2050 [486]. In parallel, according to the United Nations [198], the urban population is projected to increase by 72% by 2050, from 3.6 billion in 2011 to 6.3 billion in 2050.

This, combined with unprecedented economic growth, is expected to result in a doubling of urban water demand by 2025 [454]. Furthermore, global demand for water is expected to outstrip available resources by 40% by 2030 if current trends continue [480]. These developments are putting unprecedented stresses in aquatic ecosystems and in a broader context, as suggested by [348], will lead to the governments facing ever increasing difficulties in effectively managing their water resources. Some of the world's largest rivers including the Rio Grande, Colorado River, the Yellow River, and Indus River have dried up before they reach their river mouths [351]. Major problems in coastal waters include wastewater, oil spills, runoff effluents, fish culture, recreation, land reclamation, and eutrophication [66, 242, 286].

Eutrophication is often suggested a main threat to coastal ecosystems [107, 230, 286], as it may impact the nutrient cycles [341], induce hypoxia/anoxia conditions [141, 434], that promote harmful or toxic algal blooms [155], among others. These undesirable effects of eutrophication are often related to excessive supply of nutrients, especially nitrogen and/or phosphorus [108]. However, to control biomass growth, it is critical to understand growth of limiting nutrients [108, 157]. Overall, fresh waters are inspected to be phosphorus limited due to a high N:P ratio [163] and nitrogen fixation [399]. In contrast, marine waters are inspected to be nitrogen limited due to slow nitrogen fixation, high denitrification and sediment release of phosphorus [343]. Estuaries are in the transitional zones between marine and freshwater systems, thereby usually exhibited complicated patterns in nutrient limitation [108]. Other limiting factors such as such as temperature, light, grazin, residence time of water can be considered as the major factors that affect changes of biomass in coastal ecosystems [38].

Therefore, the challenge is to develop a management tool to address environmental problems, to improve understanding of ecosystem properties as well as to predict the results of climate and human action affecting coastal ecosystems.
Numerical model incorporates mathematical formulations that can be used to describe the hydrodynamics and water quality of an ecosystem in response to forcing factors. It can be developed based on the existing knowledge of hydrodynamics and biogeochemical processes, and it can be tested against observations. Duly calibrated water quality model can capture the time-space variations in a coastal ecosystem and therefore be a valuable tool to assess the dynamics of the coast for an efficient and effective management system [104, 191, 407].

Hydrodynamic model can be used to predict water temperature and salinity as well as understand the way coastal circulation respond to forcing factors (e.g., tidal action, freshwater inflow and weather events). For example, air temperature influences water temperature, which may promote the development of water column stratification and induce eutrophication [80, 173]. Similarly, wind has a direct impact in upwelling/downwelling [171, 372] that may affect coastal circulation. Many coastal ocean hydrodynamic models, such as regional ocean modeling system (ROMS), estuarine and coastal ocean model (ECOM), semi-implicit eulerian lagrangian finite-element model (SELFE), Princeton ocean model (POM), Estuarine Coastal and Ocean Modeling system with Sediment (ECOMSED), curvilinear grid hydrodynamic 3D model (CH3D), environmental fluid dynamics code (EFDC), advanced circulation (ADCIRC), finite volume coastal ocean model (FVCOM), unstructured-grid tidal residual in marshes (UnTrim), and others have been developed, calibrated, validated to simulate the ocean currents in complex coastal regions and applied in support of water quality management activities. Many of them (ROMS, EFDC, ECOM and CH3D) have biogeochemical modules directly coupled to hydrodynamics [236, 276].They can also conducted as a basis for water quality assessment or for coupling with biogeochemical models [254]. When the objective is to simulate changes in nutrient supply, phytoplankton growth, as well as contaminant transport, distribution and fate in coastal ecosystems, increased local grid refinement is required [236]. Tools such as Modelo Hidrodinâmico (MOHID Water), Computational Aquatic Ecosystem Dynamics Model (CAEDYM), water quality analysis simulation program

(WASP), Corps of Engineers 2-D Hydrodynamic and Water Quality Model (CE-QUAL-W2) and European Regional Seas Ecosystem Mode (ERSEM) are examples of biogeochemical models. These been mostly coupled with hydrodynamic models and have been largly used for assessing the circulation and water quality over the scale of the larger waterbody.

Although water quality modelling applications have emerged globally, 3D coupled hydrodynamic-biogeochemical modelling implementation to simulate water quality of coastal ecosystems are still missing in many countries in subtropical regions such as Moroccan Atlantic coast (North-West Africa) [379].

Moroccan Atlantic coast is the most important ecosystem on the North-West Africa. The influence of the large-scale coastal processes (e.g., azores and Canary Currents, upwelling/downwelling) (e.g., [21, 273, 390, 391] makes it very productive in terms of phytoplankton biomass (Chl-a up to $10 mg.m^{-3}$) and primary production (up to $5 gCm^{-2}.d^{-1}$) [32, 249]. Agadir area is one of the most productive ecosystems on the southwestern part of Morocco, providing crucial valuable resources for several economic activities in the region, namely fishing, aquaculture and recreational activities [91, 190, 245]. Growing population of about 624,960 habitants in 2016 and an expected increase to more than 1 million individuals in Agadir Ida-Outanane district by the end of 2021 [196], land use, industrial and urban expansion and human activities differ widely but their combined intensities give rise to immense environmental problems leading to deterioration of water quality [10, 64, 190, 245].

The main objective of this study is to develop an integrated modelling framework that can couple high-resolution downscaled weather data with a 3D hydrodynamic and biogeochemical model to simulate different physical, chemical, and biological processes in complex subtropical coastal environments.

1.2 Research Goals

The main purpose of this study is to provide a decision support tool for coastal management of North-West Africa (Moroccan Atlantic coast). More specifically, the ultimate goal is the implementation of a comprehensive integrated water qualiy modeling approach towards a better understanding the main hydrodynamic and biogeochemical features of the Moroccan Atlantic coastal water body.

The specific goals are as follows:

1. To explore the emerging trend of coastal science in Moroccan Atlantic coast between 1971 and 2021.
2. To explore the emergence of research literature on water quality modelling applications within the Atlantic area published from 1981 to 2021.
3. To improve understanding of hydrodynamic characteristics of Agadir Bay and the response of the sea surface level and physical factors, especially water temperature and salinity to physical forcing.
4. To explore the the reliability of model performance and the uncertainty associated with model forecasts.
5. To calculate the RT and estimate the possible pathways of surface passive tracers.
6. To explore the spatial and seasonal patterns in the dynamics of physic-chemical factors (water temperature, salinity and DO) and nutrient limitation nutrients (nitrogen (N), phosphorus (P) and silicium (Si)) on phytoplankton growth (diatoms and flagellates).

1.3 Outline

In **chapter II**, a comprehensive review is carried out using bibliometric analysis in conjunction with network analysis to describes qualitatively and quantitatively the progress, trends, and hotspots of coastal science in Moroccan Atlantic coast. The performance of 4891 publications (1971-2021) covering annual outputs, document types, language of publication, mainstream journals, the impact of the research by research area, coastal habitat type and study area are investigated. Afterwards, co-words, co-authorship, co-country analysis and cluster analysis are conducted using VOSviewer software.

In **chapter III**, science mapping approach is used to explore the emergence of research literature on water quality modelling applications within the Atlantic area published from 1981 to 2021. The study sought to document the general research trend, the influential journals, authors, and institutions, topical foci, identify the most frequently applied model, the water body types and the areas within which models are mainly applied. A database of 1952 potentially relevant publications (2548 individual modelling applications) are analyzed using Microsoft Excel, VOSviewer and ArcGIS.

In **chapter IV**, 3D hydrodynamic model MOHID Water coupled with a Lagrangian transport model is implemented and explored to improve our understanding of hydrodynamic features of the Agadir coast. The model is calibrated and validated against meteorological conditions, sea surface level, harmonic tidal constituents, water temperature and salinity. Thereafter, it is used to estimate the local residence time (RT) and determine the pathway of passive tracers.

In **chapter V**, a 3D coupled hydrodynamic-biogeochemical model is performed in order investigate the time-space distribution of inorganic nutrients (nitrate, phosphate and dissolved silica), and their control on phytoplankton (diatoms, flagellates) biomass on the Agadir coast. The model is calibrated and validated against satellite observations and climatology data. The model achieved satisfactory representation of the sea surface temperature, chlorophyll-a, and a reasonable agreement in the seasonal pattern of inorganic nutrients. The dynamic of phytoplankton and their response to nutrient limitations and environmental factors variations are discussed and pertinent conclusions are summarized. These chapters are based on previously published or submitted papers by the author during the time frame of this PhD research.

In **chapter VI**, a general conclusion related to the accomplishment of the objectives of this thesis, as well as recommendations for future work are provided.

CHAPTER 2

Trends and hotspots of coastal science in Moroccan Atlantic coast: A bibliometric analysis

2.1 Résumé du chapitre

Les résultats de ce chapitre ont fait l'objet d'un article soumis pour publication au journal "*Science of the Total Environment*".

Dans ce chapitre :

L'exploration scientifique des écosystèmes côtiers s'est avérée cruciale dans la mise en œuvre d'un programme de gestion basée sur les écosystèmes lorsqu'elle est efficacement analysée et communiquée à toutes les parties impliquées dans la science côtière [262]. Bien qu'un ensemble considérable de connaissances scientifiques se soit concentré sur la côte atlantique marocaine, sa gestion globale semble être un défi. Des difficultés telles que le faible financement de la recherche synthétique en science côtière pourraient entraver une gestion efficace des connaissances.

Dans cette revue, nous explorons la tendance émergente de la science côtière sur la côte atlantique marocaine en utilisant une analyse bibliométrique en conjonction avec une analyse de réseau. Nous décrivons qualitativement et quantitativement les progrès, les tendances et les points chauds des publications, les revues, les auteurs et les pays influents, l'impact de la recherche par domaine de recherche, type d'habitat côtier et zone d'étude. Nous avons identifié 1952 documents publiés entre 1971 et 2021. L'analyse des co-mots, co-auteurs, co-pays et les clusters sont visualisés à l'aide du logiciel VOSviewer. Les résultats soulignent une nette disparité dans l'évolution de la recherche, 52% du total des publications ont été produites entre 2011 et 2021. 80% d'entre eux ont été publiés sous forme d'articles de journaux. Le Journal of Materials and Environmental Science est la revue la plus active. 75% des publications sont limitées aux zones côtières et lagunes. En revanche, les habitats tels que les dayas et les oasis ont reçu peu d'attention. L'hydrobiologie et de l'écologie ont été largement investigués et progressivement approfondis. L'analyse a également révélé un biais de recherche significatif contre le littoral sud-central, les régions de l'Atlantique marocain qui ont un besoin élevé de recherche. En revanche, l'industrialisation rapide de la région du nord a pu favoriser l'établissement de nouvelles collaborations entre l'industrie locale et les scientifiques, engendrant un soutien financier privé pour les activités de recherche universitaire. En bref, cette analyse suggère que l'effort scientifique futur sur les écosystèmes côtiers atlantiques marocains devrait soulager les biais existants en augmentant la recherche multidisciplinaire sur les systèmes intégrés et en encourageant le transfert interrégional des ressources de recherche vers les zones de faible effort de recherche, avec un accent particulier sur les écosystèmes de recherche critiques du littoral Sud.

2.2 Abstract

Despite the growing focus in coastal conservation practice towards scientific evidence-based decision making, there remains a need for enhancing knowledge management and its implication in coastal management planning. Herein, we adopts bibliometric analysis in conjunction with network analysis to describes qualitatively and quantitatively the progress, trends, and hotspots of coastal science in Moroccan Atlantic coast. A total of 4891 publications from 1971 to May, 2021 were collected. The performance of publication covering annual outputs, document types, language of publication, mainstream journals, the impact of the research by research area, coastal habitat type and study area were investigated. Thereafter, co-words, co-authorship, co-country analysis and cluster analysis were conducted using VOSviewer software. The findings underscore a clear disparity in the research evolution, 52% of the total publications were produced between 2011 and 2021. 80% of them were published as journal articles. Journal of Materials and Environmental Science was the most active journal. Behind Morocco, France and Spain researchers have made the main contributions to this research area. 75% of publications have been limited to the coastlines and lagoons. In contrast, habitats such dayas and oasis have received little attention. Hydrobiology and ecology topics have being largely investigated and gradually deepened. The analysis also revealed a significant research bias against the south-central coastline, the regions of Moroccan Atlantic that have a high research need. This analysis suggests that future scientific effort on Moroccan Atlantic coastal ecosystems should relieve existing biases by increasing multidisciplinary integrated system research and encouraging inter-regional transfer of research resources to areas of low research effort, with a special emphasis on the critical research ecosystems in the southern coastline. Finally, some key recommendations were raised for strengthening the implementation of knowledge management within the concept of sustainable coastal management.

Key–Words : Coastal science, Moroccan Atlantic coast, Bibliometric analysis, Network analysis, Research trend

2.3 Introduction

The keyword 'Policy relevance' is usually used when research results can assist to solve the issues faced by society in an appropriate way [465]. Research in an ideal world would provide a consistent direction for policy to address specific societal and environmental issues [255]. In the real world, the situation is more complicated. It is difficult to draw specific guidelines from research that policymakers and managers require for the implementation of a management plan [115].

While challenging to address in the context of sustainable development concerns, there is still a pressing need for further consideration of the practical strengthening research findings to support policy-decision making [333]. The challenges of conducting scientific research that crosses traditionally distinct disciplines and involves researchers, practitioners and intermediary actors are much more complex in coastal ecosystems that are marked by tipping points and ecological thresholds in their functioning [207, 475]. The degradation of coastal ecosystems, and their complexities suggests that the coastally oriented research community has a responsibility to periodically investigate its priorities and communicate efficiently data gaps and scientific information needed to address such issues [23, 256]. Their management spans a range of sectors including environment, health and education, fisheries and conservation, coastal aquaculture, water and energy, coastal tourism, coastal development, coastal biotechnology, pollution, climate change, impact of ocean acidification in coastal ecosystems, invasive species and coastal biodiversity, coastal economy, laws, regulations and politics and poverty [68, 79, 98, 466]. Consequently, policy-makers may acquire scientific evidence from across a wide variety of disciplines including ecology, social sciences, economics etc.[109, 256]. Strengthening, however, cross-disciplinary scientific collaboration for effective management of coastal areas [385].

As coastal pressures mount, there is an increasing need for research framework programmes to conceptualize complex coastal issues, enhance research organization and lead scientist to supports the regulation, management, adaptation and resilience of coastal ecosystems [256, 340]. These pressures are largely arising from the combined effects of climate change (e.g., [317, 375, 469]), anthropogenic factors (e.g., [120, 221, 288, 461]), industry and tourism (e.g., [485, 499]), waste disposal and land-based pollution (e.g., [266, 295]), coastal cabling for communications (e.g., [282, 462]), transport and energy production (e.g., [61, 338]), seaport/shipping development, coastal groundwater extraction, coastal mining and other human activities. Imperfect legal and insufficient education, cooperation and funding for coastal ecosystems conservation [430]. It is the case of the Moroccan Atlantic coast that extends for about three thousand kilometres. The coast is a complex mosaic of different environments (coastal dunes, beaches, deltas, salty and fresh water marshes, rocky cliffs, mangroves, bays, lagoons and estuaries etc.) with great ecological, social-cultural and economic values [54, 90, 307]. Scientific understanding of these ecosystems has proven crucial in the implementation of ecosystem-based management program (EBM) when effectively analyzed and communicated with all stakeholders involved in coastal science [262, 430].

Although considerable body of scientific knowledge has centered on the Moroccan Atlantic coast, its comprehensive management appears challenged. Difficulties such as deficiency in scientifically sound planning, shortage of baseline information, lack of communication between researchers and users of science, poor funding for synthetic research in coastal science could hinder effective knowledge management. Nonetheless, most researchers focus on one/some specific researcher topic (s), to our knowledge, there is no review summarizes the research trends and revealed the emerging trend of coastal science in Moroccan Atlantic coast. Hence, a comprehensive review can be carried out using bibliometric tools, and a network analysis for clustering and mapping the relevant scientific information [428]. Herein, we review the research on coastal science in Moroccan Atlantic coast via bibliometric analysis in conjunction with network analysis using VOSviewer software.

1. A total of 4891 publications are analyzed from 1971 to May, 2021.
2. The variation in the characteristics of total publications, year of publication, document type, language of publication and journal coverage are summarized.
3. The distribution of publication outputs by research area, coastal habitat type and study area are analyzed.
4. The co-occurrence analysis of keywords, authors and countries are visualized.
5. The future directions and enabling actions that can be undertaken to facilitate the implementation of knowledge management within the concept of sustainable coastal management are discussed.

2.4 Methodology

2.4.1 Data collection

To ensure sufficient coverage, search databases include Scopus (Elsevier), Web of Science (Clarivate Analytics) and Google Scholar (Google Group) were used to compile a bibliography of all publications referring to the research on Moroccan Atlantic coastal ecosystems.

The Scopus databas (https://www.scopus.com/) holds the largest number of journals and provides outcomes of more consistent accuracy in comparison to other databases [269, 293, 296]. As checked in May 2021, Scopus was indexing more than 81 million items and over 25,000 titles from 7000 publishers worldwide and get access to 1.7 billion of cited references [158]. It has double the number of indexed journals than the Web of Science database [432].

Maintained by Clarivate Analytics, Web of Science (https://clarivate.com/webofsciencegroup/solutions/web-of-science-core-collection/) covers all journals indexed in Emerging Sources Citation Index (ESCI), Social Sciences Citation Index (SSCI), Science Citation Index Expanded (SCIE) and Arts and Humanities Citation Index (AHCI) [180]. It allows for acquiring long and complex search queries [432].

The other robust source of references used in the review was the Google Scholar database (https://scholar.google.com/), used by its turn to track, sort, analyze, and visualize publications [293]. More sources as Hal (https://hal.archives-ouvertes.fr/), Theses.fr (http://www.theses.fr/) and Otrohati (https://otrohati.imist.ma/) were used search engine for PhD defended.

Furthermore, only keywords were selected for retrieval to improve the accuracy of the results and increase the degree of correspondence with the literature. All possible combinations of keywords related to the topic were searched without language restriction between 1971 and 2021. The selected study period encompasses period of enormous change in the ecology and economy of the Moroccan Atlantic coast.

In order to allow a better understanding of the temporal evolution of the topic, documents were aggregated according to their year of publication, into six groups of nine-year intervals (except the last one) corresponding to the last five decades (1971–1980; 1981–1990; 1991–2000; 2001–2010; 2011–May, 2021). This is a sufficiently extensive period yields useful insight and establishes the general research trends. A total of 6340 documents were retrieved for further analysis.

2.4.2 Refinements of the results

The selected data included of the following information: “document title”, “author (s)”, “affiliation(s)”, “document type”, “journal title”, “language”, “year of publication”, “institution(s)”, “abstract”, “author keywords”, “citation count” and “bibliographical information” were downloaded for further examination. Full records were downloaded into a reference manager (Mendeley) where duplicates were removed, saved to CVS format and then exported to VOSviewer for a subsequent analysis. Linlog/modularity approach of normalization and citations was selected as option for weights in the visualization scale. It is important to note that the download records were manually retrieved to solve issues such as missing data. Record was standardized with same formatting to extract the relevant information. After data cleaning, 4891 documents remained for analysis (Fig. 2.1).

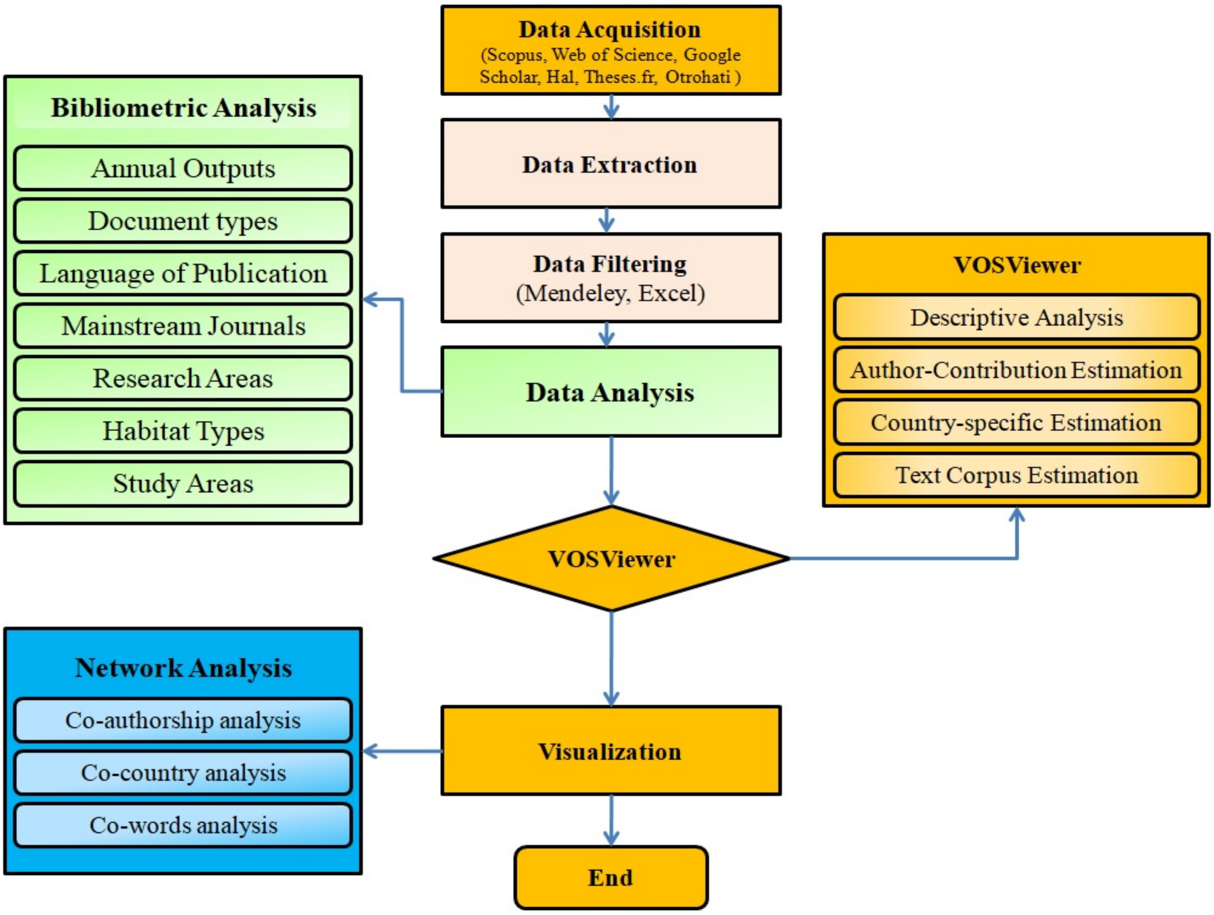

Figure 2.1: Procedure for the bibliometric analysis used in this paper.

2.4.3 Data analysis

As an indicator of scientific impact and production, the annual distribution of the published-document number and the contribution of documents for each of the authors, the number of total citations, average citations per article, impact factor (IF) of journals were investigated. The IF of a journal was obtained from the Journal Citation Reports (JCR) (`clarivate.com/products/web-of-science`). In addition, the high frequency keywords were extracted to reveal research hotspot. The impact of research by habitat type, research area and study area were anlyzed in this study.

2.4.4 Data visualization

Microsoft Excel 2017, ArcGIS (version 10.5) and VOSviewer (version 1.6.9) visualization softwares were engaged to provide visual insights of coastal research. VOSviewer [458] was used to read the data was standardized using fractionalization mode to perform a network analysis [428]. It was adopted in this study to visualize the relationships among the top productive authors, research institutions and the co-occurrences of keywords [175, 258]. Network diagrams include nodes and links. Nodes reflect different components such as author, institution, and keywords. The size of nodes in the network is proportional to the number of publications (or frequency); the larger the node, the greater the number of publications or the higher frequency [175, 260, 459]. The thickness and length of links between nodes reflect relationships of collaboration, co-authorship/co-occurrence, or co-citations [353]. The color of the node/lines reflects different clusters or years [260].

2.5 Results

2.5.1 Bibliometric analysis

2.5.1.1 Publication years, document type and language of publication

The annual distribution of the published-document number express the overall situation and research patterns, while the latter highlights the overall trend features considering different development time periods. Thus, the combination of published literature referring to the Moroccan Atlantic coastal ecosystems and fixed time window was achieved (Fig. 2.2).

Due to the small number of early publications, the present study uses 1971–1980, 1981–1990, 1991–2000, 2001–2010, and 2011–2021 respectively as first to fifth research periods. In the first decade (1971–1980), the increasing number of published documents per year was no more than 36 publications. In the second and the third decades, research grew slowly but steadily, and the annual average document number varies slightly between years. In last decade (2011–2020), the number of research documents increased rapidly, reaching a peak of 330 publications in 2020, signaling a surge in research activity throughout the coast over the last decade. It is worth mentioning that the year 2021 was represented by 194 publications considering the months of January to May.

Four-fifths of the total documents were published as journal articles (3924 publications; 80.22% of total documents) and more than three-twenty as scientific bulletins (6.9%) and theses (6%). Conference papers (3.43%), scientific reports (2.92%) and book sections (0.57%) comprised a small portion of the published documents. Almost one-twenty (4%) of documents were published as journal articles during the early phases of research (1971–1980) and more than one-half (51.68%) during the most recent period (2011–2021) (Fig. 2.2).

The languages of all publications were grouped. The result shows that French (2457 publications; 50%) and English (48%) were by far the dominant academic language in the coastal research field. Several other languages including Spanish (0.65%), German (0.29%), Arabic (0.2%), Russian (0.12%) and Portuguese (0.04%) also appeared.

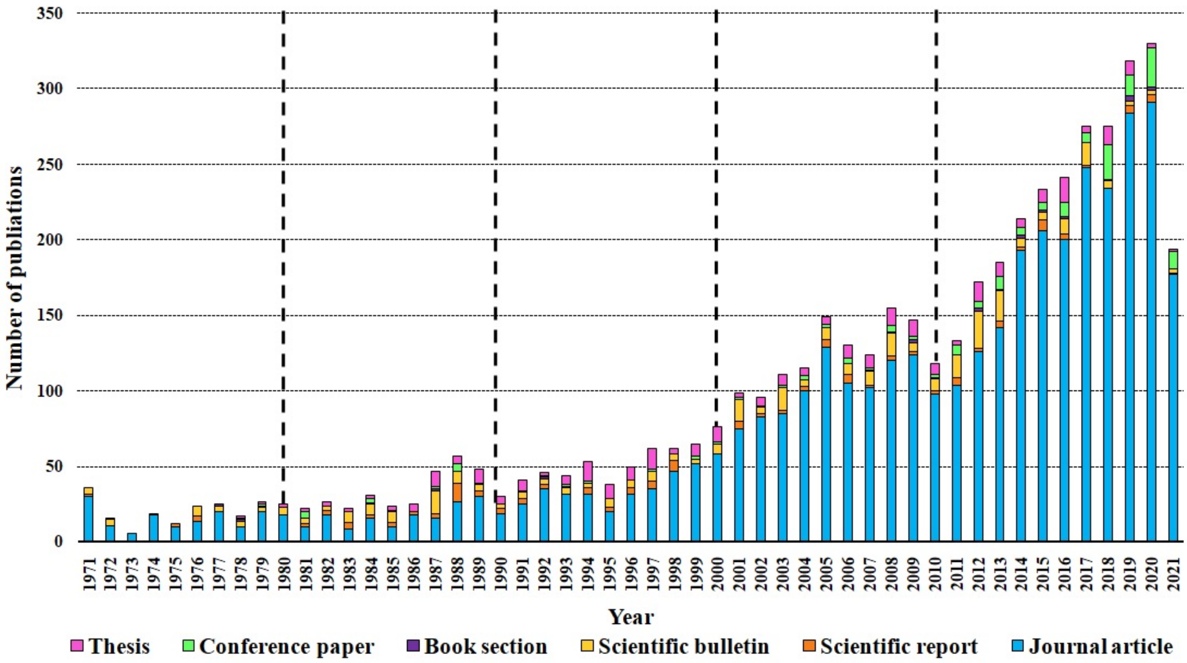

Figure 2.2: Number of publications per document type by years.

2.5.1.2 Journal publication

A total of 924 articles were published in a wide range of 1005 national and international journals. Table 2.1 summarizes the top journals (2.4%) in descending order with respect to the total number and percentage of published articles published (TP), impact factor (IF), and journal subject category. According to the category description in the SCImago Journal and Country Rank, coastal sciences covers resources concerning many aspects of the of the study of the coastal areas, among them environmental chemistry, environmental geology, water quality, oceanography, eco-toxicology, monitoring and coastal health. Journal of Materials and Environmental Science published the most articles with 126 articles (3.2%). Journal of African Earth Sciences ranked second with 70 articles (1.78%) while Deep-Sea Research Part I: Oceanographic research papers (1.07%) and AACL Bioflux (0.92%) ranked 3rd and 4th. The most commonly cited article was published in the 3rd position journal with 1188 citations. International Journal of Advanced Research ranked on top productive journal with the highest impact factor of 5.228, reporting that on average, the articles published in this journal has been cited five or more times per year. Progress in Oceanography ranked 2nd with an impact factor of 4.06 and 944 citations. More than half (58.86%) of articles have published between 2011 and 2021. From 1981 to 1990, journal with most publications was Deep-Sea Research Part I: Oceanographic research papers. They have published almost two times as many articles than the second in the table, which is Journal of African Earth Sciences. Over the time, research priorities have changed, so too has the interested journal. Comptes Rendus de l'Académie des Sciences and Comptes Rendus Biologies were the most productive journal with during the period 1991–2000 and 2001–2010, respectively. Since the 2011s, Journal of Materials and Environmental Science (126 articles) has become the preferred journal in which scientists have published their research on coastal science.

Table 2.1: The top most active journals during the period of 1971–2021 with the number of articles published, impact factor, and journal subject category

Journal title	**TP(%)**	**Citation**	**IF**	**Time period**				**Subject category***
				1981-1990	**1991-2000**	**2001-2010**	**2011-2021**	
Journal of Materials and Environmental Science	126 (3.2)	197	0.75	_	_	_	126	Pollution; Waste Management and disposal; Environmental chemistry
Journal of African Earth Sciences	70 (1.78)	619	1.603	8	7	17	38	Earth-Surface Processes; Geology
Deep-Sea Research Part I: Oceanographic research papers	42 (1.07)	1188	2.6	16	7	6	13	Aquatic Science; Oceanography
AACL Bioflux	33 (0.92)	23	0.54	_	_	1	32	Aquatic Science; Ecology, evolution, behavior and systematics
Quaternaire	32 (0.81)	252	0.412	2	10	14	6	Earth-Surface Processes; Geology
Comptes Rendus Biologies	31 (0.8)	155	1.904	_	_	25	6	Biochemistry; Genetics and Molecular; Biology; Immunology and microbiology
Arabian Journal of Geosciences	26 (0.66)	76	1.327	_	_	_	26	Environmental Science
Acta Horticulturae	26 (0.66)	38	0.26	_	1	8	17	Horticulture
Estuarine, Coastal and Shelf Science	24 (0.61)	131	2.33	1	_	8	15	Aquatic Science; Oceanography
Cretaceous Research	24 (0.61)	444	1.854	2	3	6	13	Paleontology
Comptes Rendus de l'Académie des Sciences	24 (0.61)	82	_	6	17	1	_	_
Progress in Oceanography	23 (0.6)	944	4.06	_	1	14	8	Aquatic Science; Oceanography
European Scientific Journal	23 (0.6)	0.65	_	_	_	_	23	_
Afrique SCIENCE	23 (0.6)	_	0.45	_	_	14	9	_
Revue des Sciences de l'Eau	22 (0.56)	45	0.33	1	_	9	12	Water Science and technology
Regional Studies in Marine Science	22 (0.56)	8	1.183	_	_	_	22	Animal Science and Zoology; Aquatic Science ; Ecology, evolution, behavior and systematics
Eau, l'Industrie, les Nuisances	22 (0.56)	19	0.02	_	1	3	18	Water Science and technology
Physical and Chemical News	21 (0.53)	11	0.876	_	_	8	13	Mathematical Physics
Oceanologica Acta	21 (0.53)	134	1.14	1	9	11	_	Aquatic Science; Oceanography
Marine Biology	21 (0.53)	284	2.05	5	_	9	7	Aquatic Science ; Ecology, evolution, behavior and systematics
International Journal of Advanced Research	21 (0.53)	_	6.992	_	_	_	21	Environmental Chemistry; Pollution
Hydrobiologia	21 (0.53)	521	2.385	2	6	12	1	Aquatic Science
Environmental Toxicology	21 (0.53)	76	3.258	_	3	16	2	Health, toxicology and mutagenesis; Management, monitoring, policy and law
Journal of Geophysical Research: Oceans	20 (0.5)	276	3.56	_	5	8	7	Aquatic Science; Oceanography

(TP, total publications; IF, impact factor *Data generated from SCImago Journal and Country Rank (SJR) (http://www.scimagojr.com/)).

2.5.1.3 Research area

The dynamic changing process of knowledge areas over time period is analyzed (Fig. 2.3a). Hydrobiology (33 publications; 15%) and ecology (in a broader sense) (14.7%) dominated research during the first decade (1971-1980), but with advancing time, the research began to emerge and studies were progressively used to answer a wider range of questions. Hydrology (19.7%) and marine geosciences (17%) maintained a steady growth while algology (1.47%) and energy (1.47%) dipped in the second decade (1981-1990). Microbiology/Genetic (2%) was a new research points that appeared in this decade. In the third decade (1991–2000), hydrobiology (17%) and hydrology (15.44%) continued to be a concern. Ecotoxicology (14.8%) has a sudden increase from the third to the fourth decade and become a new research hotspot during this time period. In last decade (2011–2021), ecology (14.7%) and hydrology (13.6%) became crucial issues of coastal science. Other aspects, such as modeling and remote sensing monitoring methods including geographic information system (GIS), have received much more attention since then. Otherwise, climate change and oceanography received minor attention.

2.5.1.4 Coastal habitat type

During the first decade, publications were analyzed a limited variety of coastal habitats. However, from the 207 published documents between 1971 and 1980. Almost half of them (130 publications; 48%) have been limited to the coastline studies, more than one-fifth to the cape (12.5%) and estuaries (8%). The remaining habitats (lagoons, bays and beaches) were only the focus of 15% of the documents (Fig. 2.3b). In the second decade (1981-1990), the numbers of publications investigating the coastline has increased (155 publications; 47%). Estuaries (15%) and lagoons (15%) were the focus of over than one-third of the published documents. Recently (2011-2021), more than half (1691 publications; 63%) of the publications was devoted to investigate the coastline, 11.44% was conducted to analyze lagoons, 7% for estuaries, 5.6% for bays and 4.2% for capes. The remaining 8% were split between beaches (3.4%), marshlands (1.8%), harbours (1.2%), dayas (0.8%) and oasis (0.8%).

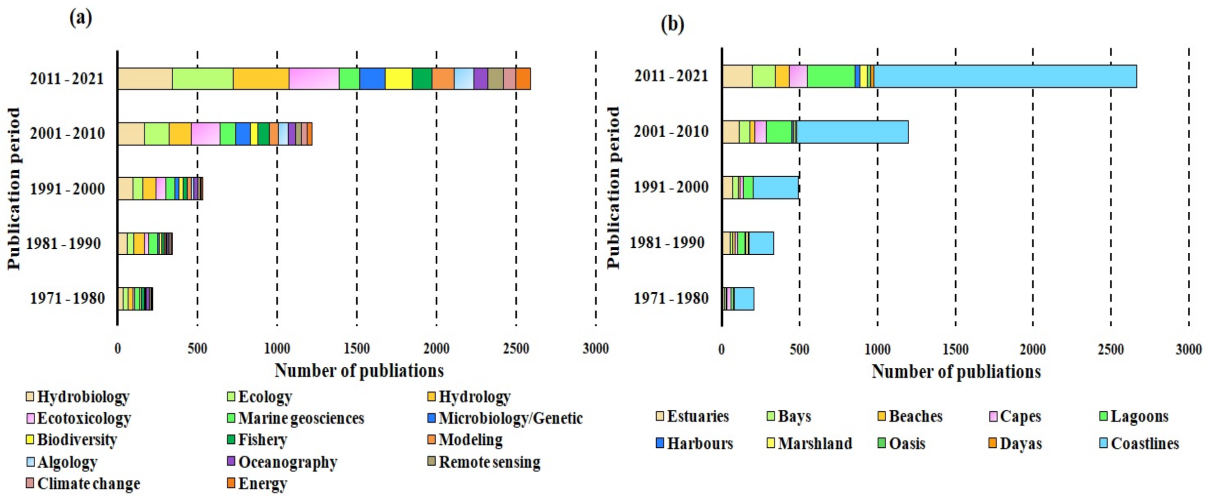

Figure 2.3: Distribution of publications by (a) research area and (b) habitat type during the last five decades: 1971-1980, 1981-1990, 1991-2000, 2001-2010 and 2011-May, 2021.

2.5.1.5 Geographic extent

Fig. 2.4 shows the Moroccan Atlantic map with the most productive areas in terms of total number the published documents. Agadir coast including Agadir Bay, Agadir harbour and Taghazout Bay had the highest volume of scientific published studies and positioned at the top of the ranking with 538 (11%) publications; Casablanca coast ranked second with 481 (9.8%) publications. This is followed by Cape Blanc, which is ranked 3rd, with production increasingly closer 255 (5.21%) publications. Essaouira coast and Oualidia lagoon ranked 4th (236 publications; 4.8%) and 5th (220 publications; 4.5%), respectively. El Jadida Bay ranked 6th with 203publications (4.15%), rabat coast ranked 7th with 203 publications (4.15%) and Moulay bouslham lagoon ranked 8th with 180 publications (3.7%). The geographic distribution of the published literature appears to be unevenly distributed across the Moroccan Atlantic coast (Fig. 2.4); Overall, the Northern Atlantic areas were clearly dominated the research throughout all analyzed period followed by the central Atlantic areas, while, areas that receive relatively little attention were situated in the southern coast.

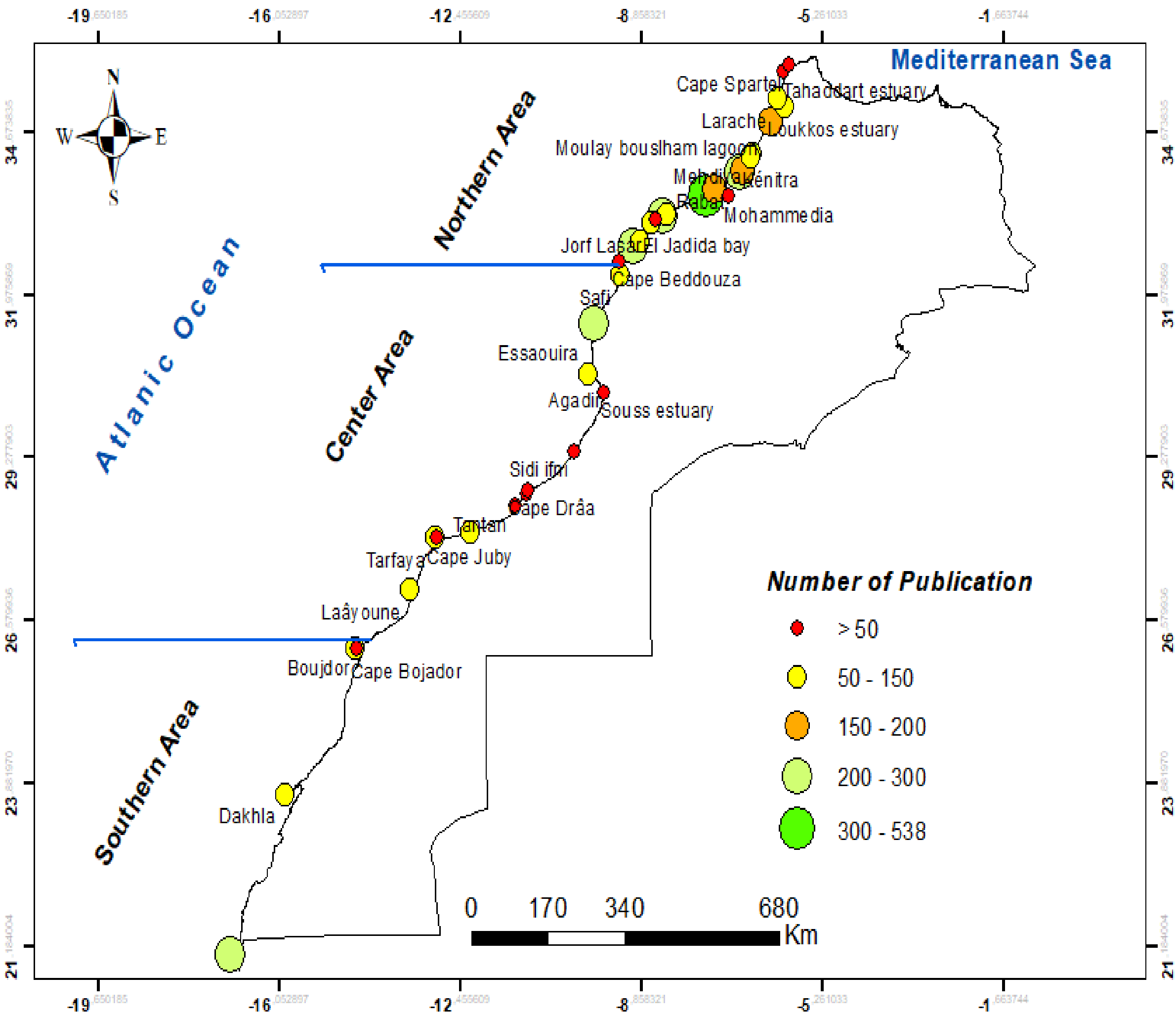

Figure 2.4: Geographical distribution of the most productive areas by of number of publications (1971–2021).

2.5.2 Network analysis

2.5.2.1 Co-words analysis

Co-word analysis is a key technology for content analysis [291]. It permits researchers to visualize the problematic networks and discover scientific research hotspots. In this section, we base on the frequency of words appearing in titles, keywords and abstracts to capture co-occurrence relationships among different keywords. We set the minimum number of keyword occurrences to 10. Of all 14409 keywords, 497 meet the threshold. The co-occurrence relationships among these 497 keywords was visualized and the total strength of the links between them was calculated. The co-occurrence map of keywords with the greatest total link strength is shown in Fig. 2.5. The size of the circle illustrates occurrences of keywords, and high occurrences typically have strong link strength. Keyword clustering divides the research contents into five clusters, where each one is distinguished by a different color. The red cluster involved the analysis of sedimentology, paleoecology, biostratigraphy, paleoceanography of the coast. The green cluster referred to the distribution of phytoplankton biodiversity in the coastal upwelling system (Moroccan Atlantic coast). The blue cluster focused on the evaluation of water quality pollution and environmental monitoring of heavy metal contamination in coastal waters. Indeed, heavy metals received focus on a high degree in coastal pollution research during the study period. Copper, cadmium and

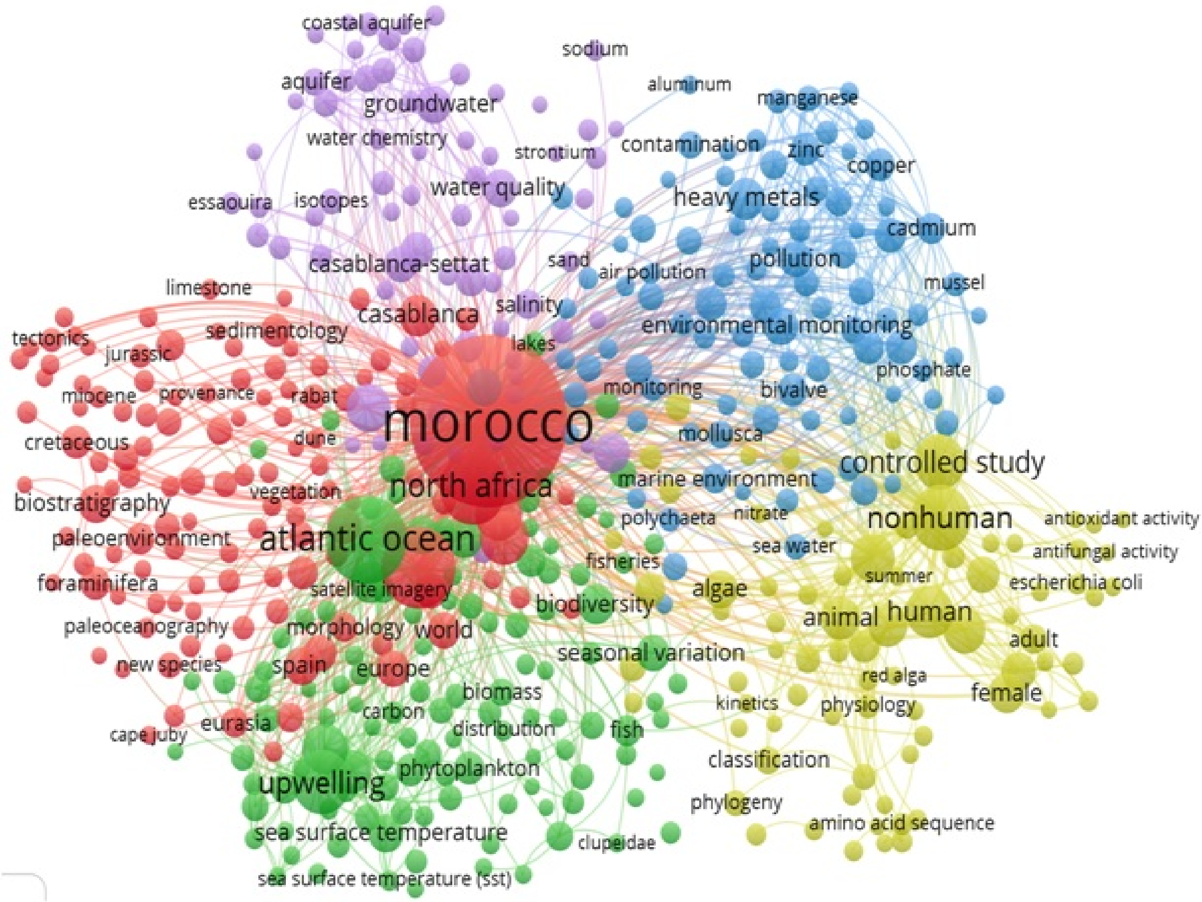

Figure 2.5: Keywords co-occurrence and clusters.

manganese addressed, respectively, more concern in coastal contamination. The purple cluster has connections with keywords mainly related to the Assessment of groundwater water quality and chemistry especially in the region of Casablanca-Settat and Essaouira. Finally, the yellow cluster involved mainly the human behaviour as an ecological driver of non-human evolution in coastal areas.

2.5.2.2 Co-authorship analysis

We set the minimum number of corporation document of an author as 8, of 7946 authors, 110 meet the threshold. For each of the 110 authors, the total strength of the co-authorship links between the authors was calculated. A collaboration network for the most productive authors was presented (Fig. 2.6). Using cluster analysis, authors were aggregated into 12 clusters, each one is marked with different color. It worth noting that Abdellatif Moukrim and Mohamed Maanan have highest publications and corporation number with other researchers.

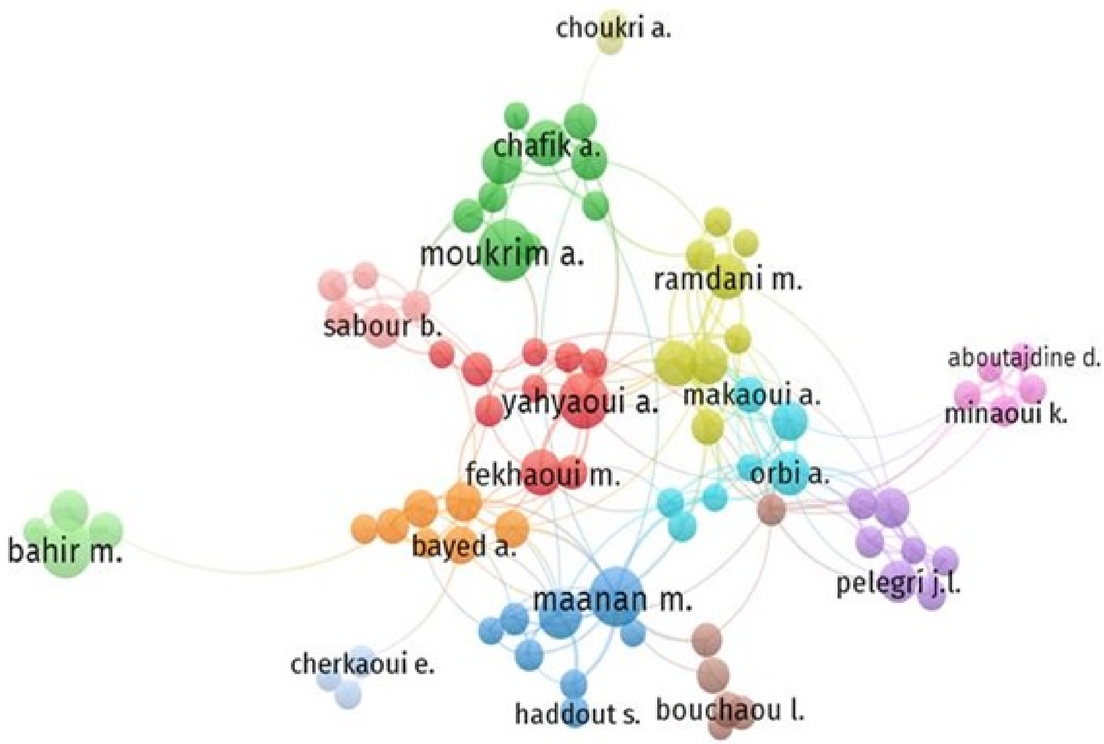

Figure 2.6: Authors' co-authorship network analysis.

2.5.2.3 Co-country analysis

As for co-country analysis, we set the minimum number of documents of a country as 10, of all 128 authors, 25 meet the threshold. For each of the 25 countries, the strength of the co-authorship links (LS) between the countries was calculated. The greatest relationship between countries of affiliation for each co-author were visualized (Fig. 2.7). The lines attach the countries whose authors have cooperated. Countries with the same color were commonly being cooperated more often than others. Generally speaking, Morocco played a central position with the highest total collaboration intensity (LS = 823). The link strength between Morocco and France was maximum (LS = 571) with 537 collaborative publications, this could be an indicator of how wide of international cooperation was carried out. Spain and Germany ranked second and third with LS = 267 and LS = 203, respectively. The cooperation between Morocco and European countries was much more active than African countries. With the continuous development of coastal science, African and Asian countries should strengthen their international cooperation with Morocco to improve their accomplishments.

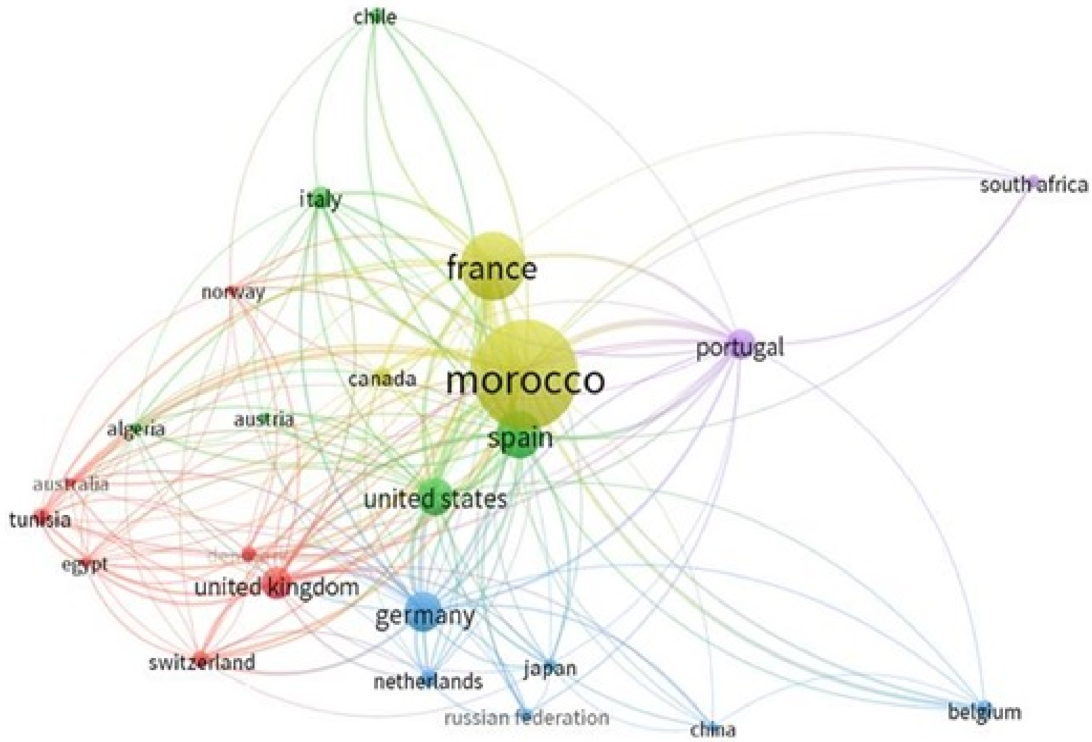

Figure 2.7: Co-country network analysis.

2.6 Discussion and concluding remarks

2.6.1 Research effort in coastal science

Although the growing pressures on coastal ecosystems are still apparent, the future of Moroccan Atlantic coast looks promising since the government understands that the use of the coast under the Coastal Blue Economy Growth (CBEG) concept with the Sustainable Development Goals (SDGs) and the United Nations Decade of Ocean Science for Sustainable Development (2021-2030) [113] requires concerted efforts on coastal science [109]. The information provided here concerning research effort in Moroccan Atlantic coast express the growing concerns about the scientific understanding of these coastal ecosystems. Indeed, 77.9% of the total publications were produced during the last two decades.
This sharp increase in the number of publications coincides with:

(a) Passage of a series of conventions (Integrated Coastal Zone Management (ICZM) protocol of the Barcelona Convention, Ramsar Convention) and legislation (law N°13-03; N° 31-06; N° 81-12) that favoured field research, data collection, and article publication;

(b) Implementation, in progress, of the National Coastal Plan and the regional plans provided for by the Coastal Law (Dahir No. 1-15-87 of July 16, 2015 ; Kingdom of Morocco, 2015) that shape their coastal monitoring requisites;

(c) Achievement of the Institutional Training Program that assisted research projects in coastal and oceanic ecosystems ; accomplish the institutional purpose and strategic planning priorities in various areas of activity: scientific research, scientific advancement, data collections, knowledge communication, contribution of science to technology.

The Atlantic coast is dominated by three main forms of ecosystem: sandy beaches (2% of the coastal line), rocky coasts with cliffs (63%) and wetlands (35%), often classified as sites of biological and ecological interest [151]. Among wetlands, coastline and lagoon valuations have appeared at consistently high levels of published literature across the period. Oualidia lagoon is among the most investigated lagoons (220 publications).

The population around the lagoon has increased from 7,741 to 18,616 inhabitants between 1971 and 2014 [154] leading to pressures as seaweed harvesting, sand extraction, traditional fisheries and oyster aquaculture [57, 60, 153, 279]. Such activities are responsible for nutrient enriched from the cultivated areas that cover 78% of the catchment [133]; input of organic matter from aquaculture and phosphate enriched from the adjacent phosphate mine [132, 133]. These nutrients stimulate an increase in chlorophyll levels within the lagoon ecosystem [152]. In conrast, scientists draw little attention to ecosystems such Khenifiss lagoon (94 publications), where the anthropic impacts are not detected at present [154]. The lagoon is a protected area that has been designated by UNESCO as a world heritage site [154]. Beside, since the implementation of the Water Framework Directive [441], the hydrobiological status of the Morocan atlantic coastal ecosytems (14%) has been considerably investigated using a set of ecological tools that enhance biological assessments in highly dynamic aquatic ecosystems [130]. We also recognize that the efforts for coastal conservation have been broader by improving the links between ecotoxicology (12%) and biological assessment tools [240, 290, 474].

In spite of the optimistic attitudes of research tendency, it is worthwhile to note that further efforts are still required in energy (2.9%), climate change (2.9%), remote sensing (3.2%) and ecosystem modelling (4.7%). Indeed, for many monitoring situations the application of statistical analysis is sometimes suitable compared to the application of numerical simulations [228]. This is attributed to the simplicity of the statistical approach in comparison to modeling and their direct implementation through low-cost specialized software yielding consistent results [228]. In contrast, a direct observation in a system is insufficient, management strategies are more effective if designed to prevent unpleasant circumstances [55]. Environmental models are suitable for coastal and marine monitoring purposes [63].

In addition to the unequal distribution of research effort between the research areas, our analysis also revealed tremendous geographical heterogeneity in the generation of scientific knowledge. In this sense, as mentioned earlier, research capacity is stronger in the northern coast with the highest number publications found in the northren coast. This disparity in research effort between the northern, central and southern coast could have different roots of climatic, economic, demographic, institutional and social character. After independence, the shift of population to the coast has continued at a steady pace. According to [304], Moroccan Atlantic cities had 14.7

million inhabitants (46.68% of the total population) in 2010 while it represented only 6 million (39.21%) in 1971. Most of them living around the Rabat-Casablanca region [307]. Industrial activity has also sought out the coastal location with more than 75% of units and 77% of new investments (Mohammedia, Safi, Jorf Lasfar) [247]. In 2012, industrial areas concentrated 89% of production, emitted 95% of exports and received 89% of investments [5]. Before 2015, Casablanca, Mohammedia and Jorf Lasfar harbors concentrated over 90% of the investments [6]. Besides growing pressure from industrial activities, by 2030, more than 3% of natural coastal areas will be subject to anthropization and about 1.5% of agricultural land will be transformed for industry, tourism or urbanization [5].

Furthermore, the Atlantic coast of Morocco receives most of the running water, particularly from the large northern watersheds of the Sebou, Oum Rbia and Tensift, which are heavily loaded with pollutants [479]. However, industrial and anthropogenic pollution, localization of the most productive research institutes/academic agencies in coastal science and a great number of persons using on the coast as a main source of income in the northern areas; placing more emphasis on local knowledge production. In addition, the rapid industrialization of northern region could have favored the establishment of new collaborations between local industry and scientists, engendering private financial support for academic research activities. In contrast, areas that are conspicuous for the research deficiency are situated in the southern coast, which may indicate more efforts should target on increasing research production in this region.

2.6.2 Impediments to the scientific knowledge managment

Fundamental to improving the management relevance of scientific research on Moroccan Atlantic coastal ecosystems is the need for coastal managers and decision-makers to draw on the scientific advancements through the access to up-to-date scientific results [81]. Indeed, researches as producers of scientific information are held to be responsible for making such information available to managers and all stakeholders involved in the coastal research. Coastal decision-makers would have a clear-sightedness of the resources they should manage and managers would fully utilize available scientific to repair ecological damage and adopt ideas related to coastal restoration practices in an integrated management of improvement informed by sound monitoring. Nonetheless, a number of impediments prohibit the efficient management and exchange of scientific knowledge.

The first mainly associated with the limited accessibility to scientific information. Indeed, the present synthetic research may not have exhausted the scientific literature in its entirety, only those freely available online are collected. As a great number of cited references or found online do not meet accessibility criteria may undermine the real representation of the current status of scientific knowledge in Moroccan Atlantic coast. This is also the case in other countries, whereby governance framework are not clearly organized making the access to scientific information much more limited, thus showing that over half of the scientific information was not freely accessible to users, due to non-open access journals. Even when scientific information was freely accessible to decision-makers, a previous study has reported that only about one-fifth (19%) of research papers revealed clear propositions for management actions [128].
Other impediments can be associated to:

(a) An inadequate scientific information collection;

(b) Inadequate mobilization and exploitation of the scientific information collected in national planning of coastal monitoring;

(c) Lack of institutional capacity and infrastructure to adopt the necessary requirements for coastal knowledge management;

(d) Poor program planning and lack of organised national data bases;

(e) Timing mismatch between need for research and implementation of a management plan [127].

Following data collection and processing, scientific article request an average of three years to be published [127]. Scientific outcomes may thus be less useful to coastal decision-makers. These disparities in access to scientific knowledge prevent an effective collaboration between scientific researchers and coastal managers, especially where the transfer to scientists and institutions lack the necessary skills [148]. Nevertheless, without improving the necessary capacity for management of scientific knowledge, governments will continue to be short of the information they require for the sustained effective management of Moroccan Atlantic coast.

2.6.3 Future recommendations for improving Knowledge management and its implication in coastal management planning

Knowledge management (KM) is key to scientific progress. It can be described as a cross-disciplinary activity that allows organizations to involve effectively the major processes of creating, storing, diffusing and using knowledge in order to accomplish their objectives more faster and efficiently [303].

Implementation of KM within the concept of sustainable development of coastal areas is required to achieve the objectives of the Integrated Coastal Zone Management (ICZM), that covers different aspects entailed in coastal evolution from information collection, exploitation and coastal planning to decision making and monitoring coastal development [263]. It has considerable implications for effective coastal research planning, admitting that serious disorganization and structural impediments to research disturbed the successful implementation of coastal adaptive governance, causing therefore coastal management feebleness.

Despite scientific efforts in understanding of Moroccan coastal ecosystems, the government still lacks an efficient research strategy to ensure that scientific knowledge feeds directly into the managers and policy makers. This section proposes some tasks to be undertaken to improve the use of scientific knowledge in management planning of Moroccan Atlantic coast.

First, the government could implement a national environmental database or clearing-house mechanism to maintain scientific knowledge visibile and accessible to all stakeholders [95, 377]. The system disseminates data needs to be carefully maintained, updated, organized according to formal data use agreement and managed by trained database curators before sharing. Such system is supposed to ensure that managers can have access to the local information to support effective coastal management. It could have tools to foster online interaction between scientists and users, allowing them to constitute virtual communities, exchange and communicate knowledge on the trends and status of coastal ecosystems. Particularly useful system includes increased funding opportunities for cross-sector collaborations [52, 114]. There may be organized forums for such interactions including scientific conferences, workshops, seminars, meetings and periodic training to foster partnerships between actors at different levels [426]. Other conventional mechanisms of dissemination as regular technical reports and policy briefs are valuable in communicating research findings, enhancing the visibility of coastal knowledge. Modern technologies, particularly digital networks can be nevertheless useful for ensuring the knowledge is provided on time [426].

On the other hand, focusing on co-production of knowledge whereby coastal policy-makers and managers contribute in scientific research should take place for sustainable research and policy [452]. Confirmed by other studies, permanent embedding scientists in managerial activities will bridge the divide between scientists and managers by understanding of scientific materials needs of managers [114, 215, 497]. The involved parties should thus be strictly engaged in environmental decision-making organizations; idea should be exchanged, understood and discussed before being executed. National Oceanic and Atmospheric Administration (NOAA) in the United States and Western Australian Department of Parks and Wildlife in Australia can be take it as successful models of organizational marine decision-making structure embedding researchers within their organizations. In addition, progress towards the sustainable management of Moroccan coastal area is widely attributed to institutional advancement. This should include institutional innovation by academic institutions, funding agencies, research funders and publishers to support scientist component for engagement activities, with both time allotments and dedicated funding [128]. This will simulate coastal scientists with benefits extending to increase coastal research productivity and improve exchange of information. At the worldwide scale, Shanley and López, 2009 have investigated 268 scientists across 29 countries and noted that 93% of contributors agreed that funding bodies are effectively improve the dissemination of research findings.

Research funders should insist through contractual engagement to make all research findings freely open access to the users of scientific knowledge, and provide supplemented funding to cover these activities charges. This method has been successfully adopted by funding agencies globally such as Australian Research Council (ARC), requiring that any ARC funding publications should be available as free electronic copies accessible repository within a 12 month [127].

Beside, the Driver–Pressure–State–Impact–Response (DPSIR) framework can be adopted to inform coastal science. This approach has the capacity to bridge the gap between scientific discipline and involved science in coastal management. Indeed, DPSIR can serve as a template for organizing advanced research and providing viable options for managing and maintaining coastal systems [256]. Increase the North – South scientific community communication through elaboration of strong social network between different stakeholders, including all producers and users of coastal knowledge. The network should also include “Grey Literature” being considered as one of the most important sources of knowledge about environmental and natural resource management [116, 170, 439]. Accordingly, scientists would use such technologies to share knowledge with the large scientific community; coastal decision makers would have access to the most recent and scientifically credible research available and managers would have possibility to access raw coastal data.

CHAPTER 3

WATER QUALITY MODELLING: REVIEW AND SCIENCE MAPPING, 1981–2021

3.1 Résumé du chapitre

Les résultats de ce chapitre ont fait l'objet d'un article soumis pour publication au journal " *Environmental Nanotechnology, Monitoring and Management*".

Dans ce chapitre :

Nous explorons l'émergence de la littérature de recherche sur les applications de modélisation de la qualité de l'eau dans l'espace atlantique en utilisant une approche de cartographie scientifique. Cette revue a cherché à documenter la tendance générale de la recherche, les journaux, les auteurs et les institutions influents, les foyers thématiques, à identifier l'approche et le modèle le plus fréquemment utilisé, les types de masses d'eau et les zones dans lesquelles les modèles sont principalement appliqués. En utilisant l'outil de recherche Scopus, nous avons identifié 1952 publications potentiellement pertinentes (2548 applications individuelles de modélisation) publiées entre 1981 et 2021. Nous utilisons Microsoft Excel, VOSviewer et ArcGIS pour analyser notre base de données. L'analyse des données comprend des statistiques descriptives, des analyses de citation, de co-citation, de co-auteurs et de co-occurrence. Les résultats ont mis en évidence une tendance à la hausse du nombre de publications au cours des deux dernières décennies. En bref, nous avons récupéré 89,33% articles, 8.06% articles de conférence, 1,63% rapports scientifiques et 0.98% documents classés comme autres. Science of the Total Environment, Ecological Modelling et Journal of the American Water Resources Association sont les revues les plus influentes. "Ramiro J. J. Neves" (Instituto Superior Técnico, Portugal), "Jeffrey G. Arnold" (USDA Agricultural Research Service, États-Unis) et "Raghavan Srinivasan" (Blackland Research and Extension Center, États-Unis) sont les auteurs les plus productifs. Plymouth Marine Laboratory, plymouth; MARETEC, Instituto superior técnico, universidade de lisboa; Virginia institute of marine science, college of william and mary, Gloucester Point and USDA-ARS Hydrology sont les institutions de recherche les plus productives. En utilisant l'analyse des co-mots, "la qualité de l'eau", "États-Unis", "bassins versants", "rivières", "modélisation hydrologique", "pollution de l'eau", "phosphore", "modèles numériques" sont les points chauds de la recherche. En outre, le SWAT (cadre de modélisation semi-empirique) a été largement appliqué au cours des deux dernières décennies et reste le modèle le plus utilisé aujourd'hui, suivi de MOHID Water, CE-QUAL et HSPF. La plupart des applications de modélisation ont porté sur le système des bassins versants (72.15%). Le nord-ouest et le nord-est de l'Atlantique ont reçu la plus grande attention, principalement les États-Unis d'Amérique 41.64%), Canada (13.81%). Cette analyse donne une image globale de l'état actuel des connaissances sur les applications de modélisation de la qualité de l'eau dans l'espace atlantique. Elle peut aider les chercheurs à comprendre l'évolution de la littérature et les inciter à améliorer encore ce domaine de recherche.

3.2 Abstract

To improuve our understanding of the application of water quality models, we use science mapping approach to explore the emergence of research literature on water quality modelling applications within the Atlantic area published from 1981 to 2021. The study sought to document the general research trend, the influential journals, authors, and institutions, topical foci, identify the most frequently applied model, the water body types and the areas within which models are mainly applied. We identified 1952 potentially relevant publications (2548 individual modelling applications). We use Microsoft Excel, VOSviewer and ArcGIS to analyze the database. Our findings highlighted an upward trend in number of publications during the past two decades. More broadly, SWAT (semi-empirical modeling frame-works) was by far the most often used model (22.4%), followed by MOHID Water (9.1%), CE-QUAL (8%) and HSPF (6.4%). Most of modelling applications have addressed watershed system (72.15%). Northwest and Northeast Atlantic have received the greatest attention, mostly the United States of America (41.64%). Our analysis provides a holistic picture of the water quality modelling applications within the Atlantic area. It can help scholars understand the evolution of littrature and inspire them to further improve this research domain.

Key–Words : Water quality, modelling, science mapping, Atlantic, VOSviewer.

3.3 Introduction

A water quality model can be described as a simplified mathematical description of contaminant fate and movement within an aquatic system that can be coupled with a mathematical description of contaminant transport from their land-based sources to receiving water bodies [4, 104]. The water quality models are essential in describing processes affecting fate and movement of contaminants [103]. They help government agencies, local authorities and environmental managers to predict the behaviour of the system in response to specified inputs under different conditions and management actions [102, 413]. This makes water quality models a critically important tools to assist in the pollution prevention, control and remediation of water body [102, 118].

Since [359] proposed one of the earliest solution of the first-order differential equation to model dissolved oxygen rise by reaeration and decreased by the decomposition of organic matters. Several water quality models classified as conceptual, empirical, stochastic, deterministic, or process-oriented have since advanced to simulate water quality processes [103, 470]. Hence, the number of model processus and parameters significantly expanded, thereby increasing the model complexities. Multiple factors contributed to this expansion including the increased computing powers, advancements in situ sensors, remote monitoring of water quality, advance in remote sensing algorithms [103, 104].

Although the water quality modeling was broadly reviewed [117–119, 225, 300, 405]. There is a need for a clear picture of the current state-of-knowledge of water quality modelling application within the Atlantic area. One of the challenges to enhance water quality models applications is the establishment of baseline information on the way how models are applied.

More specifically, this review is aimed at uncovering the current status and research trend in water quality model applications within the Atlantic area from 1981 to 2021. A quantitative analysis "science mapping [516]" of a large corpus of published literature on water quality model is employed. To our knowledge, there is no such review have published.
The review are structured around the following research questions:

1. What is the trend of the literature on water quality models published in the Atlantic area between 1981 and 2021?

2. Who are the most influential journals, authors, and institutions?

3. What topical foci have gotten the most attention?

4. What models are most frequently applied?

5. What are the water body types and areas where models are mainly addressed?

Using scopus search tool, we identified a database of 1952 publications (2548 modelling applications) published between 1981 and 2021. The database were analyzed using Excel, VOSviewer, and ArcGis. Data analysis enclosed descriptive statistics, citation, co-citation, co-authorship and co-occurrence analysis. First, our review sought to document the general research trend of research literature on water quality modelling applications within the Atlantic area published from 1981 to 2021. Second, the review uses science mapping as a means of establishing a quantitative analysis of the database. Finally, the review provide insight into models most frequently used, the water body types most frequently addressed and the areas within which models are mainly applied. The relevant conclusions are crucial for researchers to provides insights into the state-of-knowledge in water quality model applications, identify the most used model, the regions of interest, and investigate potential future research directions.

3.4 Methodology

3.4.1 Data Collection

The Scopus search engine was chosen as the data repository from which to extract published literature on water quality models. Literature review has revealed that Scopus's superior coverage of the world's research output compared to other databases makes it a better option for research reviews [193, 262, 316, 500].

Our search criteria included a broad scope in terms of document types (journal articles, books, book chapters, conference articles and other academic documents), in the belief that dependence on a large database would induce a more reliable outcome. Published literature between 1981 and May 2021 was selected, this is a sufficiently extensive period to provide useful insight into the general research trends. The following search criteria was selected to determine publications potentially relevant for our investigation: keywords water quality and model or name of the model in the publication title, abstract, author keywords and keywords plus. Referring to [22, 117–119, 174, 225, 300, 337, 405], the most frequently used water quality models were chosen (**Box 1**). All publications matching the selected criteria were extracted and downloaded for further analysis. After scanning abstract of all publications, only the models applied in Atlantic region were kept. Afterwards, a manual check was conducted to add the missing contents, remove duplicate and exclude inadequate publications.

3.4.2 Data Extraction

The bibliographic "data" depicting features of the 1952 Scopus-indexed documents were downloaded and stored in a .csv (comma-separated values) file. These "meta-data" included all information listed in Table 3.1. In the case of publications presenting several model applications or various modelled area, authors generated several individual 'meta-data' in our database. A total of 1952 publications were screened to identify 2548 individual modelling applications. A copy of the .csv file including the same database was also saved in EXCEL spreadsheets version 10.0 for further data analysis. It's worth noting that our database considers publications reporting water quality modelling applications with well-defined boundary conditions. Publications presented technical descriptions of models without practical applications are excluded from our database.

3.4.3 Data Analysis

Comprehensive assessments relied on bibliometric analysis and study summaries were conducted using different software programs. Bibliometric analysis involves descriptive statistics, citation, co-citation, co-authorship, and co-occurrence analysis to enlighten key characteristics of knowledge domains [457]. Descriptive statistics analyses of the publication growth in terms of number of publication by year, country, and journal were performed using Microsoft Excel. ArcGIS (version 10.5) was used to generate a visual map showing the geographical distribution of the modelling applications.

The impact factor (IF) is the most common index for quantifying the importance of citation frequencies and evaluating the performance of scientific journals [435]. It is computed by dividing

Box 1 keyword search and acronymlist of the water quality models searched for titles, abstract, and the keywords of the Scopus database.

Scopus search

“ water quality ” AND “model” OR:

AQUATOX, SWAT, WASP, MIKE, QUALs, HSPF, CE-QUAL, CAEDYM, EFDC, SPARROW, MOHID Water, TOMCAT, Delft-3D, ERSEM, COHERENS, DYRESM, ECOHAM, ECOLAB, NORWECOM, TELEMAC, INCA, MINLAKE, EUTRO

Table 3.1: List of “meta-data” collected for each relevant publication.

Group	Entry	Types of data
Bibliometric data	Year of publication	Open (numeric)
	Author (s) name	Open (alphanumeric)
	Author affiliation (s)	Open (alphanumeric)
	Document type	Multiple choice
	Title	Open (alphanumeric)
	Language of document	Multiple choice
	Journal name	Open (alphanumeric)
	DOI	Open (alphanumeric)
	Abstracts	Open (alphanumeric)
	Author keywords	Open (alphanumeric)
	Keywords Plus	Open (alphanumeric)
	Various citation data	Open (alphanumeric)
Modelling exercise	Model name	Open (alphanumeric)
Study area	Continent	Multiple choice
	Country	Open (text)
	Type of Water body	Multiple choice
	Name of the study area	Open (alphanumeric)

the citation number of the current year by the published articles in the first two years of a journal [378]. This review employed IF from the Journal Citation Reports in 2021 (JCR (`clarivate.com/products/web-of-science`).

Citation analysis (including authors’ influence, affiliation statistics and key words analysis) has been largely used to identify key authors, documents, and journals shaping the evolution of knowledge domains [193, 450]. It is alculated by calculating the number of times that the article was cited by other articles [258]. In this review, citation analysis was exploited to identify the extent to which each units of our database had been cited by other publications in the Scopus index “Scopus citations” [193].

Co-citation analysis is defined as the frequency with which two or more earlier units (e.g., authors, journals, keywords) are cited simultaneously by the later elements [414]. Many studies have presented a detailed description of author co-citation analysis (e.g., [302, 478]) and proved its validity as a reliable tool for examining the intellectual structure of a scientific discipline [371]. Co-authorship defines the number of publications that are co-authored by multiple authors, institutions or countries. It can be used to explore the authors’ position in scientific communities [46]. Co-occurrence or co-word analysis identifies the frequencies of words in titles, abstracts, or in text. Color clustering is based on paradigm of keyword co-occurrence among different keywords

[450]. The size of the node reflects the number of occurrences of the keyword; the larger the node, the more times it occurred in the database [253]. The thickness of the lines between nodes reflect the link strength between keywords; the thicker the line, more links occurred between the keywords [353].

3.5 Results

3.5.1 Publication trends

As previously mentioned, we found that a total of 1952 documents (2548 individual modelling applications) applying water quality models at local, regional, national or larger scales of Atlantic region had published over the past four decades (1981–2021), with an average annual publication output of 9.55. It's worth noting that our database, as large as it is, was confined to publications indexed in Scopus. Hence, it does not even represent the entirety of the published literature on the subject. Wherefore, one might infer that the use of water quality models has amassed a quite substantial body of information. This began with the publication of one documents during the 1981s (Fig. 3.1) coinciding with the widespread adoption of microcomputers in the mid 1980s [20], rose to 82 documents during the 2010s, and emerged rapidly throughout the ensuing decades to reach 134 documents published during the 2019s. The last evaluated year (2021) recorded 83 documents considering the months of January to May 2021.

Notably, the article type ranked first with 89.33% of the total publiations, followed by conference paper (8.06%) and scientific report (1.63%) (Fig. 3.1). Most of the documents were published in English (94.58%) (Not presented).

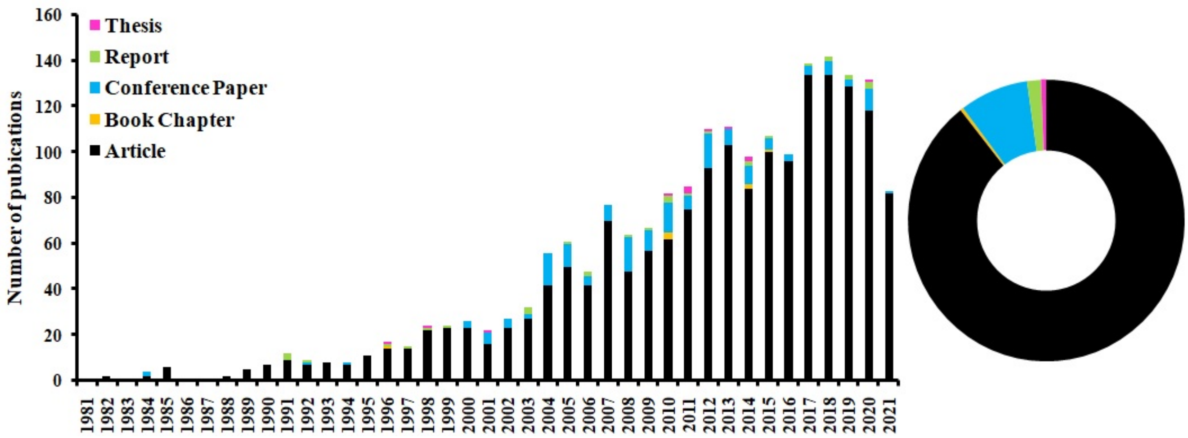

Figure 3.1: Number of publications per document type through time (left) and overall distribution (right), 1981–2021.

3.5.2 Influential Journals, Authors, and Research Institutions

The 1750 retrieved articles are published in 725 journals. The top 10 most productive journals on water quality modelling studies from 1981 to 2021, accounting for 25.65% of the total publications, are shown in Table 3.2. The obtained journals vary largely in terms of the number of publications, this may be due to various launch dates and the variations in number of articles per year. The core journals are multidisciplinary, referring mainly to ecology, environmental engineering, oceanography, water science and technology, ecological modeling, and pollution, etc. Obviously, Science of the Total Environment and Ecological Modelling have published the most articles (7.37%). Science of the Total Environment and Journal of Hydrology are the most influential in terms of impact factor (7.963 and 5.722, respectively). When sorted by total citations, Journal of the American Water Resources Association (2414 citations) and Ecological Modelling (2219 citations) evidenced the largest cited amount.

Another strength of bibliometric methods is the capacity to identifiy influential authors and research institutions [172, 329, 457]. First, **"author-citation analysis"** was performed. This approach consists of ranking authors by the number of publications and by citations to obtain insights in their research productivity [427]. Hence, authors with highly-cited publications usually dominate the conceptual tendencies [492].

In this section, authors' contribution were investigated using the "author(s)" unit from the extracted database. The top 20 productive authors by the number of publications and citation impact are listed in Table 3.3. Noted, only citations of the authors authored more than 10 publications are considered. When sorted by the number of publications by each author "Ramiro J. J. Neves" from MARETEC, Instituto Superior Técnico, Portugal (63 publications), "Dias, João Miguel"from Universidade de Aveiro, Portugal (24 publications), "Jeffrey G. Arnold" from USDA Agricultural Research Service, United States (24 publications), and "Raghavan Srinivasan" from Texas AM, Agriculture and Life Sciences, Spatial Science Laboratory (21 publications) generated the most publications. Referring to the number of citations, "Ramiro J. J. Neves", "Raghavan Srinivasan" and "Jeffrey G. Arnold" have the highest number of citations (1368, 1177 and 1160 citations, respectively).

The only surprising thing was that we had anticipated finding authors as "Daniel J. Jacob", "Jimmy R. Williams" among top 10 most productive authors. Their absence may be attributed to our database that was restricted to publications from Scopus-indexed list. For instance, Scopus offers less complete coverage of books, book chapters, and conference papers which may were the preferred way of scientific production by those authors.

To overcome this limitation of citation analysis, co-citation analysis can be performed [193]. With this aim, we used VOSviewer [457] to identify an **"author co-citation analysis"** based on the frequency of authors appearing in the references of our database. We set the minimum number of author co-citations to 10. The top 20 co-cited authors are listed in Table 3.4. "Jeffrey G. Arnold" seems to be the most influential author with a total of 147 co-citations. "Raghavan Srinivasan" ranked second with 94 co-citations. Furthermore, we noted appearance of several influential authors who had not emerged in the list of the top 20 cited authors (Table 3.3). It's the case of "Einar Svendsen", "Jimmy R. Williams" who had ranked third (58 co-citations) and quarter (54 co-citations), respectively. Total Link Strength reflects the strength of the co-authorship links between two scholars; the higher the link strength, the greater collaborative efforts between scholars. Thus, "Jimmy R. Williams", Raghavan Srinivasan" and "Einar Svendsen" had the higher Total Link Strength (5257, 3663 and 2297, respectively).

The next analysis consisted on identifying the most productive institutions (Table 3.5). Leading was the Plymouth Marine Laboratory, plymouth with 11 publications (215 citations). MARETEC, Instituto superior técnico, universidade de lisboa ranked second (10 publications, 97 citations) followed by Virginia institute of marine science, college of william and mary, Gloucester Point (6 publications, 123 citations) and USDA-ARS Hydrology and Remote Sensing Laboratory, Beltsville (6 publications, 61 citations). As expected, United States institution have absolute advantage in the total number of publications. Considering Total link strength, collaboration across organizations indicate a weak cooperation amongst organizations.

Table 3.2: Rank order of the 10 most productive journals.

Rank	**Journal**	**Number of publications**	**Impact factor (2021)**	**Citations**	**Suject category***
1	Science of the Total Environnent	66	7.963	1473	Environmental Chemistry; Environmental Engineering; Pollution; Waste ; Management and Disposal
2	Ecological Modelling	63	2.974	2219	Ecological modelling
3	Journal of the American Water Resources Association	61	3.202	2414	Ecology ; Water Science and Technology
4	Journal of Hydrology	57	5.722	1921	Water Science and Technology
5	Water (Switzerland)	42	3.103	358	Biochemistry; Water Science and Geography, Planning and Development
6	Journal of Marine Systems	38	2.542	1464	Evolution, Behavior and Systematics; Oceanography
7	Estuarine, Coastal and Shelf Science	35	2.929	1393	Aquatic Science; Sciences Oceanography
8	Environmental Modelling and Software	30	5.288	710	Ecological Modeling ; Environmental Engineering
9	Journal of Great Lakes Research	29	2.480	673	Aquatic Science Ecology ; Evolution, Behavior and Systematics
10	Journal of Coastal Research	28	0.707	393	Ecology ; Water Science and Technology

*Data generated from SCImago Journal and Country Rank (SJR) (http://www.scimagojr.com/)

Table 3.3: Rank order of the 20 most productive authors, number of publications and scopus citations, 1981 to 2021.

Rank	Author	Institution	Nation	Documents	Citations
1	Ramiro J. J. Neves	MARETEC, Instituto Superior Técnico	Portugal	63	1368
2	Raghavan Srinivasan	Texas AM, Agriculture and Life Sciences, Spatial Science Laboratory, College Station	United States	21	1177
3	Jeffrey G. Arnold	USDA Agricultural Research Service	United States	24	1160
4	J. J. Icarus Allen	Plymouth Marine Laboratory	UK	17	1098
5	Carl F. Cerco	US Army Engineer Research and Development Center, 3909 Halls Ferry Road	United States	12	493
6	Momme Butenschon	Centro Euro-Mediterraneo per i Cambiamenti Climatici	Italy	12	473
7	Ali M.Sadeghi	US Department of Agriculture – Agricultural Research Service, Hydrology and Remote Sensing Laboratory	United States	13	460
8	Flavio Martins	Escola Superior de Tecnologia, Universidade do Algarve, Campus da Penha	Portugal	17	432
9	Paulo Leitao	Departamento de Engenharia Mecânica, Instituto Superio Técnico	Portugal	14	405
10	Jürg Bloesch	Eawag - Swiss Federal Institute of Aquatic Science and Technology	Switzerland	12	400
11	João Miguel Dias	CZCM, Departamento de Física, Universdade de Aveiro	Portugal	24	359
12	Zachary M. Easton	Department of Biological and Environmental Engineering, Cornell University	United States	13	318
13	Nuno Vaz	CESAM Department of Physics, Universidade de Aveiro	Portugal	16	312
14	Marcos Mateus	MARETEC, Instituto Superior Técnico	Portugal	19	292
15	Heinz G. Stefan	St. Anthony Falls Hydraulic Laboratory, University of Minnesota, Minneapolis,	United States	14	285
16	Sabine Sauvage	Research Engineer, ECOLAB, University of Toulouse, CNRS, INPT, UPS	France	13	273
17	David D. Bosch	USDA-ARS Southeast Watershed Research Laboratory, Tifton	United States	14	269
18	Wanhong Yang	College of Social and Applied Human Sciences, University of Guelph, Guelph,	Canada	12	265
19	Paulo C. Leitão	Hidromod, Modelação em Engenharia, Lda., Av. Manuel da Maia, Lisboa	Portugal	11	262
20	Morten D. Skogen	Institute of Marine Research, Nordnes, Bergen	Norway	13	234

3.5.3 Topical Foci in water quality modelling studies

In order to identify the topical foci in research of water quality models, keywords co-occurrence analysis, (or co-word analysis) was conducted. Co-word analysis are assumed to be the most revealing indicators of the publication's content [428]. It allows researchers to visualize the emergence of these problematic networks [82].

Such as analysis allows for identification of research focus and emerging trends for future research [181]. Thus, publications with frequently co-occurring keywords denotes that the concepts behind those keywords are closely linked [516]. Table 3.6 shows the 20 most frequently used keywords, where the keywords "Water quality" (889, 17331), "United states" (422, 8642) and "Watersheds" (362, 7794) presented the most commonly co-occurring keywords and the highest total link strength. This is then followed by keywords "Rivers" (294, 6909), "Hydrological modeling" (244, 4928), and "Water pollution" (198, 4918).

Figure 3.2 shows the network visualization map of keyword co-occurrences ("All Keywords" appearing in the title, author-keywords, and index), with a threshold of at least 20 occurrences. Of the 12,589 keywords, 337 met the threshold. The hotspot keywords belonged to four distinct clusters. As expected, the central core of the co-word map is occupied by the highest co-occurrence and densely linked keyword "Water quality". The red cluster surfaces themes related to the watershed management using hydrological and water quality models. The applications consisted mainly of using SWAT model to investigate agricultural watershed of the United States. The themes in the green cluster adressed the application of water quality modeling approach for examining the eutrophication responses to climate change in estuarine and lake ecosystems. The applications consisted mainly of using CE-QUAL-W2 for exploring water quality mainly in Brazil and Europe. In contast, the themes in the blue cluster revolves around environmental monitoring and assessment of water pollution using water quality modeling approach. The yellow cluster has a less dominant set of themes associated principally with simulation of nutrients using water quality models.

Table 3.4: Rank order of the 20 influential scholars by co-citations, 1981 to 2021.

Rank	Author	Institution	Nation	Co-citations	Total link strength
1	Jeffrey G. Arnold	USDA Agricultural Research Service	United States	147	5257
2	Raghavan Srinivasan	Blackland Research and Extension Center	United States	94	3663
3	Einar Svendsen	Institute of Marine Research, Nordnes	Norway	58	2297
4	Jimmy R. Williams	Blackland Research and Extension Center	United States	54	1987
5	Morten D. Skogen	Institute of Marine Research	Norway	48	1653
6	Johannes Pätsch	Institut für Meereskunde der Universität Hamburg, Troplowitzstrasse	Germany	43	1768
7	Daniel J. Jacob	Harvard University	United States	38	1656
8	Daniel N. Moriasi	USDA Agricultural Research Service	United States	36	1641
9	Andreas Moll	Universität Hamburg, Institut für Meereskunde (IfM)	Germany	35	1482
10	Karim C. Abbaspour	Swiss Federal Institute of Aquatic Science and Technology (Eawag)	Switzerland	34	1321
11	Philip W. Gassman	Center for Agricultural and Rural Development, Iowa State University	United States	32	1326
12	Valérie Thouret	Université de Toulouse, CNRS/INSU, Laboratoire d'Aérologie, Toulouse, France	France	31	1693
13	Helmuth Thomas	Dalhousie University, Department of Oceanography	Canada	31	1531
14	Thomas Pohlmann	Institut für Meereskunde der Universität Hamburg, Troplowitzstrasse	Germany	30	1229
15	Radach Günther	Institut für Meereskunde der Universität Hamburg, Troplowitzstrasse	Germany	30	1102
16	Alberto V.Borges	Université de Liège, Unité d'Océanographie Chimique	Belgium	28	1431
17	Jarle Berntsen	Department of Mathematics, University of Bergen, Norway	Norway	26	1126
18	George L. Mellor	Atmospheric and Oceanic Sciences Program, Princeton University, Princeton	United States	26	387
19	Laurent Bertino	Nansen Environmental and Remote Sensing Center	Norway	25	909
20	Tamie L.Veith	USDA-ARS Pasture Systems and Watershed Management Research Unit, University Park	United States	24	1034

Table 3.5: Rank order of the 10 most productive institutions, 1981 to 2021.

Rank	Organization	Country	Documents	Citations	Total link strength
1	Plymouth Marine Laboratory, plymouth	United Kingdom	11	215	7
2	MARETEC, Instituto superior técnico,	Portugal	10	97	1
3	Virginia institute of marine science, college of william and mary, Gloucester Point	United States	6	123	0
4	USDA-ARS Hydrology and Remote Sensing Laboratory, Beltsville	United States	6	61	0
5	Athabasca river basin research institute (ARBRI), Athabasca university, Alberta	Canada	5	64	1
6	School of engineering, University of Guelph, guelph	Canada	5	63	9
7	INPT, UPS, laboratoire ecologie fonctionelle et environmenet, Toulouse	France	4	31	0
8	USDA Forest Service, Center for Forested Wetlands	United States	4	252	5
9	ASCE, American Society of Civil Engineers	United States	3	49	2
10	Department of Marine Sciences, University of Georgia, Athens	United States	3	37	3

3.5.4 Water quality models and their application

In their various forms and applications, SWAT was by far the most often used model, accounting for approximately 22.41% (571 applications), followed by MOHID Water (9.1%, 231), CE-QUAL (8%, 204), HSPF (6.44%, 164), MIKE (6.28%, 160), Delft-3D (5.26%, 134), ERSEM (4.51%, 115), and QUALs (4.16%, 106) (Fig. 3.3). Among QUALs, QUAL2E was the most used model (24.53%, 26), followed by QUAL2 (20.75%, 22), QUAL2KW (18.87%, 20). Nevertheless, CE-QUAL-W2, contributed the most with 115 (56.37%) of CE-QUAL applications (Not presented). Splitting the database into 10-year time windows (Fig. 3.3, 3.4) shows a positive trend in modelling applications over time.

In the first time windows (1981–1990), the applications were mostly implemented using Delft-3D (22%, 6) (Fig. 3.3); studies were mainly addressed estuarine (20.34%, 10) and lake (16.95%, 12) systems (Fig. 3.4). In the second time windows (1991–2000), the applications were mostly implemented using MINLAKE (13.47%, 18), CE-QUAL (12.21%, 16) and TOMCAT (12.21%, 16). More than 23.67% of the recorded data fall into lake system. In the last two time windows (2001-2010 and 2011-2021), modelling applications using SWAT model become dominant (15.51%, 114 and 26.66%, 441, respectively); most of them addressed watershed (23.7%, 168 and 24.5%, 398, respectively) and rivers (16.9%, 120 and 18.21%, 296, respectively) systems.

Table 3.6: Rank order of the 20 most used keywords, 1981 to 2021.

Rank	Keyword	Occurreneces	Total link strength
1	Water quality	889	17331
2	United states	422	8642
3	Watersheds	362	7794
4	Rivers	294	6909
5	Hydrological modeling	244	4928
6	Water pollution	198	4918
7	Phosphorus	190	4511
8	Numerical model	262	4710
9	Hydrodynamics	263	4358
10	Nutrients	176	4317
11	Canada	206	4375
12	Calibration	189	4258
13	Water managment	191	4106
14	Computer simulation	210	4109
15	Nitrogen	167	3909
16	Climate change	197	3772
17	Soil and water assessment tool	166	2521
18	Atlantic ocean	269	3760
19	Runoff	154	3588
20	Environmental monitoring	121	3621

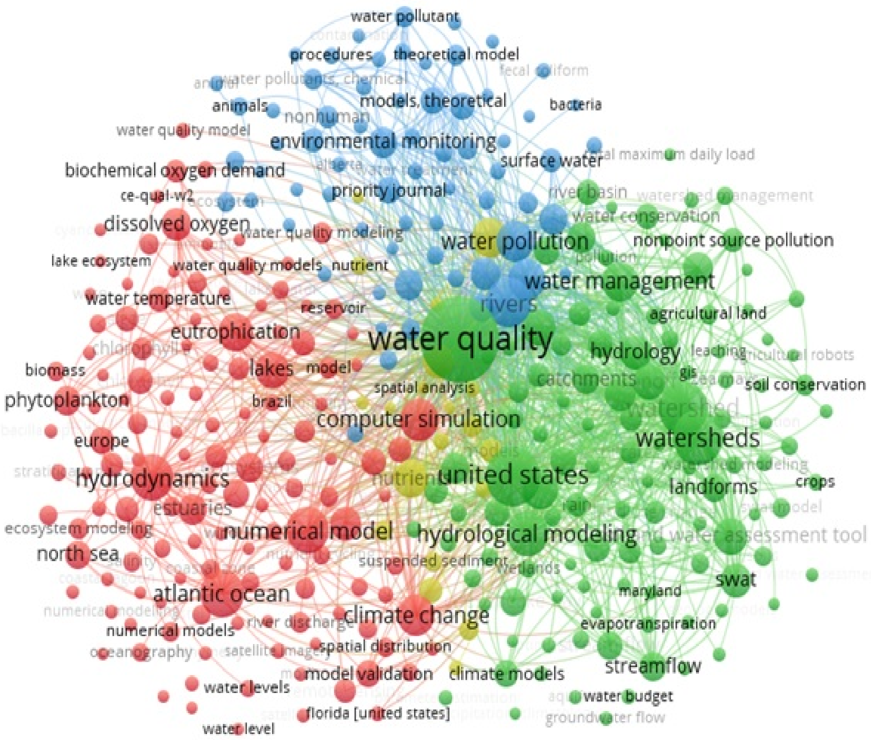

Figure 3.2: Clustering network on high frequency keywords, 1981 to 2021.

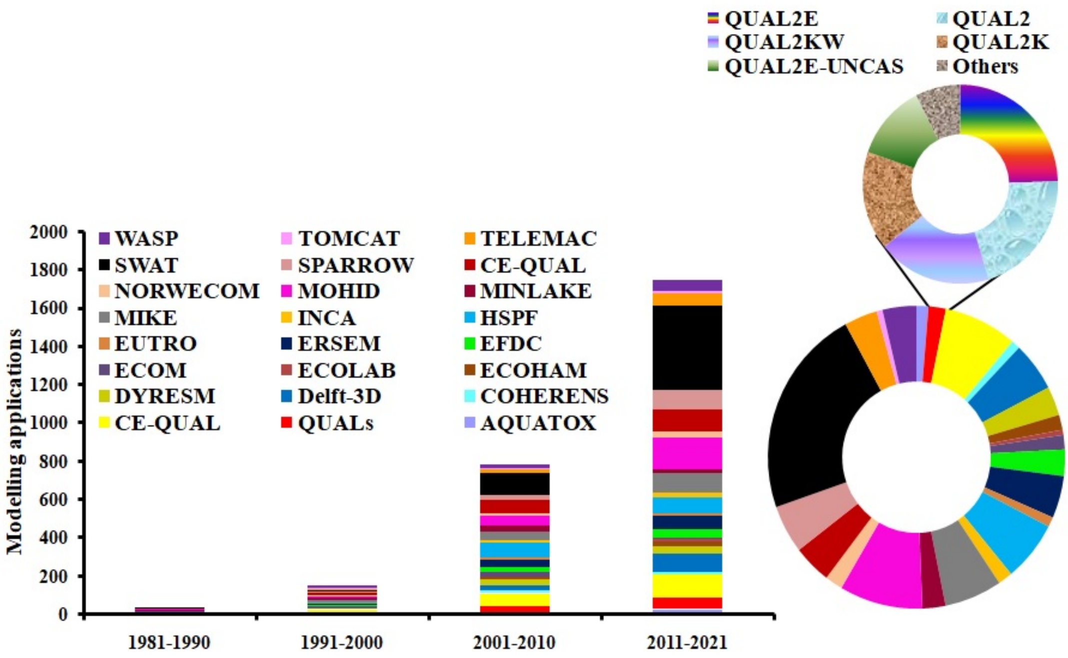

Figure 3.3: Number of publications per water quality models through 4-year time windows (left) and overall distribution (right), 1981–2021.

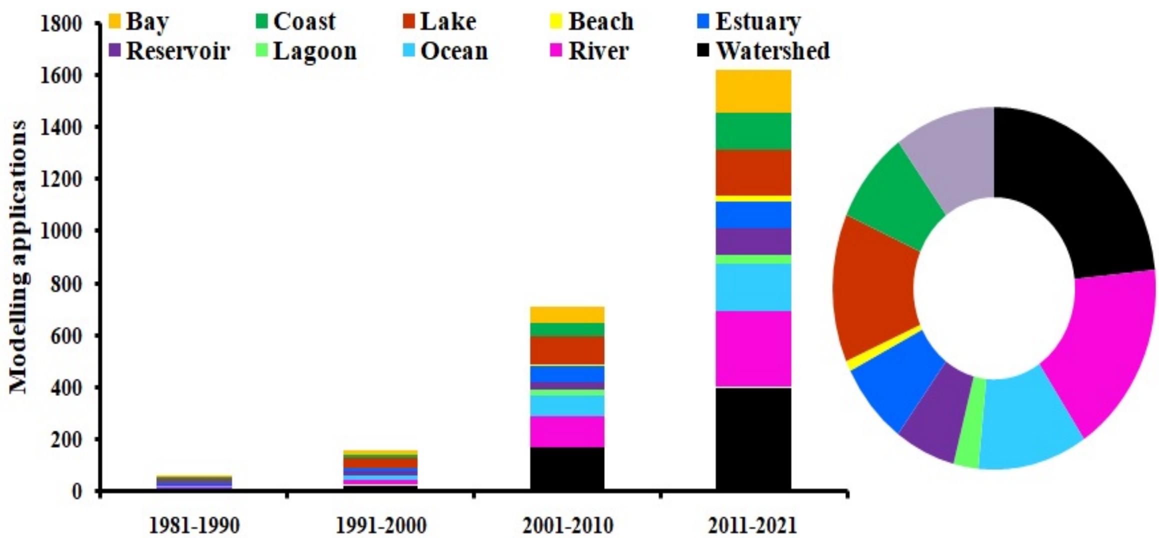

Figure 3.4: Number of publications per type of water body through 4-year time windows (left) and overall distribution (right), 1981–2021.

3.5.5 Geography of the modelling applications

Reference to the map in Figure 3.5 shows spread of the 2548 individual modelling record across different Atlantic countries. Two regions of high model applications could be observed in areas covering the Northwest and Northeast Atlantic. Whereas, few model applications can be observed in areas around the Southeast Atlantic. Statistically, United States of America (41.64%, 1061), Canada (13.81%, 332), and Portugal (7.57%, 183) had the greatest number of modelling applications. More than half of the SWAT (53.6%, 306) and CE-QUAL (60.3%, 123) applications have implemented in the United States of America; most of them addressed Maryland ecosystems (19.6%, 60 and 35.78%, 44, respectively). Over half of the MOHID applications have performed in Portugal (51.94%, 120). Nevertheless, the highest number of the HSPF applications have observed in United States of America (86.6%, 142), mostly in Virginia (36.62%, 52).

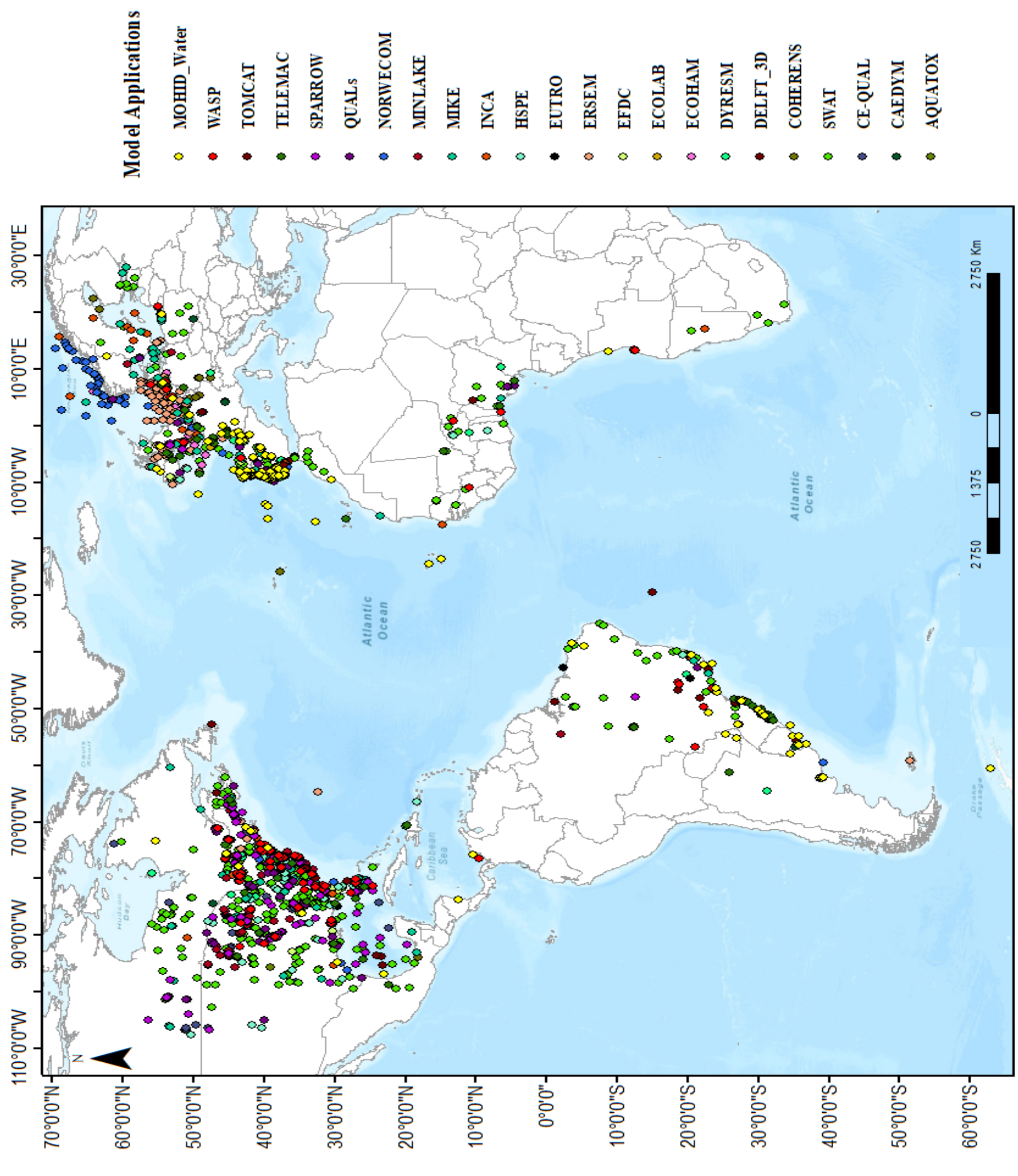

Figure 3.5: Geographical distribution of 2548 modelling applications, Atlantic, 1981–2021.

3.6 Discussion

The current review used science mapping approach as a means of exploring the emergence of literature on water quality modelling applications over the past four decades. The database contains 1952 documents (2548 individual modelling records) applying water quality models within the Atlantic area. Our database only considers studies exploring well-defined practical applications. Publications reporting technical descriptions or enhancements of models were not included.

Our interest mainly address the structure of existing research by analyzing the statistical characteristics of the literature (publications, journals, authors, and institutions) and the research hotspots. We described later the general aspects of the modelling applications. The present review are anticipated to benefit researchers who are implicated in the current research progress in water quality modelling applications within the Atlantic countries.

We believe that our database constitutes a practical source of structured literature information providing a new insight for further research direction. In the following, we highlight limitations of the review and provide interpretation of the main findings.

3.6.1 Limitations

Despite the insights provided from the review, the present work has some shortcomings. Key limitations merges from the review's delimitation to Scopus documentation. While Elsevier's Scopus bibliographic database offers widest scope of publications than the Thomson Reuters' Web of Science (WoF) [316], it provides less coverage of books, book chapters, theses, proceeding papers, and conference papers than journal articles. The use of co-citation analysis mitigated this shortcomings by capturing publications outside of our review database [450]. Therefore, future studies should incorporate more databases (e.g., Web of Science and Google Scholar) to gather vast amount of the existing literature.

3.6.2 Interpretation of the findings

3.6.2.1 Research trends and hotspots

The publication pattern on water quality modeling revealed a sharp rise of publications during the last 10-years. Several factors contributing to this growth including the great progress in computer technology, advancements of remote sensing algorithms, fast advance in remote monitoring of water quality, and progress in pre- and post-processing capabilities [103, 162]. Another possible contributing factors could be advances in understanding of processes influencing water quality, and advances in land modeling [103].

Science of the Total Environment, Ecological Modelling, Journal of the American Water Resources Association and Journal of Hydrology are the most influential journals. Considering the leading scholars, "Ramiro J. J. Neves" (Instituto Superior Técnico, Portugal), "Jeffrey G. Arnold" (USDA Agricultural Research Service, United States), and "Raghavan Srinivasan" (Blackland Research and Extension Center, United States) are the most productive authors. American authors have produced a substantial body of literature and have published the greatest number of English-language articles referring to water quality modelling. Plymouth Marine Laboratory, plymouth, MARETEC, Instituto superior técnico, universidade de lisboa, Virginia institute of marine science, college of william and mary, Gloucester Point and USDA-ARS Hydrology and Remote Sensing Laboratory, Beltsville are the most productive institutions but with limited collaboration across organizations.

Most of leading institutions are located in economically developed countries as also indicated by [492]. This reflected the advance in research experiences, scientific resources and data availability. From co-word analysis, research hotspots have been revealed, including “Water quality”, “United states”, “Watersheds”, “Rivers”, “Hydrological modeling”, “Water pollution”, “Phosphorus”, and “Numerical model”. These terms point out the combination between water quality issues and innovative technology advancements.

3.6.2.2 Evaluation of reviewed models

Among the 23 selected water quality models, a list of the most recurrent models with their key features including the acronyms, full model name, origin and model website, license agreement, operating system, dimensions, and model type are summarized in Table 3.7. Bref descriptions of the reviewed models with a consistent set of criteria: model system, conceptualization, model strengths, applicability, and their limitations are listed in Table 3.8 and 3.9. Detailed framework of some of these models (e.g., modelling equations, processes, and input data/parameters required) were investigated in other literature reviews (e.g., [22, 117, 119, 174, 300, 337, 405].

As indicated previously, a greatest number of models have been implemented over the last two decades. The applications have tended to range from simple water quality models with minimal number of processes to more complex models capable to consider a large number of interconnected variables. The application of simplified models has been frequently advocated when dealing with complex systems [481]. These models consisted on fewer and simpler relationships, with reduced complexity and calculation time, makes it ideally suited for larger-scale integrated modeling [233].

Models as QUAL2E, QUAL2K, WASP, MIKE-11 are usually applied for waste water control and water resources management but mainly remain restricted to small catchments due to the lengthy calculation time. Grey box was by far the most often used modelling approach to simulate water quality concentrations because of it capability to provide high accuracy with low computational cost [233]. Parsimonious models are considered as the simplest approach that fit the water quality modelling application has been argued that it’s a good middle ground between the variety of detailed physical models and the simpler black box models [289]. For instance, the appropriate modelling approach can be selected based mainly on the modelling goal and data available for the proper model application. Models as EFDC, WASP and MOHID Water have 1D, 2D or even 3D hydrodynamic components. Whereas, models like CAEDYM, DYRESM, ERSEM, ELCOM require biog ling with the hydrodynamic models to simulate the different components of the aquatic systems [339].

Some models may simulate steady flow (e.g., AQUATOX, QUALs, SPARROW, CE-QUAL-W2, HSPF, CAEDYM, MOHID Water, EFDC, MIKE-11). Other models, may simulate unsteady flow (e.g., Delft3D-ECO), steady flow (e.g., ERSEM) or both steady and unsteady flow (e.g., WASP). Most of them have windows based graphical interface except some models such as ERSEM, which is written in the Fortran programming language and runs on Linux or Unix environment. Concidering the process description, models like QUALs, WASP, AQUATOX are mechanistic that can use physical, biological and hydrometeorological data to simulate contaminant fate contemporaneously [440],while other models such as SWAT is semi-empirical. Moreover, models like WASP, MIKE-11, QUALs, EFDC, CAEDYM, ERSEM are deterministic. Other models, such as SIMCAT, TOMCAT are deterministic and stochastic depending upon the data type. Model complexity and data requirements may also be a decision point among water quality models since some models such as AQUATOX, WASP and ERSEM have a high complex structure. Other models like QUAl2KW, CEQUAL-W2, SWAT have intermediate level of complexity. In contrast, SPARROW was found to be a simplistic versatile model, where the determinant of interest is simulated as being either diminishing by a first-order decay (i.e. BOD and nitrate) or conservative such as chloride. Looking to data requirements, models such as AQUATOX, CAEDYM, WASP and QUAl2KW can be considered as the most data extensive models. Conversely, models like AQUATOX, WASP, QUAl2KW, CAEDYM and EFDC are able to simulate maximum number of water quality parameters.

The amount and quality of the processes involved in water quality assessment of aquatic systems may also be a constraint to select the relevant model. Models like WASP, MIKE-11, CAEDYM, EFDC, SPARROW have the ability of simulating heavy metals. WASP are SPARROW have been used more frequently to model toxicant dynamics, they have an advantage of simulating synthetic organics, conservative tracer and pesticides as well.

Other features such as open-source code, input data, modelling goal, type of water body modeled, model outputs, capabilities, model strengths and limitations among other factors, may also affect the model selection and have been summarized in Table 3.8 and 3.9.

Table 3.7: Summary of the most recurrent water quality models, Atlantic, 1981 to 2021.

	Full model name	Origin and model website	License agreement	Operating System	Dimensions /Types	Modeling approach	Application considerations	Applicability	Documentation and Supporting Information
AQUATOX	Modeling environmental fate and ecological effects in aquatic ecosystems	US EPA [1],	Open source	MS Windows XP, 7, 8, or 10	1-D, 2-D, or 3-D, Dynamic state [337] Steady flow [405]	ADE, using 4th and 5th order, Runge-Kutta integration routines [405]	Limited training/ Public Domain [337]	Reservoirs, linked reservoir segments, vertically stratified lakes, streams, small rivers, linked river segments, estuaries, ponds, coastal water and pond enclosures [118, 470, 512])	The details of AQUATOX can be found in the technical reference guide of the model [344] [2]
CAEDYM	Computational Aquatic Ecosystem Dynamics Model	[3]	Open source		0-D, Steady state, Dynamic [339]	ODEs were calculated using the first order Euler approximation [106]	Public Domain	Lakes, reservoirs, wetlands, rivers, marshes, estuaries and coastal ocean	The user manual was provided by [203]
CE-QUAL-W2	Corps of Engineers 2-D Hydrodynamic and Water Quality Model	US Army Corps of Engineers [4]	Open source	Windows, OS-X, Linux	2-D, Steady state, Dynamic [189, 490].	ADE, unequal river reaches, river branches [300]	Public Domain [438]	Stratified water bodies, narrow/shallow rivers, estuaries, lakes, reservoirs, and river basins [308]	The user manual was provided by [112]. Active user forum: [5]
Delft3D-ECO		Delft Hydraulics, Holanda [6]	Open source	Windows 32/64-bit platforms, Linux	3-D, Unsteady water flow, dynamic [275]	Finite difference approach with an ADI numerical scheme [142]	Public Domain	River, estuarine, lake, lagoon, and coastal areas [471]	The details of the EFDC model were documented by [416]

[1] https://www.epa.gov/ceam/aquatox. [2] http://www.epa.gov/waterscience/models/aquatox/download.html
[3] https://dyresm-caedym-release-package.software.informer.com/4.0/.
[4] http://cee.pdx.edu/w2/. [5] https://w2forum.cee.pdx.edu/. [6] https://www.deltares.nl/en/software/delft3d-4-suite/

Table 3.7 (continued)

EFDC	Environmental Fluid Dynamics Code	US EPA [7]	Open source	Windows 98, NT, 2000, XP	3-D, Steady-state, Dynamic [179]	ADE, explicit finite difference method [235]	Public Domain [217]	Lakes, reservoirs, rivers, oceans, estuaries, wetlands, and near-shore coastal areas [364]	The details of the EFDC model were documented by [194] and [121]
ERSEM	European Regional Seas Ecosystem Mode	[8]	Open source	Linux, Hector	1-D, Quasi-steady state [447]	Differential equation [239]	Public Domain	Estuarie, shelf seas, oceans	[9] [10]
HSPF	Hydrological Simulation Program-Fortran	US EPA [11]	Open source	Windows XP, Vista, Windows 7, or Windows 8	1-D, Steady state, Dynamic [488]	Mass balance equation [98]. The first-order kinetic approach [223]	Public Domain [453]	Channels, estuaries, irrigation systems, rivers, and other water bodies [397]	User manuals: [12], Data formatting tools: [13]
MIKE-11	Model based and Incremental Knowledge Engineering	Danish Hydraulic Institute (DHI) [14]	Not open source	Windows, Linux and Wine	1-D, Steady state, Dynamic [337]	ADE, implicit finite difference scheme for solving Saint-Venant equation [37]	Substantial training/ Significant Cost [337]	Lagoons, estuaries, reservoirs, lakes	[15]
MOHID Water	Modelo Hidrodinâmico	Instituto Superior Técnico, lisboa [16]	Open source	Windows 2000, XP or Vista, Linux, Solaris, Mac, etc.	3-D, Steady state, Dynamic [165]	ADE, Regular grid, finite elements [300]	Public Domain [164]	Lagoons, estuaries, reservoirs, watersheds, inland waters, oceans and coastal areas [379]	[17]

[7] https://www.epa.gov/ceam/environmental-fluid-dynamics-code-efdc. [8] https://ersem.com. [9] https://www.pml.ac.uk/Modelling_at_PML/Models/ERSEM. [10] https://ersem.readthedocs.io/en/latest/. [11] https://water.usgs.gov/software/HSPF/. [12] https://water.usgs.gov/software/HSPF/. [13] https://www.epa.gov/exposure-assessment-models/hspf-data-formatting-tool-desktop-hdft. [14] http://www.mikebydhi.com. [15] https://manuals.mikepoweredbydhi.help/2017/MIKE_11.htm. [16] http://www.mohid.com/pages/models/mohidwater/mohid_water_home.shtml. [17] http://wiki.mohid.com/index.php?title=Mohid_Bibliography.

Table 3.7 (continued)

QUALs	QUAL2K	Enhanced Stream Water Quality Model	US EPA [18]	Open source	Windows ME, 2000, XP	1-D, Steady flow [41]	ADE, unequal river reaches [41]	Limited training Public Domain [73, 232]	Lakes, river, stratified reservoirs, complex flows and stratified estuaries [117]	[19]
	Qual2KW		US EPA [20]			1D, Steady flow [225]	ADE, unequal river reaches [225]	Public Domain [225]		
	QUAL2E		US EPA			1-D, Steady state/Dynamic [131]	ADE, equal river reaches [337]	Limited training/ Public Domain [337]		
	QUAL2EU		US EPA [21]			1D, steady state/dynamic [374].	ADE, equal river reaches [225]	Public Domain [225]		
SPARROW		Spatially Referenced Regression Model on Watershed Attributes	[22]	Open source	Windows 95, NT	2-D, Steady state [311]	Explicit mass-balance modeling technique, non-linear regression equations [469]	Substantial training [62]	watersheds, rivers basins, baies, estuaries, reservoirs, lakes, karst basin, and coastal seas [129, 477]	[23]
SWAT		Soil Water Assessment Tools	USDA-ARS [24]	Open source	SWAT+ 2.0.4 released 15 April 2021. Windows, Linux, and MacOS.	2-D, Quasi-Dynamic [268]	Water balance equation [326]	Moderate training/ Public Domain [318]	All kinds of water bodies: estuaries, lakes, rivers, etc	[25] [26] [27]
TOMCAT		Temporal/ Overall Model for CATchments	Environment Agency, Rotherham, UK [28]		Windows, Unix, Linux	1-D, Steady-state (time-invariant) [225]	CSTR [225]	Public Domain	All Thames Water [225]	[29] [65]
WASP		Water quality Analysis and Simulation Program	US EPA [30] [31]	Open source	Windows, Mac OSX, Linux Ubuntu	1-D, 2-D, or 3-D, Steady state, Dynamic [211]	ADE, dynamic compartmental [264]	Substantial training/ Public Domain [337]	Rivers, lakes, estuaries, ponds, coastal wetlands, streams, and reservoirs	[32]

US EPA : United States Environmental Protection Agency's, CSTR: continually stirred tank reactor in series, ADI : alternating direction implicit, ADE : advection–dispersion equation, USDA-ARS : U.S. Department of Agriculture- Agricultural Research Service, ODEs : ordinary differential equations.

[18] https://www.qual2k.com/. [19] http://www.ecy.wa.gov/programs/eap/models. [20] http://www.ecy.wa.gov/programs/eap/models.html.
[21] https://www.epa.gov/ceam. [22] https://www.usgs.gov/media/images/sparrow-model. [23] https://water.usgs.gov/nawqa/sparrow/#.
[24] http://swat.tamu.edu/ [25] http://swat.tamu.edu/documentation/. [26] https://www.card.iastate.edu/swat_articles.
[27] https://swat.tamu.edu/workshops/instructional-videos. [28] http://homepages.see.leeds.ac.uk/~lecmc/slimcat.html.
[29] https://tomcat.apache.org/tomcat-3.3-doc/tomcat-ug.html.
[30] https://www.epa.gov/ceam/water-quality-analysis-simulation-program-wasp.
[31] http://www.epa.gov/athens/wwqtsc/html/wasp.html. [32] https://www.epa.gov/ceam/wasp-model-tutorials.

Table 3.8: Summary of the most recurrent water quality models on the basis of their model systems and coneptualization, Atlantic.

	Brief description	Model System	Conceptualization
AQUATOX	AQUATOX [226] is a process-based or mechanistic model [345]. It is intended to be a bioenergetic model of the combined fate and impacts of nutrients, organic chemicals and suspended and bedded sediments in aquatic ecosystems. Algorithms from CLEAN model [345] and toxic fate model PEST [346] are combined with an algorithms from ecotoxicological studies borrowed from the FGETS model [423].	AQUATOX simulates various pollutants in a well-mixed and stratified systems [238]. The water quality processes was solved using the fourth and fifth order Runge-Kutta integration method [405]. The model uses differential equations to simulate the changes of the different state variables.	The model can simulates the physical environment (e.g., flow, temperature, light, and sediment), chemical environment (e.g., pH, DO, COD, TSS, and nutrients including NH_4, NO_3, total soluble P) [15], organic toxic chemicals [515]. The food web consists of plants : Algae (diatoms flagellate, blue–greens, greens, other algae), macrophytes, periphyton and submerged aquatic vegetation; zooplankton and zoobenthos; Invertebrates : ders, clams grazers, snails, bottom and suspended sediment feeders, bacteria, fungi and predatory invertebrates ; Fish : Bottom fish, foraging fish, and game fish [496].
CAEDYM	CAEDYM [203] consists of a set of process-based partial differential equations to simulate time-varying fluxes that regulate ecological variables considering (including nutrient concentrations, phytoplankton biomass,...), accounting for processes such as nutrient cycling, oxygen dynamics, sediment–water interactions, primary and secondary production [220]. It has been applied to numerous freshwater and saline systems for investigating the effects of nutrient loading, sediment transport, climate change, microbial pollution, eutrophication, and anthropogenic influences on biological communities [67].	The biogeochemical balance equations are integrated with CAEDYM using a first order Euler approximation [106]. The biogeochemical variables are explicitly pursued to assure mass balance, nevertheless of whether static/dynamic internal state variables are simulated [383]. The partial differential equations describing the variation of the biogeochimical variables involved rate constants, changing in the model in response to various environmental variables (e.g. temperature, salinity, pH, DO, etc.) [77].	The biogeochemical structure described by CAEDYM can be configured according to the purpose of the model and the availability of data [220]. Overall, the model can simulates C, N, P, Si and DO cycles, BOD, ISS, SOD along with the biomass and metabolic processes of phytoplankton (e.g. cyanobacteria, diatoms, dinoflagellates, chlorophytes and cryptophytes), and zooplankton (e.g.copepods, cladocerans, copepodites, calanoid, rotifers and ciliates). The model can also simulates macrophytes, bacteria, the heterotrophic microbial loop components, fish, jellyfish and benthic invertebrates [451, 515].
CE-QUAL-W2	CE-QUAL-W2 [149] is a 2-D, longitudinal/vertical, hydrodynamic and water quality model. It has been extensively used in modeling hydrodynamic and biogeochemical processes of diverse water bodies worldwide [308]. It can be also used for various artificial outflows (withdrawals, spillways and pumps) [118, 403]. The boundary conditions include inflow (water temperature, discharge, nutrient concentrations), outflow discharge, and the meteorological data [308].	CE-QUAL-W2 employs a numerical scheme for direct linking of hydrodynamic and water quality variables [506]. It is based relies on the finite-difference scheme to the six laterally averaged equations of fluid motion involving momentums, hydrostatic pressure, continuity, surface wave equation, constituent concentration and transport, and temperature/density [216]. The model uses Boussinesq and hydrostatic approximations to write the different equations [111]. The model uses a state-of-the-art numerical approche (QUICKEST) to solve the advection–dispersion equations [117]. The mass balance equations calculate the fate and transport of variables based on their kinetic reaction rates presented in source and sink terms [506]. The source and sink terms depict the mass rates of variable change as a result of kinetic reactions [506].	The model is discretized into grid cells in the vertical and longitudinal dimensions. For each model cell, CE-QUAL-W2 can simulates the water temperature, water level, water velocity, flow, water density, circulation patterns and many water quality constituents including pH, DO, ISS, alkalinity, CBOD, BOD5, C cycle, N cycle, P cycle, S cycle, total iron, labile/refractory and particulate/ dissolved organic matter, conservative tracer, phytoplankton, macrophytes, epiphyte/periphyton, zooplankton and bacteria [308, 388, 515].

Table 3.8 (continued)

Delft3D-ECO	Delft3D-ECO is a 3D integrated water quality process-based model intended to simulate the processes of water-sediment interactions, water quality, eutrophication, and primary production [22]. The model been widely used in invistigating nutrient cycles, harmful algal bloom dynamics, ecological functioning of aquatic systems [471].	Delft3D-ECO incorporates the algae model BLOOM, which uses a linear programming method to simulate algal composition [22, 257]. The model explicitly simulates water quality processes assuming that the state variables distribution derived by extraction/addition of mass, diffusive transport, and adjective-dispersive transport [22].	Delft3D-ECO simulates the concentration patterns and mass flows of nutrients (C, N, P and Si cycles), salinity, DO, organic matter, sediment, more then eight phytoplankton groups (including green algae, diatoms and six groups of cyanobacteria), coliform bacteria, E.coli, Enterococci [471]. Ecophysiological processes (e.g. respiration, growth, mortality, excretion, grazing, sedimentation, vertical migration etc.) are simulated using the algae processes BLOOM in Delft3D-ECO model [195]
EFDC	EFDC [194] is a 3-D hydrodynamic and water quality model. It includes hydrodynamics, water quality, toxic contaminant, and sediment transport modules. The model is able to simulates 3-D biogeochemical processes, transport, and flow in surface aquatic systems [364]. The model can be used to simulates benthic and floating macroalgae, eutrophication, the interactions between the watershed load and nutrient flux, pollution loads, transport problems [117].	The EFDC model is implemented using momentum, continuity, heat balance and salt balance equations with hydrostatic and Boussinesq assumptions [218]. Based on hydrostatic and Boussinesq approximations, EFDC solves the 3-D primitive equations of motion for turbulent flow using a combination of finite difference and finite volume approaches in a horizontal curvilinear and vertical sigma-stretched coordinate system [347]. The model solves the Eulerian transport equations for temperature, salinity, and other variables using a second-order, mass conservation, fractional step solution. Mass balance equation consider the physical transport and kinetic changes of the water quality state variable [44]. Mass balance equation for physical transport reflect the changes in the flow velocities, turbulent diffusivities, the concentration of a water quality variable, and sink/source [44].	The water quality module solves mass balance equations for 22 state variables, including DO, C, N, P and Si cycles, 6 groups of algae (including cyanobacteria, diatoms, green algae), and fecal coliform bacteria [99, 214]. The algae could be simulated in terms of algal growth, setting, predation, death and external load [182]. Sediment transport module is driven by the net settling of POC, POP, PON, and SU that are computed by the eutrophication model. It can simulates the resulting sediment flux, the depositional flux of POM, the diagenesis of POM and the associated production of inorganic nutrients [99]
ERSEM	ERSEM [47] is a biomass and functional group-based biogeochemical model depicting the cycling of carbon and nutrients within the lower trophic level of the marine system. ERSEM is well suitable to simulate ocean carbon fluxes [252].	The ERSEM model uses a functional group approach to simulate lower-trophic level marine food web. Each functional group involved a number of components (C, N, P, Si), that are explicitly simulated using differential equations [169]. The model uses advection dispersion from GOTM to simulate the transport of nutrients [243].	The ERSEM state variables include nutrients (C, N, P, Si), DO, CO2, carbonate, organic detritus, and living organisms. Living organisms include four functional groups of phytoplankton (diatoms, pico-, nano-, and micrphytoplankton,), three zooplankton groups (heterotrophic nanoflagellates, mic- and mesozooplankton), and heterotrophic bacteria [410] .The biomass is simulated in terms of chlorophyll, C, N, P, and Si for diatoms [411]. The model considers three layers of sediment: the oxic, denitrification and anoxic layer, with total thickness of 30 cm [22].

Table 3.8 (continued)

HSPF	The HSPF is a continuous simulation, semi-distributed, lumped parameter that simulates watershed hydrology and water quality [103]. It consists of three main modules: stream/reach/reservoirs (RCHRES), pervious land module (PERLND), impervious land module (IMPLND) [250]. 8 The model has successfully been applied on various watersheds to simulate sediment transport, peak and low flows, nutrient and toxic organic pollutant concentrations [250].	HSPF simulates the flow and pollutant transport from watersheds to receiving streams. Terms of volatilization, oxidation, sorption, hydrolysis, photolysis, and biodegradation are exploited to depict the transmission and reaction processes [223]. The mass balance equations are used to simulate the transport and the fate of water quality components [259]. Interflow is computed using a linear relation between lateral flow based on the interflow-recession coefficient (IRC) and the conceptual interflow-storage volume [101]. The first-order kinetic approach is adopted to simulate sorption [223]. The linear storage approach is used to calculate baseflow [101]. The lumped parameter model is used to simulated water quality components [223, 408].	RCHERS module includes water temperature, pH, alkalinity, DO, inorganic C, organic and inorganic N and P, planktons, and their interactions with atmosphere and sediment. PERLND module includes water budget, sediment production and removal, snow melt, phosphorous and nitrogen cycles, and pesticide behavior. IMPLND module includes pollutant wash-off and overland flow [250].
MIKE-11	MIKE-11 [140] is a 1-D deterministic model that can be implemented for water resources management. It consists of a set of modules (hydrodynamic, rainfall runoff, sediment transport, advection-dispersion, eutrophication, and water quality) that can be used as stand-alone simulators or in combination [144].	MIKE-11 uses finite difference numerical approach to solve 1-D equations governing sediment transport, dynamic flows and water quality [210]. The hydrodynamic module simulates explicitly dynamic flows using ADE. The advection–dispersion module simulates the transport of solutes using conservation of mass equation [464].	The mass balances for the state variables included in the water quality module are computed using a rational extrapolation approach in an integrated two-step method with the advection–dispersion module [42]. The water quality module includes DO, C, P and N cycles, BOD, OD, phytoplankton, zooplankton and detritus, sediments, coliform. Other water quality modules include heavy metals, eutrophication, nutrient transport, iron oxidation, cohesive and non-cohesive sediment [337].
QUALs	USEPA, 1985 released a series of QUAL models including QUAL2E, QUAL2EU, QUAL2E-UNCAS, QUAL2K, and QUAL2Kw. They are 1-D steady-state water quality models developed in the microsoft windows operating system [117]. QUALs are designed to be the general dynamic models for water quality assessment. They are widely used for river simulations [117].	QUALs uses the implicit finite difference approach to solve the differential equations [337]. Numerical solution is described with ADE, that was derived from mass balance approach [337]. As 1-D steady-state models, heat, hydrological and material balances are affected by water temperature, flow and concentrations for headwater [281].	QUALs can simulate a wide variety of constituents including temperature, pH, alkalinity, ISS, DO, SOD, slowly and fast-reacting CBOD, N and P cycles, phytoplankton, detritus, chlorophyll, coliform bacteria, algae, periphyton and pathogenic bacteria [281].
SPARROW	SPARROW [400] is a hybrid statistical and process-based model, that has been extensively used to investigate diffuse pollutant sources and transport in surface waters [469].	The SPARROW modeling approach adopts a nonlinear least squares regression restrained by mass-balance to describe the relationships between spatially referenced watershed and streamflow and channel features [469]. The nonlinear regression model involves transport processes, non-conservative transport processes, surface-water flow paths, and mass-balance constraints on model losses, inputs, and outputs [504].	The model accounts for source and sink processes over different timescales. Source processes, considere delivery rates from different catchments, export coefficients and attenuation coefficients [477].

Table 3.8 (continued)

	The model performs well in analyzing changes in nutrients loading, environmental factors, and assessing water quality [129].	The model incorporates a fully integrated streamflow network that considers water resource diversions, storage, inflows, and human impact [311].	The model applications mainly focus on either total carbon, total nitrogen or total phosphorus loadings, suspended sediment and Escherichia coli [401, 477]. Transport module can simulates the dynamic of the salinity, temperature, drifter and near field. Variables such as velocity, depth, and mixing are coupled to the water quality, sediment transport, and toxic contaminant modules [323].
SWAT	SWAT [36] is a continuous-time, physically-based, semi-distributed, process-based river basin model [469]. It was implemented to assess the nonpoint source pollution risk and management effects on water quality [35, 491].	SWAT uses water balance equation [143] to simulate the hydrological cycle. A SWAT based coupled modeling system has been emerged as one of the most widely used system worldwide to evaluate water quantity and quality. It can simulate, hydrological processes, sediment erosion, plants, nutrients, chemical yields, pesticide, bacteria, pathogens, and other variables [117].	SWAT incorporates three sub-modules: hydrologic process, the pollution load and the soil erosion [7, 491]. Hydrologic routines within SWAT model account for vadose zone processes (i.e., evaporation, plant uptake, percolationto lower layers, lateral flows and infiltration), groundwater flows, snowfall and mel [117]. The model can simulates dissolved oxygen, CBOD, nutrients, Phytoplankton, sediments and trace chemicals [515].
TOMCAT	The TOMCAT model [65] is a stochastic, deterministic model that describes the distributions of flow and concentrations of key determinands (temperature, DO, BOD, ammonia, and DO) assuming Monte Carlo approach and CSTR method [300]. It was implemented to support in the process of setting effluent quality standards at different stations of the River Thames and its tributaries (UK water) within the objective of improving water quality assessments [225, 374].	TOMCAT's river system consider several events witch are defined at the rivers, abstractions, confluences, monitoring sites, and effluent discharges [448]. Three fundamental processes connect these events: internal alterations and flow from groundwater and runoff, input, and flow mixing mass balance [119, 448]. The flows and concentrations of determinands are simulated using mass balance approach that does not represent ADE [300]. Chemical processes are simulated using a first-order decay equation, taking into account in-stream removal [229]. DO is simuated using the Streeter Phelps equation [119, 229].	TOMCAT structure is outlined by the mean monthly air temperatures, the number of sub-catchments to be investigated, the number of shots, and the number of seasons [119]. The model run required two types of input data: physical parameters defining as rate constants; flow and quality data supplied as input to the simulating process [448]. Boundary conditions including flow and water quality constituents of reach and runoff are provided as single/seasonal distributions [374]. Various parameters are provided for each user-defined reach, including: reach length, depth, mean cross-sectional area, scale factor for runoff, catchment number for diffuse runoff, thermal equilibrium rate constant, oxygen exchange rate and decay rate and concentration of NH4 and BOD [225, 374].
WASP	WASP [20] is a 3D deterministic model furnishing dynamic compartment-modeling for water body. It consists of three kinetic submodels (DYNHYD for hydrodynamics, EUTRO for water quality, and TOXI for the transport of suspended sediments and pollutants). WASP7 has additional modules as advanced EUTRO, HEAT and MERCURY [405].	WASP is based on the concept of flexible compartmentalization. It integrates the mass balance equation over a completely mixed finite segment using finite differences equation [482]. The model uses advection dispersion and kinetic formulations to simulate the processes of transport, transformation, and loading [280]. The transport information include internal stream transport algorithms and external hydraulic / hydrodynamic models using linkage options [482]. The Hydrodynamic Program (DYNHYD), Environmental Fluid Dynamics Code (EFDC) and a kinematic wave model were incorporated directly into the WASP model [482, 483].	WASP includes DO, P , N and Si cycles, CBOD, DOC, particulate detritus, phytoplankton and periphyton (bottom algae), coliform bacteria, solute chemicals, nanochemicals, inorganic solids, heavy metals, mercury, pesticides, conservative tracer, cohesive and non-cohesive sediment sediments, sediment diagenesis [17]. The linkage with hydrodynamic and sediment transport models provide flows, volumes, depths, velocities, sediment fluxes, temperature and salinity [482]

US EPA : United States Environmental Protection Agency's, CSTR: continually stirred tank reactor in series, ADI : alternating direction implicit, ADE : advection–dispersion equation, USDA-ARS : U.S. Department of Agriculture- Agricultural Research Service, ODEs : ordinary differential equations.

Table 3.9: Summary of the most recurrent water quality models on the basis of their model strengths and limitations, Atlantic.

	Strengths	Limitations
AQUATOX	- AQUATOX is an integral part of the BASINS modeling system and can be coupled to the other watershed models as HSPF and SWAT [315]. - It has a flexible structure that investigates a variety of environmental stressors and their effects on aquatic systems [150]. - It simulates the direct and indirect impacts on the resident organisms [150]. - The model includes nominal range sensitivity analysis, Latin hypercube sampling strategies for uncertainty analysis and time-varying process analysis [476].	-The model requires considerable data, the interactions between state variables are not completely understood [118, 344]. -Surrogate data provides significant uncertainty in food-web interactions and simulation outputs [185] and can not coupled with the hydrodynamic models [150]. -The model does not include the stochasticity of taxa abundance and diversity [186]. -The limitations of implementing AQUATOX model for prospective risk assessment incorporate the deficiency of impact indicators and standard ecological scenarios [270]. -The model has been limited to pesticides in artificial streams [386], metals and luxury uptake [405]. -The deficiency of single-species toxicity and aquatic life history data required for food web parameterization [287]. -The linked segments have an indistinguishable set of state variables. The links between them are supposed to be either uni-directional or bidirectional [405]. -Algal bioenergetics does not account for internal nutrients [337, 405]. -Non-living particulate organic material and decomposers are simulated together under the term of detritus [118, 344].
CAEDYM	-It has been extensively used as a water quality management tool [125]. -It has a flexible ecological configuration that canconfigured with various levels of complexity to achieve model purpose [22, 380]. -It provides the option of selecting the 'components' to model, and solving for the equilibrium speciation of the solution using optional gas/mineral phases incorporated [319]. -It has faster model run time [380].	-CAEDYM can not simulate the transport of variables, it has to be coupled with an appropriate hydrodynamics model (e.g. 1D DYRESM, 2D DYRIM, 2D DIVAST, 3D ELCOM) [339, 451]. -The model is not suited to examining geochemistry [204, 319]. -CAEDYM necessitates an the external hydrodynamic vecteur that provide information on water temperature, salinity and velocity [451]. -It has a complex biogeochemical structure [125]. -The model does not include toxic components, metals and sediment compartment [515].
CE-QUAL-W2	-The model has earned a reputation for being the preferred model providing a robust predictive modeling code [498, 514]. -The model may be coupled with BASINS modeling system (including QUAL2E, HSPF and SWAT) [117, 267]. -The model assumes particle swarm optimization (PSO) when assessing eutrophication process to maximize a river–reservoir system's trash loading capacity [118, 298]. -It is well-suited to investigate the deep and narrow waterbodies where lateral fluctuation in hydrodynamic and water quality process is negligible [137]. - It is well-suited for predominantly longitudinal variations (i.e. narrow and long reservoirs) [102, 112]	-The model implementation is a complex and time consuming task [150]. -The laterally averaged equations of the hydrodynamics and transport equations make the variations in water temperatures, velocities, and water constituent concentrations insignificant, that may be unsuitable for large waterbodies [118]. -The hydrostatic assumption is not satisfied in all fluid motion scenarios. -The laterally averaged of complete homogeneity along the lateral direction is not met in broad rivers [30]. -The equations describing the algal processes are oversimplified, compromising the model accuracy to simulates the algal growth [117, 388]. -The model doest not incorporates Zooplankton, SOD and metals [515].
Delft3D-ECO	-Delft3D-ECO modelling approach has provided a broad range of application has provided a broad range of application Large applications in tropical, temperate, oligotrophic, stratified, fresh, and brackish water. -It incorporates biological, physical, chemical, processes [471]. It is able to integrate outcomes from diverse processes with different temporal resolutions [22].	-Unsatisfactory representation of water-sediment interaction processes [22]. Inadequate simulation of phytoplankton mortality rates in tropical waters [195]. -The model does not incorporates microbial loop [471]. -It is not well-suited for aquatic systems of small depths, periodic anoxia and extensive tidal flats [22]. -It is not well-suited for complex phytoplankton kinetics [22].
EFDC	- The prediction ability of the model makes them a widely used realistic 3-D ecological model of water systems [507]. - It is considered one of the models recommended by USEPA [507]. -EFDC model is proved to be a reliable tool for water source protection and water quality management [22]. -The model accurately reproduced the time-space distribution of water quality indicators [22, 507]). - It is to model hydraulic control structures, drying and wetting and wave induced currents.	-There are no advanced module of zooplankton in the EFDC model [219]. -The model has a large spatial resolution (approximately 1,000 m long). It is not suitable for appropriate simulation of any occurrence with a spatial scale smaller than the cell width and length. Such modeling practices necessitate smaller scales [159]. -The model does not include Zooplankton and detritus compartments [515].

Table 3.9 (continued)

ERSEM	-The model can be coupled to many hydrodynamic models in 1-D or 3-D, to provide information on water temperature, salinity, general circulation... [22]. -It provides a pelagic-benthic coupling [227].- The model incorporates a large number of processes that significantly affect the ecosystem dynamics.-It rovides a better simulation of the effect of nutrient limitation on cells [59].	-The model has one of the most complex lower trophic level modelling structure [59]. -It is not well-suited for large ecosystems [22].
ERSEM	-HSPF typify the model categories that have been of main interest to the water quality assessment [103]. -It has a flexible modeling framework that can simulate hydrologic and associated water quality processes on diverse regional scales and land use types [250]. -The model has the ability to adapt to a wide variety of watershed conditions, including a wide range of surface water and groundwater issues at numerous spatiotemporal scales [499]. -Its flexibility, simplicity rendered HSPF suitable for application in large watershed for long time periods [493]. -The model has a special empirical processes for assessing runoff founded on the Stanford Watershed Model [367]. Based on a robust data and sophisticated hydrological model, the model performed adequately low flow and peak flow at different time scales [278]. -It explicitly integrates soil contaminant runoff processes considering in-stream hydraulic and sediment–chemical interactions [306].	-The HSPF model impediments incorporate a complex biogeochemical structure [117] and requires a high level of expertise and experience to select relevant parameters [499]. -The model accuracy depends upon “good quality” meteorological data [150]. -HSPF is not well-suited to directly simulate conveyance systems nor the variety of stormwater control measures (SCMs) [493]. -It is not suited to simulate monthly sediment yield and streamflow in extreme weather conditions [499]. -HSPF doest not incorporates the spatial distribution of watersheds [9]. -It is limited to 1-D flow and well-mixed reservoirs, rivers [150]. -It requires extensive calibration [150]. -The use of storage-based equation or the nonlinear flows prevent the adequate simulation the flood waves or the intense single-event storm [499]. - Relies on empirical approach to depict many physical processes [9]. -One of HSPF’s major flaws is the absence of explicit SCM representation [314, 493]. - Require a relatively large number of parameters in the model calibration [306].
MIKE-11	-The model has earned a reputation as the most well known 1-D numerical modelling of the pollutant transport in the river environments [309]. -It is well-suited to various levels of water quality complexity and can deal with complex flow patterns such as loops backflows [119]. -It is well-suited to investigate the effect of catchment inflow on the physical and biological processes [437]. -The model incorporates parameter estimation routines [119]. -Given a limited dataset, the model can be calibrated using a variety of parameter combinations, any of these could be the most accurate representation of the in-stream dynamics [119].	-Mike-11 is considered as a complex model and the accuracy of the outputs depends upon “good quality” flow, a comprehensive discretization of the watershed as well as water quality time series [229]. -The model requires a large amounts of data for model operation and calibration [337, 448]. -It does not incorporate wind effects and urban drainage [376]. -It does not consider secondary currents and neglects bank erosion processes [306]. -It is seldom used to simulate chemical concentrations at a catchment scale [229].
MOHID Water	-The model robustness, reliability and the diversity of vertical coordinates make MOHID one of the most used models [168]. -It allows the implementation a tree of one-way nested models with no restrictions on the number of nesting domains; That provides efficient overlapping of different scales for investigating of local processes [251]. -It provides a flexible parameterization that can be configured with different levels of trophic complexity [301]. -It is suited for simulating heterotrophic bacteria in the water column [22]	-The model does not incorporate metals cycle into biogeochemical cycle [22, 515].
QUALs	-QUALs has been widely used for the environmental management of rivers [174]. -Easy accessibility, comprehensive formulations, frequent upgrades [405]. -It is well-suited to dendritic rivers and non-point source pollution [150]. -TQUAL2K has earned a reputation for being a powerful tool in the comparative assessment of potential water quality enhancement strategies [96, 502]. -QUAL2E has been widely used to investigate the fate and transport of contaminants in medium-sized rivers [150, 511]. -It is well-suited to simulate the contaminants behavior in well-mixed rivers [150].	-The model provides 1-D simulation, while flow is supposed to be in a steady state [117]. -It is not well-suited to simulate branches of the river system [117]. -It is not well-suited to simulate denitrification processes, macrophytes growth, and suspended sediment movement [150]. -Some of the QUAL models are moderately sensitive to nitrification rate, point source flow, CBOD and highly sensitive to water depth [174, 281]. -No uncertainty component is incorporated [117]

Table 3.9 (continued)

SPARROW	-SPARROW induces the implementation of large-scale regional models with mass balance constraints [311]. -Based on regression approache, SPARROW model is well suitable for large basins [469]. -The model is an empirical model that simulates the long-term variability of watershed processes [311]. -Less data is required compared to numerical mechanistic models [129]. -Sound conceptual foundation and simple physical structure of mass transport within the landscape [234]. -In comparison to statistical and deterministic models, the use of process-based approache enhanced model interpretability, simulation reliability and reduced computational cost [311].	-As a "black box" model, SPARROW describes a limited number of process [118] -As an empirical model, SPARROW is not suitable for short-term (less than annual) water-quality records that dynamic mechanistic models can provide [311]. -A ramification of SPARROW's propagated structure is the spatial transmission of model error, that provides in turn a significant statistical issue [477]. -Simulation requires a large number of water-quality monitoring stations [118].
SWAT	-SWAT was justified as being suitable for large-scale applications, due to its solid physical basis [35, 491]. It can be applied to diverse spatio-temporal scales from small watershed (e.g., 10 km2) to a river basin and provide higher long-term prediction accuracy [18]. -It had the ability to be easily implemented in data-scarce regions [177]. -SWAT had the ability to fill the gaps in weather record [16, 443]. -Alternative calibration approaches (i.e., SWAT-CUP (Calibration and Uncertainty Programs)) have been developed to streamline calibration time and improve the model's performance [467]. -The model shows good performance in long-term sediment yield rate prediction [184].	-Modelling of soil temperature, sediment, soluble-phosphorous and nitrate loadings, and baseflow discharge are sensitive to season change, generating a low accuracy of SWAT prediction when applied to areas with significant winter snow cover [117, 365]). -The model does not incorporates bacterial growth [104] and Metals reactions [515]. -It is not well-suited to simulate sub-daily events (i.e., storm event, diurnal changes of dissolved oxygen) [174]. -It is not well-suited to simulate the seasonal dynamics of sediment load delivery at a ssmall catchment outlet. -Low temporal resolution [16, 147]. -Concerns related to large prediction uncertainties associated with model structure and input parameters have resulted in limited use of the model [16, 334]. -SWAT requires numerous data to make calibration process tedious [16].
TOMCAT	-TOMCAT was designed to be a simpler model, easy to use, allows fast runs (auto-calibration), and appropriate for simulating determinants in freshwater [374]. -Useful to organizations such as water utility companies for simulating lowland rivers [119]. -Reduced amount of input data [229]. -Requires a limited imput data [300]. -The model can produce the impact of storm water by diverting waste discharges to a substitute outlet [374]. -It can provide annual and monthly statistics [374].	-TOMCAT has limited functionality concerning the number of processes involved, it does not incorporate some relevant processes for water quality (e.g. respiration, photosynthesis, sediment dynamics) [300]. -It is note suitable for simulating in-stream concentrations of down-the-drain chemicals as results of ewage treatment [229]. -The model only assumes the river's cross-sectional area, which can affect the reliability of the flow velocity outputs [374]. - As a stochastic model, is sensitive to the type/form of the input data [119].
WASP	-The WASP flexibility has ensured the wide use and longevity of the model [370]. -It can simulate water quality in 1-D or 2-D or 3-D [405]. -It can be coupled with hydrodynamic and sediment transport models to provide water temperature, salinity, circulation and sediment fluxes. -The volume control structure allows for the application of the mass-conservation concept [405] . -The model can be combined withtion, metals, toxics, nutrient, and sediment transport [150]. -It has been extensively used to simulate heavy metals, PCBs and organic compounds in diverse aquatic ecosystems [482]. -The user can control the state variables to simulate and parameterize [482]. -The algal death could be convert to CBOD [225].	-Model calibration and its application to simulate some water quality parameters requires extensive amount of data and a significant amount of time [150, 337]. -It is not well-suited to simulate sinkable/floatable materials, near-field effects or mixing zones [118, 150]. -It is not well-suited to simulate microalgae and periphyton dynamics [150, 337]. -It does not incorporate some variable processes (i.e. non-aqueous phase liquids, metals speciation, segment drying, and mixing zone processes) [150]. -It is not able to simulate successfully the variation of suspended solids loading in the river [150, 225]. -Linking with multi-dimensional hydrodynamic models requires substantial site-specific linking efforts [225].

3.6.2.3 Spatio-temporal trends in model applications

In their various forms and applications, SWAT was cleary the most applied water quality model. It covers approximately 22.41% of the total applications. Simular results were provided by [117]. Most of modelling applications have addressed watershed system. The popularity of SWAT reflects its capability to performs further analyses of different water management scenarios [494]. It is capable to simulates the effects of land management activities on water and agricultural chemical yields in complex watersheds with various management conditions over different timescales [213]. 19.6% of the SWAT applications were implemented to addresse Maryland ecosystems, make it the most commonly used model in the United States of America (53.6%). Overall, we underline a general tendency of the models to be applied within the three distinct countries of the Northwest and Northeast Atlantic; United States of America (41.64%, 1061), Canada (13.81%, 332), and Portugal (7.57%, 183). Otherwise, Southeast Atlantic seem to be poorly represented by water quality models. A possible explanation can be probably related to more publishing in books, book chapters, and the technical reports, inadequacy of infrastructure, lack of knowledge, fewer scientific resources and limited data availability [16, 384].

3.7 Conclusion

The present study reviews the literature in water quality modelling applications within the Atlantic area from 1981 to 2021. 1952 publications (2548 individual modelling applications) were retrieved. The document types consisted of 89.33% articles, 8.06% conference paper, 1.63% scientific report and 0.98% classified as others. English was the most used language, accounting for 94.58%. Number of publications has shown an upward trend in the past two decades. Among the most productive journals, Science of the Total Environment and Ecological Modelling have the largest number of publications.

Considering number of publications, citations and co-citations, “Ramiro J. J. Neves” (Instituto Superior Técnico, Portugal), “Jeffrey G. Arnold” (USDA Agricultural Research Service, United States), and “Raghavan Srinivasan” (Blackland Research and Extension Center, United States) are the most productive authors. Plymouth Marine Laboratory, plymouth, MARETEC, Instituto superior técnico, universidade de lisboa, Virginia institute of marine science, college of william and mary, Gloucester Point and USDA-ARS Hydrology and Remote Sensing Laboratory, Beltsville are the most productive research institutions. Using co-word analysis, “Water quality”, “United states”, “Watersheds”, “Rivers”, “Hydrological modeling”, “Water pollution”, “Phosphorus”, and “Numerical model” are the research hotspots.

Further, SWAT (semi-empirical modeling frame-works) has been extensively applied during the last two decades and remains the most used model today, followed by MOHID Water, CE-QUAL, and HSPF. 72.15% most of modelling applications have addressed watershed system. The other systems received little attention.

The geographical distribution of modelling applications suffers from a significant imbalance with greater numbers of applications in the Northwest and Northeast Atlantic areas. Overall, United States of America, Canada, and Portugal stood out with the greatest number of studies. Fewer studies was observed in Southeast Atlantic. The main contribution of our review is to offers a holistic picture of the modelling applications within the Atlantic area. Briefly, the quantitative and qualitative analysis findings can help scholars identify impactful, authors, institutions for future collaborations and inspire them to further improve this research domain.

CHAPTER 4

Three-dimensional hydrodynamic modelling of the Moroccan Atlantic coast: A case study of Agadir bay

4.1 Résumé du chapitre

Les résultats de ce chapitre ont fait l'objet d'un article soumis pour publication au "Journal of sea research".

Dans ce chapitre :

Le modèle de simulation est essentiel pour prévoir l'hydrodynamique et les processus environnementaux associés aux eaux côtières. Cependant, peu de modèles de simulation de ce type sont utilisés pour les masses d'eau de la côte atlantique marocaine. Comme première étape vers notre objectif final de développer une approche de modélisation intégrée pour une meilleure compréhension de la dynamique des eaux côtières atlantiques marocaines, cette étude a mis en œuvre un modèle hydrodynamique 3D de la baie d'Agadir. Le modèle a été calibré et validé par rapport aux conditions météorologiques, niveau de la surface de la mer, constituants harmoniques de la marée, ainsi que la température et la salinité de l'eau, en utilisant une combinaison de mesures *in-situ* disponibles, données satellitaires et flotteurs ARGO. Malgré quelques divergences, les résultats ont révélé une bonne correspondance entre les simulations et les observations, ce qui souligne la faisabilité du modèle pour prédire les principales caractéristiques dynamiques de la baie d'Agadir. Le modèle hydrodynamique validé a été inclus avec la masse injectée de traceurs en utilisant le modèle de transport lagrangien. Dans l'ensemble, l'hydrodynamique de la zone est dominée par des marées semidiurnes (M2) et régie par des vents d'ouest et de nord-ouest avec une température de l'air relativement élevée (maximum de 30°C) et une humidité relative élevée (maximum de 95%). L'analyse des structures verticales de la température et de la salinité de l'eau a révélé que la thermocline et l'halocline étaient situées près de surface. L'eau de mer relativement plus chaude et plus salée occupait les eaux de surface, tandis que les eaux profondes étaient relativement froides et fraîches. L'interaction entre la topographie de la baie d'Agadir et la tension du vent local pourrait induire une circulation double-gyre: une grande circulation cyclonique près du rivage et une autre en pleine mer. Les conditions de la saison hivernale consistent en un niveau élevé de vitesse des vents provenant principalement du S-SE, ce qui entraîne une augmentation des vitesses horizontales, qui s'écoulent principalement vers le nord-ouest. En revanche, les vents locaux de NW poussent les eaux de surface au large vers le sud pendant les conditions de la saison estivale. Les simulations de Lagrangien model fournissent des informations sur le TR et les voies possibles des traceurs passifs de surface. Des RT plus faibles (de 3 à 9 jours) ont été observés en été et plus élevés (de 5 à 15 jours) en hiver. Les traceurs semblent être piégés à l'intérieur d'un tourbillon cyclonique côtier, favorisant le transport vers le nord et l'augmentation des TR dans la baie sud, ce qui en fait une région côtière susceptible d'être polluée. En outre, la validation des simulations lagrangiennes et l'évaluation de différents scénarios de dispersion des traceurs passifs devraient être réalisées dans le futur, afin de consolider les connaissances sur la dispersion des particules polluées ainsi que leur zone d'accumulation dans la baie d'Agadir.

4.2 Abstract

Coastal areas are a noteworthy source of commercial and economic fortunes for surrounding municipalities throughout the Moroccan Atlantic coast. Thus, a deep knowledge of local hydrodynamics and environmental processes associated is integral to effective coastal management. 3D hydrodynamic model that includes a Lagrangian particle simulation can participate to this understanding of dynamics. The model was calibrated and validated against meteorological conditions, sea surface level, harmonic tidal constituents, water temperature and salinity using a combination of available in-situ measurements, satellite, and ARGO floats data. Subsequently, it was used to determine the pathway of passive tracers and estimate the local residence time (RT). Despite some discrepancies, the findings revealed a good match between simulations and observations, which underlines the feasibility of the model in predicting the main dynamic features of the Agadir Bay. Overall, the hydrodynamics of the area is tidal dominated by semidiurnal tides (M2) and governed by westerly and northwesterly winds. Passive tracer simulations showed strong seasonal and spatial variability, conditioning the obtained RTs, with mean values much shorter during summer (3 to 9 days) than winter (5 to 15 days). The tracers look to be trapped inside a coastal cyclonic eddy that increases the RTs in the southern Bay, making it an area with highest likelihood of accumulation of pollutants while favoring the northward transport and decrease RTs in the northern Bay.

Key–Words : 3D hydrodynamic model, Lagrangian model, Moroccan Atlantic coast, Agadir Bay, residence time.

4.3 Introduction

As a part of the Canary Current System, natural dynamic of Moroccan Atlantic coastal ecosystems has been greatly influenced by the large-scale coastal processes (e.g., upwellings, downwellings, eddies, and coastal currents) (e.g., [21, 51, 212, 249, 273, 332, 352, 390, 391]). Such forces pump massive quantities of kinetic energy to the system that contributes to diverse circulation patterns. Moreover, heat energy exchange is a crucial factor when investigation the hydrodynamic features of coastal areas. However, with increasing environmental pressures and associated natural drivers (e.g., storm surges, hurricanes, sea-level rise) on the one hand and anthropogenic activities (e.g., industrial and urban expansion, fisheries, aquaculture, maritime traffic docking at the harbors, etc.) on the other hand, energy fluxes could be altered [12, 244].

Changes in these forces affect water stratification, water circulation and residence time (RT). Furthermore, changes in coastal hydrodynamics influence dispersion of pollutants originated from wastewater discharges and runoff, which is especially important in urban coastal areas [40]. Therefore, knowledge about hydrodynamics, RT and understanding the way pollutants dispersion responds to coastal circulation is crucial to the management of these water bodies, as Agadir Bay, being crucial to establish the local water quality and to enable local authorities to design contingency, adaptation, and mitigation measures.

[11] carried out some experiments to quantify the concentration of pesticide in different areas of the Bay, indicating the contamination increases from northern to southern Bay. A full description of contamination paths, concentration and seasonality is yet to be performed. Therefore, an estimate of the residence times of the coastal water under different circumstances may be useful in investigating the impact of such contamination. In general, areas with high RT would have excellent water quality [231, 277, 358].

Given the limited time-space coverage of in-situ measurements, the coastal waters of Agadir Bay generally suffer from scarcity of data; the field data and experimental knowledge are especially limited regarding local hydrodynamics variables, and therefore it is extremely limited the knowledge about local hydrodynamic processes and features. Hydrodynamic models have been widely used to simulate coastal circulation in response to forcing factors [40]. The impact of these forcing, which are mainly tides, atmospheric pressure and wind stress forcing, rely on system characteristics [1].

Recently, several hydrodynamic models have been implemented, validated and used in research for better understanding of how systems respond to external forces. For example, Delft3D (e.g., [258, 429, 495]), ROMS (e.g., [235, 355, 503]), TELEMAC (e.g., [209, 368, 393, 406]), ADCIRC (e.g.,[222, 473]), FVCOM (e.g., [100, 197, 418]), MIKE3 (e.g., [468]), SHYFEM (e.g.,[53, 123]), SELFE (e.g.,[188, 505]), HYDROTAM-3D [89] and MARS-3D (e.g., [72, 398].

To our knowledge no previous study has simulated the local scale hydrodynamic processes of the Agadir Bay. To fulfil these knowledge gaps, a three-dimensional (3D) MOHID Water modelling system has been implemented and explored in the present study. It is worth noting that MOHID Water model has successfully been applied to investigate various dynamic aspects occurring on the water columns [25, 135, 176, 305, 360, 366, 392, 442], being so, a useful tool for coastal dynamic evaluation [138].

In the present study, a three-dimensional (3D) hydrodynamic model MOHID Water coupled with a Lagrangian transport model were implemented, in order to improve our understanding of hydrodynamic features of the Bay, to estimate the local residence time and to determine the pathway of passive tracers.

4.4 Materials and methods

4.4.1 Study area

The Agadir coast is one of the most extensive coastal areas in Moroccan Atlantic coast (Fig. 4.1). It is the central part of a 35 km long sandy shoreline bound in the north by Cape Arhdis and in the southwest by Cape Aglou.The Agadir Bay (30°25’ N, 9°38’ W) represents the western limit of the city of Agadir; extending over almost 6 km as the crow flies, oriented in a south-west/north-east direction between the large Agadir harbor and the Oued Souss estuary. It is open to the Souss Massa plain covering an area of about 23,950 km^2 [27].

The geomorphological characteristics of the coast comprise a wider continental shelf, shallower and with lower slopes than the one on the north of Cap Ghir. The specific orientation of the coast, which is clearly deflected towards the west, is responsible for the constant regularity of the winds blowing over these regions; a situation that generates important upwelling events nears the coast [321]. According to the Hydraulic basin Agency of Agadir, the area is characterized by an arid to semi-arid climate with the highest average rainfalls recorded between November 2016 (165.7 mm) and February 2017 (283 mm) [244].

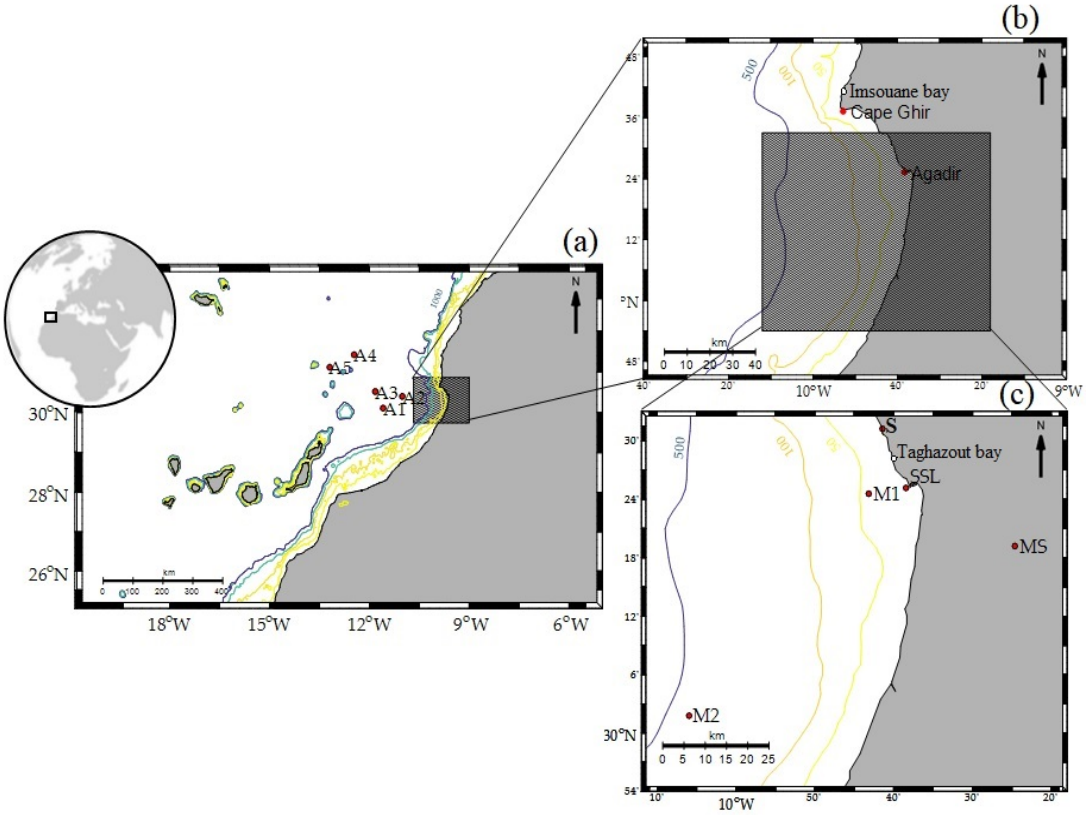

Figure 4.1: Model domain showing the location of the stations used for the atmospheric and the hydrodynamic model validation (red dots) a) MACOMS (Domain 1) with A1–A5 - ARGO floats location; b) ACMS (Domain 2); c) Agadir Bay (Domain 3) with MS – Meteorological station; SSL – Sea surface level; M1 – Wind near the coast; M2 – Wind at the open ocean; S – Surface water temperature and salinity. Bathymetry is presented with contours for 50, 100, 500 and 1000 m.

4.4.2 Model implementation and exploitation

4.4.2.1 Hydrodynamic model

The 3D-MOHID Water model resolves the Navier-Stokes equations using the Boussinesq and hydrostatic approximations [138, 168].

The finite volume approach is used to discretize the MOHID equations enabling the execution of several types of vertical coordinates at the same time.
The equations solved in the model are:

$$\frac{du}{dx} + \frac{\partial v}{\partial y} + \frac{\partial w}{\partial z} = 0 \tag{4.1}$$

$$\frac{\partial u}{\partial t} + \frac{v\partial u}{\partial x} + \frac{v\partial u}{\partial y} + \frac{w\partial u}{\partial z} - fv = -\frac{1}{\rho_r}\frac{\partial p}{\partial x} + \frac{\partial}{\partial x}\left(A_h\frac{\partial u}{\partial x}\right) + \frac{\partial}{\partial y}\left(A_k\frac{\partial u}{\partial y}\right) + \frac{\partial}{\partial z}\left(A_v\frac{\partial u}{\partial z}\right) \tag{4.2}$$

$$\frac{\partial v}{\partial t} + \frac{v\partial v}{\partial x} + \frac{v\partial v}{\partial y} + \frac{w\partial v}{\partial z} + fu = -\frac{1}{\rho_r}\frac{\partial p}{\partial x} + \frac{\partial}{\partial x}\left(A_h\frac{\partial v}{\partial x}\right) + \frac{\partial}{\partial y}\left(A_k\frac{\partial v}{\partial y}\right) + \frac{\partial}{\partial z}\left(A_v\frac{\partial v}{\partial z}\right) \tag{4.3}$$

$$\frac{\partial \rho}{\partial z} + \rho g = 0 \tag{4.4}$$

u, v and z : the components of the velocity in the x , y and z directions respectively; f : the Coriolis parameter; A_v and A_h : the coefficient of turbulent viscosities in the horizontal and vertical directions; ρ : the pressure; ρ_r: the reference density.

The temporal discretization is accomplished using a semi-implicit algorithm ADI (Alternating Direction Implicit) [331]. This algorithm resolves issues related to the explicit methods, responsible for long-term model instability and simplifies the resolution of the sea surface level and the horizontal velocities. The algorithm of [312] is also used to solve the water density non-linear state equation that depends on pressure, salinity and water temperature. The spatial resolution of the hydrodynamic model is achieved using a downscaling technique of nested domains [83, 251]. The vertical turbulence is computed by coupling MOHID with the General Ocean Turbulence Model (GOTM), consisting of a generic library with different turbulence closure structure for the parameterization of vertical turbulent fluxes in water column [75]. More information on the software is available in `http://mohid.com/`. Three different nested domains are implemented using a one-way downscaling approach: D1) Moroccan Atlantic Coast Operational Model System (MACOMS) (Domain 1) – 2D barotropic model with an horizontal resolution of 0.04° (4 km) and 50 vertical layers (7 sigma + 43 Cartesian until the bottom), covering the Moroccan Atlantic coast and providing information to the higher resolution nested domain, resulting in a grid of 238 × 359 cells with maximum depths around 5300 m; D2) Agadir Coast Model System (ACMS) (Domain 2) – 3D baroclinic model with 0.02° (2 km) horizontal resolution, covering the area ranging from 29°44' to 30°51'N and from 10°40' to 9°37'W, resulting in a grid of 56 × 56 cells with maximum depths around 2133 m; D3) Agadir Bay (Domain 3) – 3D baroclinic model based on an equally spaced Cartesian horizontal grid with a resolution of 500 m. The last domain receives its open boundary conditions from the lower resolution ACMS domain and covers the area comprised between 45.00° and 34.38° N and 12.60° and 5.10° W, resulting in a grid of 24 × 21 cells and maximum depths around 133 m (Table 4.1). The bathymetry was provided from Multinational Response and Preparedness to Oil and Chemical Spills project (MARPOCS; http://www.maretec.org/en/projects/current/MARPOCS) and run with mode-splitting time steps of 90 s, 20 s and 20 s for for D1, D2 and D3, respectively. Daily profiles of seawater temperature and salinity were interpolated from the Copernicus Marine Environment Monitoring Service (CMEMS; https://www.copernicus.eu/) and imposed at the open sea boundary. The tidal oceanic forcing was determined from the harmonic components extracted from the FES2012 (Finite Element Solution) model at numerous locations along the boundary. At the atmospheric boundary, the model was forced with results from a previous implementation of the Weather Research and Forecasting (WRF) model (http://www.actionmodulers.pt), covering the entire domain, with hourly results for a 3 km grid resolution [445].

Table 4.1: Model setup configuration for the Agadir Bay domain

Settings	Domains		
	D1 - MACOMS	**D2 - ACMS**	**D3 - Agadir Bay**
Area	Moroccan Atlantic coast	Agadir coast	Agadir Bay
Model characterization	2D – Barotropic	3D – Baroclinic	3D – Baroclinic
Grid corners	Lon: -20.79 – -6.51 Lat: 25.04 – 34.55	Lon: -10.67 – -9.63 Lat: 29.74 – 30.86	Lon: -9.91 – -9.61 Lat: 30.23 – 30.55
Depth	Min: 15 m Max: 5300 m	Min: 15 m Max: 2133 m	Min: 5 m Max: 133 m
Cells dimension	238 × 359	56 × 56	24 × 21
Vertical Grid	7 Sigma Layer 43 Cartesian layers	7 Sigma Layer 33 Cartesian layers	7 Sigma Layer 17 Cartesian layers
Horizontal Grid	4 km	2 km	500 m
Time steps	90 seconds	20 seconds	20 seconds
Tides	FES2012 [88]	From Domain 1	From Domain 2
OBC Water	From MercatorOcéan [1]	From Domain 1	From Domain 2
OBC Atmosphere	WRF [445]	WRF [445]	WRF [445]
OBC Nutrients	–	WOA13 [2]	Domain 2
Discharges	No	No	No
Turbulence	–	GOTM [3] [74]	GOTM [4] [74]
Bottom stress	Rugosity of 0.0025 $m^2 s^{-1}$	Rugosity of 0.0025 $m^2 s^{-1}$	Rugosity of 0.0025 $m^2 s^{-1}$

[1] https://www.copernicus.eu/. [2] https://odv.awi.de/data/ocean/. [3] General Ocean Turbulence Model. [4] General Ocean Turbulence Model.

4.4.2.2 MOHID Lagrangian model

The Lagrangian model was used to simulate RT in the Agadir Bay using the methodology described in previous works [69, 231, 285, 395]. The model uses the concept of passive tracers [8], where each tracer is considered a floating object identified by its volume, own origin, and spatial coordinates (x, y, z), and each is attributed a time to achieve random movement. The position of each tracer depends on the velocity in each grid cell as well as its location in the previous time step. Tracer movement is determined integrating its velocity, resulting from the addition of the Eulerian transient current velocity produced by the hydrodynamic model with a random component of velocity, using a Runge-Kutta scheme, according to the approach followed by [272]. Thus, the Lagrangian model utilize the surface current fields produced by the 3D baroclinic model to describe the distribution of tracers and the trajectory generated by the non-turbulent velocity field, which results indirectly from the advective term introduced in the Navier-Stokes equation. The dispersion of the tracers is regulated using monitoring boxes to estimate their RT in each box. The boxes were filled with equal volumes of Lagrangian tracers. The RT is computed

assuming the time taken by 80% of the tracers to leave each monitor box. This attribute is used to ensure the expulsion of most particles from the boxes [284, 285].
The water fraction f_{ij} inside the box i in each instant of time t with origin from box j is calculated as:

$$f_{ij} = \frac{V_{ij}(t)}{V_{ij}(0)} \tag{4.5}$$

Where,$V_{ij}(t)$ is the tracer's volume issued in box j, located inside box i at time t. $V_{ij}(0)$ is the volume of water inside box i at the inception of the simulation (t ¼ 0).
Surface currents simulated in the present study using the hydrodynamic model, with a time step of 3600 s, are used to estimate tracers' trajectories and RT, assuming that particles remain on the surface. For the Lagrangian simulations, a time step of 600 s is used.

4.4.2.3 Model evaluation and data collection

To determine the model's accuracy, a large set of observational data from various data providers was used to validate the model and to verify its ability to predict the key dynamic features of the study region. For the validation purpose, the model was simulated from 1/01/2017 to 30/12/2018; period corresponding to high atmospheric and hydraulic conditions in Agadir coast (Hydraulic basin Agency of Agadir) and high data availability. Nevertheless, hourly and daily air temperature, humidity, atmospheric pressure, wind velocity data were obtained from GMAD station at Agadir-Al Massira International Airport (-9.42 N - 30.32 W) (approximately 26 km South-East of the Agadir Bay) (https://www.ogimet.com/metars.phtml). Temporal evolution of the wind velocity was also evaluated using the field data from the same meteorological station (https://www.tutiempo.net/agadir.html). Data of sea surface level (SSL) was retrieved from French Navy's Hydrographic Department (Shom) (www.shom.fr), with an hourly time step in Agadir harbor location (-9.61 N, 30.41 W). In-situ measurements from I. Lamine expedition [244] were compared with time series of simulated surface seawater temperature (SST) and surface seawater salinity (SSS). The monthly sampling of seawater was carried out at the S station located south of the Taghazout Bay resort (30.52N, -9,69W), near the tourist-campground (Atlantica Parc Imourane, 14 km from Agadir). One liter of seawater was collected at low tide at 9 or 10 a.m, at a depth of 50 cm in a sterilized and labelled bottle. Furthermore, spatial distribution of SST was validated using remote sensing data from ODYSSEA satellite images (http://marine.copernicus.eu/ [39]). These images are a multi-sensor merged high-resolution level 4 product with 0.02° resolution, available every 24 hours. ARGO profiling floats data was downloaded through the US component of the international Argo Program (www.argo.ucsd.edu) and used to validate vertical profiles of water temperature and salinity of the regional model domain. The model's accuracy was also assessed comparing the major tidal constituents amplitude and phase predicted by the model and obtained from Shom data. Tide Harmonic Analysis Toolbox [350], based on the classic FORTRAN tidal analysis packages written by Mike Foreman (http://www.dfo-mpo.gc.ca/science/datadonnees/tidal-marees/index-eng.html) was used to extract the harmonic tidal components from SSL data. Afterwards, distribution maps of the main tidal harmonic constituents (M2, K1, M4) determined from MOHID SSL predictions were plotted, aiming to characterize the tidal propagation along the Bay. Moreover, the capability of the model to reproduce the observed variables was evaluated using Pearson correlation coefficient (r), Root Mean Square Error (RMSE), average error bias (BIAS), Model Skill Score (MSS). Eqs. (4.6), (4.7), (4.8) and (4.9) express r, RMSE, BIAS and MSS, respectively:

$$R=\frac{\sum_{i=1}^{N}\left(X_{\text{madel}}-\overline{X_{\text{abs}}}\right)\left(X_{\text{abs}}-\overline{X_{\text{abs}}}\right)}{\sqrt{\sum_{i=1}^{N}\left(X_{\text{model}}-\overline{X_{\text{madel}}}\right)^{2}}\sqrt{\sum_{i=1}^{N}\left(X_{\text{obs}}-\overline{X_{\text{abs}}}\right)^{2}}} \tag{4.6}$$

$$\text{RMSE}=\sqrt{\frac{1}{N}\sum_{i=1}^{N}\left(X_{\text{model}}-X_{\text{obs}}\right)^{2}} \tag{4.7}$$

$$\text{BIAS}=\sum_{i=1}^{N}\frac{1}{N}\left(X_{\text{model}}-X_{\text{obs}}\right) \tag{4.8}$$

$$\text{MSS}=1-\frac{\sum_{i=1}^{N}\left(X_{\text{model}}-X_{\text{obs}}\right)^{2}}{\sum_{i=1}^{N}\left(\left|X_{\text{model}}-\overline{X_{\text{model}}}\right|+|X_{\text{obs}}-\overline{X_{\text{obs}}}\right)^{2}} \tag{4.9}$$

N: the number of records in the time series; X_{obs} and X_{model} : the observed and model outputs variables and the overbar represent the mean of the variables.

4.5 Results

4.5.1 Meteorological model

Given the importance of atmospheric boundary conditions for the proper reproduction of the coastal environment by the hydrodynamic model, daily time series of air temperature, relative humidity, atmospheric pressure and wind intensity provided by the WRF atmospheric model are compared with data obtained from GMAD meteorological station of the Agadir-Al Massira International Airport (station MS – Fig. 4.1). For the seasonal analysis, the study period extends from 1/01/2018 to 31/12/2018, in which meteorological data were available every 1 hour. Seasonal configurations are sequentially divided into four seasons: winter (21-Dec, Jan, Feb, 19-Mar), spring (20-Mar, Apr, May, 20-Jun), Summer (21-Jun, July, Aug, 21-Sep), and Autumn (22-Sep, Oct, Nov, 20-Dec). Overall, the observed air temperature and humidity fluctuation shows that both variables differ alternately (Fig. 4.2).

During summer, the air temperature progressively increased and peaked in September, when it frequently reached a maximum of 30 °C and the humidity was minimal (42%). During winter, the air temperature dropped to the lowest level (10 °C) in November; conversely, the humidity rose and reached (95%) in the same period. The annual trend of the observed winds exhibits irregular pattern; however, the period between 12 of April and 25 of May has the most intense event, in which the observed wind intensity reaches more than 5 ms^{-1}. The minimum wind intensity was found to be 0.54 ms^{-1} in June and the maximum was 7.2 ms^{-1} in April. The simulation for low-value observations of wind intensities are well matched, but the BIAS grows rapidly with higher values, yielding RMSE and BIAS mean values of 25.92 and -1.38 ms^{-1}, respectively (Table 4.2). This may be because WRF model does not entirely resolve the complex topography in the vicinity of a branch of the Atlas Mountains that extends for more than 150 km around the study area [50]. Such issues are well aligned by several authors [178, 389]. Small differences between simulated and observed air temperature were prevalent during winter. Nevertheless, the mean value of the correlation coefficient was high (0.7) whereas BIAS was low (0.52 °C), suggesting that these deviations have a minimal repercussion in quality of the model outputs. In contrast, the observed relative humidity was underestimated by the model, which is confirmed by the negative mean values of BIAS (-1.88%) in combination with large RMSE values (35.20%). A good reproduction is noticed for the atmospheric pressure, with a correlation coefficient of 0.94 and RMSE mean values of 5.23 hPa.

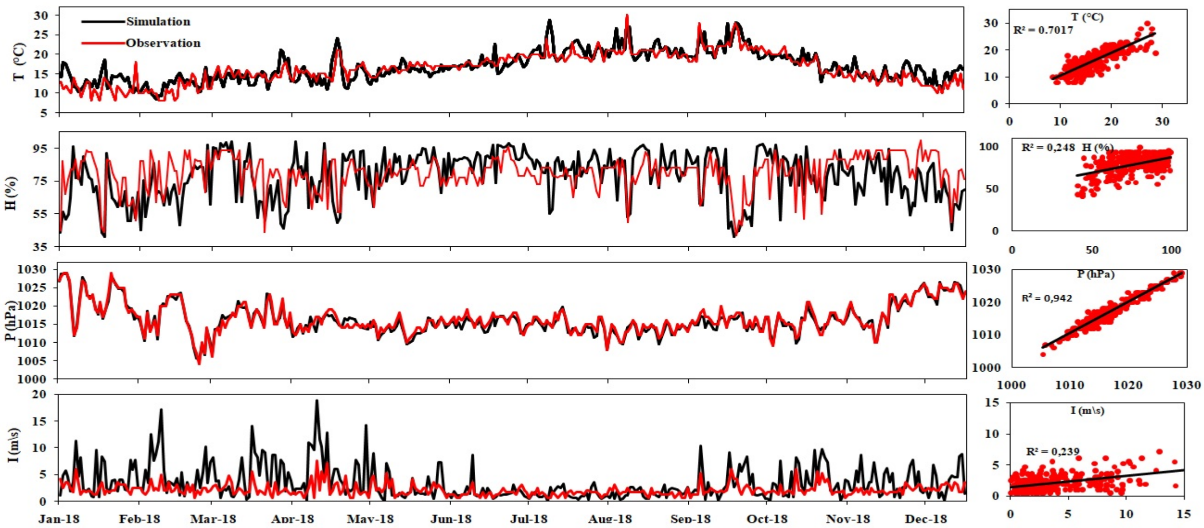

Figure 4.2: Comparison between WRF outputs and GMAD station data for air temperature (T), humidity (H), atmospheric pressure (P) and wind intensity (I) for 2018 (left). Red line represents GMAD station data and the black line the WRF outputs. Correlation and performance results for the WRF model vs meteorological data (right). Squared correlation coefficient (R^2).

Next, MS observations and WRF model outputs, as well as WRF simulations at two additional stations (M1: near the coast (-9.72 N, 30.41 W); M2: at the open ocean (-10.10 N, 29.93 W) – Fig. 4.1) are compared to identify the dominant wind configuration, in terms of the frequent wind speed and directions in the outermost domain (Fig. 4.3). Results reveal higher wind intensities at sea comparing to land, reaching values of around 21 ms^{-1} near-shore and 33 ms^{-1} at the open ocean. The morphology assessment of wind roses (Fig. 4.3a) from both WRF outputs and observations, furnish close results in terms of the frequent wind speed and directions, confirming that the main wind blows from the W and NW sector. Given the observed data, more than 16% of winds have speeds between 8 and 12 ms^{-1}, and 15% of winds have speeds between 4 to 8 ms^{-1}. Winds from the E quadrant are the least frequent, with a frequency of 1.6%, while the S winds have a frequency of 8%. Moving to the coast, the wind veers to the NW and the intensity markedly increases, presenting more than 19% of the local wind intensity amplitude, which varies between 12 and 16 ms^{-1} near-shore. In the open ocean, the evolution of the wind intensity is slightly different from the near-shore area, which is rather variable, ranging from northwest to west. The wind seasonal fluctuation was then evaluated for the near-shore station (Fig. 4.4). The overall view of the wind roses indicates that this area exhibits an irregular wind pattern, where the strength and the direction of such winds are altered in seasonal scales. In winter, the wind

Table 4.2: Statistical results used to assess the agreement between WRF model outputs and GMAD station observations for 2018. R^2 — Squared correlation coefficient; RMSE — root mean square error; BIAS — average error.

	Air temperature (°C)	**Humidity (%)**	**Atmospheric pressure (hPa)**	**Wind intensity ($m.s^{-1}$)**
R^2	0.70	0.24	0.94	0.23
RMSE	9.69	35.20	5.23	25.92
BIAS	0.52	-1.88	1.08	-1.38

speed reaches 14.4% and 16.2%, mostly associated to winds from the NW and S-SE direction, respectively. The summer season shows a strong influence of winds from NW (19.3%). There wind intensities increase comparatively to the winter, with 50% of the winds with intensities higher than 8 ms^{-1}. NW wind direction still dominates the wind configuration during the remaining seasons, with about 16.8% of the occurrences in spring.

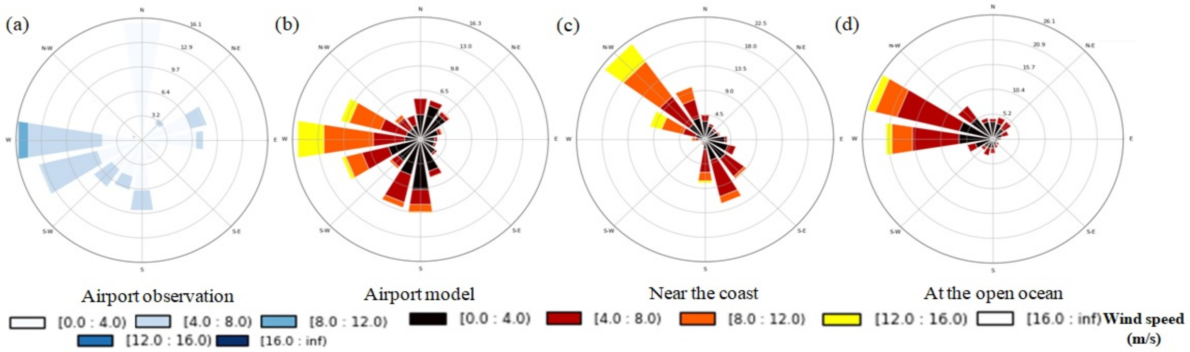

Figure 4.3: Comparison of wind roses for the annual average wind measured at Airport station (a) and simulated by WRF for (b) Airport station (-9.42 N - 30.32 W), (c) near-shore (-9.72 N, 30.41 W) and (d) the open ocean (-10.10 N, 29.93 W) from 1/01/2018 to 31/12/2018. (Note that the color scales are different between observed and simulated data).

4.5.2 Hydrodynamic processes

4.5.2.1 Tides

Simulated time series of SSL at Agadir harbor (9.61 N, 30.41 W) (SSL, locations marked in Fig. 4.1c) from 01/05/2017 to 31/12/2017 were compared with those extracted at the same location from Shom data. The station and the period were selected due to Shom data availability. Preliminary results are analyzed to assess the overall reliability of the model's forecast accuracy for Agadir Bay, rather than to perform an in-depth validation, which requires further comparisons with field measurements at different locations and over a longer period. The mean SSL during the model validation period was 3.49 m; the highest level was observed in June and peaked on 25 June (Fig. 4.5a). The goodness-of-fit statistics in Fig. 4.5b of monthly variation of SSL

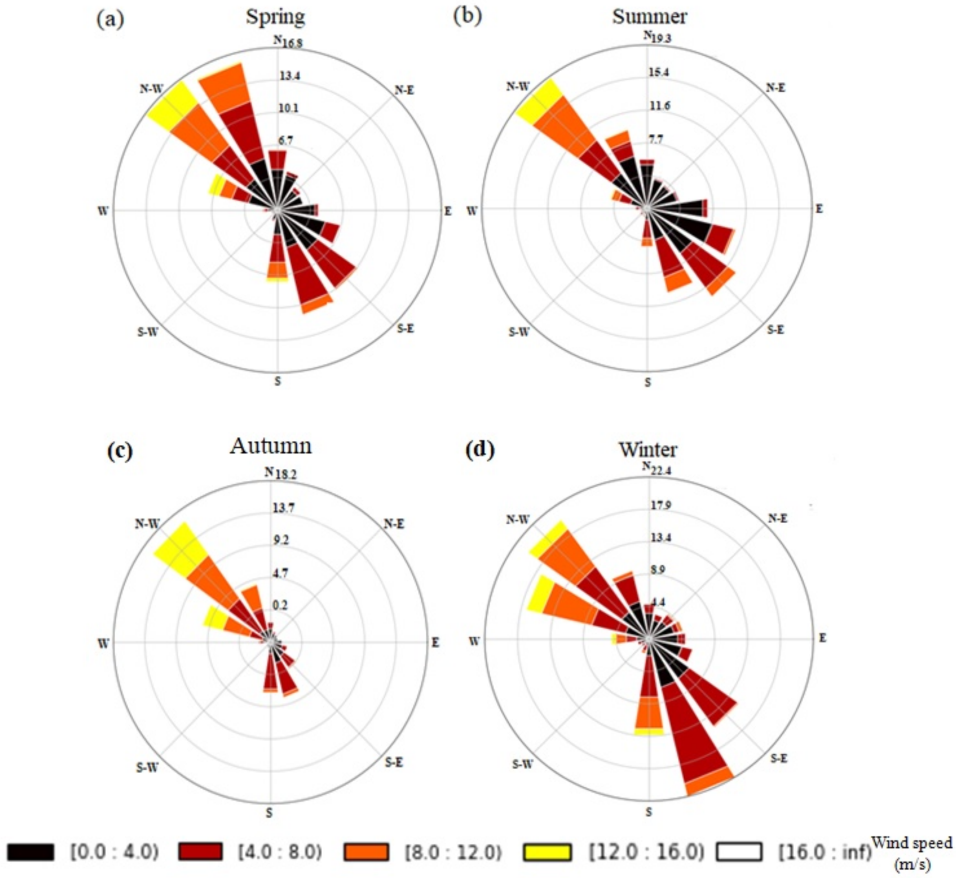

Figure 4.4: Seasonally average simulated wind speed and direction at the near-shore station (-9.72 N, 30.41 W) during (a) spring (b) summer and (c) autumn and (d) winter, 2018.

from 01/06/2017 to 30/06/2017 reveal that the tidal model accurately reproduces the frequency distribution of tidal cycle, with Pearson correlation coefficient higher than 0.99 and MSS main values close to 1 Table 4.3). The elevation difference between datasets is considered negligible (average 0.005 m). Nevertheless, the mean RMSE (0.35 m) and BIAS (0.004 m) values were quite low, suggesting that this discrepancy was of minimal consequence. The amplitude and the phase of the principal tidal constituents are accurately captured as shown by the harmonic analysis in Table 4.4. The averaged differences between the datasets are often smaller than 0.01 m for the amplitude and 11 degrees for the phase. The bulk of tidal energy is accounted for the semi-diurnal constituents, which are the major tidal constituents in the Agadir bay. The principal lunar M2 showed the highest amplitude and accounted for 58.5% of the tidal amplitude of the total harmonic's components presented in Table 4.4. Constituent O1 (principal lunar diurnal) and the high frequency constituent M6 (sixth diurnal tide) are less accurate considering their weaker amplitudes.

The simulated amplitude and phase maps for the most representative harmonic constituents (M2 for semi-diurnal, K1 for diurnal and M4 for the main non-linear shallow water constituent) are shown in Fig. 4.6. The results for the higher harmonic constituent (M2) demonstrate that its amplitude increases progressively in the shallower areas, reaching a maximum of approximately

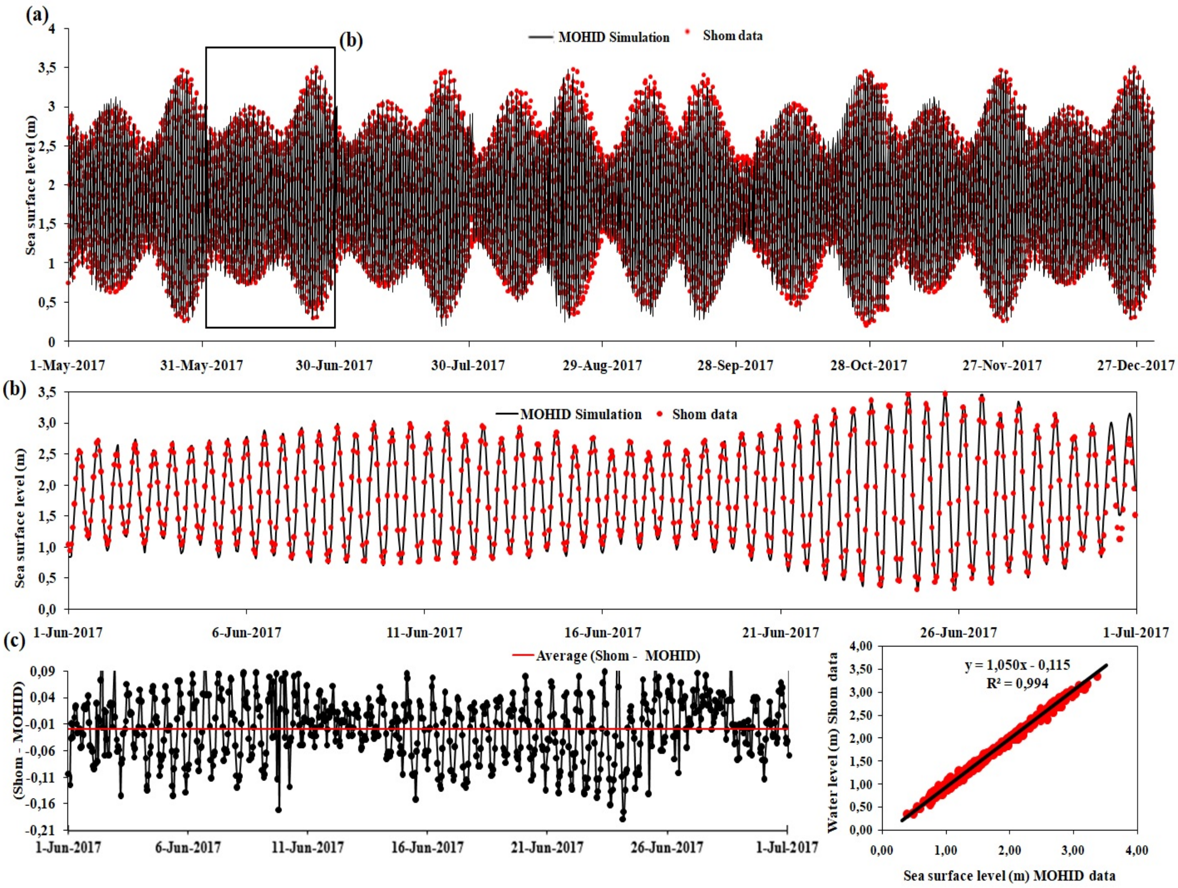

Figure 4.5: Comparison between MOHID simulation (black line) and Shom times series (red dots) of sea surface level (m) at Agadir harbor from (a) 01/05/2017 to 31/12/2017 and (b) 01/06/2017 to 30/06/2017. (c) Difference between Shom data and MOHID forecast for the Agadir harbor, June 2017 (left). Correlation and performance results for the MOHID model vs Shom data (right). R^2 — Squared correlation coefficient.

Table 4.3: Quantitative assessment between MOHID sea surface level outputs and Shom times series at Agadir harbor, June 2017. n — number of observations; R^2— Squared correlation coefficient; RMSE — root mean square error; BIAS — average error; MSS — model Skill Score.

	Average (min-max) MOHID Simulation	**Average (min-max) Shom data**	**n**	R^2	**RMSE (m)**	**BIAS (m)**	**MSS (m)**
Agadir harbor	1.84 (0.29– 3.49)	1.85 (0.31– 3.51)	720	0.99	0.35	0.004	0.99

80 cm near the coast. K1 tidal amplitude presents a pattern like that of M2, increasing toward the inshore areas along the deepest lower Bay. The amplitude of the shallow waters constituent (M4) is negligible over the Bay, but decrease irregularly to the open ocean. In terms of tidal phase, differences in tidal propagation between the northern and southern Bays were found. Indeed, it

Table 4.4: Frequency (cph), amplitude (m) and phase (degrees) of the principal tidal constituents determined from Shom data and computed with MOHID model in Agadir harbor. SNR is the square ratio between amplitude and amplitude error.

Harmonic constituent	Frequency (cph)	Shom Tide Amplitude (m)	Shom Tide Phase (degrees)	SNR	MOHID Simulation Amplitude (m)	MOHID Simulation Phase (degrees)	SNR
Q1	0.0372	0.0171	250.27	43	0.0135	235.48	14
O1	0.0387	0.0457	295.25	0.030	0.0513	287.78	0.02
K1	0.0417	0.0819	45.19	0.012	0.0884	38.61	0.077
J1	0.0432	0.0072	106.38	8.5	0.0108	114.31	9.9
N2	0.0789	0.2473	25.67	29	0.2612	27.35	0.011
M2	0.0805	0.9820	43.16	0.045	1.0223	44.42	0.001
S2	0.0833	0.2633	64.32	35	0.2814	67.35	0.011
M4	0.1610	0.0143	139.40	13	0.0176	147.02	45
M6	0.2415	0.0045	335.82	1.9	0.0143	237.60	26

was found a minor phase delay as M2 tide propagates southward. K1 phase lag is locally lower and follows an inverse pattern, increasing from northern to southern Bay. The lower values of M4 phase were identified close to the Agadir harbor, where the M4 higher amplitudes were found in consequence of the local shallower depths that induce the higher bottom friction.

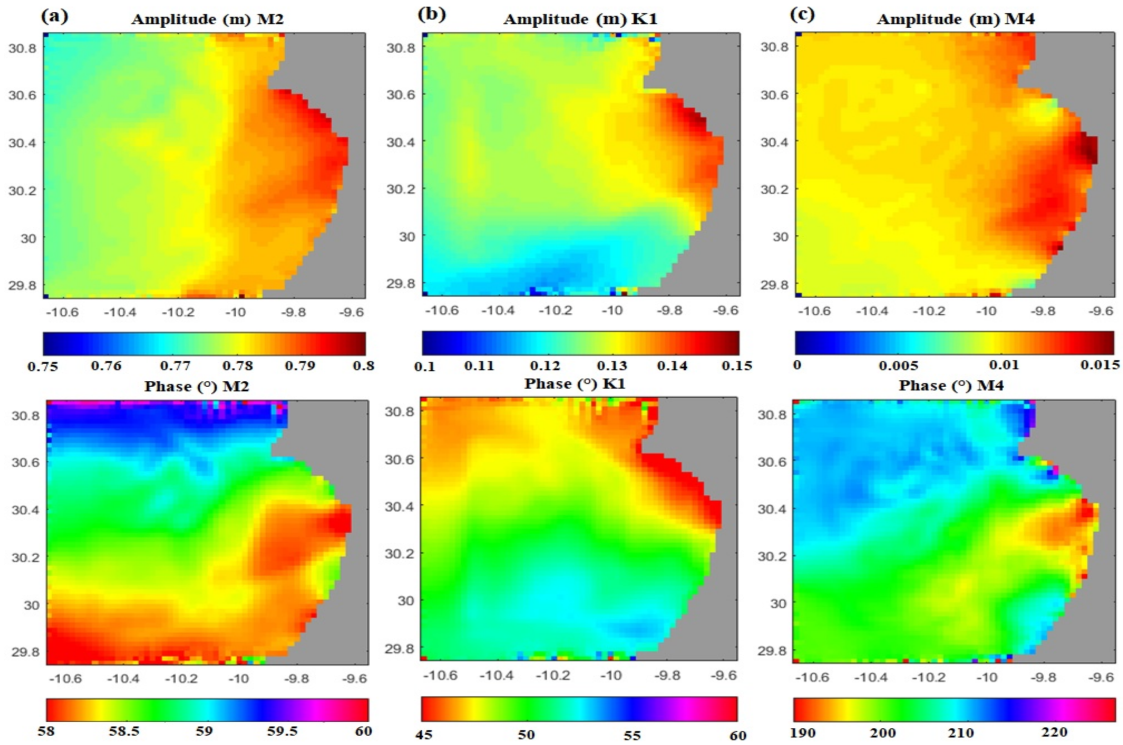

Figure 4.6: Amplitude (m) and phase (degrees UT) for (a) the semi-diurnal, (b) diurnal and (c) non-linear tidal constituents, using the MOHID 3D – Baroclinic model predictions for the Agadir Bay domain. (Note that the color scales are different in each panel of the figure).

4.5.2.2 Water temperature and salinity

• Comparison with in-situ data, satellite and ARGO floats

In-situ data, satellite product and ARGO floats profiles were interpolated over the model grid and compared to the simulated water temperature and salinity. First, the seasonal variation of SST and SSS were analyzed comparing time series of model results and measurements from I. Lamine expedition [244] at S station (30.52N, -9,69W) (Fig. 4.1) from 01/01/2017 to 01/01/2018, considering the availability of data. The surface water warmed up and reached a maximum of 24.95°C in August. In winter, the SST dropped to 16.89 °C by the end of December. The observed data are directly compared with model output, revealing the ability of the model to replicate the seasonal fluctuations of the measured SST data, as shown in Fig. 4.7a. The model did not capture all the observed data, especially the annual variation of SSS (Fig. 4.7b). Indeed, the seasonal cycle of measured SSS was well pronounced, with the lowest value (26.9 psu) occurring in February and the highest (37.9 psu) in August. Next, simulated SSTs are horizontally interpolated for each layer and compared with ODYSSEA satellite imagery for spring, summer, autumn 2017 and winter 2018 (Fig. 4.8). A general decreasing of SST in areas off the Bay and the generation of a coastal band of warmer water during the spring and summer seasons is apparent in both satellites and simulated data. In autumn and winter, the cold Canary Current flows southeastwards across Canary Islands. Visual comparisons between satellite and simulated data indicates that model simulations for SST were reasonably good particularly for the spring and summer seasons.

As for vertical distribution, the model configuration was validated by comparing simulated and observed vertical profiles of water temperature and salinity available for the region under study. ARGO profiling floats data from 2017 was selected for model validation because that was the one with the highest number of buoys within the regional domain. However, the ARGO floats data from the five buoys location (Fig. 4.1; A1–A5) were interpolated for different time instants onto the nearest model grid (Fig. 4.9). The general water temperature and salinity patterns decrease gradually toward the deep waters; high values (20.33 °C and 36.56 psu) were observed at the subsurface and defined an established thermocline and halocline near the surface. At 2000 m depth, the bottom temperature and salinity reached their minimum values of 4.38 °C and 35.16 psu, respectively. A visual comparison between simulated and observed values of water temperature and salinity reveals that model captured reasonably well the observed data at shallow depths. Differences between simulated and observed values were relatively higher at the deep layers, especially in summer.

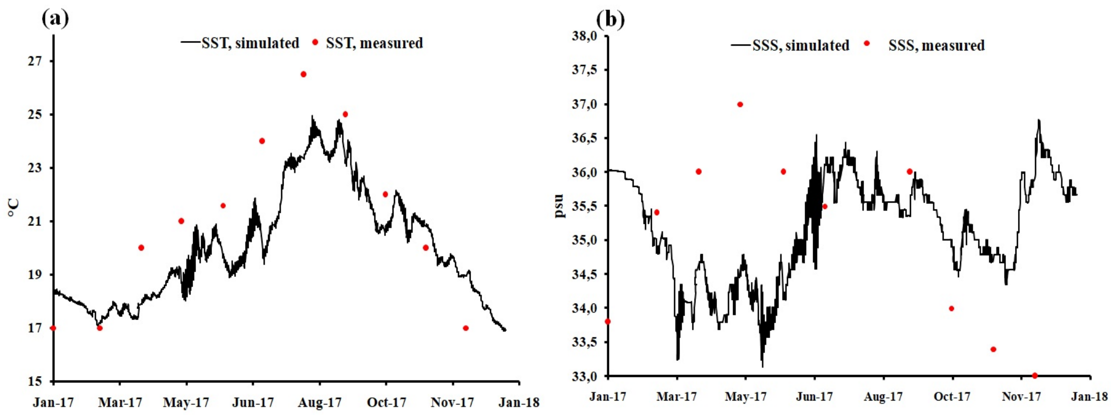

Figure 4.7: Comparison between simulated (black lines) surface seawater temperature (SST, (a)) (°C) and sea surface salinity (SSS, (b)) (psu) (black lines) and the corresponding measurements (red dots) at the surface layer of the Agadir area (station S, 30.52N, -9,69W) for the period January-December 2017.

• **Model skill assessment** A quantitative assessment of model accuracy is given by the performance of the goodness-of-fit statistics (Tables 4.5) and 4.6, where the statistical comparison between observed and simulated horizontal and vertical profiles of temperature and salinity is provided. Overall, the accuracy of the local model configuration to reproduce the seasonal variation of SST of the study region was adequate, as demonstrated by the Pearson and RMSE values of 0.825–2.57 °C, respectively (Table 4.5). Discrepancies with observed values may be explained by the used input values at the inflow boundaries. The agreement is less satisfactory considering SSS temporal distribution, as reflected by a higher RMSE (0.707 psu) and a negligible correlation coefficient (-0.441). Such discrepancies are expected as the area is governed by a large variety of environmental factors that are not accounted in the model (e.g., waves, freshwater discharges from Souss and Massa rivers), leading to some limitations in simulating SSS in the area. Horizontal comparison between simulated and satellite SSTs showed that the spatial thermal structure was adequately reproduced by the model, even if they tend to be

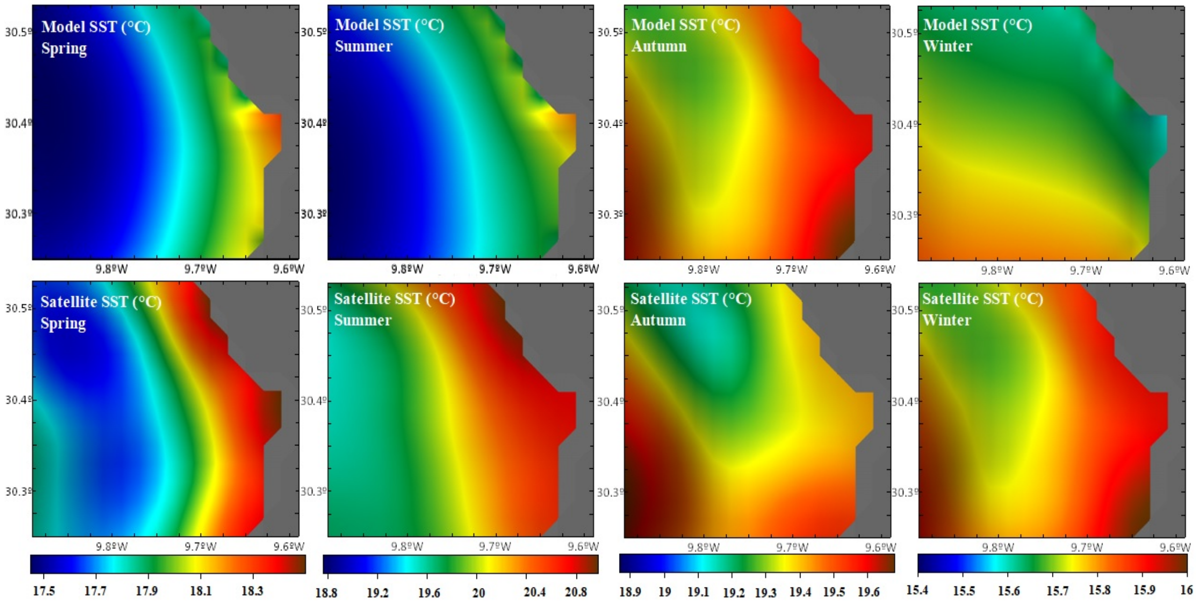

Figure 4.8: Comparison between ODYSSEA seasonal surface seawater temperature (SST) images (top) and MOHID results (bottom) for spring, summer, autumn and winter 2017 periods. (Note that the color scales are different in each panel of the figure).

slightly underestimated in all seasons (BIAS ranging between -0.75 and -0.19 °C) (Table 4.5). Indeed, correlation coefficient higher than 0.73 and RMSE lower than 0.64 °C were obtained for water temperature simulations during the spring season. In contrast, slightly lower correlation coefficient (0.378) and higher RMSE values (0.881 °C) were obtained during the summer season simulation compared to the other seasons. Such a discrepancy could be associated to uncertainties in the model near-shore wind configuration (e.g., [110, 391]), but also considering that satellite data provides skin sea temperature whereas model results correspond to a 1 m thickness layer, leading to an underestimation (BIAS = - 0.752 °C) of simulated SSTs, when compared with the satellite products. These discrepancies corroborate that mentioned in the literature, where differences between 1 and 1.5 °C are detected [420]. Vertically, a good agreement between model simulations and ARGO floats was accomplish, highlighting the appropriateness of the model implemented to reproduce thermocline and halocline patterns and all temperature and salinity vertical variability. The skill assessment confirmed this model-data agreement (Table 4.6). Indeed, correlation coefficients higher than 0.99°C/0.96 psu and RMSE lower than 0.93 °C/0.12 psu were obtained for temperature and salinity comparisons, respectively. A decrease in model accuracy was obtained at deeper depths, in this situation, model simulations tended to underestimate water temperatures and salinity. The largest discrepancies between both datasets occurred for ARGO 4, as demonstrated by RMSE values (0.932 °C – 0.122 psu). This disagreement could be attributed to the turbulence parameterization, satellite maneuvers and algorithm selection. Overall, considering the uncertainties, the complexity of the near-shore processes, the environmental factors that are not accounted in the model, the comparisons with temperature data are reasonable.

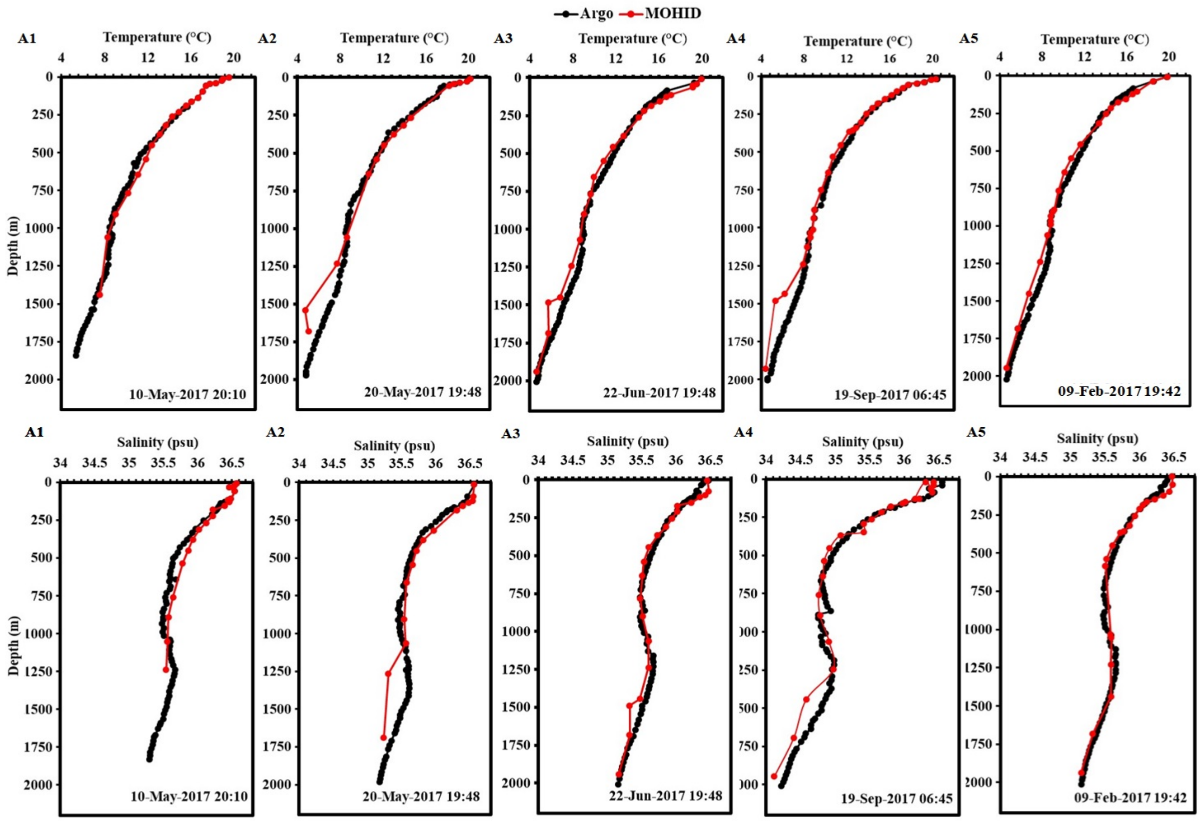

Figure 4.9: Water temperature and salinity comparison between MOHID simulation (red line) and ARGO float (black line) at different location (see Fig. 4.1 for the buoys locations) and time instants. From left to right, A1 (February 9, 2017), A2 (May 10, 2017); A3 (May 20, 2017); A4 (June 22, 2017); A5 (September 19, 2017).

Table 4.5: Quantitative assessment between model results and observations for surface seawater temperature (SST) and surface seawater salinity (SSS) for the period January-December 2017. n—number of observations; r— Pearson correlation coefficient; RMSE—Root mean square error; BIAS—average error.

		Model average	**Observations average**	**n (per day)**	**Pearson (r)**	**RMSE**	**BIAS**
Time series	**SST**	18.98	18.92	12	0.825	2.57	5.103
	SSS	35.133	31.915	12	-0.441	0.707	9.731
Spatial distribution	**Spring**	17.707	17.904	89	0.734	0.636	-0.197
	Summer	19.344	20.096	91	0.378	0.881	-0.752
	Autumn	18.964	19.38	80	0.563	0.716	-0.416
	Winter	15.706	16.002	89	0.730	0.519	-0.295

Table 4.6: Quantitative assessment between model results and observations for vertical profiles of water temperature and salinity. n—number of observations; r— Pearson correlation coefficient; RMSE—Root mean square error; BIAS—average error.

					Water Temperature (°C)			Salinity (psu)		
		Location	**Time**	**n**	**Pearson (r)**	**RMSE**	**BIAS**	**Pearson (r)**	**RMSE**	**BIAS**
Winter	**A1**	30.66N, 12.71W	09/02 19:42	105	0.997	0.817	0.305	0.997	0.074	0.044
Spring	**A2**	30.06N, 10.95W	10/05 20:10	83	0.997	0.363	-0.273	0.987	0.079	-0.497
	A3	30.39N, 11.00W	20/05 19:48	92	0.994	0.641	-0.298	0.965	0.122	-0.021
Summer	**A4**	30.15N, 11.83W	22/06 19:48	53	0.995	0.932	0.484	0.990	0.122	0.060
	A5	30.85N, 12.27W	9/09 06:45	102	0.998	0.447	-1.27	0.993	0.06	0.009

4.5.2.3 Residual circulation and residence time

Even if no current velocities data were available for the model validation, the good agreement between the meteorological data simulations and observations, as well as SSL, temperature and salinity, is a solid indicator of the validity of the implemented hydrodynamic model [394]. From the hydrodynamic model outputs, we can derive more information describing the coastal dynamics of the study region, such as residual circulation and residence time of water. The residual circulation was computed by averaging the transient velocities at each grid cell over the simulation period (from January-2017 to December-2018). Referring to the surface current circulation pattern, the model suggested a residual flow field with a double gyre circulation pattern; a large near-shore cyclonic circulation and another one at the open ocean (Fig. 4.10). Lagrangien simulations provide knowledge about the behavior of tracers released from any location of the model [381].

In what follows, Lagrangian tracers were used to simulate RT from five boxes selected according to previous knowledge of ecological characteristics of the study area [11], from the north to the south (Fig. 4.11a): box 1 limited by Cap Ghir, box 2 represents Anza Beach, box 3 the Souss estuary, box 4 the Massa estuary and box 5 the Southern Bay. Fig. 4.11b represents the instant when the tracers start leaving the Bay, showing their pathway within the Agadir Bay. RT values during July and October 2017, where atmospheric conditions and tidal circulation are strong were selected to represent the temporal variation of RTs (Fig. 4.12).

Overall, the simulation shows that in July all particles leave the Bay during the first 15 days (Fig. 4.12a, b). RT for three northern boxes is 3 days, for box 4 is 6 days and 9 days for the southern Bay (box 5) (Fig. 4.12a). During October, the RTs are 5 days in the northern box 1, 2 days for box 3, 7 days for box 4 and 15 days for the southern Bay (box 5). After 13 days, the water from boxes 1, 2, 3 and 4 was fully renewed (Fig. 4.12a, b). Furthermore, Fig. 4.12c shows that after 6 days during July, the volume of the tracers is below 50% of the total volume of the Bay. During October, the volume of the tracers reaches 50% of the total volume of the Bay after 10 days. This suggests that the RT of the whole Bay displayed a clear temporal variation, with its smallest value in July and largest in October. This variation suggested that during July the Bay

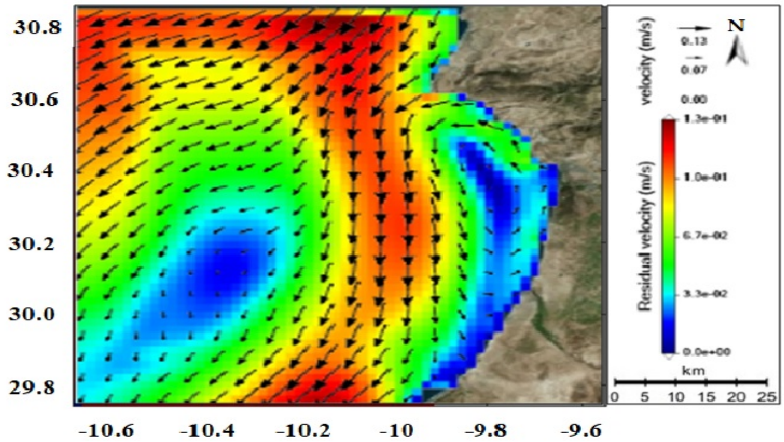

Figure 4.10: Surface residual circulation (ms^{-1}) in Agadir Bay (average of model velocities from January-2017 to December-2018).

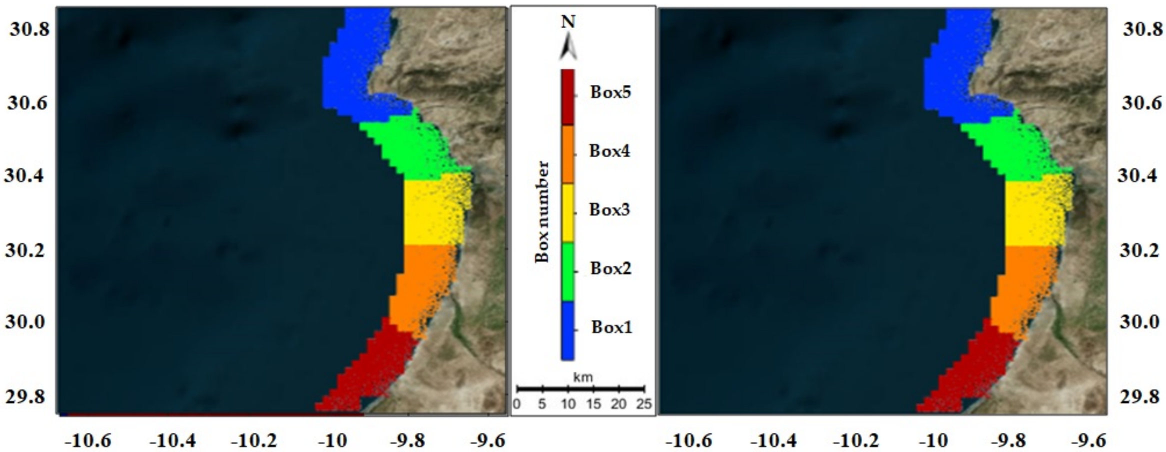

Figure 4.11: Agadir Bay filled with Lagrangian tracers at the beginning of the simulation (a) and after 1 day of simulation (b).

has a short retention for soluble particles, indicating that particles discharged in July would be quickly transported out of the Bay. In contrast, particles released during October have the longest retention time in the Bay.

4.6 Discussion

4.6.1 Hydrodynamic processes

The implementation of models to coastal areas, with scientific or management intentions, should be based on evaluation of their predictive capabilities [40, 206]. Thus, validation should be based on comparison with observed data using goodness-of-fit evaluation measure. In the present

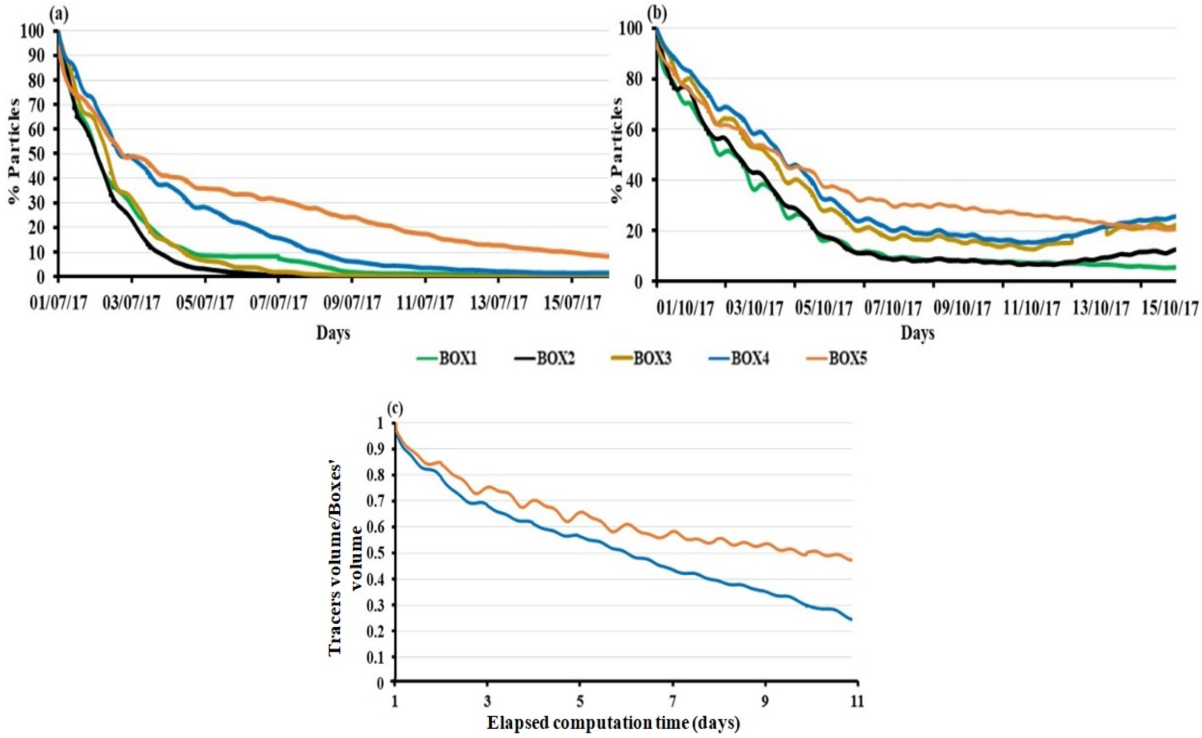

Figure 4.12: Temporal evolution of tracers emitted in each box in (a) summer and (b) winter 2017. (c) Temporal evolution of the ratio between the tracers' volume and the boxes' volume.

work, the use of a simple morphology assessment comparing model results and observations revealed a useful insight into the SSL and the harmonic tidal characterization. The preliminary results highlight the model's accuracy to reproduce the seasonal variability of SSL. Differences in tidal distribution could be attributed to the Bay morphology convergence/divergence, the bottom friction influence and advective effects [138, 139, 330]. The results from amplitude and form ratio ((O1 + K1) / (M2 + S2) [363]) show that the tide is semidiurnal and that its principal tidal component is the principal lunar (M2). This result is consistent with the known mainly semi-diurnal character of the Moroccan Atlantic ocean [13, 28, 307, 320]. As a shallow water constituent, the amplitude of M4 is negligible, but is strongly influenced by changes in the Bay morphology, namely by the shallower depths where the tidal wave from the Atlantic ocean is amplified within the coast according to local topography and low bathymetry [202] modelisation. In addition to the increase in amplitude for shallow areas, a phase delay is observed as tide propagates in the Northward/Southward direction. Moreover, the tides are amplified in the coastal area due to strong shoaling and narrowing effects, reaching more than 0.79, 0.15 and 0.015 m near the Agadir harbor for M2, K1 and M4 constituents, respectively. Therefore, a significant effect of the shallower continental shelves and the coastline concavity was found on local tidal circulation. Moreover, the changes in the local coastal dynamics are reflected in the distribution of water properties. In fact, it was found an important seasonal coastal variability in averaged water temperature, with a mean SST value of 18.9 °C. The thermal gain from the increased air temperature during summer is mainly governed by the meteorological conditions, particularly at the arid to semi-arid setting of Souss [28], which gives rise to the warm water pools. This allowed water evaporation to increase to maximum levels; consequently, SSS reached 37.9 psu in August. During winter, the coastal area displays a distinctive level of water temperature and salinity. However, the SST range was weak, hardly reaching 22 °C, whereas SSS drops to less than 27 psu in February.

Vertical profiles of seawater temperature and salinity revealed a thermocline and halocline near the surface, associated with warmer and saltier surface waters and cooler and fresher deeper waters. This situation seems to be influenced by the weather patterns and the wind induced circulation characterized by the W and NW winds that dominate the study area. The sporadic warm winds "Chergui" occasionally blow from the E, associated with the "Saharan depressions" [27, 28], and may contribute to extreme air temperatures, beyond 30°C in summer 2018. Further, the near-shore circulation could be driven by the local winds acting on the surface. In summer (Fig. 4.13a), an irregular pattern with surface currents (< 0.3 ms^{-1}) is simulated near the shoreline, in consequence of the restrictions to water movement induced by the shallower depths and the higher bottom friction [183]. The predominantly NW winds induce strong southwards near-shore circulation. In the offshore area, surface water moves southwestward and spread with an approximate velocity of 0.4 ms^{-1}. The model velocities are high in comparison to measurements achieved in Cape Ghir (0.1 ms^{-1}, [425]). In winter, the circulation of the surface water masses in the inshore areas is generally NW-directed due to the predominantly S-SE wind conditions. As a result of the interaction between predominantly winds and the coast topography, a large cyclonic eddy dominates the circulation pattern in the inshore area of the Agadir Bay [379].

The analysis of the residual circulation calculated by averaging Eulerian circulation over the simulation period confirms these findings (Fig. 4.10). The lowest residual velocities are found near the coast (< 0.03 ms^{-1}), and the flow vectors induce specific circular distribution. Indeed, the movements of residual circulation pathways reveal the presence of coastal cyclonic eddy, typical of this region. A similar structure was reported in previous studies [192, 273, 297, 391, 425]. This may be induced by the SW-NE orientation of the Bay [244] and by the differences in the bottom friction due to the local bathymetry. As the wind blows over a surface of a variable depth ecosystem, it accelerates the shallow waters more strongly than the deeper waters [271].

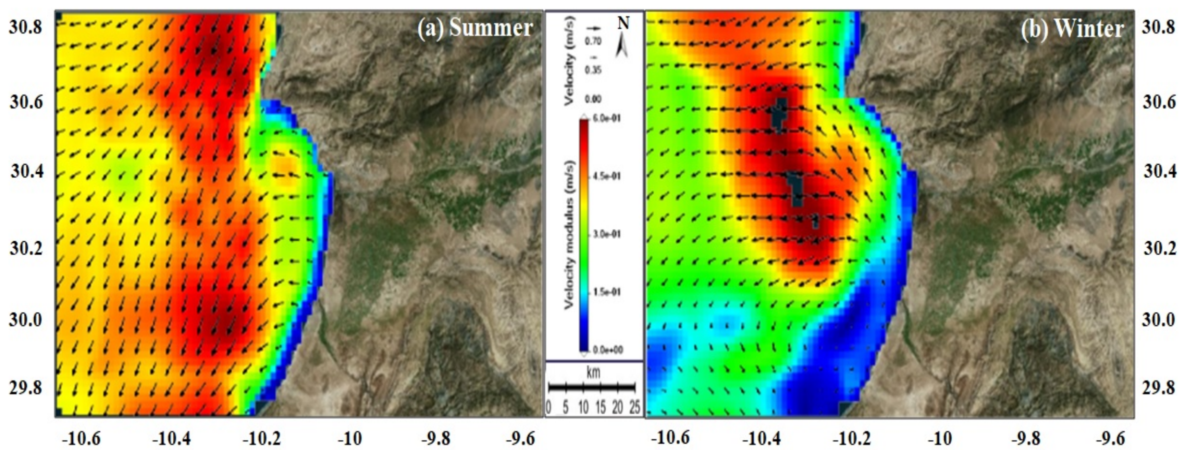

Figure 4.13: Simulated velocity modulus (ms^{-1}) at the surface of Agadir Bay averaged over summer 2017 (a) and (b) winter 2018 seasons.

4.6.2 Particles trajectories and residence time

The behavior of the tracers shows its quick response to the Agadir Bay hydrodynamics'. This is noticeable from the time-space distribution of the RT, with lower RTs ranging from 3 to 9 days in summer and higher RTs ranging from 5 to 15 days in winter, depending on box location. These results remain low in comparison to the other studies; e.g., Tagus estuary, Portugal (between 10 and 20 days, [167]); Marennes-Oléron Bay, French Atlantic coast (10 days, [134]).The shortest RTs in the northern boxes may be explained by the slow mixing between box waters and incoming waters form the Atlantic Ocean. Tracers were transported by the surface currents in the coastal boundary layer, which is part of a large near-shore cyclonic eddy. Tracers originating north of the Bay left these areas over a shorter time and transported to the south, when winds blew from the NW. Nevertheless, RTs of tracers released in areas along the southern Bay of the region was longer.

The local geomorphology restricts tracer's circulation at the southern boxes, within which tracers are trapped for a long time, but allows released tracers to scatter faster in the northern box in response to the typical hydrodynamic activities favored by the coastline shape and the orientation of the Cape. The investigation of the residual circulation pathways corroborates these outcomes (Fig. 4.10). Indeed, it appeared that tracers are trapped inside a large near-shore cyclonic eddy which favors their northward movement and decrease RT in the northern Bay. Other factors as winds, the Bay-shelf water exchange [145, 224, 284, 357, 373, 472, 501], and tidal exchange [284, 387] contribute to regulate the spatial and temporal variation of RT.

Such outcomes are well aligned with [501] results for the average RT in the Daya Bay (South China Sea), obtained using a 3D barotropic model and considering the large-scale coastal circulation in the open boundaries (upwelling, downwelling). Under these conditions they found 16 days for tidal forcing, and 18 days when the waves are considered. The obtained higher RT in summer was related to the mean surface circulation as the water column is stratified during this season, whereas the lower RT in winter was linked with the depth-mean circulation as the water column is mixed. Accordingly, the tides increase the RT whereas the winds reduce the RT by increasing local surface wind–driven circulation.

4.6.3 Model improvement

Main limitations in the present model implementation could be attributed to the scarcity of field measurements that may have limited the validation of some model outputs. In fact, deviations in the simulated surface salinities were somewhat expected, since there river discharges were not incorporated in the model. Therefore, improved model skills may be gained by integrating freshwater drainage in the model implementation. In addition, the resolution of the imposed WRF forcing should be enhanced to better address the wind field variability.

It is worth noting that this was a preliminary investigation, which aims to contribute to increase the knowledge about an important area that has been practically unexplored to date from the hydrodynamic point of view. Notwithstanding, to get a more realistic picture of the main dynamic features of the study area, a more robust validation with extensive field measurements with greater spatial extent over a longer period should be carried out. This would require additional validation of the coastal circulation and of the dispersal of passive tracers against in-situ Eulerian (ADCPs) or Lagrangian (surface drifters) data.

4.6.4 Conclusion

A 3D MOHID hydrodynamic model coupled with a Lagrangian transport model was implemented and validated for the Agadir Bay (Moroccan Atlantic coast) to analyse hydrodynamic functioning and estimate the RT of the study area. The model was calibrated and validated against meteorological conditions, sea surface level, harmonic tidal constituents, water temperature and salinity using a combination of available in-situ measurements, satellite, and ARGO floats data. Nevertheless, it was clear that the available data were limited and more current speeds and directions are needed to perform a comprehensive model calibration and validation study in the future.

Bearing in mind the weaknesses precisely above, quantitative and qualitative assessment of model accuracy revealed a reasonable validation of the model, which highlights the ability of the model in reproducing dynamic behavior in the regional-scale atmospheric and hydrodynamic of the Bay. The area is mainly characterized by relatively high air temperature (maximum of 30°C), high relative humidity (maximum of 95%), dominated westerly and northwesterly wind directions and governed by the semidiurnal tide (M2).

The analysis of the water temperature and salinity vertical structures revealed that the thermocline and halocline were located near the surface layers. Relatively warmer and saltier seawater occupied the surface water, while the deep waters were relatively cool and fresh. The interaction between Bay's topography and the local wind stress could induce a double-gyre circulation a large near-shore cyclonic circulation and another one at the open ocean. Winter season conditions consist of high level of winds speed coming predominantly from the S-SE resulted in increased horizontal velocities, which predominantly flow northwestward. In contrast, local NW winds drive the offshore surface water to the south during the summer season conditions.

Lagrangien simulations provide information about the RT and the possible pathways of surface passive tracers. Lower RTs (from 3 to 9 days) were found in summer, and higher (from 5 to 15 days) in winter. The tracers are trapped inside a coastal cyclonic eddy, favoring the northward transport and the RT increase in the southern Bay, making this a coastal region susceptible to pollution. Nevertheless, validation of Lagrangian simulations against observed surface tracers' trajectories should be performed to assure the reliability of the model results. An assessment of different scenarios for dispersal of passive tracers should be accomplish in the future, to consolidate the knowledge about dispersion of polluted particles as well as their area of accumulation within the Agadir Bay.

CHAPTER 5

MODELING INVESTIGATION OF THE NUTRIENTS AND PHYTOPLANKTON DYNAMICS IN THE MOROCCAN ATLANTIC COAST: A CASE STUDY OF AGADIR COAST

5.1 Résumé du chapitre

Les résultats de ce chapitre ont fait l'objet d'un article publié en 2021 au journal "*Ecological Modelling*" (https://doi.org/10.1016/j.ecolmodel.2021.109510). **Dans ce chapitre :**

Pour contrôler la prolifération du phytoplancton dans les zones côtières, il est essentiel de comprendre les facteurs limitant la croissance, qui peuvent être la température, l'azote (N), phosphore (P), silicium (Si) ou d'autres facteurs environnementaux [108, 157]. En général, les eaux douces sont souvent considérées limitées en P en raison d'un rapport N:P élevé dans les sources fluviales [163] et de la fixation de l'azote [399], tandis que les eaux marines sont souvent considérées comme étant principalement limitées en N en raison de la libération de P par les sédiments, de la lenteur de la fixation de l'azote et de la dénitrification élevée [343]. Les estuaires se trouvent dans les zones de transition entre les systèmes d'eau douce et les systèmes marins, et présentent donc souvent des schémas plus complexes de limitation des nutriments [108]. L'information est rare lorsqu'il s'agit de la dynamique du phytoplancton dans la baie d'Agadir. Dans ce contexte, pour comprendre la distribution saisonnières et spatiales des nutriments inorganiques dissous, et leur contribution à la croissance du phytoplancton dans la baie d'Agadir, un modèle 3D hydrodynamique-biogéochimique à haute résolution est mis en œuvre. Un accent particulier a été consacré au décryptage de la dynamique des assemblages planctoniques (Chl-a, diatomées et flagellés), en réponse aux variable physico-chimiques (température de l'eau, salinité et DO) et à la disponibilité des nutriments inorganiques dissous (NO_3,PO_4 et SiO_4). Le performance du modèle a été évaluées par rapport à des produits satellitaires (ODYSSEA pour la SST et MODIS pour le Chl-a) et des données climatologiques (WOA2018). Malgré certaines divergences dans la distribution temporelle de la SSS et de l'OD qui sont probablement attribuées à des processus manquants et à certaines lacunes dans le cycle hydrologique du modèle atmosphérique, les résultats ont démontré une représentation satisfaisante de la SST, de la Chl-a, et un accord raisonnable dans le modèle saisonnier des nutriments inorganiques. A partir des concentrations en nutriments et des rapports stœchiométriques; on peut affirmer que les niveaux de NO_3 peuvent être l'élément clé contrôlant la distribution du phytoplancton dans la baie d'Agadir. Le rapport moyen N:P était inférieur au rapport classique de Redfield de 16:1 (N:P = 0.4), ce qui suggère que la plupart de l'azote disponible a été incorporé par le phytoplancton (largement dominé par les flagellés) dans le cycle biogéochimique local et fait évoluer la zone vers une limitation de l'azote. Par contre, le faible rapport N:P pourrait être attribué à la plus grande absorption d'azote par les flagellés, à l'injection possible de phosphore par les filaments d'upwelling associés à un tourbillon cyclonique ou au recyclage plus rapide du phosphore par rapport à l'azote dans les eaux côtières de surface. Les fortes concentrations simulées de SiO_4 conduisent à un appauvrissement stœchiométrique en P par rapport à Si (rapports Si:P > 16:1) et à une forte déficience en N par rapport à Si (rapports N:Si < 1:1) dans notre zone d'étude. En outre, la distribution du phytoplancton révèle les plus grandes réponses aux niveaux de nutriments et aux paramètres environnementaux avec une grande variabilité saisonnière. Les flagellés ont dominé le Chl-a total dans les couches supérieures de la colonne d'eau pendant les périodes de printemps et d'été coïncidaient avec le réchauffement des températures de l'eau, des salinités plus élevées, une stratification intense et des concentrations plus faibles de nutriments (NO_3 et PO_4). Alors qu'une augmentation considérable de la biomasse des diatomées a été simulée après l'été en réponse à une température de l'eau plus basse et à des concentrations en SiO_4 plus élevées. Ceci a des répercussions majeures sur le flux de carbone dans la zone, car les assemblages phytoplanctoniques dominés par les flagellés contribuent à une faible exportation de carbone vers les eaux plus profondes par rapport aux diatomées [126].

5.2 Abstract

Although the environmental status of the Moroccan Atlantic coastal waters has been researched in previous studies, there is still a lack of knowledge about its biogeochemical functioning. Especially for the Agadir coast where measurements are quite scarce, realistic ecological models can help identifying the key mechanisms driving fluctuations in such coastal areas. Here we implemented a three-dimensional (3D) coupled hydrodynamic-biogeochemical model in order investigate the time-space distribution of inorganic nutrients (NO_3, PO_4 and SiO_4), and their control on phytoplankton (diatoms, flagellates) biomass on the Agadir coast. Model performance was evaluated against satellite observations and climatology data. The model achieved satisfactory representation of the sea surface temperature, chlorophyll-a, and a reasonable agreement in the seasonal pattern of inorganic nutrients. Based on nutrient concentrations and their stoichiometric ratio; the study points to nitrate as the key factor controlling phytoplankton distribution (largely dominated by flagellates). Nitrate depletion occurs faster than phosphate and silicate, thus driving the area towards nitrogen limitation.

Key–Words : Biogeochemical model, Agadir coast, diatoms, flagellates, nitrogen limitation.

5.3 Introduction

Sustained by upwelling events and interactions with terrestrial inputs, the coastal waters off North-West Africa in the Canary Current System including the Moroccan Atlantic coast are very productive in terms of phytoplankton biomass (Chl-a up to 10 $mg.m^{-3}$) and primary production (up to 5 $gCm^{-2}.d^{-1}$) [32, 33, 249]. This makes this coast a very productive area in terms of pelagic and demersal resources [32, 97]. Recently, coastal development has been unavoidable in parallel with economic growth within Morocco. Consequently, coastal marine ecosystems have been disrupted and several environmental problems have occurred, such as pollution of coastal water, eutrophication, depletion of fish diversity and degradation of marine ecological habitats [10, 64].

Understanding and managing the ecological changes occurring under climatic and anthropogenic pressure is a scientific and coastal manager's challenge as well. Within this context, numerical models could contribute to the coastal management improving the current knowledge on the nutrients and plankton dynamics, supplementing the time-space constraints of observations. Over the last years, there has been an increase in the use of models as management support tools to describe the water quality of coastal and marine environments; CE-QUAL-W2 (e.g., [112, 506]), QUAL2E (e.g., [73, 419]), RWQM (e.g., [124]), WASP7 and 8 (e.g., [85, 105, 237]).

The Agadir coast, part of the Moroccan Atlantic coastal areas, was chosen for the development of a numerical coastal model for North-West Africa. Given its geographical location as a part of the Canary Current System, the concavity of its coastline and the influence of the Atlas Mountains, the area is characterised by a permanent upwelling, responsible for a high productivity [21]. It is, therefore, an important resource for fishing, aquaculture and recreational activities which has been under local impacts, typically associated with strong human pressure, industrial and urban expansion; dredging and pollution discharges disturb its ecological balance [11, 12, 244, 324]. Understanding the ecological behaviors of this area remains necessary to address coastal management questions. Unfortunately, given the limited spatial and temporal coverage of observation networks, a major part of the Moroccan Atlantic coastal waters, including the Agadir coast suffers usually from data sparsity. The information is poorer when it comes to biogeochemical field data.

A coupled modeling system able of comprehensively capturing the cycle of biogeochemical processes occurring in water column could facilitate ecological analysis of ecosystem dynamics, making it a useful tool for investigating nutrient and plankton variability in coastal areas. Although the biogeochemical variables in the coastal areas off the Canary Current System (North-West Africa) has been restrictively discussed in previous studies (e.g.,[34, 199, 200, 273, 274, 391]), there is still a lack of knowledge about its biogeochemical functioning of the Agadir coast. To our knowledge, no high-resolution numerical model has yet been implemented to describe the biogeochemical properties of this area. To fulfil these knowledge gaps, the biogeochemical dynamics of lower trophic levels of the Agadir coast through the development and the assessment of a three-dimensional (3D) MOHID Water modelling system has been investigated. The flexibility of the MOHID Water allows the simulation of a large variety of ecological, physical and chemical processes occurring in the water column, sediment and air interfaces, being so, considered a powerful tool to investigate the dynamic aquatic ecosystems [92, 138, 146, 300, 361]).

The main purpose of this study is to provide a decision support tool for coastal management of North-West Africa (Moroccan Atlantic coast). To accomplish this objective, numerical simulations of a high-resolution local configuration of 3D MOHID Water are performed over the Agadir coastal waters. Special emphasis is given to describe the spatio-temporal distribution of inorganic dissolved nutrients, and their contribution to phytoplankton (diatoms and flagellates) dynamics. Time-series, surface and depth maps of the simulated physicochemical fields (including water temperature, salinity and dissolved oxygen), inorganic nutrients (nitrate, phosphate and dissolved silica) and planktonic assemblages (chlorophyll-a, diatoms, flagellates and zooplankton) are carried out for the period 2017-2018; selected according to the data availability. Model validation is investigated by comparing simulated surface variables with monthly climatological and remote sensing data. A quantitative validation using statistical (correlation coefficient, difference of mean values, standard deviation and root mean square errors) and graphical analysis (Taylor diagram) are then executed to assess the model performance. Finally, the dynamic of phytoplankton and their response to nutrients and environmental factors variations are discussed and pertinent conclusions are summarized.

5.4 Materials and methods

5.4.1 Study area

Located on the south-western Atlantic coast of Morocco, the Agadir coast is the central part of a 35 km long shoreline bound between Cape Ghir in the north and Cape Aglou in the southwest (Fig. 5.1). The coast exhibit wide morphological and geological variation. It is characterized by an alternation of rocky coast in the north and sandy coast in the south [27]. The orientation of the coast towards the west generates an important upwelling event because of its shallow depth and the constant regularity of the northeast (NE) winds in this area [321].

Agadir Bay and the adjacent smaller Anza beach north of the commercial port are the most important morphological characteristics of the region. Influenced by the Atlas Mountains, the Atlantic ocean and Sahara, the area is characterized by an arid to semi-arid climate [29]. Average annual temperatures range from 14°C in winter and 26.7°C in summer although temperatures may rise to over 40°C under the influence of Sahara winds [244]. The rainy season mainly occurs in the fall and in the first weeks of winter with average annual rainfall of about 300 mm/year according to data obtained from the Regional Office of the Development of Agricultural Souss Massa. Relatively energetic waves from the North largely dominate the area in both winter and summer, presenting approximately 67% of the incident waves and only 5.75% from the south. Furthermore, the dominant winds in the area are from the west-northwest (WNW) to the west (W), favourable for the generation of Aeolian dunes in the semi-arid climate of Souss Massa.

The area is mainly governed by mesotidal and semidiurnal tides with a mean neap tidal range of 1.3 m and a mean spring tidal range of 2.9 m. Tidal currents was relatively weak (order of 0.1 $m.s^{-1}$) and maintained a circular pattern within the coast [28].

5.4.2 Model description

Numerical simulations are performed using MOHID Water Modelling System (`www.mohid.com`). The model consists of a set of coupled modules that aim to simulate the main physical and biogeochemical processes in aquatic ecosystems [310]. It is based on the finite volume concept, where the equations are applied macroscopically at each cell in the grid, using divergent flux that assures the conservation in the transport of properties. The hydrodynamic model solves the momentum and primitive continuity equations for the surface elevation supposing hydrostatic and Boussinesq approximation [455].

Furthermore, the model is implemented assuming a semi-implicit time step integration for

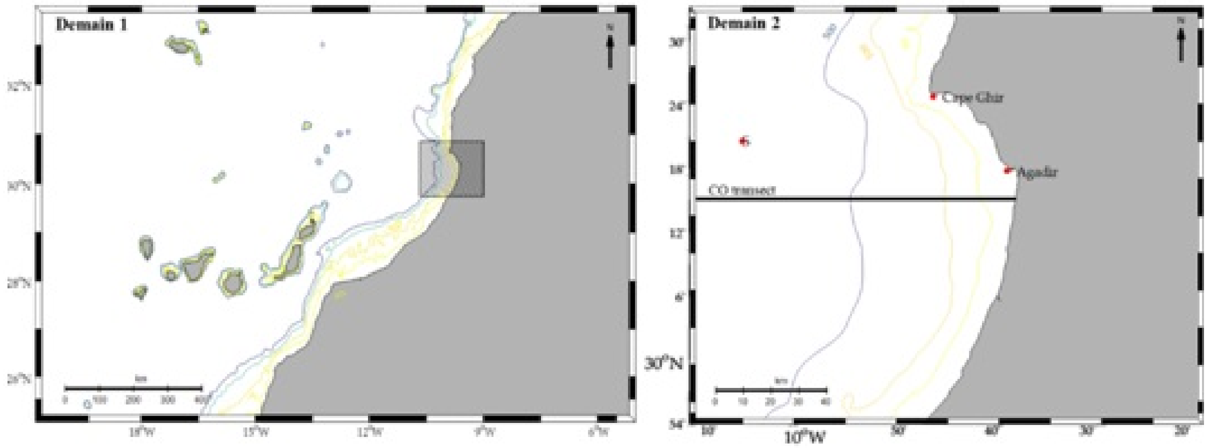

Figure 5.1: Downscaled model domain from Domain 1 (4km resolution) to Domain 2 (2km resolution) with bathymetric contours. "S" indicate the position of the investigated station (30.5N, -10.5W) used for time series validation. The "CO" transect is labeled as a black line.

its temporal discretization, using a Cartesian and sigma coordinates for its vertical discretization and an Arakawa C grid for its horizontal discretization [294]. The transport event for a given biogeochemical property (P), are calculated using a 3D advection-diffusion differential equation [84].

$$\frac{dP}{dt} = \frac{\partial P}{\partial t} + u_j \frac{\partial P}{\partial x_j} = \frac{\partial}{\partial x_j}\left(k_\theta \cdot \frac{\partial P}{xj}\right) + (\text{ Sources } - \text{ Sink }) \tag{5.1}$$

Where P is the property concentration, j is the index for the Cartesian coordinate (x,y,z), k is the turbulent mass diffusion coefficient. The sink and source terms for biogeochemical properties are computed in each cell of the grid, and in each time instant using a biogeochemical model [394]. The state variables and processes are computed for a control volume, regardless of any transport scheme. The control volume approach consists of splitting the water body into finite segments (or control volumes) [94], solving for each one of them a series of linear equations representing the interdependence of various properties and calculating the mass balances considering the sources and sinks within each volumes. The biogeochemical processes are mainly adapted based on formulations originally developed by the US Environmental Protection Agency (EPA) [513]. The conceptual structure and the accounted processes are reported in Fig. 5.2. Model state variables as well as a list of parameters values are given in tables 5.1 and 5.2. Thus, inorganic and detrital organic forms of nitrogen (N), phosphorus (P) and silica (Si) have been explicitly simulated, being are driven by very different remineralisation rates. The ammonia (NH_4) equation considers respiration, mineralisation processes, phytoplankton uptake as well as the fraction of phytoplankton and zooplankton mortality that is directly supplied into the system. In oxygenated water column, NH_4 is oxidized to NO_3 by nitrification and conversely, NO_3 is lost by denitrification to nitrogen gas (N_2). The kinetics of denitrification reaction is simulated as a function of NO_3, dissolved oxygen (DO) and temperature availability in the system [31].

The model considers the organic and inorganic phosphorus forms; the inorganic phosphorus (PO_4) considers mineralisation processes, phytoplankton uptake as well as the fraction of phytoplankton and zooplankton mortality that is released into the water column in inorganic form. Fraction of the organic phosphorus settles to the sediment and another part is mineralized into

PO_4. The DO mass balance equation considers the production of oxygen by primary producers, the consumption of oxygen and the exchange of oxygen between water column and atmosphere. The model considers two major groups of producers in the ecosystem, diatoms (Dia) and autotrophic flagellates (Fla) and various organic matter components. Primary producers' uptake inorganic nutrients (NH_4,NO_3,PO_4 and dissolved silica (DSi)) and follow an exponential growth model. Their variation is dependent on several factors mainly, oxygen, light incidence, and nutrients availability [185]. The process is governed by equation:

$$\frac{\mathrm{d}\Phi_{\mathrm{Phy}}}{\mathrm{dt}} = \left(\mu^{\mathrm{Phy}} - r^{\mathrm{Phy}} - ex^{\mathrm{Phy}} - m^{\mathrm{Phy}}\right).\Phi_{\mathrm{Phy}} - G^{\mathrm{Phy}} \tag{5.2}$$

Were t is time (day); Φ_{Phy} is phytoplankton biomass ($mgC.L^1$); μ^{Phy} is gross growth rate (day^1); r^{Phy} is total respiration rate (day^1); ex$^{\mathrm{Phy}}$ is excretion rate (day^1); m^{Phy} is natural mortality rate (day^1); G^{Phy} is grazing rate (day^1) (More equations are given in Appendix).

Phytoplankton growth rates are linearly dependent on nutrient uptake rates [460]. The model assumed also that both zooplankton (mirozooplankton (ciliate) and mesozooplankton) types are simulated with Redfield Ratio (106C:16N:1P) such that their growth relies on the grazing rate and maximum growth rate. Grazing, in turn, depends on food density and size as well as the food encounter rate. The microzooplankton graze on flagellates and detrital particulate matter whereas the mesozooplankton graze on diatoms, flagellates, and microzooplankton at rates determined by zooplankton swimming speed, food size and density, and particle encounter rate [45]. Grazing and mortality result in the accumulation of detritus, and dissolved inorganic and organic nutrients through remineralisation. Dissolved organic material (refractory dissolved organic nitrogen (DONr), refractory dissolved organic phosphorus (DOPr), dissolved non-refractory organic nitrogen (DONnr) and non-refractory dissolved organic phosphorus (DOPnr), dissolved silica) are simulated with Redfield Ratio (106C:16N:1P). Particulate organic material (particulate organic nitrogen (PON), particulate organic phosphorus (POP)) are remineralised to NH_4 and PO_4, respectively, and biogenic silica (BSi) to DSi. They are generally produced by inefficient feeding, plankton mortality, and zooplankton excretion. During these transformations, DON is released in the water column and rendered available to the phytoplankton either as NH_4. The DOP is mineralized to PO_4 and rendered become available to the phytoplankton.

Table 5.1: Model state variables.

State Variable	Units
Organism	
Flagellate	mgC/L
Diatom	mgC/L
Mesozooplankton	mgC/L
Ciliate (Microzooplankton)	mgC/L
Nitrogen	
Ammonia	mgN/L
Nitrite	mgN/L
Nitrate	mgN/L
Particulate Organic Nitrogen	mgN/L
Dissolved Organic Nitrogen Non Refractory	mgN/L
Dissolved Organic Nitrogen Refractory	mgN/L
Phosphorus	
Inorganic Phosphorus	mgP/L
Particulate Organic Phosphorus	mgP/L
Dissolved Organic Phosphorus Non Refractory	mgP/L
Dissolved Organic Phosphorus Refractory	mgP/L
Silica	
Dissolved Silica	mgSi/L
Biogenic Silica	mgSi/L
Oxygen	
Dissolved Oxygen	mgO_2/L

Table 5.2: Model parameters.

Parameter	Units	Value	Reference
Nitrogen			
PON decomposition rate at reference temperature	d^{-1}	0.1	[444]
PON decomposition temperature coefficient	–	1.02	[136]
DONre mineralization rate at reference temperature	d^{-1}	0.01	[362]
DONre mineralization temperature coefficient	–	0.02	[362]
Nitrification rate at reference temperature	d^{-1}	0.06	[362, 449]
Nitrification half-saturation constant	mgO_2/ L	2	[160]
Denitrification half-saturation constant	mgO_2 L	0.1	[283]
Nitrification temperature coefficient	–	1.08	[160]
Denitrification rate at reference temperature	–	0.125	[160]
Denitrification temperature coefficient	d^{-1}	1.045	[160]
DONnr mineralization rate at reference temperature	d^{-1}	0.1	[336]
DONnr mineralization temperature coefficient	–	1.02	[136]
Phosphorus			
POP mineralization rate at reference temperature	d^{-1}	0.2	[444]
POP mineralization temperature coefficient	–	1.08	[160]
DOPre mineralization rate at reference temperature	d^{-1}	0.03	[160]
DOPre mineralization temperature coefficient	–	1.064	[456]
DOPnr mineralization rate at reference temperature	d^{-1}	0.1	[283]
DOPnr minreralization temperature coefficient	–	1.064	[456]
Phosphorus or. Nitrogen			
Nutrient regeneration half-saturation constant	–	1	[136]
Fraction of PON available for mineralization	–	0.7	[136]
Silica			
Biogenic silica dissolution rate in the water column at the reference temperature	d^{-1}	0.03	[160]
Biogenic silica dissolution temperature coefficient	–	1.02	[160]

Oxygen			
Oxygen/carbon ratio in CO2	–	2.67	[136]
Photosynthesis oxygen/carbon ratio	–	2.67	[456]
Oxygen/nitrogen ratio in nitrate	–	3.43	[136, 444]
Oxygen/nitrogen ratio in Phosphate	–	2.06	[136, 444]
phytoplankton oxygen/carbon Ratio	–	2.67	[136]
Mesozooplankton respiration oxygen/carbon ratio	–	2.67	[136]
Microzooplankton respiration oxygen/carbon ratio	–	2.67	[136]
Bacteria oxygen/carbon ratio (Redfield)	–	1.4	[362]
Organic matter nitrogen/carbon ratio (Redfield)	–	0.18	[136]
Organic matter phosphorus/carbon ratio (Redfield)	–	0.024	[136]
Minimum oxygen concentration for growth	–	10e-5	[362]
Flagellates			
Flagellates maximum gross growth rate	d^{-1}	2.0	[160, 248]
Endogenous respiration constant for flagellates	d^{-1}	0.0175	[160, 362]
Fraction of actual photosynthesis which is oxidized by photorespiration for flagellates	–	0.125	[136]
Excretion constant for flagellates	–		[136, 362]
Maximum mortality rate for flagellates	d^{-1}	0.07	[362]
Mortality half-saturation rate for flagellates	mgC/L.d^{-1}	0.02	[136, 362]
Assimilation efficiency of the flagellates by zooplankton		0.3	[362]
Nitrogen half-saturation constant for flagellates	d^{-1}	0.5	[136, 446]
Phosphorus half-saturation constant for flagellates	mgN/L	0.014	[160, 456]
Optimum light intensity for flagellates photosynthesis	mgP/L	0.001	[160]
Minimum temperature of the optimal interval for flagellates photosynthesis	W/m^2	121	[160]
Maximum temperature of the optimal interval for flagellates photosynthesis	°C	13	[136]
Minimum tolerable temperature for flagellates photosynthesis	°C	25	[136]
Maximum tolerable temperature for flagellates photosynthesis	°C	5	[136]
Constant1 to control temperature response curve shape on flagellates	°C	35	[136]
Constant2 to control temperature response curve shape on flagellates	–	0.05	[313]
Constant3 to control temperature response curve shape on flagellates	–	0.98	[136]
Constant4 to control temperature response curve shape on flagellates	–	0.98	[313]
Flagellates nitrogen/carbon Ratio	mgN/mgC	0.18	[160, 161]
Flagellates phosphorus/carbon Ratio	mgP/mgC	0.024	[160, 161]
Fraction of soluble inorganic material excreted by flagellates		0.4	[136, 362]
Fraction of dissolved organic material excreted by flagellates	–	0.5	[136, 362]
Diatoms			
Diatoms maximum gross growth rate	d^{-1}	3	Calibrated
Diatoms endogenous respiration constant	d^{-1}	0.0175	[160, 362]
Fraction of actual photosynthesis which is oxidized by photorespiration for diatoms	–	0.125	[136]
Diatoms excretion constant	–	0.07	[136, 362]
Maximum mortality rate for diatoms	d^{-1}	0.02	[362]
Half-saturation for mortality for diatoms	mgC/L.d^{-1}	0.3	[136, 362]
Assimilation efficiency of diatoms by zooplankton	d^{-1}	0.8	[136, 446]
Nitrogen half-saturation constant for diatoms	mgN/L	0.015	[160]
Phosphorus half-saturation constant for diatoms	mgP/L	0.002	[160]
Silicate half-saturation constant for diatoms	mgSi/L	0.08	[160]
Optimum light intensity for diatoms photosynthesis	W/m^2	121	[136]
Minimum temperature of the optimal interval for diatoms photosynthesis	°C	8	[136]
Maximum temperature of the optimal interval for diatoms photosynthesis	°C	10	Calibrated
Minimum tolerable temperature for diatoms growth	°C	4	[136]
Maximum tolerable temperature for diatoms growth	°C	37	[136]
Constant1 to control temperature response curve shape on diatoms	–	0.1	Calibrated
Constant2 to control temperature response curve shape on diatoms	–	0.98	[160, 161]
Constant3 to control temperature response curve shape on diatoms	–	0.98	[160, 161]
Constant4 to control temperature response curve shape on diatoms	–	0.02	[136]

Diatoms nitrogen/carbon ratio	mgN/mgC	0.18	[136]
Diatoms phosphorus/carbon ratio	mgP/mgC	0.024	[48]
Diatoms silica/carbon ratio	mgSi/mgC	0.6	[160]
Fraction of soluble inorganic material excreted by diatoms	–	0.4	Calibrated
Fraction of dissolved organic material excreted by diatoms	–	0.5	Calibrated
Mezooplankton			
Zooplankton maximum gross growth rate	d^{-1}	0.15	[136, 160]
Zooplankton nitrogen/carbon ratio	mgN/mgC	0.15	[160]
Zooplankton phosphorus/carbon ratio	mgP/mgC	0.024	[160]
Soluble inorganic fraction on the zooplankton excretions	–	0.4	Calibrated
Dissolved organic fraction excreted by zooplankton	–	0.5	Calibrated
Minimum temperature of the optimal interval for zooplankton growth	°C	13	Calibrated
Maximum temperature of the optimal interval for zooplankton growth	°C	25	[136]
Minimum temperature zooplankton growth	°C	5	[136]
Minimum temperature of the optimal interval for zooplankton growth	°C	35	[136]
Constant1 to control temperature response curve shape	–	0.05	[313]
Constant2 to control temperature response curve shape	–	0.98	[313]
Constant3 to control temperature response curve shape	–	0.98	[313]
Constant4 to control temperature response curve shape	–	0.02	[313]
Rate of zooplankton consumption of carbon by respiration and non-predatory mortality	d^{-1}	0.036	[160]
Ivlev grazing constant	l/mgC	13	[136]
Zooplankton predatory mortality rate: predation by higher trophic levels	d^{-1}	0.02	[160]
Minimum prey concentration for zooplankton grazing	mgC/L	0.0045	[136]
Minimum ciliates concentration for zooplankton grazing	mgC/L	0.0045	[136]
Minimum phytoplankton concentration for zooplankton grazing	mgC/L	0.0045	[136]
Diatoms minimum concentration for predation	mgC/L	0.0045	[136]
Zooplankton excretion Rate at 0º	mgC/L	0.02	Calibrated
Constant for zooplankton excretion curve	mgC/L	1.0305	Calibrated
Constant for zooplankton mortality curve	–	0.0	Calibrated
Minimum rate for zooplankton natural mortality	d^{-1}	0.001	Calibrated
Maximum rate for zooplankton natural mortality	d^{-1}	0.04	[24]
Half-saturation constant for grazing	mgC/L	0.85	[136]
Capture efficiency of phytoplankton by zooplankton	–	0.8	[136]
Capture efficiency of ciliates by zooplankton	–	0.2	Calibrated
Capture efficiency of diatoms by zooplankton	–	0.8	Calibrated
Zooplankton maximum ingestion rate	–	1	[362]
Assimilation coefficient of phytoplankton by zooplankton	–	0.8	[136]
Assimilation coefficient of ciliates by zooplankton	–	0.8	[136]
Assimilation coefficient of diatoms by zooplankton	–	0.8	[136]
Proportion of phytoplankton in zooplankton ingestion	–	1.0	Calibrated
Proportion of ciliates in zooplankton ingestion	–	0.0	Calibrated
Proportion of diatoms in mesozooplankton ingestion		0.0	Calibrated
Ciliates (microzooplankron)			
Ciliates nitrogen/carbon ratio	mgN/mgC	0.16	Calibrated
Ciliates phosphorus/carbon ratio	mgP/mgC	0.024	Calibrated
Minimum concentration of bacteria for ciliates grazing		0.0045	Calibrated
Minimum concentration of flagellates for ciliates grazing	mgC/L	0.0045	Calibrated
Minimum concentration of prey for ciliates grazing	mgC/L	0.0045	Calibrated
Ciliates respiration rate at the reference temperature	d^{-1}	0.02	[48]
Ciliates excretion rate	–	0.02	Calibrated
Constant for ciliates excretion curve	mgC/L	1.0350	Calibrated
Constant for ciliates mortality curve	–	0.0	Calibrated
Minimum rate for ciliates natural mortality	–	0.0	Calibrated
Maximum rate for ciliates natural mortality	d^{-1}	0.044	[24]
Half-saturation constant for ciliates grazing	mgC/L	0.85	[24]
Capture efficiency of bacteria by ciliates	–	0.5	Calibrated
Capture efficiency of flagellates by ciliates	–	0.5	Calibrated
Ciliates maximum ingestion rate	–	1	Calibrated
Assimilation coefficient of bacteria by ciliates	–	0.5	[160]
Assimilation coefficient of flagellates by ciliates	–	0.5	[48]
Proportion of bacteria in ciliates ingestion	–	0.5	Calibrated
Proportion of flagellates in ciliates ingestion	–	0.5	Calibrated

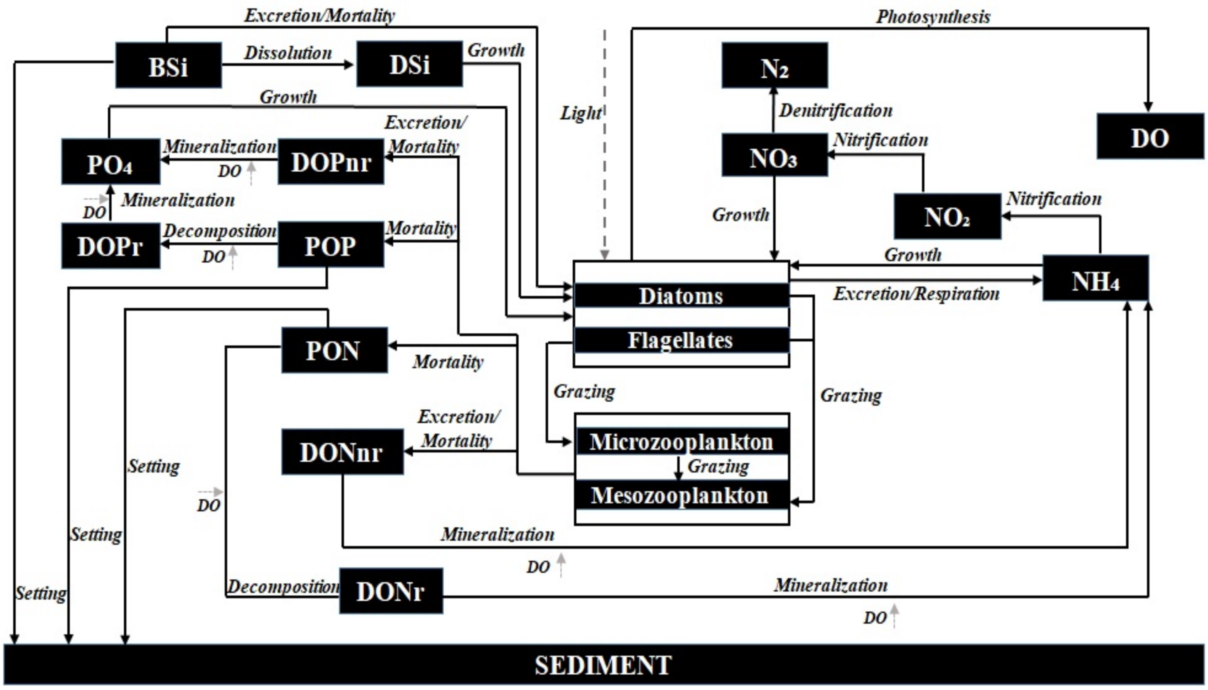

Figure 5.2: Biogeochemical conceptual model representing state variables (black boxes) and processes (arrows).(Nitrogen gas (N_2), ammonia(NH_4), nitrate (NO_3), nitrite(NO_2), inorganic phosphorus (PO_4), dissolved silica (DSi), biogenic silica (BSi), refractory dissolved organic nitrogen (DONr), refractory dissolved organic phosphorus (DOPr), dissolved non-refractory organic nitrogen (DONnr), non-refractory dissolved organic phosphorus (DOPnr, particulate organic nitrogen (PON), particulate organic phosphorus (POP), dissolved oxygen (DO)).

5.4.3 Model implementation

The model was implemented using the downscaling approach of nested domains, described by [299]. Two domains of nested grids with different resolutions were used (Fig. 5.1). The local high-resolution domain, Agadir Coast Model System (ACMS) (Domain 2), receives its open boundary conditions from the lower resolution regional domain, the Moroccan Atlantic Coast Operational Model System (MACOMS) (Domain 1) which open boundary condition (seawater temperature and salinity) combines low-frequency Copernicus Marine Environment Monitoring Service (CMEMS) outputs with tidal levels simulated using the same horizontal resolution (ACMS domain).

In operational modelling system, the one-way downscaling approach using an intermediate regional model application between CMEMS and a local domain has the advantage of running a number of local applications in parallel. This allows simulations to be available in a short time period, as MACOMS can run independently of its receiving local application. MACOMS domain is an implementation of 2D barotropic model with 0.04° horizontal resolution, regional domain resulting in a grid of 238 × 359 cells and maximum depths around 5300 m (Table 5.3). ACMS domain resulting of an implementation of 3D baroclinic model with 0.02° horizontal resolution, a grid of 56 × 56 cells and a maximum depths reaching 2133 m (Table 5.3).

The model has been set up using the bathymetry provided from MARPOCS (Multinational Response and Preparedness to Oil and Chemical Spills) project (http://www.maretec.org/en/

projects/current/MARPOCS) and run with mode-splitting time steps of 90 s and 20 s respectively for 2D and 3D calculations.

Air temperature, relative humidity, wind speed and direction, mean sea level pressure, cloudiness and radiation data provided from WRF (Weather Research and Forecasting Model) implemented by Action Modulers (http://www.actionmodulers.pt) were used to force the model. The tidal forcing was obtained from the harmonic components extracted from the FES2012 with 3km resolution, version of the FES (Finite Element Solution) global tidal model [87]. The monthly climatological 3D boundary for inorganic nutrients was derived from World Ocean Atlas 2013 (WOA13, https://odv.awi.de/data/ocean/). The WOA13 data provides vertical fields of inorganic nutrients (NO_3,PO_4, and SiO_4) and dissolved oxygen on a 1.00° grid, defined at 37 standard depth levels with distances between values increasing with depth starting with 5 m intervals at the surface and 25 m intervals from 100 m depth onwards.

Table 5.3: Main characteristics of the implemented nested model domains

Settings	MACOMS domain	ACMS domain
Area	Moroccan Atlantic coast	Agadir coast
Model characterization	2D – Barotropic	3D – Baroclinic
Grid corners	Lon: -20.79 – -6.51	Lon: -10.67 – -9.63
	Lat: 25.04 – 34.55	Lat: 29.74 – 30.86
Depth	Min: 15 m	Min: 15 m
	Max: 5300 m	Max: 2133 m
Cells dimension	238 × 359	56 × 56
Vertical Grid	7 Sigma Layer	7 Sigma Layer
	43 Cartesian layers	33 Cartesian layers
Horizontal Grid	4 km	2 km
Time steps	90 seconds	20 seconds
Tides	FES2012 [88]	From Domain 1
OBC Water	From MercatorOcéan [1]	From Domain 1
OBC Atmosphere	WRF [445]	WRF [445]
OBC Nutrients	–	WOA13 [2]
Discharges	No	No
Turbulence	–	GOTM [3] [74]
Bottom stress	Rugosity of 0.0025 m^2s^{-1}	Rugosity of 0.0025 m^2s^{-1}

[1] https://www.copernicus.eu/. [2] https://odv.awi.de/data/ocean/. [3] General Ocean Turbulence Model.

5.4.4 Model validation

The model performance is evaluated through the comparison with remote sensing and climatological data.Satellite level 4 products generated by the ODYSSEA with 0.02° spatial resolution (http://marine.copernicus.eu/ [39]) are spatially averaged to fit the model grid and compared with the simulated sea surface temperature (SST). Monthly mean chlorophyll-a (Chl-a) derived from the Moderate Resolution Imaging Spectroradiometer (MODIS) sensor onboard NASA's Aqua database (https://neo.sci.gsfc.nasa.gov/view.php?datasetId=MY1DMM_CHLORA) is used to examine the Chl-a concentration (January – December 2017) in the surface layer of the station "S" (30.5N, -10.5W) (Fig. 5.1), choosed according to the data availability.

Namely SST, sea surface salinity (SSS), DO, NO_3,PO_4, and SiO_4 are validate using tan Atlas 2018 (WOA2018; hemonthlyclimatologicaldataprovidedfromWorldOcehttps://odv.awi.de/data/ocean/) at the station "S". Furthermore, quantitative analysis is investigated using graphical and statistical skill assessment including; correlation coefficient (r), difference of mean values (bias), root mean squared error (RMSE), standard deviation (SD) and, graphically, the Taylor's diagram [436].

5.5 Results

5.5.1 Spatial variability of hydrographical condition

The spring (20-Mar, Apr, May, 20-Jun), summer (21-Jun, July, Aug, 21-Sep), and winter (21-Dec, Jan, Feb, 19-Mar) horizontal distribution of SST predicted by the model and collected by ODYSSEA are presented in Fig. 5.3. General SST cross-shore gradient is detected; this gradient is accentuated in the south-western coast, in result of the cold-water inflow coming from the north. The horizontal signature of the SST seasonal pattern is captured by the model with nevertheless some discrepancies near to the boundaries. The model skill in reproducing the SST distribution was graphically summarized in a quantitative way using the Taylor diagram. The diagram investigates overall position of the simulated SST with respect to the ODYSSEA products in terms of r, RMSE and SD [436].

Results are depicted in Fig. 5.3 and associated statistical indices are calculated in Table 5.4. As a whole, spatial distribution of SST presents relatively good scores in all skill indexes, even if they tend to be slightly underestimated in spring and summer (BIAS = -0.129 and -0.177°C, respectively) (Table 5.4).The diagram clearly confirms the good agreement between simulated and satellite SST fields, with correlation coefficient up to 0.87. Of the three seasons, the simulated SST in closest agreement with the satellite product in terms of high correlation (r = 0.86) and low error (RMSE = 0.55°C) is provided during the winter period. In contrast, this agreement decrease slightly during the spring period with r = 0.74, RMSE = 0.68°Cand SD = 0.61°C and the summer period with r = 0.72, RMSE = 0.69°C and SD = 0.67°C. Likewise, SSS increased as the offshore distance increased (Fig. 5.5a, b, c). However, the near-shore region affected by diluted waters and the offshore region affected by high salinity associated with warmer surface waters declined in winter (Fig. 5.5c). In contrast, surface DO was patchily distributed, with a mass water of higher concentrations coming from the north simulated in spring and summer (Fig. 5.5d, e). In winter, the DO concentrations decreased as the distance from the near-shore region increased (Fig. 5.5f).

Table 5.4: Statistical results used to assess the agreement between ODYSSEA satellite sea surface temperature (SST) and MOHID SST simulations. n-number of observations; r- correlation coefficient; RMSE- root mean square error; SD- standard deviation; BIAS- average error.

	MOHID Average(°C)	**ODYSSEA Average(°C)**	**n (per day)**	**Correlation (r)**	**RMSE (°C)**	**SD (°C)**	**BIAS (°C)**
Spring	18.491	18.621	89	0.742	0.682	0.613	-0.129
Summer	19.711	20.988	91	0.724	0.692	0.667	-0.177
Winter	16.065	16.059	89	0.866	0.553	1.104	0.007

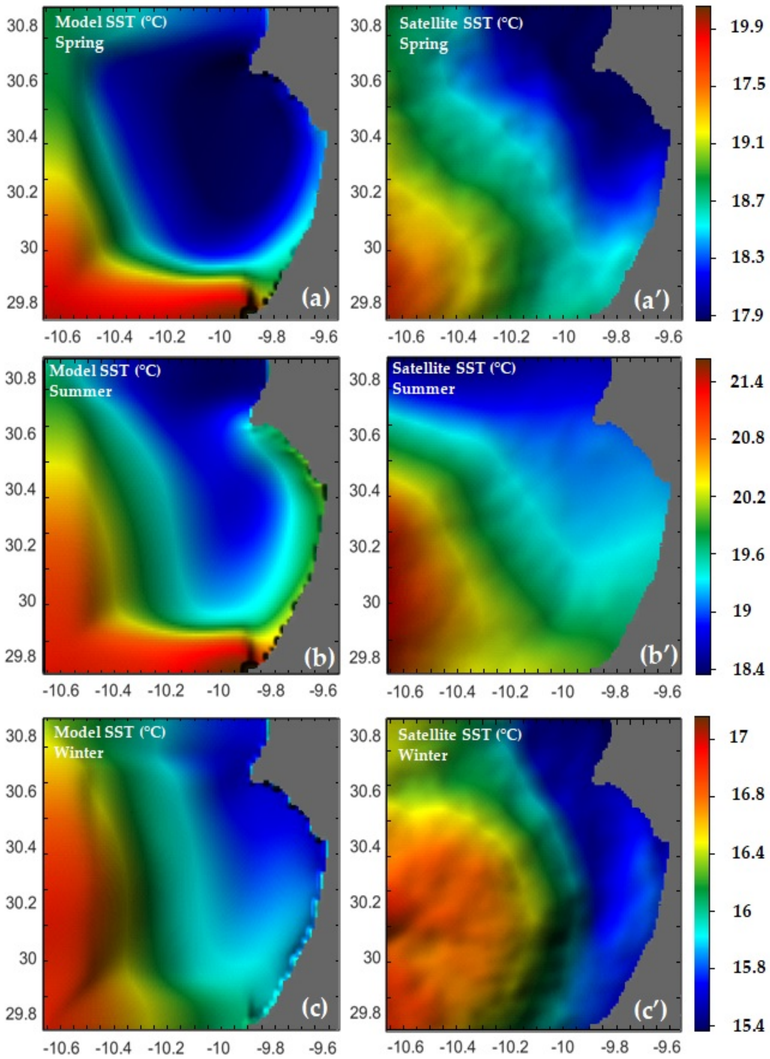

Figure 5.3: Sea surface temperature (SST) from (left) satellite ODYSSEA and (right) MOHID outputs during (a, a') spring, (b, b') summer and (c, c') winter 2017-2018 (Note that each panel has its own scale).

Vertical sections (up to 1500 m) of physicochemical parameters were illustrated selecting the "CO" transect (Transect with high mean cross-shore variables gradient) from the Agadir coast, across the continental shelf to the offshore region (Fig. 5.1). Indeed, the water temperature, salinity and DO concentration of "CO" transect exhibited stratified distributions in both seasons (summer and winter). The temperature and salinity decreased as the depth increased with strong negative downward gradient of around 17 units difference between surface and bottom layers for water temperature, 1.8 units for salinity. As the temperature increased, the microorganisms became more active; nonetheless, the leaping layers hindered the water exchange between the surfaces to the bottom layers, inducing in a drop of the DO levels on the bottom (Fig. 5.6).

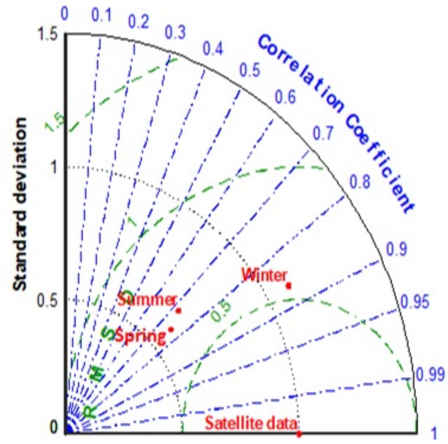

Figure 5.4: Taylor diagram quantifying model skill of sea surface temperature (SST) against ODYSSEA satellite product acquired in spring, summer and winter 2017-2018. The correlation coefficient (r) between simulated and satellite SST is given along the arch of the diagram by the azimuthal angle. The centred root mean square difference (RMSD) is represented by the green arc and the normalized standard deviation (SD) is proportional to the radial distance from the origin.

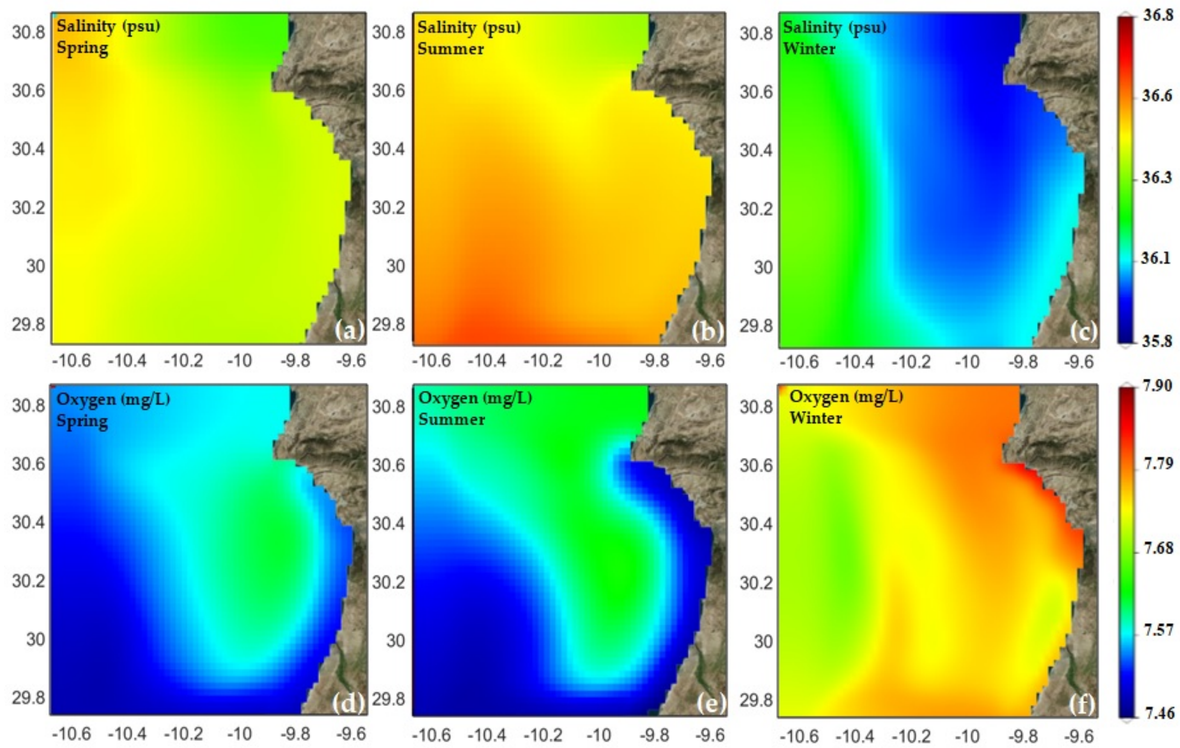

Figure 5.5: Surface distribution of simulated (a, b, c) salinity (psu) and (d, e, f) dissolved oxygen (mg/L) in spring, summer and winter 2017-2018.

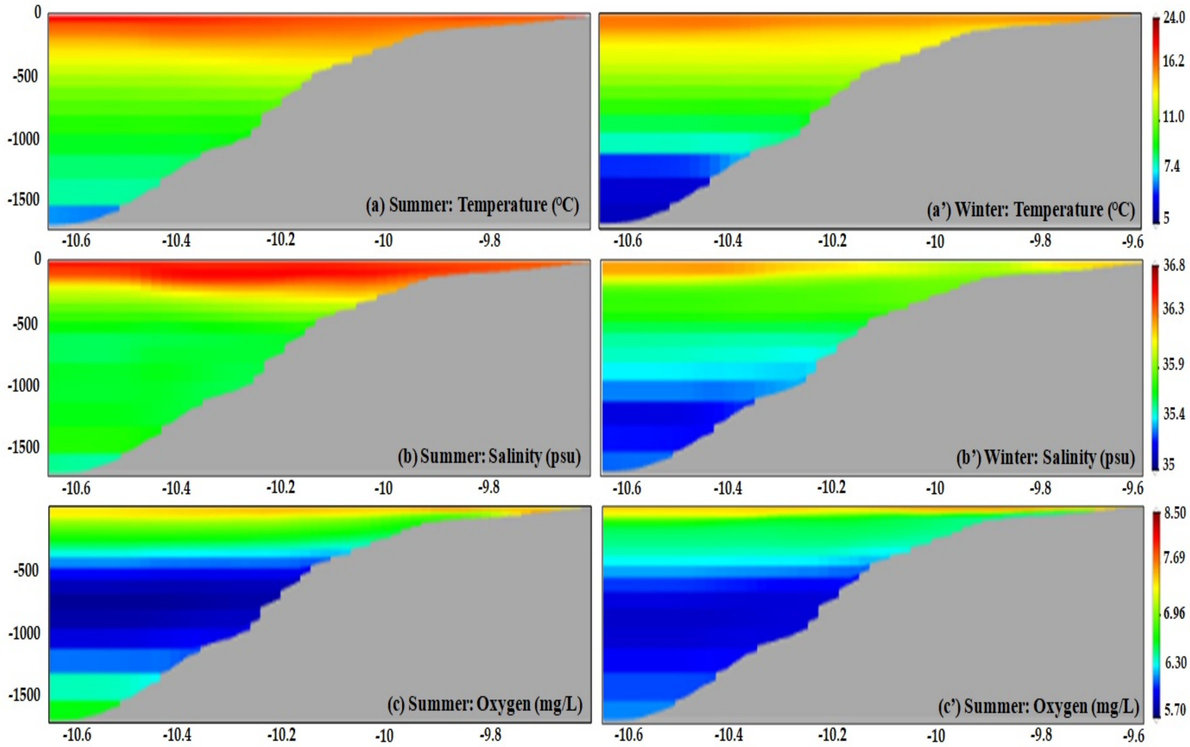

Figure 5.6: Vertical distributions of simulated (a, a') temperature (°C), (b, b') salinity (psu) and (c, c') dissolved oxygen (mg/L) along the "CO" transect (black line in Fig.5.1) in summer and winter 2017-2018.

5.5.2 Spatial variability of nutrient concentrations and plankton biomass

Spatial distributions of surface NO_3,PO_4 and SiO_4 concentrations in Agadir coastal area were simulated during spring, summer and winter 2017-2018 (Fig. 5.7). The anomalously high NO_3 concentrations were limited to the northern area during the spring period and could be associated to the boundary conditions (Fig. 5.7a). In contrast, the central part of the coast seems to be favoured by high NO_3 concentrations during summer and winter periods (Fig. 5.7b, c). The PO_4 distribution exhibits a different pattern as NO_3. Areas with low concentrations were located in a narrow coastal band in spring (Fig. 5.7d). In summer, coastal circulation loads of PO_4 concentrations to accumulate in the central part of the coast; offshore extensions were detected during the winter period (Fig. 5.7e, f). The SiO_4 concentrations were found to be higher for all seasons in comparison with NO_3 and PO_4. Thus, SiO_4 is unlikely to be the principal limiting factor for diatom distribution in our area. In spring, the SiO_4 concentrations were higher than those in summer and exhibited decreasing trends as distance from the near-shore coast increased (Fig. 5.7g). During summer and winter periods, the lowest SiO_4 concentrations were limited to the central part of coast, the rest of the domain was relatively rich in SiO_4 (Fig. 5.7h, i).

Furthermore, the vertical profiles of NO_3,PO_4 and SiO_4 of "CO" transect displayed stratified distributions (Fig. 5.8). The nutrient concentrations gradually increased with increasing depth, and high values were simulated in the bottom layers in response to the bottom currents and remineralisation of organic material.

On the other hand, the simulated surface phytoplankton (in terms of C-biomass) varies substantially from the coast to the open ocean, showing a strong longitudinal decreasing trend of diatoms in spring and winter (Fig. 5.9a, c). In contrast, the central part of the coast seems to be favoured by high biomass of diatoms during the summer period (Fig. 5.9b). Simulated surface flagellate has a similar footprint to the diatoms distribution trends although with greater magnitude (Fig. 5.9d, e, f). Nevertheless, lower values of simulated zooplankton biomass were limited to the nearshore area in spring and to the central part of the coast in summer (Fig. 5.9g, h), whereas, the winter season exhibited a high zooplankton biomass near the coast, which begins to decrease gradually to the offshore area (Fig. 5.9i).

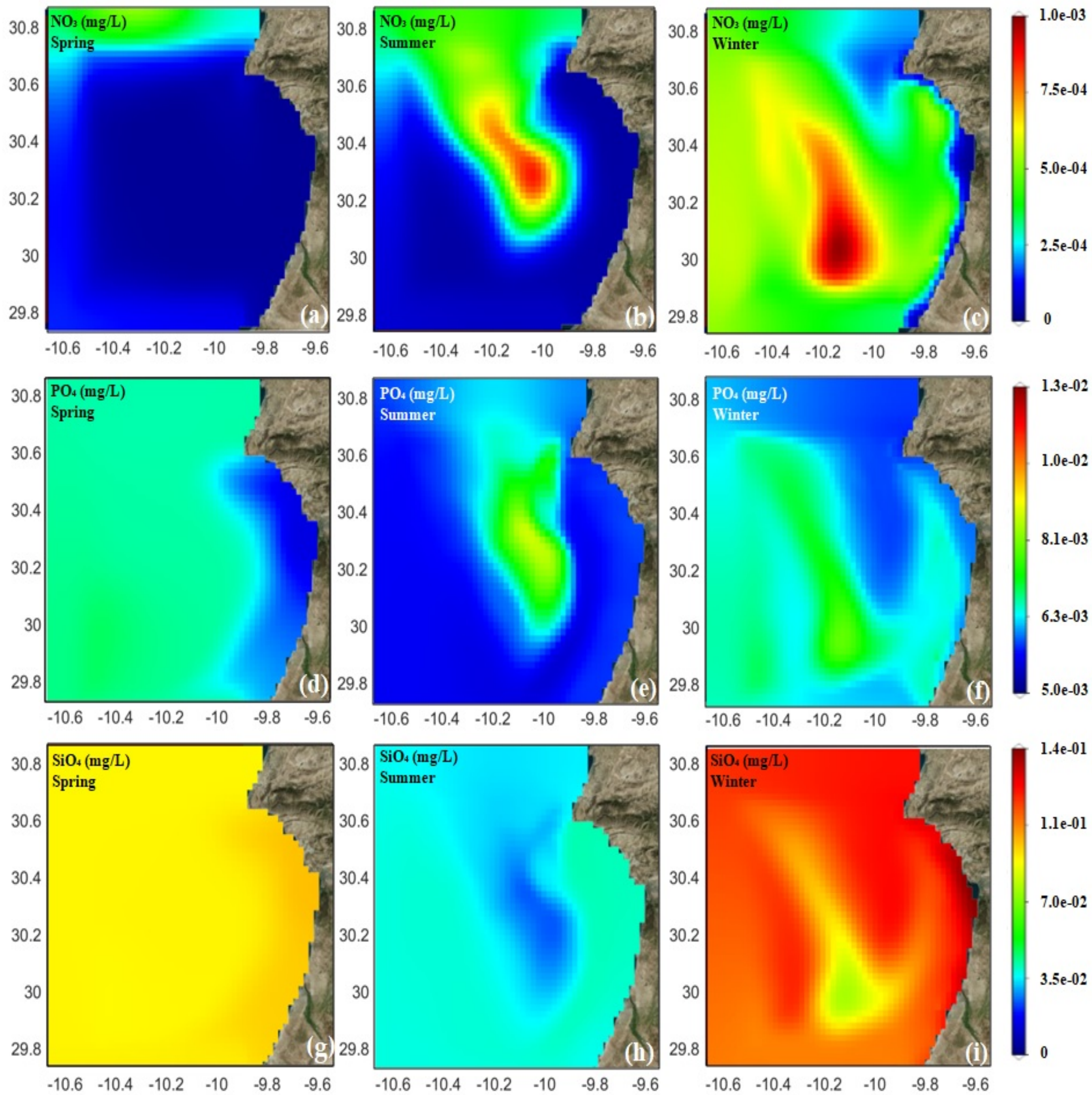

Figure 5.7: Surface distribution of simulated (a, b, c) NO_3 (mg/L), (d, e, f) PO_4 (mg/L) and (g, h, i) SiO_4 (mg/L) in spring, summer and winter 2017-2018.

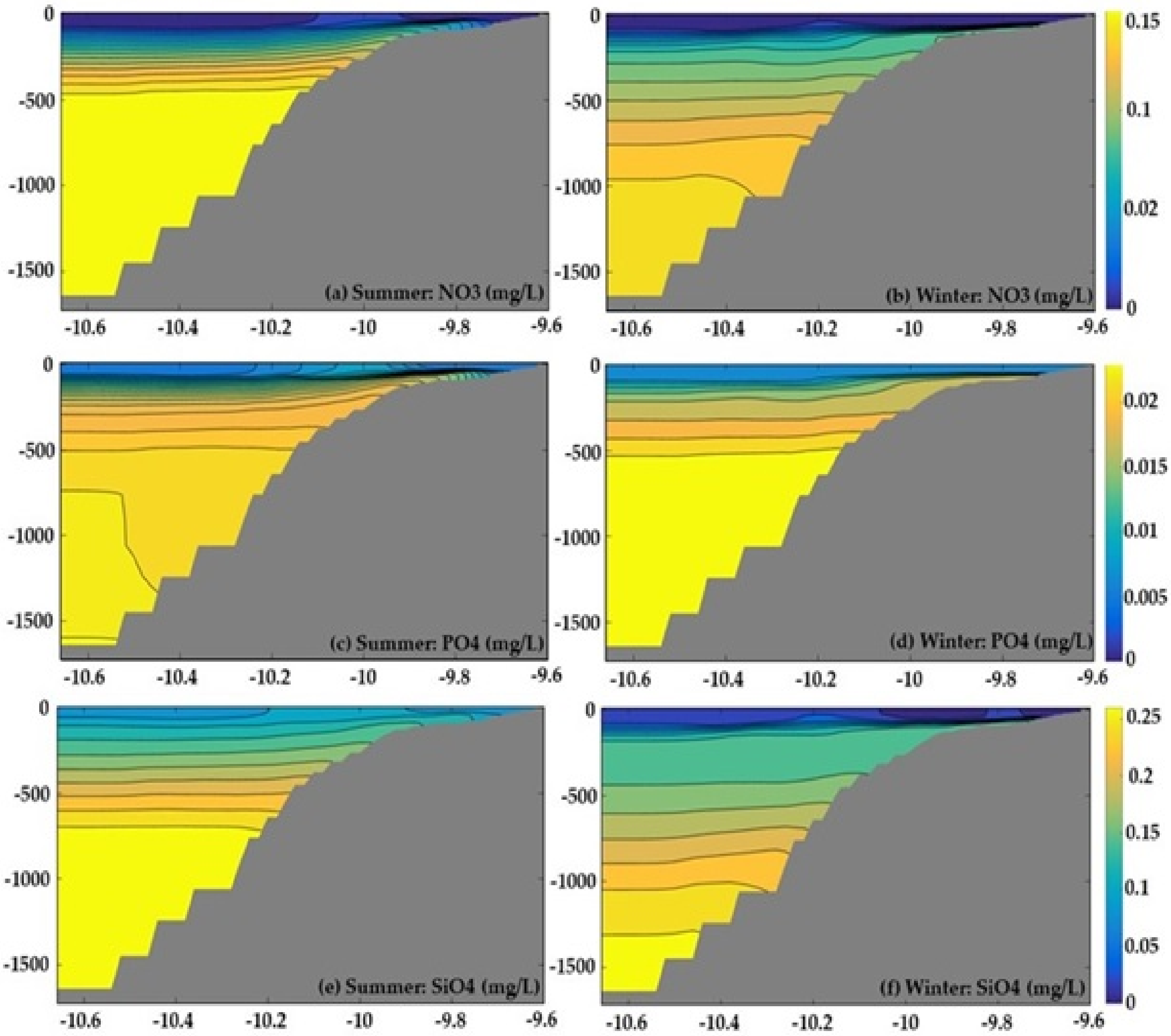

Figure 5.8: Vertical distributions of simulated (a, b) NO_3 (mg/L), (c, d) PO_4 and (e, f) SiO_4 (mg/L) along the "CO" transect (black line in Fig. 5.1) in summer and winter 2017-2018.

5.5.3 Temporal variation – validation with climatology and satellite data

To understand changes in phytoplankton distribution in relation to physical and biogeochemical variables, we analyzed annual variation (January December 2017) of SST, SSS, DO and inorganicnutrients by averaging the monthly climatology data and compared with simulated findings from station "S" (30.5N, -10.5W) (Fig. 5.10).

We summarize graphically in a quantitative way the model performance using the Taylor diagram. For temperature, we analyzed the seasonal pattern of the mean SST, which indicated that the study area warmed up and attained maximum temperature during summer. In winter, the surface water has cooled down rapidly and attained minimum temperature in February. The model captured not only the seasonal variability in SST climatology, but also the range of the observations (Fig. 5.10a). Meanwhile, the average SSS climatology data showed higher values in winter and spring than that in summer and fall. The model does not matches SSS climatology

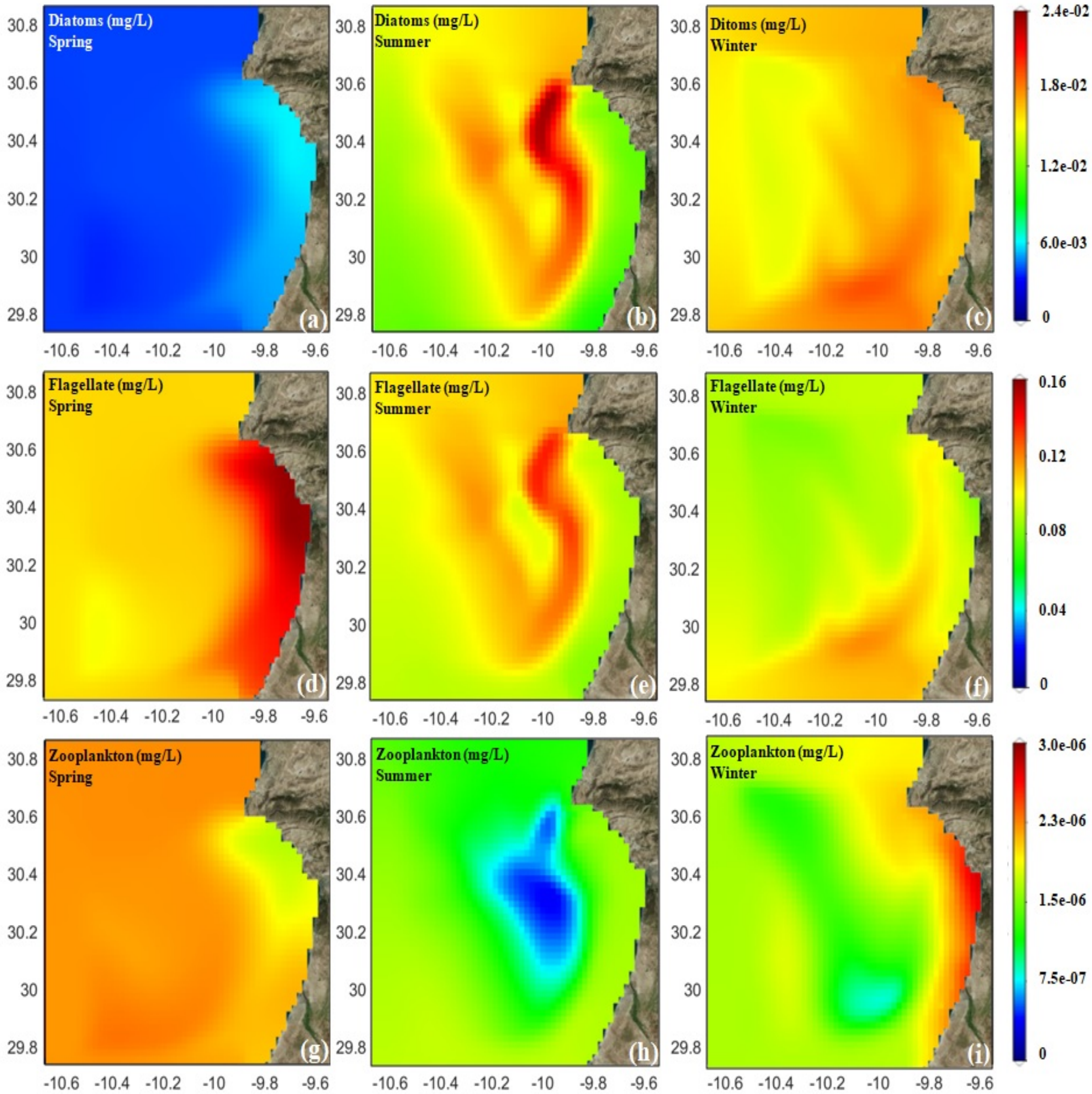

Figure 5.9: Surface distribution of simulated (a, b, c) diatoms (mg C/L), (d, e, f), flagellate (mg C/L) and (g, h, i) zooplankton (mg/L) in spring, summer and winter 2017-2018.

data indicating a shift in timing of the monthly variability (Fig. 5.10b) and leading to a higher error (RMSE =1.67 psu) (Fig. 5.11). The surface DO average climatology concentrations reached the maximum in the winter. Thereafter, the DO variation remained a decreasing trend and dropped to the minimum average in fall. The model relatively captured the general annual trend with an underestimation mainly in the late period of investigation (Fig. 5.10c). A decreasing trend in inorganic nutrients (NO_3 and PO_4) systematically occurred from the early spring, leading to ample variations in NO_3 concentrations explained mostly by the denitrification processes and the phytoplankton uptake (see later discussion). The model captured seasonal signature of the climatological pattern, except a slight time-lag of the winter peak and an overall overestimation in January and the early February and underestimation in the rest of the year (Fig. 5.10d). Seasonal changes in PO_4 concentrations were consistently associated with higher values in winter followed by a sharp decrease in summer. Overall, the model captured reasonably seasonal pattern, despite some discrepancies could be related to the used constant input values at the inflow boundaries (Fig. 5.9e). The general SiO_4 trends show that the highest values were getting later in the year. A continuous increase in SiO_4 concentrations with time was simulated in agreement with the climatology data (Fig. 5.10f). On the other hand, given the scarcity of field data, time series of the sea surface Chl-a (estimated using the conversion factor from simulated total phytoplankton carbon-biomass as defined in [246] are assessed using MODIS-Aqua satellite data. Overall, the average concentration in spring and summer was higher than that in fall and winter.

The model captured reasonably well seasonal variability in Chl-a concentrations, particularly good agreement is observed in spring and summer. In winter, the model has a tendency to underestimate surface Chl-a concentrations, most notably in the early period of investigation (January and February) (Fig. 5.10g). The flagellate biomass distribution displays a similar pattern as Chl-a (Fig. 5.10h). However, simulated flagellate growth starts at late February, followed by the bloom peak in March and April. The simulated biomass decreased in the late spring, and the second summer bloom of lower magnitude was manifested. After a summer bloom decline biomass attains even lower values in fall and reaches its annual minimum values in the November, probably due to combined zooplankton grazing, light and nutrient limitation. Compared to the flagellate, the diatoms seasonal signature is less marked where biomass tended to remain low throughout the year. Their simulated biomass slowly but steadily increased, reaching the maximum values in late December (Fig. 5.10h).

The visualization of the models' performance using the Taylor diagram confirmed the agreement model–climatology data (Fig. 5.11). From the Taylor skill indexes, one can identify PO_4 and NO_3 tend to be the most skillful among the all model variables, with high correlation coefficient ($r > 0.8$), low error (RMSE < 0.6 mg/L) and normalised standard deviations close to 1 (SD = 0.91 and 1.07 mg/L, respectively). Chl-a, SST and SiO_4 present a moderate correlation ($0.68 < r < 0.7$) and the correct variability (SD 0.7). DO is a bit out of phase with the observed one, which results in its low correlation and error (r = 0.17, RMSE = 1.19 mg/L and SD = 0.86 mg/L). The low skill scores for DO suggests that it is difficult to validate since many components interact with oxygen, and contribute to oxygen production and consumption, such as the exchange of oxygen between water column and atmosphere, photosynthetic oxygen production, respiratory consumption by phytoplankton and consumption of oxygen by degradation of organic matter [354, 388]). Furthermore, SSS appears with a negative correlation (r= -0.3) and high error (RMSE =1.67 psu), as the model fails to capture the observed evolution of the climatology data. Theses discrepancies can be due of the fact that the freshwater discharges from Souss and Massa rivers are not accounted in the model.

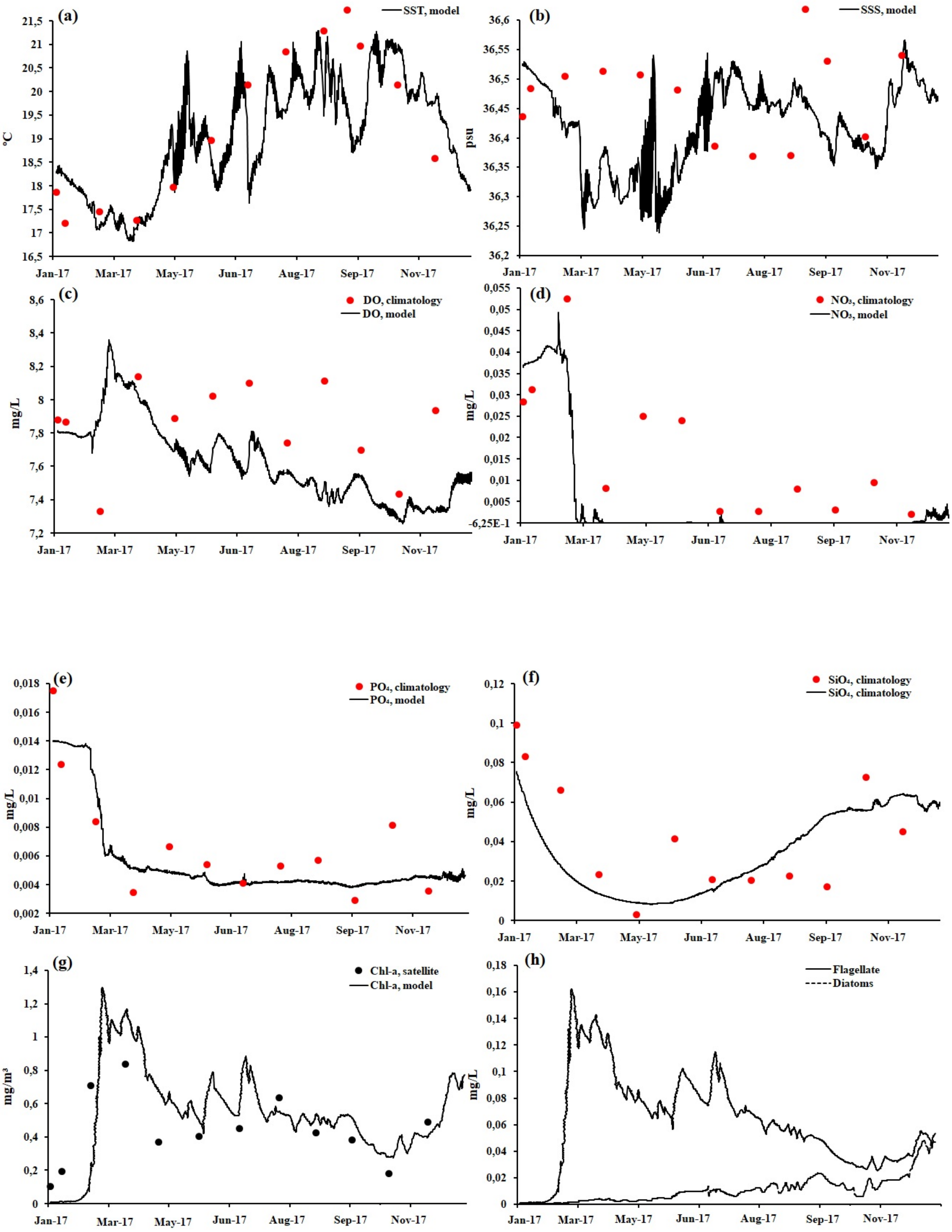

Figure 5.10: Comparison of (e-f) simulated sea surface temperature (SST), sea surface salinity (SSS), dissolved oxygen (DO) and nutrients (NO_3,PO_4,SiO_4) concentrations (mg/L) (lines) and the corresponding WOA2018 climatology data (red dots).(g) Simulated Chlorophyll-a (Chl-a) concentration (mg/m^3) (line) and the corresponding MODIS-Aqua satellite products (black dots) at the surface layer of the Agadir area (station "S") for the period January-December 2017. (h) Time series (January-December 2017) of phytoplankton biomass (diatoms and flagellates) (mg C/L) at the surface layer of station "S".

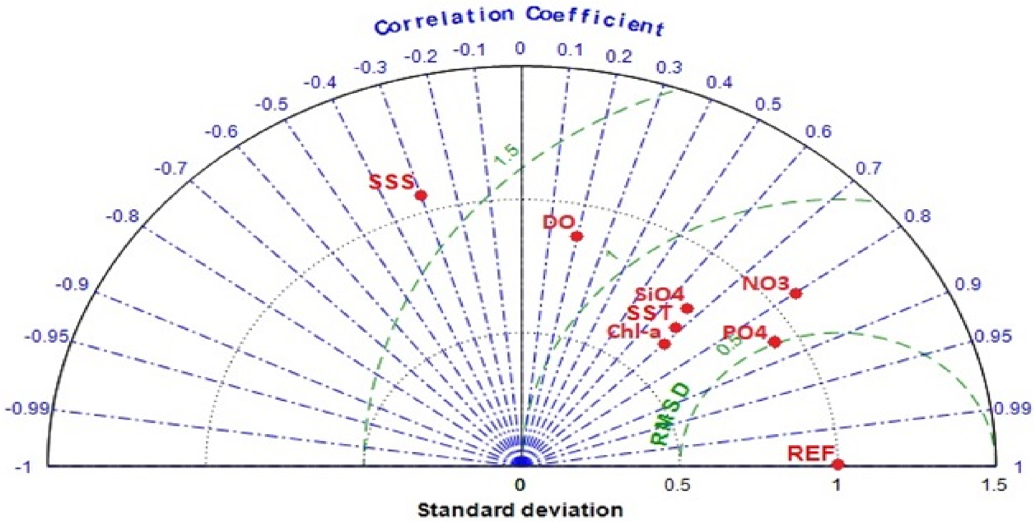

Figure 5.11: Taylor diagram displaying the model–data correspondence of the annual variability (January December 2017) of model outputs and WOA2018 climatology data of sea surface temperature (SST), sea surface salinity (SSS), dissolved oxygen (DO), nitrate (NO_3), phosphate (PO_4) and silica (SiO_4); MODIS-Aqua satellite data for chlorophyll-a (Chl-a) in the surface layer of the Agadir area (station "S").

5.6 Discussion

5.6.1 Spatio-temporal dynamics of phytoplankton

The dominance of simulated flagellates was somewhat surprising as several studies report that diatoms typically dominate Moroccan Atlantic coastal food chains [156, 327, 417]. Except for [21] that report a low to moderate (20–68%) contribution of diatoms to total phytoplankton in the Cape Ghir (Fig. 5.1). There are a number of explanations for the lack of diatoms in this area. The first can be associated to the strong water column stratification that provides beneficial conditions to favor flagellated group of the phytoplankton assemblages, as flagellates are more adapted to stratified and stable waters with low nutrient concentrations (e.g., [261, 421]). Another possible explanation can be attributed to the way phytoplankton responded to the time–space changes in upwelling conditions (SST, SSS. . .) that affect the nutrient levels in water column. In fact, many flagellate species are characterized by higher surface/volume ratios compared to the diatoms group. They are able to access alternative phosphorus sources [78] and to use various forms of reduced nitrogen when N: P ratios are minimal [21, 322].

At the spatial scale, the general shift in maximum flagellates and diatoms between the shelf and the open ocean during the spring period coincides with the spatial gradient of the surface inorganic nutrients (Fig. 5.7, 5.9).Thereafter, the possible injection of nutrients by coastal upwelling events could have improved phytoplankton proliferation in the central part of the coast during the summer period when coastal upwelling is more intense [122, 391]. In winter, the transport of high nutrient water to the offshore areas supported by the Atlantic water advection could favors proliferation of phytoplankton in waters further offshore [21]. Besides this spatial distribution, increases in Chl-a concentrations in studied station "S" (30.5N, -10.5W) generate a major spring peak of 1.3 mg/m^3 in March and a minor summer peak of 0.1 mg/m^3

in July. Outside those two peaks, Chl-a levels oscillate between approximately 0.008 and 1.3 mg/m^3.This range of values remains lower in comparison to those observed by [208] near the coastline (30.56N, -9.76W) (0.77 – 1.95 mg/m^3). Surface distribution of simulated flagellates show similar trends with well-pronounced spring bloom that could be attributed to the higher nutrient availability combined with adequate light conditions (not shown) in the upper stratified water column. Nutrient concentrations become then relatively low and simulated flagellate levels decrease to 0.058 mg C/L in late May. Afterward, flagellate growth conditions apparently improved due to sufficient light irradiance supported by the increase in surface solar heating, generating relatively high flagellate levels in July. After summer, inorganic nutrients (NO_3 and PO_4) are dropped to low levels in the surface water column and solar heating is decreased. Consequently, the simulated flagellate levels reach their annual minima in fall and winter. The diatom assemblages show less seasonal variability. Their amplitude remained low throughout our simulations, gradually increasing until the early winter. This low pattern could be partly confined to the changes in the nutrient molar ratios and the absence of adequate conditions for diatom growth (relatively high nutrient concentrations and low water temperatures [487, 508] (discussed in next section).

5.6.2 Response of phytoplankton to nutrients and environmental factors variations

Nutrients availability appeared to be the main factor controlling the phytoplankton distribution in Moroccan Atlantic coastal waters where the upwelling events are strong (e.g., [21, 156, 417]. In this context, our findings reveal a sign of nutrient depletion, supporting the claim that the phytoplankton dynamics in the area may be controlled by the annual variation in nutrients. This is particularly relevant for NO_3, as the simulated concentrations drops to low levels (0.0001 mg/L) during the first flagellate bloom (early spring). This low concentration can be designed as an index of limitation for fast photosynthesis in coastal waters [241]. Furthermore, the average N:P ratio was lower than the classical Redfield ratio of 16:1 (N:P = 0.4), suggesting that most of the available nitrogen has been incorporated by flagellate into the local biogeochemical cycle and move the coast towards nitrogen limitation. The low N:P ratio could be then attributed to the higher nitrogen uptake by the flagellate dominated blooms in the study area; the injection of phosphorous into the surface waters caused by the upwelling of deep Atlantic waters or to the faster recycling of phosphorous relative to nitrogen in the surface coastal waters. Furthermore, although NO_3 is recognized to be rapidly exhausted in upwelling filaments, the nutrient-rich water upwelled off North-West Africa [50] is advected offshore at the surface layers as showed by the relatively high nutrient concentrations in the offshore waters [391]. The exhaustion of nitrogen to the analytical limit during phytoplankton blooms has been previously detected in Cape Ghir during the three cruises (June, August and October 2009). In these cruises, NO_3 concentrations were close to the detection limit and inorganic N:P ratios were lower than 6 [21]. In addition, this notion of the primary production growth being nitrogen limited has been reported by various investigators in many areas of the North Atlantic Ocean (e.g.,[14, 166, 396]). By contrast, the distribution of flagellates is less sensitive to the low phosphate concentrations (0.003 –0.014 mg/L) due to their ability to secrete alkaline phosphatase in response to limited phosphorus availability (e.g., [86, 257, 509, 510]. Meanwhile, the relative larger size of flagellates when comparing to diatoms makes it more adapted to take advantage of PO_4, mainly delivered from the Atlantic Ocean via coastal upwelling events [265].On the other hand, it is interesting to note that the high simulated concentrations of SiO_4 (between 0.008 and 0.075 mg/L) in comparison with NO_3 and PO_4 lead to stoichiometric P impoverishment relative to Si (Si:P ratios > 16:1) [349] and strong deficiency of N relative to Si (N:Si ratios < 1:1) [369] in our station. These findings illustrate the preferential uptake of NO_3 by phytoplankton and suggest that SiO_4 is not limiting factor in the surface waters of the study area. Nutrient ratios and levels cannot account alone for phytoplankton distribution as environmental parameters are fundamental factors in shaping the distribution of diatoms and flagellates in the study areas.

Temperature is assumed to have an indirect effect on the phytoplankton dynamics, affecting the processes of sinking, grazing, and nutrient assimilation as well as the rate of biochemical reactions in water column [421]. However, spatial distribution of simulated and satellite SST (Fig. 5.3) with a narrow band of cold waters in the nearshore area confirms the influence of the cold upwelling filament off North-West Africa [32, 391]. Previous studies (e.g., [21, 335, 484] pointed out the permanent coastal upwelling off Cape Ghir (31N) with maximum intensity in summer. This filament propagates more than 100 km offshore associated with a cyclonic eddy, mainly influenced by the local bottom topography, the concave configuration of the coastline and the presence of the Canary Islands (e.g., [50, 192, 352, 352, 391]).

The analysis of the horizontal and vertical ("CO" transect) residual velocities calculated by averaging the transient velocities at each grid point over the simulation period (from January-2017 to December-2018) reinforces these findings (Fig. 5.12). Thus, the south-west/north-east orientation of the coast and the differences in the bottom friction affect residual current velocity and induce a coastal cyclonic eddy, typical of this region. Cyclonic eddy tend to increase NO_3 and PO_4 concentrations in the central parts of the coast during the summer period, thereby controlling the phytoplankton growth in the area (Fig. 5.7, 5.9). Temporal distribution of simulated SST shows seasonal variations with fluctuations ranging from 16.82 °C in March to 21.30 °C in August 2017. In situ SST measurements have reported a wider range of SST variation, from 14.9 °C in February 2016 to 26.6 °C August 2017 [244] compared to the other areas as Imessouane Bay (Southwest, Moroccan Atlantic coast) (19.2 °C to 21.9°C) [19].Furthermore, it is interesting to note that in our station, phytoplankton blooming produced by rapid growth of flagellates is most common in the early spring and summer when SST is increasing. After spring, flagellates biomass declined rapidly while that of diatoms continued to increase (Fig. 5.10).Warming temperatures resulting in inorganic nutrients decline levels as a consequence of intense stratification can explain in part the persistence of flagellates at higher levels than diatoms, which are still present in our station during summer but with low biomass [415]. Diatoms ability to grow well at low water temperature [49]; witness the fact that they start growing in the early winter reaching a maximum in December. This can be also attributed to the optimal water temperature range for the growth of diatoms (15–20°C for *S. costatum*) compared to that for flagellates (20–27°C for *P. donghaiense*) [431, 489].

Besides water temperature, salinity can strongly influence phytoplankton composition and biomass. Previous studies (e.g., [43, 201, 292] have endorsed the tight relationship between salinity level and phytoplankton dynamic. In our study, the range of simulated SSS values (36.23 – 36.56 psu) were indicative of the influence of North Atlantic Central West Water [21]. When compared to other Atlantic Moroccan areas, the range for in situ SSS is narrower than that simulated by our model. Minimum value of 31.26 psu (February 2017) and a maximum value of 37.9 psu (August 2017) was observed in Taghazout Bay [244]. The range between 36.1 and 36.8 psu were observed in Imessouane Bay [19]. This could explain the dominance of large flagellate that may result from the salinity optimum for flagellates (36.7–37.7 psu for *P. arcuatum*) [412] (20–37 psu for *A. minutum*) [187]. It is consistent with other studies (e.g., [328]) showing that flagellates dominate marine brackish salinities but diatoms are able to persist at hypersaline waters.In addition, changes in ambient DO concentrations could also a main factor considered to affect phytoplankton distribution and composition [58, 325, 422]. From our simulation, it can be observed that the horizontal distribution of phytoplankton is similar to that of DO concentrations. A strip of high sea surface phytoplankton simulated in the central part of the coast during the summer period coincides well with the DO maximum concentrations (Fig. 5.5e).Vertically, nutrients are depleted in the surface water column and an enrichment of DO is simulated (higher than 8.5 mg/L), with a sharp decrease to the bottom (less than 2 mg/L).

From these findings, Agadir waters are relatively well oxygenated compared to Taghazout Bay (6.9 – 8.5 mg/L) [244]. Overall, the relatively high DO concentrations can be mostly attributed to the important circulation of water [27] that improves oxygen levels inside the coast and the photosynthetic release of oxygen by the high flagellate blooms.

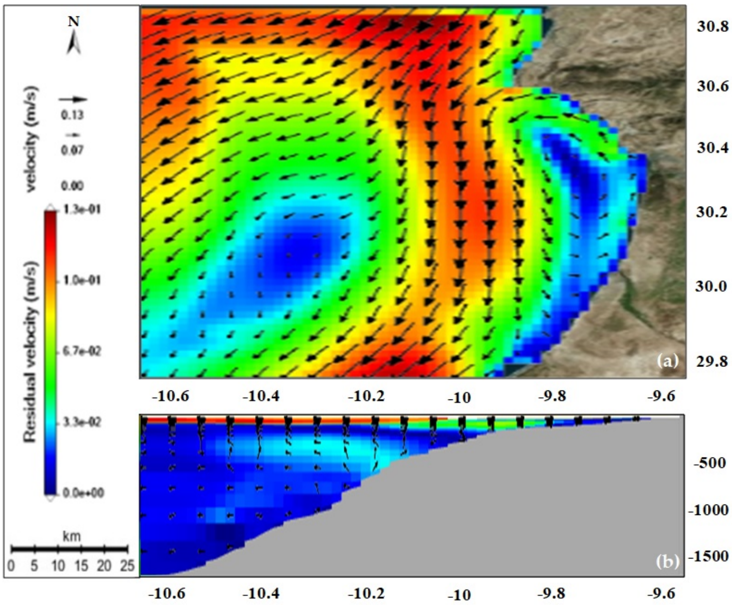

Figure 5.12: Residual current velocity distribution over surface (a) and depth "CO transect" (b) layers (ms^{-1}) in Agadir coast (average of model velocities from January-2017 to December-2018)).

5.7 Conclusion

To our knowledge, this paper is the first biogeochemical modeling investigation of the of southern Moroccan Atlantic coast (Agadir coast) using a high-resolution three-dimensional coupled hydrodynamic-biogeochemical model. Special emphasis was dedicated to deciphering of planktonic assemblages (Chl-a, diatoms and flagellates) dynamics, in response to physicochemical fields (water temperature, salinity and DO), inorganic dissolved nutrients (NO_3,$PO_4 and SiO_4$) availability. The model performance was investigated by comparison with satellite products (ODYSSEA for SST and MODIS for Chl-a) and climatology data (WOA2018). Despite aforementioned bias in temporal distribution of SSS and DO which is probably attributed to missing processes and some gaps in the hydrological cycle of the atmosphere model; It is undisputed that our model reveals an adequate reproduction of spatial pattern of SST and seasonal signature of SST, Chl-a and PO_4. Furthermore, the underestimation of the simulated NO_3 concentrations is likely a result of applied nutrient boundary conditions. From nutrient concentrations and stoichiometric ratios; it can be asserted that the NO_3 levels may be the key element controlling phytoplankton distribution in the Agadir coast. The possible injection of nutrients through upwelling filaments associated with a cyclonic eddy could be responsible for the nutrients enrichment in the surface layers of water column; improving, therefore, proliferation of phytoplankton in the central part of the coast in summer and toward the open ocean in winter.Biological variables reveal the largest responses to nutrient levels and environmental parameters with high seasonal variability. The flagellates dominated total Chl-a in the upper layers of water column during spring and summer periods were coincident with warming water temperatures, higher salinities, intense stratification and lower nutrient (NO_3 and PO_4) concentrations. Whereas considerable increased in diatoms biomass has been simulated after summer in response to lower water temperature and higher SiO_4 concentrations. This has major repercussions for the flow of carbon in the area, as flagellates dominated phytoplankton assemblages contribute to low carbon export to deeper waters compared to diatoms [126]. In sum, the proposed 3D hydrodynamic-biogeochemical model can be considered to be an interesting descriptor of the biogeochemical behaviour of Moroccan Atlantic coastal waters. Even if it is able to simulate reasonably seasonal cycles of inorganic dissolved nutrients and Chl-a further work is still needed to improve system representation.

Chapter 6

General conclusion

As the first step toward our final goal to provide a decision support tool for coastal management of North-West Africa (Moroccan Atlantic coast).

First, the emerging trend of coastal science in Moroccan Atlantic coast was explored using bibliometric analysis in conjunction with network analysis. 1952 documents were analyzed to describes qualitatively and quantitatively the progress, trends, and hotspots of publications, between 1971 and 2021. Next, science mapping approach was used to explore the emergence of research literature on water quality modelling applications within the Atlantic area published from 1981 to 2021.

A database of 1952 potentially relevant publications (2548 individual modelling applications) were analyzed to document the general research trend and identify the most frequently applied model, the water body types as well as the areas within which models were mainly applied. Afterwards, 3D hydrodynamic-biogeochemical model of Agadir bay was set up to understand the dynamics that control nearshore water quality. To model all of the complex features in the area accurately, the extended model was refined to a high resolution of 500 m.

The hydrodynamic model was externally derived by meteorological data, tidal oceanic forcing and boundary conditions of Agadir bay. It was used to calculate SSL, harmonic tidal constituents and physical factors. The model was included with the injected mass of tracers using Lagrangian transport model and used to calculate RT and estimate the pathway of passive tracers. The pre-computed scalar transport and boundary conditions from the hydrodynamic solution were then used to conduct biogeochemical calculations in an offline coupled mode. The model was used to explore the time-space patterns in the dynamics of physico-chemical parameters and nutrient limitation on phytoplankton growth. The refined model was calibrated and validated using a combination of available in-situ measurements, satellite products, climatology and ARGO floats data. However, it was clear that the available data were limited and more surface drifters and current speeds and directions as well as phytoplankton biomass are required for any more comprehensive model calibration and validation study in the future.

The main conclusions drawn from this study can be summarised as follows:

1. The analysis of research trend of coastal science in Moroccan Atlantic coast suggests that future scientific effort on Moroccan Atlantic coastal ecosystems should relieve existing biases by increasing multidisciplinary integrated system research and encouraging inter-regional transfer of research resources to areas of low research effort, with a special emphasis on the critical research ecosystems in the southern coastline. Some key recommendations were raised for strengthening the implementation of knowledge management within the concept of sustainable coastal management.

2. The analysis of 1952 publications (2548 individual modelling applications) provides a holistic picture of the water quality modelling applications within the Atlantic area. Main findings highlighted an upward trend in number of publications during the past two decades. SWAT (semi-empirical modeling frame-works) was by far the most often used model. A great number of modelling applications have located in the Northwest and Northeast Atlantic, mostly the United States of America, most of them addressed watershed system.

3. Implementation of the 3D hydrodynamic-biogeochemical model has led to a comprehensive description of the ecological behavior of a subtropical bay (Moroccan Atlantic coast). The simulations improved our understanding of the way the hydrodynamics and different environmental forcing may influence the dynamics of nutrient and the limitation of N and P on phytoplankton growth in Agadir bay.

4. Despite some discrepancies on MOHID implementation, model accuracy revealed a good match between simulations and observations, which underlines the feasibility of the model in simulation the main dynamic features of the Agadir bay.

It worth noting that the optimal use of the model requires continuous testing and calibration with assimilation of the relevant data as they become available. With the understanding in hydrodynamics and biogeochemical variation, the model can also be used to understand the fate and transport of emerging contaminants and identify the potential sources of pollution in the area.

Chapter 7

Appendix

Table 7.1: Model equations.

Variable	Description	Units
Flagellates		
	μ^f *Grossgrowthrate*	1/d
	r^f *Totalrespirationrate*	1/d
$\mathrm{dFla} / \mathrm{dt}=\left(\mu^f - r^f - ex^f - m^f\right) \cdot \mathrm{Fla} - G^f$	ex^f *Excretionrate*	1/d
	m^f *Naturalmortalityrate*	1/d
	G^f *Grazingrate*	mgC/l. d^{-1}
Diatoms		
	μ^d *Grossgrowthrate*	1/d
	r^d *Totalrespirationrate*	1/d
$\mathrm{dDia} / \mathrm{dt}=\left(\mu^d - r^d - ex^d - m^d\right) \cdot \mathrm{Dia} - G^d$	ex^d *Excretionrate*	1/d
	m^d *Naturalmortalityrate*	1/d
	G^d *Grazingrate*	mgC/l. d^{-1}
Mesozooplankton		
	μ^z *Grossgrowthrate*	1/d
	r^z *Totalrespirationrate*	1/d
$\mathrm{dZoo} / \mathrm{dt}=\left(\mu^z - r^z - ex^z - m^z\right) \cdot \mathrm{Zoo} - G^z$	ex^z *Excretionrate*	1/d
	m^z *Naturalmortalityrate*	1/d
	G^z *Grazingrate*	mgC/l. d^{-1}
Ciliate		
	μ^c *Grossgrowthrate*	1/d
	r^c *Totalrespirationrate*	1/d
$\mathrm{dCil} / \mathrm{dt}=\left(\mu^c - r^c - ex^c - m^c\right) \cdot \mathrm{Cil} - G^c$	ex^c *Excretionrate*	1/d
	m^c *Naturalmortalityrate*	1/d
	G^c *Grazingrate*	mgC/l. d^{-1}
Ammonia (NH_4)		
$\frac{\mathrm{dNH4}}{\mathrm{dt}} = \left[f^f_{\mathrm{inorg}} \left(ex^f + r^f\right) \cdot \alpha^f_{N:c} - \beta^f_{NH4} \cdot \mu^f \cdot \alpha^f_{N:C}\right] \cdot \mathrm{Fla}$	f^X_{inorg} *Fractionofinorganicmate–* rial excreted by X	–
$+ \left[f^d_{\mathrm{inorg}} \left(ex^d + r^d\right) \cdot \alpha^d_{N:C} - \beta^d_{NH4} \cdot \mu^d \cdot \alpha^d_{N:C}\right] \cdot \mathrm{Dia}$	$\alpha^X_{N:c}$ *Nitrogen/Carbonratio*	mgN/mgC
$+ \left[f^z_{\mathrm{inorg}} \left(ex^z + r^z\right) \cdot \alpha^z_{N:C}\right] \cdot Zoo$	β^X_{NH4} *Ammoniapreferencefactor*	–
$+ \left[f^z_{\mathrm{inorg}} \left(ex^c + r^c\right) \cdot \alpha^c_{N:C}\right] \cdot \mathrm{Cil}$	K^{DONr}_{min} *DONrmineralizationrate*	1/d
$+ K^{DON}_{\mathrm{min}} \cdot \mathrm{DONr} + K^{DONnr}_{\mathrm{min}} \cdot \mathrm{DONnr}$	K^{DONnr}_{min} *DONnrmineralizationrate*	1/d
$+ f^f_{\mathrm{orgP}} \cdot K^{\mathrm{PON}}_{dec} \cdot \mathrm{PON} - K_{\mathrm{nit}} \cdot NH_4$	f^X_{orgP} *FractionofPONavailable* for mineralization	–
	K^{PON}_{dec} *PONdecompositionrate*	1/d
	K_{nit} *Nitrificationrate*	1/d
Nitrite (NO_2)		
$\frac{\mathrm{dNO_2}}{\mathrm{dt}} = K_{nit} \cdot NH4 - K_{nit} \cdot NO2$	K_{nit} *Nitrificationrate*	1/d
Nitrate (NO_3)		
$\frac{\mathrm{dNO3}}{\mathrm{dt}} = -\left(1 - \beta^f_{NH4}\right) \cdot \alpha^f \cdot \mu^f \cdot \mathrm{Fla}$	β^f_{NH4} *Ammoniapreferencefactor*	–
$-\left(1 - \beta^d_{NH4}\right) \cdot \alpha^d \cdot \mu^d \cdot \mathrm{Dia}$	K_{nit} *Nitrificationrate*	1/d
$+ K_{\mathrm{nit}} \cdot \mathrm{NO2} - K_{\mathrm{dnit}} . \mathrm{NO3}$	K_{dnit} *Denitrificationrate*	1/d

Particulate Organic Nitrogen (PON)

$$
\begin{aligned}
\frac{\mathrm{dPON}}{\mathrm{dt}} = & \left[\left(1-f_{inorg}^{f}\right)\left(1-f_{orgD}^{f}\right)\left(ex^{f}+m^{f}\right)\right]\cdot\alpha_{N:C}^{f}\cdot \mathrm{Fla} \\
& +\left[\left(1-f_{inorg}^{d}\right)\left(1-f_{orgD}^{d}\right)\left(ex^{d}+m^{d}\right)\right]\cdot\alpha_{N:C}^{d}\cdot \mathrm{Dia} \\
& +\left[\left(1-f_{inorg}^{z}\right)\left(1-f_{orgD}^{z}\right)\left(ex^{c}+m^{c}\right)\right]\cdot\alpha_{N:c}^{c}\cdot \mathrm{Cil} \\
& +\left(\delta_{N}^{c}+\varphi_{N}^{c}\right)\cdot \mathrm{Cil} \\
& +\left[\left(1-f_{inorg}^{z}\right)\left(1-f_{orgD}^{z}\right)\left(r^{z}+m^{z}+p^{z}\right)\right]\cdot\alpha_{N:c}^{z}\cdot \mathrm{Zoo} \\
& +\left(\delta_{N}^{z}+\varphi_{N}^{z}\right)\cdot Zoo \\
& -\left(1-f_{orgP}\right)\cdot K_{dec}^{\mathrm{PON}}\cdot PON \\
& -f_{\mathrm{orgP}}\cdot K_{\mathrm{dec}}^{\mathrm{PON}}\cdot PON
\end{aligned}
$$

f_{inorg}^{X} Fraction of inorganic material excreted by X		–
f_{orgD}^{X} Dissolved organic fraction excreted by X		–
$\alpha_{N:C}^{X}$ Nitrogen/Carbon ratio		mgN/mgC
δ_{N}^{Y} Non assimilated material by Y	–	1/d
φ_{N}^{Y} Stoichiometric food web losses		1/d
f_{orgP} Fraction of PON available for mineralization		–
$\cdot K_{\mathrm{dec}}^{\mathrm{PON}}$ PON decomposition rate		1/d

Dissolved Organic Nitrogen Non Refractory (DONnr)

$$
\begin{aligned}
\frac{\mathrm{dDONnr}}{\mathrm{dt}} = & \left[\left(1-f_{\mathrm{inorg}}^{f}\right)\cdot f_{\mathrm{orgD}}^{f}\cdot\left(ex^{f}+r^{f}\right)\cdot\alpha_{N:c}^{f}\cdot Fla\right] \\
& +\left[\left(1-f_{\mathrm{inorg}}^{d}\right)\cdot f_{\mathrm{orgD}}^{d}\left(ex^{d}+r^{d}\right)\cdot\alpha_{N:c}^{d}\cdot \mathrm{Dia}\right] \\
& +\left[\left(1-f_{\mathrm{inorg}}^{c}\right)\cdot f_{\mathrm{orgD}}^{c}\cdot ex^{c}\cdot \mathrm{Cil}\right] \\
& +\left[\left(1-f_{\mathrm{inorg}}^{z}\right)\cdot f_{\mathrm{orgD}}^{z}\cdot ex^{z}\cdot\alpha_{N:c}^{z}\cdot Zoo\right] \\
& -K_{\mathrm{min}}^{DONr}.\ \mathrm{DONnr}
\end{aligned}
$$

f_{inorg}^{X} Fraction of inorganic material excreted by X		–
$\alpha_{N:c}^{X}$ Nitrogen/Carbon ratio		mgN/mgC
f_{orgD}^{X} Dissolved organic fraction excreted by X		–
K_{min}^{DONr} DON remineralization rate		1/d

Dissolved Organic Nitrogen Refractory (DONre)

$$
\frac{\mathrm{dDONre}}{\mathrm{dt}}=\left(1-f_{\mathrm{orgP}}\right)\cdot K_{\mathrm{dec}}^{\mathrm{PON}}\cdot \mathrm{PON}-K_{\mathrm{min}}^{\mathrm{DONre}}.\ \mathrm{DONre}
$$

f_{orgP} Fraction of PON available for mineralization		–
$K_{\mathrm{dec}}^{\mathrm{PON}}$ decomposition rate		1/d
$K_{\mathrm{min}}^{\mathrm{DONre}}$ DON remineralization rate		1/d

Inorganic Phosphorus (IP)

$$
\begin{aligned}
\frac{\mathrm{dIP}}{\mathrm{dt}} = & \left[f_{inorg}^{f}\left(ex^{f}+r^{f}\right)\cdot\alpha_{P:C}^{f}-\mu^{f}\cdot\alpha_{P:c}^{f}\right]\cdot Fla \\
& +\left[f_{inorg}^{d}\left(ex^{d}+r^{d}\right)\cdot\alpha_{P:c}^{d}-\mu^{d}\cdot\alpha_{P:c}^{d}\right]\cdot \mathrm{Dia} \\
& +\left[\left(f_{\mathrm{inorg}}^{z}\cdot ex^{c}+r^{c}\right)\cdot\alpha_{P:c}^{c}\right]\cdot \mathrm{Cil} \\
\vdots & +\left[\left(f_{inorg}^{z}\cdot ex^{c}+r^{c}\right)\cdot\alpha_{P:c}^{z}\right]\cdot Zoo+K_{\mathrm{min}}^{DOPre}\cdot \mathrm{DOPre}\ \Big] \\
& +K_{\mathrm{min}}^{DOPnr}.\ \mathrm{DOPnr}\ +f_{\mathrm{orgP}}\,K_{dec}^{POP}\cdot POP\Big]
\end{aligned}
$$

f_{inorg}^{X} Fraction of inorganic material excreted by X		–
$\alpha_{P:C}^{X}$ Phosphorus/Carbon ratio		mgP/mgC
K_{min}^{DOPre} DOP remineralization rate		1/d
K_{min}^{DOPnr} DOPnr mineralization rate		1/d
f_{orgP} Fraction of PON available for mineralizationd		–
K_{dec}^{POP} POP decomposition rate at reference temperature		1/d

Particulate Organic Phosphorus (POP)

$$
\begin{aligned}
\frac{\mathrm{dPOP}}{\mathrm{dt}} = & \left[\left(1-f_{\mathrm{inorg}}^{f}\right)\cdot\left(1-f_{\mathrm{orgD}}^{f}\right)\cdot\left(ex^{f}+r^{f}\right)+m^{f}\right]\cdot\alpha_{P:C'}^{f}\cdot Fla \\
& +\left[\left(1-f_{\mathrm{inorg}}^{d}\right)\cdot\left(1-f_{\mathrm{orgD}}^{d}\right)\cdot\left(ex^{d}+r^{d}\right)+m^{d}\right]\cdot\alpha_{P:C}^{d}\cdot \mathrm{Dia} \\
& +\left[\left(1-f_{\mathrm{inorg}}^{z}\right)\cdot\left(1-f_{\mathrm{orgD}}^{z}\right)\cdot ex^{c}+m^{c}\right]\cdot\alpha_{P:c}^{c}\cdot Cil \\
& +\left(\delta_{P}^{c}+\varphi_{P}^{c}\right)\cdot \mathrm{Cil} \\
& +\left[\left(1-f_{\mathrm{inorg}}^{z}\right)\cdot\left(1-f_{\mathrm{orgD}}^{z}\right)\cdot ex^{z}+m^{z}+p^{z}\right]\cdot\alpha_{P:C}^{z}\cdot \mathrm{Zoo} \\
& +\left(\delta_{P}^{z}+\varphi_{P}^{z}\right)\cdot \mathrm{Zoo} \\
& -\left(1-f_{\mathrm{orgP}}\right)\cdot K_{\mathrm{dec}}^{\mathrm{POP}}\cdot \mathrm{POP}-f_{\mathrm{orgP}}\cdot K_{\mathrm{dec}}^{\mathrm{POP}}\cdot \mathrm{POP}
\end{aligned}
$$

f_{inorg}^{X} Fraction of inorganic material excreted by X		–
f_{orgD}^{X} Dissolved organic fraction excreted by X		–
$\alpha_{P:C}^{X}$ Phosphorus/Carbon ratio		mgN/mgC
pZ Zooplankton predatory mortality rate: predation by higher trophic		1/d
$forgP$ Fraction of PON available for mineralization		–

Particulate Organic Phosphorus non Refractory (DOPnr)

$$\frac{\text{dPOPnr}}{\text{dt}} = \left[\left(1-f_{inorg}^{f}\right)\cdot f_{orgD}^{f}\cdot\left(ex^{f}+r^{f}\right)\cdot\alpha_{P:c'}^{f}Fla\right] + \left[\left(1-f_{inorg}^{d}\right)\cdot f_{orgD}^{d}\cdot\left(ex^{d}+r^{d}\right)\cdot\alpha_{P:c}^{d}\cdot Dia\right] + \left[\left(1-f_{inorg}^{z}\right)\cdot f_{orgD}^{z}\cdot ex^{c}\cdot\alpha_{P:c}^{c}\cdot Cil\right] + \left[\left(1-f_{inorg}^{z}\right)\cdot f_{orgD}^{z}\cdot ex^{z}\cdot\alpha_{P:c}^{z}\cdot Z_{0o}\right] - K_{\min}^{DOPr}\cdot \text{DOPnr}$$

f_{inorg}^{X} *Fraction of inorganic* material excreted by X —
f_{orgD}^{X} *Dissolved organic fraction* excreted by X —
$\alpha_{P:c}^{X}$ *Phosphorus/Carbon ratio* mgN/mgC
$K_{\min}^{DOPr}$ *DOPr mineralization rate at* reference temperature 1/d

Dissolved Organic Phosphorus Refractory (DOPre)

$$\frac{\text{dDOPre}}{\text{dt}} = \left(1-f_{\text{orgP}}\right)\cdot K_{\text{dec}}^{\text{POP}}\cdot POP - K_{\min}^{\text{DOPre}}\,.\,\text{DOPre}$$

f_{orgP} *Fraction of PON available* for mineralization — 1/d
$K_{\text{dec}}^{\text{POP}}$ *POP decomposition rate at* reference temperature 1/d
$K_{\min}^{\text{DOPre}}$ *DOPre mineralization rate at* reference temperature

Dissolved Silica (DSi)

$$\frac{\text{dDSi}}{\text{dt}} = -\mu^{di}\cdot\alpha_{Si:C}^{di}\cdot Dia + f_{\text{orgP.}}\,K_{dec}^{\text{BioSi}}\cdot BioSi$$

$\alpha_{Si:C}^{di}$ *Diatoms Silica/Carbon ratio* 1/d
$f_{\text{orgP.}}$ *Fraction of PON available* for mineralization mgS/mgC

Biogenic Silica (BSi)

$$\frac{\text{dBioSi}}{\text{dt}} = \left[\left(1-f_{\text{inorg}}^{d}\right)\left(1-f_{\text{orgD}}^{d}\right)\left(ex^{d}+r^{d}\right)+m^{d}\right].\alpha_{\text{si:C}^{d}}^{d}.\,\text{Dia} + G_{zoo}^{d}.\,\text{Zoo} - f_{\text{orgP}}\,K_{\text{dec}}^{\text{Biosi}}\,.\,\text{BioSi}$$

K_{dec}^{BioSi} *decomposition rate* 1/d
f_{inorg}^{d} *Fraction of inorganic* material excreted by Diatoms —
f_{orgD} *Dissolved organic fraction* excreted by Diatoms —
$\alpha_{\text{si:C}^{d}}^{d}$ *Diatoms Silica/Carbon ratio* mgS/mgC
G_{zoo}^{d} *Mesozooplankton grazing on* Diatoms 1/d
f_{orgP} *Fraction of PON available for* Mineralization —
$K_{\text{dec}}^{\text{Biosi}}$ *BioSi decomposition rate* 1/d

Dissolved Oxygen (O_2)

$$\frac{dO_2}{\text{dt}} = \left(\mu^{f}\cdot\alpha_{O:C}^{\text{photo}} + \left(1-\beta_{NH4}^{f}\right)\cdot\mu^{f}\cdot\alpha_{O:N}^{NO3}\cdot\alpha_{N:C}^{f} + \mu^{f}\cdot\alpha_{O:P}^{IP}\cdot\alpha_{P:c}^{f} - r^{f}\cdot\alpha_{O:C}^{\text{plankton}}\right)\cdot\text{Fla} + \left(\mu^{d}\cdot\alpha_{O:C}^{\text{photo}} + \left(1-\beta_{NH4}^{d}\right)\cdot\mu^{d}\cdot\alpha_{O:N}^{NO3}\cdot\alpha_{N:C}^{d} + \mu^{d}\cdot\alpha_{O:P}^{IP}\cdot\alpha_{P:C}^{d} - r^{d}\cdot\alpha_{O:C}^{\text{plankton}}\right)\cdot\text{Dia} + \left(r^{c}\cdot\alpha_{O:C}^{C}\cdot\text{Cil} + r^{z}\cdot\alpha_{O:c}^{z}\cdot Z_{00}\right) - K_{\min}^{DONre}\cdot\alpha_{O:N}^{\min}\cdot DONre - K_{dec}^{PON}\cdot\alpha_{O:N}^{\min}\cdot PON - K_{\min}^{DONnr}\cdot\alpha_{O:N}^{\min}\cdot DONnr - K_{dec}^{POP}\cdot\alpha_{O:P}^{\min}\cdot POP - K_{\min}^{DOPre}\cdot\alpha_{O:P}^{\min}\cdot\text{DOPre} - K_{\min}^{DOPnr}\cdot\alpha_{O:P}^{\min}\cdot DOPnr\Big) - K_{nit}^{oxy}\cdot\text{NH}_4 - K_{dnit}^{oxy}\cdot\text{NO}_3$$

$\alpha_{O:C}^{\text{photo}}$ *Photosynthesis* Oxygen:Carbon ratio mgO/mgC
β_{NH4}^{X} *Ammonia preference factor* —
$\alpha_{O:N}^{NO3}$ *Oxygen* /Nitrogen ratio in Nitrate mgO/mgC
$\alpha_{O:P}^{IP}$ *Oxygen/Nitrogen ratio in* Phosphate mgO/mgC
$\alpha_{O:C}^{\text{plankton}}$ *Oxygen/Carbon ratio in* plankton respiration mgO/mgC
$K_{\min}^{DOPre}$ *DOPre mineralization rate* 1/d
$K_{\min}^{DOPnr}$ *DOPnr mineralization rate* 1/d
$K_{\min}^{DONre}$ *DONre mineralization rate* 1/d
$K_{\min}^{DONnr}$ *DONnr mineralization rate* 1/d
$\alpha_{O:C}^{X}$ *Oxygen* /Carbon Ratio in respiration mgO/mgC
$\alpha_{O:C}^{IP}$ *Oxygen* /Nitrogen Ratio in Phosphate mgO/mgC
$\alpha_{O:P}^{\min}$ *Oxygen Consumption in* Phosphorus mgO/mgP/d
$\alpha_{O:N}^{\min}$ *Oxygen Consumption in Nitrogen* mgO/mg

BIBLIOGRAPHY

[1] *Estuaries: a physical introduction, 2nd edn. john wiley sons, new york, p 195*.

[2] *United nations framework convention on climate change) (2013). decision 9/cp.19*.

[3] *Country population statistics and projections 1950–2050, report food and agric. of the u.n., rome*, (1996).

[4] *Water quality modeling: An overview*, 2009.

[5] *Elaboration de la stratégie nationale de gestion intégrée du littoral. phase 2: diagnostic stratégique du littoral –synthèse*, (2017).

[6] *Ministère de l'Equipement, 2016. Les ports du Maroc en chiffres, 126 p.*, 2019.

[7] K. C. ABBASPOUR, E. ROUHOLAHNEJAD, S. VAGHEFI, R. SRINIVASAN, H. YANG, AND B. KLØVE, *A continental-scale hydrology and water quality model for europe: Calibration and uncertainty of a high-resolution large-scale swat model*, Journal of hydrology, 524 (2015), pp. 733–752.

[8] J. T. ADU, *A mathematical model development for simulating in-stream processes of non-point source pollutants.*, PhD thesis, 2018.

[9] J. T. ADU AND M. V. KUMARASAMY, *Assessing non-point source pollution models: a review.*, Polish Journal of Environmental Studies, 27 (2018).

[10] I. AGMOUR, N. ACHTAICH, Y. EL FOUTAYENI, ET AL., *Carrying capacity influence on the incomes of seiners exploiting marine species in the atlantic coast of morocco*, Mathematical biosciences, 305 (2018), pp. 10–17.

[11] M. AGNAOU, M. NADIR, A. A. ALLA, L. BAZZI, Z. EL ALAMI, AND A. MOUKRIM, *Organochlorine pesticides level evaluation in a morocco southernwetland: Massa estuary*, J Mater Environ Sci, 8 (2017), pp. 3496–3501.

[12] ——, *The occurrence and spatial distribution of pesticides in sea water of the agadir bay (south of morocco)*, ecosystems, 13 (2018), p. 14.

[13] A. AGOUZOUK AND I. BESSA, *Circulation marine de la baie de cintra (sud du maroc) par modèle hydrodynamique 2d*.

[14] S. AGUSTI, C. M. DUARTE, D. VAQUÉ, M. HEIN, J. M. GASOL, AND M. VIDAL, *Food-web structure and elemental (c, n and p) fluxes in the eastern tropical north atlantic*, Deep Sea Research Part II: Topical Studies in Oceanography, 48 (2001), pp. 2295–2321.

[15] A. AKKOYUNLU AND Y. KARAASLAN, *Assessment of improvement scenario for water quality in mogan lake by using the aquatox model*, Environmental Science and Pollution Research, 22 (2015), pp. 14349–14357.

[16] G. AKOKO, T. H. LE, T. GOMI, AND T. KATO, *A review of swat model application in africa*, Water, 13 (2021), p. 1313.

[17] E. AKOMEAH, K.-E. LINDENSCHMIDT, AND S. C. CHAPRA, *Comparison of aquatic ecosystem functioning between eutrophic and hypereutrophic cold-region river-lake systems*, Ecological Modelling, 393 (2019), pp. 25–36.

[18] T. ALEMAYEHU, A. V. GRIENSVEN, B. T. WOLDEGIORGIS, AND W. BAUWENS, *An improved swat vegetation growth module and its evaluation for four tropical ecosystems*, Hydrology and Earth System Sciences, 21 (2017), pp. 4449–4467.

[19] A. AMAZZAL, E. AIT-TALBORJT, J. HERMAS, AND N. HAFIDI, *Importance of hydrological parameters in the distribution of planktonic eggs and larvae in an upwelling zone (imessouane bay, moroccan atlantic coast)*, Caspian Journal of Environmental Sciences, 18 (2020), pp. 1–12.

[20] K. R. AMBROSE, D. E. RICE, M. M. GOODMAN, AND F. KNAPP, *Effect of 3-methyl-branching on the metabolism in rat hearts of radioiodinated iodovinyl long chain fatty acids*, European journal of nuclear medicine, 13 (1987), pp. 374–379.

[21] V. ANABALÓN, J. ARÍSTEGUI, C. MORALES, I. ANDRADE, M. BENAVIDES, M. CORREA-RAMÍREZ, M. ESPINO, O. ETTAHIRI, S. HORMAZABAL, A. MAKAOUI, ET AL., *The structure of planktonic communities under variable coastal upwelling conditions off cape ghir (31 n) in the canary current system (nw africa)*, Progress in Oceanography, 120 (2014), pp. 320–339.

[22] E. ANAGNOSTOU, A. GIANNI, AND I. ZACHARIAS, *Ecological modeling and eutrophication—a review*, Natural Resource Modeling, 30 (2017), p. e12130.

[23] J. M. ANDERIES, O. BARRETEAU, AND U. BRADY, *Refining the robustness of social-ecological systems framework for comparative analysis of coastal system adaptation to global change*, Regional Environmental Change, 19 (2019), pp. 1891–1908.

[24] V. ANDERSEN, P. NIVAL, AND R. P. HARRIS, *Modelling of a planktonic ecosystem in an enclosed water column*, Journal of the Marine Biological Association of the United Kingdom, 67 (1987), pp. 407–430.

[25] S. ANGELETTI, J. O. PIERINI, AND P. M. CERVELLINI, *Suspended sediment contribution resulting from bioturbation in intertidal sites of a sw atlantic mesotidal estuary: data analysis and numerical modelling*, Scientia Marina, 82 (2018).

[26] M. ANHICHEM, M. DELLAL, R. CHFIRI, A. YAHYAOUI, AND S. BENBRAHIM, *Étude de la qualité des eaux et des sédiments de la baie de dakhla au maroc. qualité physico-chimique et contamination métallique*, Bull. Soc. Zool. Fr, 142 (2017), pp. 185–202.

[27] I. AOUICHE, L. DAOUDI, E. J. ANTHONY, M. SEDRATI, A. EL MIMOUNI, AND P. DUSSOUILLEZ, *Alongshore variations in morphology and incident wave energy on a human-impacted coast: Agadir, morocco.*, Journal of Coastal Research, (2016), pp. 1027–1031.

[28] I. AOUICHE, L. DAOUDI, E. J. ANTHONY, M. SEDRATI, E. ZIANE, A. HARTI, AND P. DUSSOUILLEZ, *Anthropogenic effects on shoreface and shoreline changes: Input from a multi-method analysis, agadir bay, morocco*, Geomorphology, 254 (2016), pp. 16–31.

[29] I. AOUICHE, L. DAOUDI, A. HARTI, E. ZIANE, AND B. OUAHMANE, *Etude multidisciplinaire de l'impact des aménagements côtiers sur l'évolution du littoral de la baie d'agadir (maroc atlantique)*, in Actes du Colloque Quaternaire du Nord-Ouest de l'Afrique, 2013, pp. 21–22.

[30] A. AREFINIA, O. BOZORG-HADDAD, A. OLIAZADEH, AND H. A. LOÁICIGA, *Reservoir water quality simulation with data mining models*, Environmental Monitoring and Assessment, 192 (2020), pp. 1–13.

[31] G. B. ARHONDITSIS AND M. T. BRETT, *Eutrophication model for lake washington (usa): Part i. model description and sensitivity analysis*, Ecological modelling, 187 (2005), pp. 140–178.

[32] J. ARÍSTEGUI, E. D. BARTON, X. A. ÁLVAREZ-SALGADO, A. M. P. SANTOS, F. G. FIGUEIRAS, S. KIFANI, S. HERNÁNDEZ-LEÓN, E. MASON, E. MACHÚ, AND H. DEMARCQ, *Sub-regional ecosystem variability in the canary current upwelling*, Progress in Oceanography, 83 (2009), pp. 33–48.

[33] J. ARÍSTEGUI AND M. F. MONTERO, *Temporal and spatial changes in plankton respiration and biomass in the canary islands region: the effect of mesoscale variability*, Journal of Marine Systems, 54 (2005), pp. 65–82.

[34] J. ARÍSTEGUI, M. F. MONTERO, N. HERNÁNDEZ-HERNÁNDEZ, I. J. ALONSO-GONZÁLEZ, F. BALTAR, M. L. CALLEJA, AND C. M. DUARTE, *Variability in water-column respiration and its dependence on organic carbon sources in the canary current upwelling region*, Frontiers in Earth Science, 8 (2020), p. 349.

[35] J. G. ARNOLD, D. N. MORIASI, P. W. GASSMAN, K. C. ABBASPOUR, M. J. WHITE, R. SRINIVASAN, C. SANTHI, R. HARMEL, A. VAN GRIENSVEN, M. W. VAN LIEW, ET AL., *Swat: Model use, calibration, and validation*, Transactions of the ASABE, 55 (2012), pp. 1491–1508.

[36] J. G. ARNOLD, R. SRINIVASAN, R. S. MUTTIAH, AND J. R. WILLIAMS, *Large area hydrologic modeling and assessment part i: model development 1*, JAWRA Journal of the American Water Resources Association, 34 (1998), pp. 73–89.

[37] A. ASADI, A. MOGHADDAM NIA, B. BAKHTIARI ENAYAT, H. ALILOU, E. AHMADISHARAF, E. KIMUTAI KANDA, AND E. CHESSUM KIPKORIR, *An integrated approach for prioritization of river water quality sampling points using modified sanders, analytic network process, and hydrodynamic modeling*, Environmental Monitoring and Assessment, 193 (2021), pp. 1–15.

[38] I. ASCIONE, *Development and application of a processoriented model for benthic marine systems*, PhD thesis, PhD thesis. Lisbon University, Portugal, 200pp, 2014.

[39] E. AUTRET, F. PAUL, P. TANDÉO, AND B. HACKETT, *For level 3 and 4 odyssea sst products over the global ocean and north western shelves—sst _ glo _ sst _ l3 _ nrt _ observations _ 010 _ 010—sst _ nws _ sst _ l4 _ nrt _ observations _ 010 _ 003, 2017*, EU Copernicus Marine Service–Public: Brussels, Belgium, (2017).

[40] I. C. AZEVEDO, A. A. BORDALO, AND P. M. DUARTE, *Influence of river discharge patterns on the hydrodynamics and potential contaminant dispersion in the douro estuary (portugal)*, Water research, 44 (2010), pp. 3133–3146.

[41] O. BABAMIRI AND S. MAROFI, *A multi-objective simulation–optimization approach for water resource planning of reservoir–river systems based on a coupled quantity–quality model*, Environmental Earth Sciences, 80 (2021), pp. 1–19.

[42] H. K. BACH AND J. K. JENSEN, *Modelling of the water quality of a proposed impounded lake of a tidally influenced river*, Ecological modelling, 74 (1994), pp. 77–90.

[43] H. BADSI, H. O. ALI, M. LOUDIKI, AND A. AAMIRI, *Phytoplankton diversity and community composition along the salinity gradient of the massa estuary*, American Journal of Human Ecology, 1 (2012), pp. 58–64.

[44] S. BAE AND D. SEO, *Changes in algal bloom dynamics in a regulated large river in response to eutrophic status*, Ecological Modelling, 454 (2021), p. 109590.

[45] M. E. BAIRD AND S. M. EMSLEY, *Towards a mechanistic model of plankton population dynamics.*, Journal of Plankton Research, 21 (1999).

[46] N. BALOIAN, J. A. PINO, G. ZURITA, V. LOBOS-OSSANDÓN, AND H. MAURER, *Twenty-five years of journal of universal computer science: A bibliometric overview*, JUCS-Journal of Universal Computer Science, 27 (2021), p. 3.

[47] J. BARETTA, W. EBENHÖH, AND P. RUARDIJ, *The european regional seas ecosystem model, a complex marine ecosystem model*, Netherlands Journal of Sea Research, 33 (1995), pp. 233–246.

[48] J. BARETTA-BEKKER, J. BARETTA, A. HANSEN, AND B. RIEMANN, *An improved model of carbon and nutrient dynamics in the microbial food web in marine enclosures*, Aquatic microbial ecology, 14 (1998), pp. 91–108.

[49] J. BARETTA-BEKKER, J. BARETTA, M. LATUHIHIN, X. DESMIT, AND T. PRINS, *Description of the long-term (1991–2005) temporal and spatial distribution of phytoplankton carbon biomass in the dutch north sea*, Journal of Sea Research, 61 (2009), pp. 50–59.

[50] E. BARTON, J. ARISTEGUI, P. TETT, M. CANTÓN, J. GARCIA-BRAUN, S. HERNÁNDEZ-LEÓN, L. NYKJAER, C. ALMEIDA, J. ALMUNIA, S. BALLESTEROS, ET AL., *The transition zone of the canary current upwelling region*, Progress in Oceanography, 41 (1998), pp. 455–504.

[51] A. BASSET, L. SABETTA, A. FONNESU, D. MOUILLOT, T. DO CHI, P. VIAROLI, G. GIORDANI, S. REIZOPOULOU, M. ABBIATI, AND G. CARRADA, *Typology in mediterranean transitional waters: new challenges and perspectives*, Aquatic Conservation: Marine and Freshwater Ecosystems, 16 (2006), pp. 441–455.

[52] P. Beier, L. J. Hansen, L. Helbrecht, and D. Behar, *A how-to guide for coproduction of actionable science*, Conservation Letters, 10 (2017), pp. 288–296.

[53] D. Bellafiore, W. J. McKiver, C. Ferrarin, and G. Umgiesser, *The importance of modeling nonhydrostatic processes for dense water reproduction in the southern adriatic sea*, Ocean Modelling, 125 (2018), pp. 22–38.

[54] Z. BENMASSAOUD and B. IBNKHALDOUN, *La gestion intégrée des zones côtières: Outil juridique de préservation du littoral marocain*, Journal d'Economie, de Management, d'Environnement et de Droit, 3 (2020), pp. 86–98.

[55] U. Bergström, G. Sundblad, A.-L. Downie, M. Snickars, C. Boström, and M. Lindegarth, *Evaluating eutrophication management scenarios in the baltic sea using species distribution modelling*, Journal of Applied Ecology, 50 (2013), pp. 680–690.

[56] A. Berraho, H. Abdelouahab, T. Baibai, S. Charib, J. Larissi, A. Agouzouk, and A. Makaoui, *Short-term variation of zooplankton community in cintra bay (northwest africa)*, Oceanologia, 61 (2019), pp. 368–383.

[57] K. Beryouni, Y. Méar, A. Murat, E. Poizot, and M. Chaibi, *Geographical variability of environmental parameters versus gps precision: Toward a better sampling strategy*, Marine pollution bulletin, 64 (2012), pp. 2507–2518.

[58] S. Biswas, K. J. Hussain, N. Das, B. Russell, K. Satpathy, and S. Mishra, *Imprint of monsoonal patterns on the fish assemblage in coastal waters of south-east india: A case study*, Journal of fish biology, 85 (2014), pp. 773–799.

[59] J. Blackford, J. Allen, and F. J. Gilbert, *Ecosystem dynamics at six contrasting sites: a generic modelling study*, Journal of Marine Systems, 52 (2004), pp. 191–215.

[60] M. Bocci, D. Brigolin, F. Pranovi, M. Najih, D. Nachite, and R. Pastres, *An ecosystem approach for understanding status and changes of nador lagoon (morocco): application of food web models and ecosystem indices*, Estuarine, Coastal and Shelf Science, 171 (2016), pp. 133–143.

[61] S. Bonamano, V. Piermattei, A. Madonia, F. Paladini de Mendoza, A. Pierattini, R. Martellucci, C. Stefanì, G. Zappalà, G. Caruso, and M. Marcelli, *The civitavecchia coastal environment monitoring system (c-cems): a new tool to analyze the conflicts between coastal pressures and sensitivity areas*, Ocean Science, 12 (2016), pp. 87–100.

[62] N. L. Booth, E. J. Everman, I.-L. Kuo, L. Sprague, and L. Murphy, *A web-based decision support system for assessing regional water-quality conditions and management actions 1*, JAWRA Journal of the American Water Resources Association, 47 (2011), pp. 1136–1150.

[63] A. Borja, J.-C. Marques, C. Olabarria, and V. Quintino, *Marine research in the iberian peninsula: A pledge for better times after an economic crisis*, Journal of Sea Research, 83 (2013), pp. 1–8.

[64] Y. BOUNDIR, M. HASNI, F. RAFIK, H. SABRI, N. BAHAMMOU, M. CHEGGOUR, H. ACHTAK, O. CHERIFI, ET AL., *First study of the ecological status in the atlantic coast of morocco using the brown seaweed cystoseira tamariscifolia*, Applied Ecology and Environmental Research, 17 (2019), pp. 14315–14331.

[65] K. BOWDEN AND S. BROWN, *Relating effluent control parameters to river quality objectives using a generalised catchment simulation model*, Water Science and Technology, 16 (1984), pp. 197–206.

[66] R. E. BOWEN AND M. H. DEPLEDGE, *Rapid assessment of marine pollution (ramp)*, Marine Pollution Bulletin, 53 (2006), pp. 631–639.

[67] B. BRACHT-FLYR AND S. C. FRITZ, *Combining lake core records with the limnologic model dyresm-caedym to evaluate lake response during the little ice age and medieval climate anomaly*, Journal of Paleolimnology, 56 (2016), pp. 79–92.

[68] F. BRANDÃO, Z. BREDA, AND C. COSTA, *Innovation and internationalization as development strategies for coastal tourism destinations: The role of organizational networks*, Journal of Hospitality and Tourism Management, 41 (2019), pp. 219–230.

[69] F. BRAUNSCHWEIG, F. MARTINS, P. CHAMBEL, AND R. NEVES, *A methodology to estimate renewal time scales in estuaries: the tagus estuary case*, Ocean Dynamics, 53 (2003), pp. 137–145.

[70] A. C. BRITO, A. NEWTON, P. TETT, AND T. F. FERNANDES, *How will shallow coastal lagoons respond to climate change? a modelling investigation*, Estuarine, Coastal and Shelf Science, 112 (2012), pp. 98–104.

[71] B. W. BROOK, J. C. BUETTEL, AND S. HONG, *Constrained scenarios for twenty-first century human population size based on the empirical coupling to economic growth*, arXiv preprint arXiv:2109.14209, (2021).

[72] S. E. BRUMER, V. GARNIER, J.-L. REDELSPERGER, M.-N. BOUIN, F. ARDHUIN, AND M. ACCENSI, *Impacts of surface gravity waves on a tidal front: a coupled model perspective*, Ocean Modelling, 154 (2020), p. 101677.

[73] H. H. BUI, N. H. HA, T. N. D. NGUYEN, A. T. NGUYEN, T. T. H. PHAM, J. KANDASAMY, AND T. V. NGUYEN, *Integration of swat and qual2k for water quality modeling in a data scarce basin of cau river basin in vietnam*, Ecohydrology & Hydrobiology, 19 (2019), pp. 210–223.

[74] H. BURCHARD, *GOTM-a General Ocean Turbulence Model. Theory, Applications and Test Cases. Tech. Rep. EUR 18745 EN. European Commission*, Springer Science & Business Media, 1999.

[75] ——, *Applied turbulence modelling in marine waters*, vol. 100, Springer Science & Business Media, 2002.

[76] M. BURFORD, C. CAREY, D. HAMILTON, J. HUISMAN, H. PAERL, S. WOOD, AND A. WULFF, *Perspective: Advancing the research agenda for improving understanding of cyanobacteria in a future of global change*, Harmful Algae, 91 (2020), p. 101601.

[77] D. F. BURGER, D. P. HAMILTON, AND C. A. PILDITCH, *Modelling the relative importance of internal and external nutrient loads on water column nutrient concentrations and phytoplankton biomass in a shallow polymictic lake*, Ecological Modelling, 211 (2008), pp. 411–423.

[78] A. BURSON, M. STOMP, L. AKIL, C. P. BRUSSAARD, AND J. HUISMAN, *Unbalanced reduction of nutrient loads has created an offshore gradient from phosphorus to nitrogen limitation in the n orth s ea*, Limnology and Oceanography, 61 (2016), pp. 869–888.

[79] J. A. BURT AND A. BARTHOLOMEW, *Towards more sustainable coastal development in the arabian gulf: Opportunities for ecological engineering in an urbanized seascape*, Marine pollution bulletin, 142 (2019), pp. 93–102.

[80] K. BURT, D. HAMOUTENE, G. MABROUK, C. LANG, T. PUESTOW, D. DROVER, R. LOSIER, AND F. PAGE, *Environmental conditions and occurrence of hypoxia within production cages of atlantic salmon on the south coast of newfoundland*, Aquaculture Research, 43 (2012), pp. 607–620.

[81] P. CABRAL, H. LEVREL, J. SCHOENN, E. THIÉBAUT, P. LE MAO, R. MONGRUEL, C. ROLLET, K. DEDIEU, S. CARRIER, F. MORISSEAU, ET AL., *Marine habitats ecosystem service potential: A vulnerability approach in the normand-breton (saint malo) gulf, france*, Ecosystem services, 16 (2015), pp. 306–318.

[82] M. CALLON, J.-P. COURTIAL, W. A. TURNER, AND S. BAUIN, *From translations to problematic networks: An introduction to co-word analysis*, Social science information, 22 (1983), pp. 191–235.

[83] F. J. CAMPUZANO, M. D. MATEUS, P. C. LEITÃO, P. C. LEITÃO, V. H. MARÍN, L. E. DELGADO, A. TIRONI, J. O. PIERINI, A. F. SAMPAIO, P. ALMEIDA, ET AL., *Integrated coastal zone management in south america: A look at three contrasting systems*, Ocean & Coastal Management, 72 (2013), pp. 22–35.

[84] L. CANCINO AND R. NEVES, *Three-dimensional model system for baroclinic estuarine dynamics and suspended sediment transport in a mesotidal estuary*, WIT Transactions on The Built Environment, 10 (1970).

[85] D. M. CANU, G. ROSATI, C. SOLIDORO, L.-E. HEIMBÜRGER, AND A. ACQUAVITA, *A comprehensive assessment of the mercury budget in the marano–grado lagoon (adriatic sea) using a combined observational modeling approach*, Marine Chemistry, 177 (2015), pp. 742–752.

[86] X. CAO, L. WAN, J. XIAO, X. CHEN, Y. ZHOU, Z. WANG, AND C. SONG, *Environmental effects by introducing potamogeton crispus to recover a eutrophic lake*, Science of the total environment, 621 (2018), pp. 360–367.

[87] L. CARRERE, F. LYARD, M. CANCET, A. GUILLOT, AND L. ROBLOU, *Fes 2012: a new global tidal model taking advantage of nearly 20 years of altimetry*, 20 Years of Progress in Radar Altimatry, 710 (2013), p. 13.

[88] L. CARRÈRE, F. LYARD, M. CANCET, L. ROBLOU, AND A. GUILLOT, *Fes 2012: a new tidal model taking advantage of nearly 20 years of altimetry measurements*, in ocean surface topography science team 2012 meeting, Venice-Lido, Italy, 2012, pp. 22–29.

[89] K. CEBE AND L. BALAS, *Water quality modelling in kaş bay*, Applied Mathematical Modelling, 40 (2016), pp. 1887–1913.

[90] D. CHAHID, A. LENOBLE, L. BOUDAD, AND B. V. VLIET-LANOË, *Enregistrements sédimentaires d'événements de haute énergie, exemples de la côte atlantique de rabat-skhirat (maroc)*, Quaternaire. Revue de l'Association française pour l'étude du Quaternaire, 27 (2016), pp. 155–169.

[91] A. CHAHOURI, N. EL OUAHMANI, A. EL AZZAOUI, B. YACOUBI, A. BANAOUI, AND A. MOUKRIM, *Combined assessment of bacteriological and environmental indicators of fecal contamination in agadir bay ecosystems (south-west morocco)*, International Journal of Environmental Science and Technology, (2021), pp. 1–14.

[92] Y. S. CHANG, J.-Y. JIN, J. Y. CHOI, W. M. JEONG, S. K. HYUN, C. S. CHUNG, AND J. D. DO, *Three dimensional numerical modeling using a multi-level nesting system for identifying a water layer suitable for scallop farming in tongyeong, korea*, Aquacultural Engineering, 89 (2020), p. 102058.

[93] C. CHANGE, *Synthesis report. contribution of working groups i, ii and iii to the fifth assessment report of the intergovernmental panel on climate change.[core writing team, rk pachauri and la meyer*, 2014.

[94] S. C. CHAPRA, *Surface water-quality modeling*, Waveland press, 2008.

[95] P. CHASEK, W. ESSAHLI, M. AKHTAR-SCHUSTER, L. C. STRINGER, AND R. THOMAS, *Integrated land degradation monitoring and assessment: horizontal knowledge management at the national and international levels*, Land Degradation & Development, 22 (2011), pp. 272–284.

[96] A. CHAUDHARY, B. R. YADAV, AND D. N. RATHA, *Prediction of Water Quality of a Stream Carrying Industrial Treated Waste Water Using QUAL2K*, PhD thesis, 2018.

[97] F. P. CHAVEZ AND M. MESSIÉ, *A comparison of eastern boundary upwelling ecosystems*, Progress in Oceanography, 83 (2009), pp. 80–96.

[98] C.-F. CHEN, K.-Y. CHONG, AND J.-Y. LIN, *A combined catchment-reservoir water quality model to guide catchment management for reservoir water quality control*, Water and Environment Journal, (2021).

[99] L. CHEN, Z. YANG, AND H. LIU, *Assessing the eutrophication risk of the danjiangkou reservoir based on the efdc model*, Ecological Engineering, 96 (2016), pp. 117–127.

[100] T. CHEN, Q. ZHANG, Y. WU, C. JI, J. YANG, AND G. LIU, *Development of a wave-current model through coupling of fvcom and swan*, Ocean engineering, 164 (2018), pp. 443–454.

[101] Y. Chen, C.-Y. Xu, X. Chen, Y. Xu, Y. Yin, L. Gao, and M. Liu, *Uncertainty in simulation of land-use change impacts on catchment runoff with multi-timescales based on the comparison of the hspf and swat models*, Journal of Hydrology, 573 (2019), pp. 486–500.

[102] A. Chinyama, G. Ochieng, I. Nhapi, and F. Otieno, *A simple framework for selection of water quality models*, Reviews in Environmental Science and Bio/Technology, 13 (2014), pp. 109–119.

[103] K. Cho, Y. Pachepsky, M. Ligaray, Y. Kwon, and K. H. Kim, *Data assimilation in surface water quality modeling: A review*, Water Research, (2020), p. 116307.

[104] K. H. Cho, Y. A. Pachepsky, D. M. Oliver, R. W. Muirhead, Y. Park, R. S. Quilliam, and D. R. Shelton, *Modeling fate and transport of fecally-derived microorganisms at the watershed scale: state of the science and future opportunities*, Water research, 100 (2016), pp. 38–56.

[105] Z. Chong, Y. Wei, and Y. Zhifeng, *Environmental flows management strategies based on the spatial distribution of water quality, a case study of baiyangdian lake, a shallow freshwater lake in china*, Procedia Environmental Sciences, 2 (2010), pp. 896–905.

[106] S.-W. Chung, J. Imberger, M. Hipsey, and H. Lee, *The influence of physical and physiological processes on the spatial heterogeneity of a microcystis bloom in a stratified reservoir*, Ecological Modelling, 289 (2014), pp. 133–149.

[107] J. E. Cloern, *Our evolving conceptual model of the coastal eutrophication problem*, Marine ecology progress series, 210 (2001), pp. 223–253.

[108] J. E. Cloern, S. Foster, and A. Kleckner, *Phytoplankton primary production in the world's estuarine-coastal ecosystems*, Biogeosciences, 11 (2014), pp. 2477–2501.

[109] K. L. Cochrane, W. H. Sauer, and S. Aswani, *Science in the service of society: Is marine and coastal science addressing south africa's needs?*, South African Journal of Science, 115 (2019), pp. 1–7.

[110] F. Colas, J. C. McWilliams, X. Capet, and J. Kurian, *Heat balance and eddies in the peru-chile current system*, Climate dynamics, 39 (2012), pp. 509–529.

[111] T. M. Cole and E. M. Buchak, *Ce-qual-w2: A two-dimensional, laterally averaged, hydrodynamic and water quality model, version 2.0. user manual.*, tech. rep., ARMY ENGINEER WATERWAYS EXPERIMENT STATION VICKSBURG MS ENVIRONMENTAL LAB, 1995.

[112] T. M. Cole and S. A. Wells, *Ce-qual-w2: A two-dimensional, laterally averaged, hydrodynamic and water quality model, version 3.5*, (2006).

[113] I. O. Commission et al., *United nations decade of ocean science for sustainable development 2021–2030 implementation plan version 2.0*, 2020.

[114] C. N. Cook, M. B. Mascia, M. W. Schwartz, H. P. Possingham, and R. A. Fuller, *Achieving conservation science that bridges the knowledge–action boundary*, Conservation Biology, 27 (2013), pp. 669–678.

[115] C. N. Cook, S. J. Nichols, J. A. Webb, R. A. Fuller, and R. M. Richards, *Simplifying the selection of evidence synthesis methods to inform environmental decisions: A guide for decision makers and scientists*, Biological Conservation, 213 (2017), pp. 135–145.

[116] D. M. Cossarini, B. H. MacDonald, and P. G. Wells, *Communicating marine environmental information to decision makers: Enablers and barriers to use of publications (grey literature) of the gulf of maine council on the marine environment*, Ocean & Coastal Management, 96 (2014), pp. 163–172.

[117] C. M. d. S. B. Costa, L. da Silva Marques, A. K. Almeida, I. R. Leite, and I. K. de Almeida, *Applicability of water quality models around the world—a review*, Environmental Science and Pollution Research, 26 (2019), pp. 36141–36162.

[118] C. M. d. S. B. Costa, I. R. Leite, A. K. Almeida, and I. K. de Almeida, *Choosing an appropriate water quality model—a review*, Environmental Monitoring and Assessment, 193 (2021), pp. 1–15.

[119] B. Cox, *A review of currently available in-stream water-quality models and their applicability for simulating dissolved oxygen in lowland rivers*, Science of the total environment, 314 (2003), pp. 335–377.

[120] D. Cozzolino, N. Greggio, M. Antonellini, and B. M. S. Giambastiani, *Natural and anthropogenic factors affecting freshwater lenses in coastal dunes of the adriatic coast*, Journal of Hydrology, 551 (2017), pp. 804–818.

[121] P. M. Craig, *User's manual for efdc_explorer: a pre/post processor for the environmental fluid dynamics code*, Dynamic Solutions, LLC, Knoxville, TN, (2011).

[122] T. E. Cropper, E. Hanna, and G. R. Bigg, *Spatial and temporal seasonal trends in coastal upwelling off northwest africa, 1981–2012*, Deep Sea Research Part I: Oceanographic Research Papers, 86 (2014), pp. 94–111.

[123] A. Cucco, G. Quattrocchi, A. Olita, L. Fazioli, A. Ribotti, M. Sinerchia, C. Tedesco, and R. Sorgente, *Hydrodynamic modelling of coastal seas: the role of tidal dynamics in the messina strait, western mediterranean sea*, Natural Hazards and Earth System Sciences, 16 (2016), pp. 1553–1569.

[124] F. Cui, C. Park, and M. Kim, *Application of curve-fitting techniques to develop numerical calibration procedures for a river water quality model*, Journal of environmental management, 249 (2019), p. 109375.

[125] Y. Cui, G. Zhu, H. Li, L. Luo, X. Cheng, Y. Jin, and D. Trolle, *Modeling the response of phytoplankton to reduced external nutrient load in a subtropical chinese reservoir using dyresm-caedym*, Lake and Reservoir Management, 32 (2016), pp. 146–157.

[126] D. Cushing, *A difference in structure between ecosystems in strongly stratified waters and in those that are only weakly stratified*, Journal of plankton research, 11 (1989), pp. 1–13.

[127] C. Cvitanovic, C. Fulton, S. Wilson, L. van Kerkhoff, I. Cripps, and N. Muthiga, *Utility of primary scientific literature to environmental managers: an international case study on coral-dominated marine protected areas*, Ocean & Coastal Management, 102 (2014), pp. 72–78.

[128] C. Cvitanovic, A. Hobday, L. van Kerkhoff, and N. Marshall, *Overcoming barriers to knowledge exchange for adaptive resource management; the perspectives of australian marine scientists*, Marine policy, 52 (2015), pp. 38–44.

[129] Y. Dai, Y. Lang, T. Wang, X. Han, L. Wang, and J. Zhong, *Modelling the sources and transport of ammonium nitrogen with the sparrow model: A case study in a karst basin*, Journal of Hydrology, 592 (2021), p. 125763.

[130] Z. Daief, A. Borja, L. Joulami, M. Azzi, A. Fahde, and H. Bazairi, *Assessing benthic ecological status of urban sandy beaches (northeast atlantic, morocco) using m-ambi*, Ecological Indicators, 46 (2014), pp. 586–595.

[131] H. Dalun and M. O. Abdullah, *Regional leachate discharge, monitoring and the associated riverine pollutants propagation model simulation of sungai sarawak in malaysia*, Journal of Cleaner Production, 303 (2021), p. 127091.

[132] Z. Damsiri, K. Elkalay, and K. Khalil, *Modelling the biogeochemical cycle of the oualidia lagoon (atlantic, morocco)*, Int. J. Adv. Res, 3 (2015), pp. 18–30.

[133] Z. Damsiri, L. Natij, K. Khalil, M. Loudiki, J. Richir, H. El Himer, and K. Elkalay, *Seasonal characterization of the nutrients state in oualidia lagoon (moroccan atlantic coast)*, Journal of Materials and Environmental Science, 8 (2017), pp. 67–77.

[134] V. David, M. Ryckaert, M. Karpytchev, C. Bacher, V. Arnaudeau, N. Vidal, D. Maurer, and N. Niquil, *Spatial and long-term changes in the functional and structural phytoplankton communities along the french atlantic coast*, Estuarine, Coastal and Shelf Science, 108 (2012), pp. 37–51.

[135] H. de Pablo, J. Sobrinho, M. Garcia, F. Campuzano, M. Juliano, and R. Neves, *Validation of the 3d-mohid hydrodynamic model for the tagus coastal area*, Water, 11 (2019), p. 1713.

[136] P. M. N. de Pina, *An integrated approach to study the Tagus estuary water quality*, 2001.

[137] B. Debele, R. Srinivasan, and J.-Y. Parlange, *Coupling upland watershed and downstream waterbody hydrodynamic and water quality models (swat and ce-qual-w2) for better water resources management in complex river basins*, Environmental Modeling & Assessment, 13 (2008), pp. 135–153.

[138] R. Deus, D. Brito, I. A. Kenov, M. Lima, V. Costa, A. Medeiros, R. Neves, and C. Alves, *Three-dimensional model for analysis of spatial and temporal patterns of phytoplankton in tucuruí reservoir, pará, brazil*, Ecological modelling, 253 (2013), pp. 28–43.

[139] R. Deus, D. Brito, M. Mateus, I. Kenov, A. Fornaro, R. Neves, and C. Alves, *Impact evaluation of a pisciculture in the tucuruí reservoir (pará, brazil) using a two-dimensional water quality model*, Journal of Hydrology, 487 (2013), pp. 1–12.

[140] DHI, *Water and Development, Horsholm, Denmark*, 2009.

[141] R. J. DIAZ AND R. ROSENBERG, *Spreading dead zones and consequences for marine ecosystems*, science, 321 (2008), pp. 926–929.

[142] P. DISSANAYAKE, H. HOFMANN, AND F. PEETERS, *Comparison of results from two 3d hydrodynamic models with field data: Internal seiches and horizontal currents*, Inland waters, 9 (2019), pp. 239–260.

[143] K. DOUGLAS-MANKIN, R. SRINIVASAN, AND J. ARNOLD, *Soil and water assessment tool (swat) model: Current developments and applications*, Transactions of the ASABE, 53 (2010), pp. 1423–1431.

[144] C. DOULGERIS, P. GEORGIOU, D. PAPADIMOS, AND D. PAPAMICHAIL, *Ecosystem approach to water resources management using the mike 11 modeling system in the strymonas river and lake kerkini*, Journal of environmental management, 94 (2012), pp. 132–143.

[145] J. DU AND J. SHEN, *Water residence time in chesapeake bay for 1980–2012*, Journal of Marine Systems, 164 (2016), pp. 101–111.

[146] B. DUARTE, J. VALENTIM, J. DIAS, H. SILVA, J. MARQUES, AND I. CAÇADOR, *Modelling sea level rise (slr) impacts on salt marsh detrital outwelling c and n exports from an estuarine coastal lagoon to the ocean (ria de aveiro, portugal)*, Ecological modelling, 289 (2014), pp. 36–44.

[147] C. DUKU, H. RATHJENS, S. ZWART, AND L. HEIN, *Towards ecosystem accounting: a comprehensive approach to modelling multiple hydrological ecosystem services*, Hydrology and Earth System Sciences, 19 (2015), pp. 4377–4396.

[148] S. M. DURANT, R. GROOM, B. KULOBA, A. SAMNA, U. MUZUMA, P. GADIMANG, R. MANDISODZA-CHIKEREMA, A. IPAVEC, N. MITCHELL, D. IKANDA, ET AL., *Bridging the divide between scientists and decision-makers: how behavioural ecologists can increase the conservation impact of their research?*, Philosophical Transactions of the Royal Society B, 374 (2019), p. 20190011.

[149] J. EDINGER AND E. BUCHAK, *A hydrodynamic, two-dimensional reservoir model: The computational basis*, Contract DACW27-74-C-0200, report, US Army Eng. Div., Ohio River. Cincinnati, Ohio, (1975).

[150] M. T. EJIGU, *Overview of water quality modeling*, Cogent Engineering, 8 (2021), p. 1891711.

[151] M. EL-AGBANI, M. FEKHAOUI, A. BAYED, AND J. SCHOUTEN, *The khnifiss lagoon and adjacent waters: hydrology and hydrodynamics [morocco]*, Travaux de l'Institut Scientifique (Morocco), (1988).

[152] F. EL ASRI, H. ZIDANE, A. ERRHIF, M.-N. TAMSOURI, M. MAANAN, M. M. IDRISSI, AND D. MARTIN, *Polychaete diversity and assemblage structure in the oualidia lagoon, moroccan atlantic coast*, Journal of the Marine Biological Association of the United Kingdom, 98 (2018), pp. 1337–1346.

[153] F. El Asri, H. Zidane, M. Maanan, M. Tamsouri, and A. Errhif, *Taxonomic diversity and structure of the molluscan fauna in oualidia lagoon (moroccan atlantic coast)*, Environmental monitoring and assessment, 187 (2015), pp. 1–10.

[154] B. El Mahrad, S. Abalansa, A. Newton, J. D. Icely, M. Snoussi, and I. Kacimi, *Social-environmental analysis for the management of coastal lagoons in north africa*, Frontiers in Environmental Science, 8 (2020), p. 37.

[155] M. El-Sheekh, M. M. Abdel-Daim, M. Okba, S. Gharib, A. Soliman, and H. El-Kassas, *Green technology for bioremediation of the eutrophication phenomenon in aquatic ecosystems: a review*, African Journal of Aquatic Science, (2021), pp. 1–19.

[156] H. Elghrib, L. Somoue, N. Elkhiati, A. Berraho, A. Makaoui, N. Bourhim, S. Salah, and O. Ettahiri, *Distribution du phytoplancton dans les zones d'upwelling de la côte atlantique marocaine située entre les latitudes 32° 30 n et 24° n*, Comptes Rendus Biologies, 335 (2012), pp. 541–554.

[157] J. J. Elser, M. E. Bracken, E. E. Cleland, D. S. Gruner, W. S. Harpole, H. Hillebrand, J. T. Ngai, E. W. Seabloom, J. B. Shurin, and J. E. Smith, *Global analysis of nitrogen and phosphorus limitation of primary producers in freshwater, marine and terrestrial ecosystems*, Ecology letters, 10 (2007), pp. 1135–1142.

[158] Elsevier, *How scopus works: Information about scopus product features. elsevier.com. retrieved may 23, 2021, from*, (2021).

[159] A. Environment, *Hydrodynamic and Water Quality Model of the North Saskatchewan River.12th Floor, Baker Centre. Edmonton, Alberta, Canada T5J 1G4*, 2009.

[160] EPA, *Rates, constants and kinetics formulations in surface water quality modeling*, 1985.

[161] P. Falkowski, R. Scholes, E. Boyle, J. Canadell, D. Canfield, J. Elser, N. Gruber, K. Hibbard, P. Högberg, S. Linder, et al., *The global carbon cycle: a test of our knowledge of earth as a system*, science, 290 (2000), pp. 291–296.

[162] M. Fengyun, *Progress in water quality monitoring based on remote sensing and gis*, in 2010 International Conference on Challenges in Environmental Science and Computer Engineering, vol. 2, IEEE, 2010, pp. 208–211.

[163] K. Fennel and J. M. Testa, *Biogeochemical controls on coastal hypoxia*, Annual review of marine science, 11 (2019), pp. 105–130.

[164] R. Fernandes, R. Neves, F. Braunschweig, and D. Brito, *A new modelling toolkit for managing oil and chemical spills in western europe and morocco's atlantic coast: the lisbon agreement and marpocs project*, in Proceedings of the Thirty-Ninth AMOP Technical Seminar on Environmental Contamination and Response. Environment Canada, 2016.

[165] R. Fernandes, R. Neves, C. Viegas, P. Leitão, and L. Hidromod, *Integration of an oil and inert spill model in a framework for risk management of spills at sea: a case study for the atlantic area*, in 36th AMOP Technical Seminar on Environmental Contamination and Response, 2013, pp. 4–6.

[166] A. FERREIRA, P. GARRIDO-AMADOR, AND A. C. BRITO, *Disentangling environmental drivers of phytoplankton biomass off western iberia*, Frontiers in Marine Science, 6 (2019), p. 44.

[167] V. F. FONSECA, P. REIS-SANTOS, B. DUARTE, H. N. CABRAL, M. I. CAÇADOR, N. VAZ, J. M. DIAS, AND M. P. PAIS, *Roving pharmacies: Modelling the dispersion of pharmaceutical contamination in estuaries*, Ecological Indicators, 115 (2020), p. 106437.

[168] M. FOSSATI AND I. PIEDRA-CUEVA, *A 3d hydrodynamic numerical model of the río de la plata and montevideo's coastal zone*, Applied Mathematical Modelling, 37 (2013), pp. 1310–1332.

[169] G. GAL, V. MAKLER-PICK, AND N. SHACHAR, *Dealing with uncertainty in ecosystem model scenarios: application of the single-model ensemble approach*, Environmental modelling & software, 61 (2014), pp. 360–370.

[170] S. GALAFASSI, L. NIZZETTO, AND P. VOLTA, *Plastic sources: a survey across scientific and grey literature for their inventory and relative contribution to microplastics pollution in natural environments, with an emphasis on surface water*, Science of the Total Environment, 693 (2019), p. 133499.

[171] A. GALÁN, M. J. ZIRBEL, G. S. SALDÍAS, F. CHAN, AND R. LETELIER, *The role of upwelling intermittence in the development of hypoxia and nitrogen loss over the oregon shelf*, Journal of Marine Systems, 207 (2020), p. 103342.

[172] M. GALVAGNO, *The intellectual structure of the anti-consumption and consumer resistance field: An author co-citation analysis*, European Journal of Marketing, (2011).

[173] A. K. GAMPERL, O. O. AJIBOYE, F. S. ZANUZZO, R. M. SANDRELLI, C. P. ELLEN DE FÁTIMA, AND A. BEEMELMANNS, *The impacts of increasing temperature and moderate hypoxia on the production characteristics, cardiac morphology and haematology of atlantic salmon (salmo salar)*, Aquaculture, 519 (2020), p. 734874.

[174] L. GAO AND D. LI, *A review of hydrological/water-quality models*, Frontiers of Agricultural Science and Engineering, 1 (2015), pp. 267–276.

[175] Y. GAO, L. GE, S. SHI, Y. SUN, M. LIU, B. WANG, Y. SHANG, J. WU, AND J. TIAN, *Global trends and future prospects of e-waste research: a bibliometric analysis*, Environmental Science and Pollution Research, 26 (2019), pp. 17809–17820.

[176] C. GARNEAU, S. DUCHESNE, AND A. ST-HILAIRE, *Comparison of modelling approaches to estimate trapping efficiency of sedimentation basins on peatlands used for peat extraction*, Ecological Engineering, 133 (2019), pp. 60–68.

[177] P. W. GASSMAN, M. R. REYES, C. H. GREEN, AND J. G. ARNOLD, *The soil and water assessment tool: historical development, applications, and future research directions*, Transactions of the ASABE, 50 (2007), pp. 1211–1250.

[178] T. M. GIANNAROS, D. MELAS, AND I. ZIOMAS, *Performance evaluation of the weather research and forecasting (wrf) model for assessing wind resource in greece*, Renewable Energy, 102 (2017), pp. 190–198.

[179] D. Glaser, J. R. Rhea, D. R. Opdyke, K. T. Russell, C. K. Ziegler, W. Ku, L. Zheng, and J. Mastriano, *Model of zebra mussel growth and water quality impacts in the seneca river, new york*, Lake and Reservoir Management, 25 (2009), pp. 49–72.

[180] C. S. Goh, H.-Y. Chong, L. Jack, and A. F. M. Faris, *Revisiting triple bottom line within the context of sustainable construction: A systematic review*, Journal of Cleaner Production, 252 (2020), p. 119884.

[181] K. H. Goh and K. F. See, *Twenty years of water utility benchmarking: A bibliometric analysis of emerging interest in water research and collaboration*, Journal of Cleaner Production, 284 (2021), p. 124711.

[182] R. Gong, L. Xu, D. Wang, H. Li, and J. Xu, *Water quality modeling for a typical urban lake based on the efdc model*, Environmental Modeling & Assessment, 21 (2016), pp. 643–655.

[183] C. J. González, E. Reyes, Ó. Álvarez, A. Izquierdo, M. Bruno, and R. Mañanes, *Surface currents and transport processes in the strait of gibraltar: Implications for modeling and management of pollutant spills*, Ocean & Coastal Management, 179 (2019), p. 104869.

[184] S. N. Gosling, J. Zaherpour, N. J. Mount, F. F. Hattermann, R. Dankers, B. Arheimer, L. Breuer, J. Ding, I. Haddeland, R. Kumar, et al., *A comparison of changes in river runoff from multiple global and catchment-scale hydrological models under global warming scenarios of 1 c, 2 c and 3 c*, Climatic Change, 141 (2017), pp. 577–595.

[185] L. Grechi, A. Franco, L. Palmeri, A. Pivato, and A. Barausse, *An ecosystem model of the lower po river for use in ecological risk assessment of xenobiotics*, Ecological Modelling, 332 (2016), pp. 42–58.

[186] A. Gredelj, A. Barausse, L. Grechi, and L. Palmeri, *Deriving predicted no-effect concentrations (pnecs) for emerging contaminants in the river po, italy, using three approaches: Assessment factor, species sensitivity distribution and aquatox ecosystem modelling*, Environment international, 119 (2018), pp. 66–78.

[187] D. Grzebyk, C. Béchemin, C. J. Ward, C. Vérité, G. A. Codd, and S. Y. Maestrini, *Effects of salinity and two coastal waters on the growth and toxin content of the dinoflagellate alexandrium minutum*, Journal of Plankton Research, 25 (2003), pp. 1185–1199.

[188] M. Guerreiro, A. B. Fortunato, P. Freire, A. Rilo, R. Taborda, M. C. Freitas, C. Andrade, T. Silva, M. Rodrigues, X. Bertin, et al., *Evolution of the hydrodynamics of the tagus estuary (portugal) in the 21st century*, Revista de Gestão Costeira Integrada-Journal of Integrated Coastal Zone Management, 15 (2015), pp. 65–80.

[189] S.-R. Ha, G.-J. Bae, D.-H. Park, and J. Cho, *Improvement of pre-and post-processing environments of the dynamic two-dimensional reservoir model ce-qual-w2 based on gis*, Water Science and Technology, 48 (2003), pp. 79–88.

[190] M. B. Haddad, G. E. De-la Torre, M. R. Abelouah, S. Hajji, and A. A. Alla, *Personal protective equipment (ppe) pollution associated with the covid-19 pandemic along the coastline of agadir, morocco*, Science of The Total Environment, 798 (2021), p. 149282.

[191] M. A. Hafeez, Y. Nakamura, T. Suzuki, T. Inoue, Y. Matsuzaki, K. Wang, and A. Moiz, *Integration of weather research and forecasting (wrf) model with regional coastal ecosystem model to simulate the hypoxic conditions*, Science of the Total Environment, 771 (2021), p. 145290.

[192] E. Hagen, C. Zulicke, and R. Feistel, *Near-surface structures in the cape ghir filament off morocco*, Oceanologica Acta, 19 (1996), pp. 577–598.

[193] P. Hallinger and J. Kovačević, *A bibliometric review of research on educational administration: Science mapping the literature, 1960 to 2018*, Review of Educational Research, 89 (2019), pp. 335–369.

[194] J. M. Hamrick, *A three-dimensional environmental fluid dynamics computer code: Theoretical and computational aspects*, (1992).

[195] H. Han, F. Los, D. Burger, and X. Lu, *A modelling approach to determine systematic nitrogen transformations in a tropical reservoir*, Ecological Engineering, 94 (2016), pp. 37–49.

[196] HCP, *Annuaire statistiques régional souss massa, regional direction of souss massa*, (1016).

[197] W. He, A. Jiang, J. Zhang, H. Xu, Y. Xiao, S. Chen, and X. Yu, *Comprehensive hydrodynamic fitness of an estuary channel and the effects of a water diversion inflow*, Estuaries and Coasts, (2021), pp. 1–11.

[198] G. K. Heilig, *World urbanization prospects: the 2011 revision*, United Nations, Department of Economic and Social Affairs (DESA), Population Division, Population Estimates and Projections Section, New York, 14 (2012), p. 555.

[199] S. Hernández-León, M. Gomez, and J. Arístegui, *Mesozooplankton in the canary current system: The coastal–ocean transition zone*, Progress in Oceanography, 74 (2007), pp. 397–421.

[200] S. Hernández-León, S. Putzeys, C. Almeida, P. Bécognée, A. Marrero-Díaz, J. Arístegui, and L. Yebra, *Carbon export through zooplankton active flux in the canary current*, Journal of Marine Systems, 189 (2019), pp. 12–21.

[201] M. Hernando, I. R. Schloss, G. Malanga, G. O. Almandoz, G. A. Ferreyra, M. B. Aguiar, and S. Puntarulo, *Effects of salinity changes on coastal antarctic phytoplankton physiology and assemblage composition*, Journal of Experimental Marine Biology and Ecology, 466 (2015), pp. 110–119.

[202] K. Hilmi, *Modélisation numérique de la circulation de deux milieux paraliques du littoral marocain: la lagune de oualidia (atlantique) et la lagune de nador (méditerranée)*, (2005).

[203] M. Hipsey, J. Romero, J. Antenucci, and D. Hamilton, *Computational aquatic ecosystem dynamics model: Caedym v2*, Contract Research Group, Centre for Water Research, University of Western Australia, 90 (2006).

[204] M. R. Hipsey, S. U. Salmon, and L. M. Mosley, *A three-dimensional hydro-geochemical model to assess lake acidification risk*, Environmental modelling & software, 61 (2014), pp. 433–457.

[205] J. C. Ho, A. M. Michalak, and N. Pahlevan, *Widespread global increase in intense lake phytoplankton blooms since the 1980s*, Nature, 574 (2019), pp. 667–670.

[206] J. T. Holt, J. I. Allen, R. Proctor, and F. Gilbert, *Error quantification of a high-resolution coupled hydrodynamic–ecosystem coastal–ocean model: Part 1 model overview and assessment of the hydrodynamics*, Journal of Marine Systems, 57 (2005), pp. 167–188.

[207] M. S. Hossain, J. A. Dearing, M. Rahman, and M. Salehin, *Recent changes in ecosystem services and human well-being in the bangladesh coastal zone*, Regional Environmental Change, 16 (2016), pp. 429–443.

[208] M. Idhalla, H. Nhhala, J. Kassila, E. Ait Chattou, A. Orbi, and A. Moukrim, *Comparative production of two mussel species (perna perna and mytilus galloprovincialis) reared on an offshore submerged longline system in agadir, morocco*, Int J Sci Eng Res, 8 (2017).

[209] I. Iglesias, P. Avilez-Valente, J. L. Pinho, A. Bio, J. M. Vieira, L. Bastos, and F. Veloso-Gomes, *Numerical modeling tools applied to estuarine and coastal hydrodynamics: A user perspective*, IntechOpen, 2019.

[210] D. H. Institue, *Mike11 a modeling system for rivers and channels*, Reference Manual, (2009).

[211] M. M. Iqbal, M. Shoaib, P. Agwanda, and J. L. Lee, *Modeling approach for water-quality management to control pollution concentration: A case study of ravi river, punjab, pakistan*, Water, 10 (2018), p. 1068.

[212] B. Ismail, M. Ahmed, H. Karim, I. Mohammed, A. Aziz, and A. Mohamed, *Analysis of coastal upwelling index along the moroccan atlantic coast using wavelets from 1967 to 2016*.

[213] A. Izady, K. Davary, A. Alizadeh, A. Ziaei, S. Akhavan, A. Alipoor, A. Joodavi, and M. Brusseau, *Groundwater conceptualization and modeling using distributed swat-based recharge for the semi-arid agricultural neishaboor plain, iran*, Hydrogeology Journal, 23 (2015), pp. 47–68.

[214] M. Jang, D. Seo, J. Kim, and J. Kim, *Spatiotemporal algal bloom prediction of geum river, korea using the deep learning models in company with the efdc model*, in Proceedings of the 2020 Summer Simulation Conference, 2020, pp. 1–11.

[215] L. D. Jenkins, S. M. Maxwell, and E. Fisher, *Increasing conservation impact and policy relevance of research through embedded experiences*, Conservation Biology, 26 (2012), pp. 740–742.

[216] L. C. JEZNACH, A. MOHAN, J. E. TOBIASON, AND D. A. RECKHOW, *Modeling crude oil fate and transport in freshwater*, Environmental Modeling & Assessment, 26 (2021), pp. 77–87.

[217] Z.-G. JI AND K.-R. JIN, *An integrated environmental model for a surface flow constructed wetland: Water quality processes*, Ecological Engineering, 86 (2016), pp. 247–261.

[218] H. JIA, S. WANG, M. WEI, AND Y. ZHANG, *Scenario analysis of water pollution control in the typical peri-urban river using a coupled hydrodynamic-water quality model*, Frontiers of Environmental Science & Engineering in China, 5 (2011), pp. 255–265.

[219] L. JIANG, Y. LI, X. ZHAO, M. R. TILLOTSON, W. WANG, S. ZHANG, L. SARPONG, Q. ASMAA, AND B. PAN, *Parameter uncertainty and sensitivity analysis of water quality model in lake taihu, china*, Ecological Modelling, 375 (2018), pp. 1–12.

[220] H. F. JONES, D. ÖZKUNDAKCI, C. G. MCBRIDE, C. A. PILDITCH, M. G. ALLAN, AND D. P. HAMILTON, *Modelling interactive effects of multiple disturbances on a coastal lake ecosystem: Implications for management*, Journal of environmental management, 207 (2018), pp. 444–455.

[221] J.-B. JOUFFRAY, R. BLASIAK, A. V. NORSTRÖM, H. ÖSTERBLOM, AND M. NYSTRÖM, *The blue acceleration: the trajectory of human expansion into the ocean*, One Earth, 2 (2020), pp. 43–54.

[222] B. R. JOYCE, W. J. PRINGLE, D. WIRASAET, J. J. WESTERINK, A. J. VAN DER WESTHUYSEN, R. GRUMBINE, AND J. FEYEN, *High resolution modeling of western alaskan tides and storm surge under varying sea ice conditions*, Ocean Modelling, 141 (2019), p. 101421.

[223] K. S. JUN, E.-S. CHUNG, J.-Y. SUNG, AND K. S. LEE, *Development of spatial water resources vulnerability index considering climate change impacts*, Science of the total environment, 409 (2011), pp. 5228–5242.

[224] X. KANG, M. XIA, J. S. PITULA, AND P. CHIGBU, *Dynamics of water and salt exchange at maryland coastal bays*, Estuarine, Coastal and Shelf Science, 189 (2017), pp. 1–16.

[225] P. R. KANNEL, S. R. KANEL, S. LEE, Y.-S. LEE, AND T. Y. GAN, *A review of public domain water quality models for simulating dissolved oxygen in rivers and streams*, Environmental Modeling & Assessment, 16 (2011), pp. 183–204.

[226] Y. KARAASLAN ET AL., *Derivation of environmental quality standards by ecological risk assessment approach using aquatox model*, Journal of Environmental Protection and Ecology, 18 (2017), pp. 71–83.

[227] T. KARPOUZOGLOU, B. VLASWINKEL, AND J. VAN DER MOLEN, *Effects of large-scale floating (solar photovoltaic) platforms on hydrodynamics and primary production in a coastal sea from a water column model*, Ocean Science, 16 (2020), pp. 195–208.

[228] I. KARYDIS, P. GRATSANIS, C. SEMERTZIDIS, AND M. AVLONITIS, *Webgis design & implementation for pest life-cycle & control simulation management: The case of olive-fruit fly*, Procedia Technology, 8 (2013), pp. 526–529.

[229] V. Keller, *Risk assessment of "down-the-drain" chemicals: Search for a suitable model*, Science of the Total Environment, 360 (2006), pp. 305–318.

[230] W. Kemp, J. M. Testa, D. J. Conley, D. Gilbert, and J. D. Hagy, *Temporal responses of coastal hypoxia to nutrient loading and physical controls*, Biogeosciences, 6 (2009), pp. 2985–3008.

[231] I. A. Kenov, A. C. Garcia, and R. Neves, *Residence time of water in the mondego estuary (portugal)*, Estuarine, Coastal and Shelf Science, 106 (2012), pp. 13–22.

[232] A. S. Keraga, *Assessment and Modeling of Surface Water Quality Dynamics in Awash River Basin, Ethiopia*, PhD thesis, Addis Ababa Institute of Technology, School of Chemical and Bio Engineering . . . , 2019.

[233] I. Keupers and P. Willems, *Development and testing of a fast conceptual river water quality model*, Water research, 113 (2017), pp. 62–71.

[234] D.-K. Kim, S. Kaluskar, S. Mugalingam, A. Blukacz-Richards, T. Long, A. Morley, and G. B. Arhonditsis, *A bayesian approach for estimating phosphorus export and delivery rates with the spatially referenced regression on watershed attributes (sparrow) model*, Ecological Informatics, 37 (2017), pp. 77–91.

[235] J. Kim, D. Seo, M. Jang, and J. Kim, *Augmentation of limited input data using an artificial neural network method to improve the accuracy of water quality modeling in a large lake*, Journal of Hydrology, 602 (2021), p. 126817.

[236] T. Kim and T. Khangaonkar, *An offline unstructured biogeochemical model (ubm) for complex estuarine and coastal environments*, Environmental Modelling & Software, 31 (2012), pp. 47–63.

[237] C. D. Knightes, R. B. Ambrose Jr, B. Avant, Y. Han, B. Acrey, D. C. Bouchard, R. Zepp, and T. Wool, *Modeling framework for simulating concentrations of solute chemicals, nanoparticles, and solids in surface waters and sediments: Wasp8 advanced toxicant module*, Environmental Modelling & Software, 111 (2019), pp. 444–458.

[238] A. Koelmans, A. Van der Heijde, L. Knijff, and R. Aalderink, *Integrated modelling of eutrophication and organic contaminant fate & effects in aquatic ecosystems. a review*, Water Research, 35 (2001), pp. 3517–3536.

[239] C. Kohlmeier and W. Ebenhöh, *Modelling the ecosystem dynamics and nutrient cycling of the spiekeroog back barrier system with a coupled euler–lagrange model on the base of ersem*, Ecological Modelling, 202 (2007), pp. 297–310.

[240] H. Kouali, H. Achtak, A. Chaouti, K. Elkalay, and A. Dahbi, *Assessment of trace metal contamination in surficial fine-grained sediments and mussel, mytilus galloprovincialis from safi areas in the northwestern atlantic coast of morocco*, Regional Studies in Marine Science, 40 (2020), p. 101535.

[241] E. Kudryavtseva, S. Aleksandrov, T. Bukanova, O. Dmitrieva, and I. Rusanov, *Relationship between seasonal variations of primary production, abiotic factors and phytoplankton composition in the coastal zone of the south-eastern part of the baltic sea*, Regional studies in Marine Science, 32 (2019), p. 100862.

[242] M. KUPPUSAMY AND V. GIRIDHAR, *Factor analysis of water quality characteristics including trace metal speciation in the coastal environmental system of chennai ennore*, Environment international, 32 (2006), pp. 174–179.

[243] Y. S. KWON, H. S. LA, J. JUNG, S. H. LEE, T.-W. KIM, H.-W. KANG, AND S. LEE, *Exploring the roles of iron and irradiance in dynamics of diatoms and phaeocystis in the amundsen sea continental shelf water*, Journal of Geophysical Research: Oceans, 126 (2021), p. e2020JC016673.

[244] I. LAMINE, A. A. ALLA, M. BOUROUACHE, AND A. MOUKRIM, *Monitoring of physicochemical and microbiological quality of taghazout seawater (southwest of morocco): Impact of the new tourist resort" taghazout bay"*, Journal of Ecological Engineering, 20 (2019).

[245] I. LAMINE, A. A. ALLA, M. B. HADAD, H. EL HABOUZ, M. NADIR, AND A. MOUKRIM, *Population dynamics of donax trunculus on the sandy beach of taghazout (southern morocco)*, Regional Studies in Marine Science, 33 (2020), p. 100912.

[246] C. LANCELOT, Y. SPITZ, N. GYPENS, K. RUDDICK, S. BECQUEVORT, V. ROUSSEAU, G. LACROIX, AND G. BILLEN, *Modelling diatom and phaeocystis blooms and nutrient cycles in the southern bight of the north sea: the miro model*, Marine Ecology Progress Series, 289 (2005), pp. 63–78.

[247] A. LAOUINA, *Note de recherche–le littoral dans le développement du maroc et de sa politique atlantique*, Norois, (2019), pp. 41–54.

[248] B. Q. LAP, K. MORI, AND E. INOUE, *The water quality analysis simulation program wasp5, part a: Model documentation, version 5.10 the water quality analysis simulation program wasp5, part a: Model documentation, version 5.10, 1993*.

[249] C. LATHUILIÈRE, V. ECHEVIN, AND M. LÉVY, *Seasonal and intraseasonal surface chlorophyll-a variability along the northwest african coast*, Journal of Geophysical Research: Oceans, 113 (2008).

[250] S. LEE, G. W. MCCARTY, G. E. MOGLEN, X. LI, AND C. W. WALLACE, *Assessing the effectiveness of riparian buffers for reducing organic nitrogen loads in the coastal plain of the chesapeake bay watershed using a watershed model*, Journal of Hydrology, 585 (2020), p. 124779.

[251] P. LEITÃO, H. COELHO, A. SANTOS, AND R. NEVES, *Modelling the main features of the algarve coastal circulation during july 2004: A downscaling approach*, Journal of Atmospheric & Ocean Science, 10 (2005), pp. 421–462.

[252] S. G. LELES, J. BRUGGEMAN, L. POLIMENE, J. BLACKFORD, K. J. FLYNN, AND A. MITRA, *Differences in physiology explain succession of mixoplankton functional types and affect carbon fluxes in temperate seas*, Progress in Oceanography, 190 (2021), p. 102481.

[253] C. LEONG, *Narratives and water: A bibliometric review*, Global Environmental Change, 68 (2021), p. 102267.

[254] A. LEVASSEUR, L. SHI, N. C. WELLS, D. A. PURDIE, AND B. A. KELLY-GERREYN, *A three-dimensional hydrodynamic model of estuarine circulation with an application to southampton water, uk*, Estuarine, Coastal and Shelf Science, 73 (2007), pp. 753–767.

[255] L. LEVINE, *Connecting research to policy: Understanding macro and micro policy-makers and their processes*, First Monday, (2020).

[256] R. L. LEWISON, M. A. RUDD, W. AL-HAYEK, C. BALDWIN, M. BEGER, S. N. LIESKE, C. JONES, S. SATUMANATPAN, C. JUNCHOMPOO, AND E. HINES, *How the dpsir framework can be used for structuring problems and facilitating empirical research in coastal systems*, Environmental Science & Policy, 56 (2016), pp. 110–119.

[257] M. LI, L. LI, X. SHI, L. LIN, AND S. LIN, *Effects of phosphorus deficiency and adenosine 5-triphosphate (atp) on growth and cell cycle of the dinoflagellate prorocentrum donghaiense*, Harmful Algae, 47 (2015), pp. 35–41.

[258] Q. LI, H. ZHANG, AND X. HONG, *Knowledge structure of technology licensing based on co-keywords network: A review and future directions*, International Review of Economics & Finance, 66 (2020), pp. 154–165.

[259] Z. LI, C. LUO, K. JIANG, R. WAN, AND H. LI, *Comprehensive performance evaluation for hydrological and nutrients simulation using the hydrological simulation program–fortran in a mesoscale monsoon watershed, china*, International journal of environmental research and public health, 14 (2017), p. 1599.

[260] Y.-D. LIANG, Y. LI, J. ZHAO, X.-Y. WANG, H.-Z. ZHU, AND X.-H. CHEN, *Study of acupuncture for low back pain in recent 20 years: a bibliometric analysis via citespace*, Journal of pain research, 10 (2017), p. 951.

[261] Y. K. LIM, S. H. BAEK, M. LEE, Y. O. KIM, K.-H. CHOI, AND J. H. KIM, *Phytoplankton composition associated with physical and chemical variables during summer in the southern sea of korea: implication of the succession of the two toxic dinoflagellates cochlodinium (aka margalefidinium) polykrikoides and alexandrium affine*, Journal of Experimental Marine Biology and Ecology, 516 (2019), pp. 51–66.

[262] C. O. LIMA AND J. BONETTI, *Bibliometric analysis of the scientific production on coastal communities' social vulnerability to climate change and to the impact of extreme events*, Natural Hazards, 102 (2020), pp. 1589–1610.

[263] T. LIN, V. VAN ONSELEN, AND L. VO, *Coastal erosion in vietnam: Case studies and implication for integrated coastal zone management in the vietnamese south-central coastline*, in IOP Conference Series: Earth and Environmental Science, vol. 652, IOP Publishing, 2021, p. 012009.

[264] Y.-P. LIN, H. MUKHTAR, K.-T. HUANG, J. R. PETWAY, C.-M. LIN, C.-F. CHOU, AND S.-W. LIAO, *Real-time identification of irrigation water pollution sources and pathways with a wireless sensor network and blockchain framework*, Sensors, 20 (2020), p. 3634.

[265] E. LITCHMAN, C. A. KLAUSMEIER, O. M. SCHOFIELD, AND P. G. FALKOWSKI, *The role of functional traits and trade-offs in structuring phytoplankton communities: scaling from cellular to ecosystem level*, Ecology letters, 10 (2007), pp. 1170–1181.

[266] D. LIU AND W. XING, *Analysis of china's coastal zone management reform based on land-sea integration*, Marine Economics and Management, (2019).

[267] L. LIU, M. S. PHANIKUMAR, S. L. MOLLOY, R. L. WHITMAN, D. A. SHIVELY, M. B. NEVERS, D. J. SCHWAB, AND J. B. ROSE, *Modeling the transport and inactivation of e. coli and enterococci in the near-shore region of lake michigan*, Environmental science & technology, 40 (2006), pp. 5022–5028.

[268] M. LIU, X. CHEN, H. YAO, AND Y. CHEN, *A coupled modeling approach to evaluate nitrogen retention within the shanmei reservoir watershed, china*, Estuarine, Coastal and Shelf Science, 166 (2015), pp. 189–198.

[269] W. LIU, Y. ZHANG, L. WU, X. YANG, AND L. SHI, *Characteristics and trends of oral leukoplakia research: a bibliometric study of the 100 most cited articles*, Medicine, 98 (2019).

[270] A. LOMBARDO, A. FRANCO, A. PIVATO, AND A. BARAUSSE, *Food web modeling of a river ecosystem for risk assessment of down-the-drain chemicals: A case study with aquatox*, Science of the Total Environment, 508 (2015), pp. 214–227.

[271] J. F. LOPES AND J. M. DIAS, *Residual circulation and sediment distribution in the ria de aveiro lagoon, portugal*, Journal of Marine Systems, 68 (2007), pp. 507–528.

[272] J. F. LOPES AND C. SILVA, *Temporal and spatial distribution of dissolved oxygen in the ria de aveiro lagoon*, Ecological modelling, 197 (2006), pp. 67–88.

[273] E. LOVECCHIO, N. GRUBER, AND M. MÜNNICH, *Mesoscale contribution to the long-range offshore transport of organic carbon from the canary upwelling system to the open north atlantic*, Biogeosciences, 15 (2018), pp. 5061–5091.

[274] E. LOVECCHIO, N. GRUBER, M. MÜNNICH, AND Z. LACHKAR, *On the long-range offshore transport of organic carbon from the canary upwelling system to the open north atlantic*, Biogeosciences, 14 (2017), pp. 3337–3369.

[275] J. LU, H. LI, X. CHEN, AND D. LIANG, *Numerical study of remote sensed dredging impacts on the suspended sediment transport in china's largest freshwater lake*, Water, 11 (2019), p. 2449.

[276] R. A. LUETTICH JR, L. D. WRIGHT, R. SIGNELL, C. FRIEDRICHS, M. FRIEDRICHS, J. HARDING, K. FENNEL, E. HOWLETT, S. GRAVES, E. SMITH, ET AL., *Introduction to special section on the us ioos coastal and ocean modeling testbed*, Journal of Geophysical Research: Oceans, 118 (2013), pp. 6319–6328.

[277] C. H. M DE ABREU, M. D. L. C. BARROS, D. C. BRITO, M. R. TEIXEIRA, AND A. C. D. CUNHA, *Hydrodynamic modeling and simulation of water residence time in the estuary of the lower amazon river*, Water, 12 (2020), p. 660.

[278] S. MA, J. ZHANG, AND Y. SONG, *Integrated water quality model and its application in baihe river basin*, in IOP Conference Series: Earth and Environmental Science, vol. 330, IOP Publishing, 2019, p. 032018.

[279] M. MAANAN, A. C. RUIZ-FERNANDEZ, M. MAANAN, P. FATTAL, B. ZOURARAH, AND M. SAHABI, *A long-term record of land use change impacts on sediments in oualidia lagoon, morocco*, International Journal of Sediment Research, 29 (2014), pp. 1–10.

[280] R. Q. MACASIEB, C. R. OROZCO, AND A. C. RESURRECCION, *Application of coupled hec-hms and us epa wasp for transport modelling of mercury in the mining-impacted ambalanga river*, ASEAN Engineering Journal, 11 (2021), pp. 158–176.

[281] T. C. MACHOLO, *Water quality modeling study for Umhlangane River, South Africa.*, PhD thesis, 2016.

[282] J. MADER, J. HORSTMANN, J. DEL RIO, AND R. NAIR, *Report on the status of hf-radar systems and cabled coastal observatories*, (2016).

[283] M. S. MALHADAS, M. MATEUS, D. BRITO, AND R. NEVES, *Trophic state evaluation after urban loads diversion in a eutrophic coastal lagoon (óbidos lagoon, portugal): a modeling approach*, Hydrobiologia, 740 (2014), pp. 231–251.

[284] M. S. MALHADAS, R. J. NEVES, P. C. LEITÃO, AND A. SILVA, *Influence of tide and waves on water renewal in óbidos lagoon, portugal*, Ocean Dynamics, 60 (2010), pp. 41–55.

[285] M. S. MALHADAS, A. SILVA, P. C. LEITÃO, AND R. NEVES, *Effect of the bathymetric changes on the hydrodynamic and residence time in óbidos lagoon (portugal)*, Journal of Coastal Research, (2009), pp. 549–553.

[286] T. C. MALONE AND A. NEWTON, *The globalization of cultural eutrophication in the coastal ocean: causes and consequences*, Frontiers in Marine Science, 7 (2020), p. 670.

[287] L. MALTBY, R. BROWN, J. H. FABER, N. GALIC, P. J. VAN DEN BRINK, O. WARWICK, AND S. MARSHALL, *Assessing chemical risk within an ecosystem services framework: Implementation and added value*, Science of the Total Environment, 791 (2021), p. 148631.

[288] G. MANEAS, E. MAKOPOULOU, D. BOUSBOURAS, H. BERG, AND S. MANZONI, *Anthropogenic changes in a mediterranean coastal wetland during the last century—the case of gialova lagoon, messinia, greece*, Water, 11 (2019), p. 350.

[289] G. MANNINA AND G. VIVIANI, *A parsimonious dynamic model for river water quality assessment*, Water Science and Technology, 61 (2010), pp. 607–618.

[290] D. MANSOURI, R. FEGROUCHE, H. ALLAMI, AND M. FADLI, *Bioaccumulation of some metallic elements in the gills, the muscle and the liver of the eel (anguilla anguilla l.) and the cabot mullet (mugil cephalus l.) of the estuary of oued sebou (morocco)*, (2018).

[291] G. MAO, N. HUANG, L. CHEN, AND H. WANG, *Research on biomass energy and environment from the past to the future: A bibliometric analysis*, Science of The Total Environment, 635 (2018), pp. 1081–1090.

[292] H. G. MARSHALL, R. V. LACOUTURE, C. BUCHANAN, AND J. M. JOHNSON, *Phytoplankton assemblages associated with water quality and salinity regions in chesapeake bay, usa*, Estuarine, Coastal and Shelf Science, 69 (2006), pp. 10–18.

[293] A. MARTÍN-MARTÍN, E. ORDUNA-MALEA, M. THELWALL, AND E. D. LÓPEZ-CÓZAR, *Google scholar, web of science, and scopus: A systematic comparison of citations in 252 subject categories*, Journal of informetrics, 12 (2018), pp. 1160–1177.

[294] F. MARTINS, P. LEITÃO, A. SILVA, AND R. NEVES, *3d modelling in the sado estuary using a new generic vertical discretization approach*, Oceanologica Acta, 24 (2001), pp. 51–62.

[295] N. K. T. MARTUTI, R. PRIBADI, N. DEWI, W. SIDIQ, AND S. NUGRAHA, *The dynamics of coastline and mangrove ecosystems in coastal area of mangkang kulon subdistrict, semarang*, in IOP Conference Series: Earth and Environmental Science, vol. 550, IOP Publishing, 2020, p. 012011.

[296] G. MASI, S. MANZI, AND M. C. BIGNOZZI, *Gender balance in construction material research: The analysis of alkali-activated materials by a bibliometric study using scopus database*, Frontiers in Materials, 7 (2020), p. 321.

[297] E. MASON, F. COLAS, J. MOLEMAKER, A. F. SHCHEPETKIN, C. TROUPIN, J. C. MCWILLIAMS, AND P. SANGRÀ, *Seasonal variability of the canary current: A numerical study*, Journal of Geophysical Research: Oceans, 116 (2011).

[298] F. MASOUMI, A. AFSHAR, AND S. T. PALATKALEH, *Selective withdrawal optimization in river–reservoir systems; trade-offs between maximum allowable receiving waste load and water quality criteria enhancement*, Environmental monitoring and assessment, 188 (2016), pp. 1–16.

[299] M. MATEUS, P. LEITÃO, H. DE PABLO, AND R. NEVES, *Is it relevant to explicitly parameterize chlorophyll synthesis in marine ecological models?*, Journal of Marine Systems, 94 (2012), pp. S23–S33.

[300] M. MATEUS, R. D. S. VIEIRA, C. ALMEIDA, M. SILVA, AND F. REIS, *Score—a simple approach to select a water quality model*, Water, 10 (2018), p. 1811.

[301] M. D. MATEUS AND G. FRANZ, *Sensitivity analysis in a complex marine ecological model*, Water, 7 (2015), pp. 2060–2081.

[302] K. W. MCCAIN, *Mapping authors in intellectual space: A technical overview*, Journal of the American society for information science, 41 (1990), pp. 433–443.

[303] K. J. MCHOMBU, *Harnessing knowledge management for africa's transition to the 21st century*, Information development, 23 (2007), pp. 25–42.

[304] S. MELLAS, F. LEONE, R. OMIRA, M. GHERARDI, M.-A. BAPTISTA, B. ZOURARAH, M. PÉROCHE, AND É. LAGAHÉ, *Le risque tsunamique au maroc: modélisation et évaluation au moyen d'un premier jeu d'indicateurs d'exposition du littoral atlantique*, Physio-Géo. Géographie physique et environnement, (2012), pp. 119–139.

[305] R. MENDES, M. C. SOUSA, M. DECASTRO, M. GÓMEZ-GESTEIRA, AND J. M. DIAS, *New insights into the western iberian buoyant plume: Interaction between the douro and minho river plumes under winter conditions*, Progress in Oceanography, 141 (2016), pp. 30–43.

[306] W. S. MERRITT, R. A. LETCHER, AND A. J. JAKEMAN, *A review of erosion and sediment transport models*, Environmental modelling & software, 18 (2003), pp. 761–799.

[307] N. Mhammdi, F. Medina, Z. Belkhayat, R. El Aoula, M.-A. Geawahri, and A. Chiguer, *Marine storms along the moroccan atlantic coast: An underrated natural hazard?*, Journal of African Earth Sciences, 163 (2020), p. 103730.

[308] C. Mi, T. Shatwell, J. Ma, V. C. Wentzky, B. Boehrer, Y. Xu, and K. Rinke, *The formation of a metalimnetic oxygen minimum exemplifies how ecosystem dynamics shape biogeochemical processes: A modelling study*, Water research, 175 (2020), p. 115701.

[309] H. Milišić, E. Hadžić, A. Mulaomerović-Šeta, H. Kalajdžisalihović, and N. Lazović, *Mathematical modeling of surface water quality*, in International Symposium on Innovative and Interdisciplinary Applications of Advanced Technologies, Springer, 2018, pp. 138–156.

[310] C. Miller and G. Pinder, *The object-oriented design of the integrated water modelling system mohid*, 2004.

[311] M. P. Miller, P. D. Capel, A. M. García, and S. W. Ator, *Response of nitrogen loading to the chesapeake bay to source reduction and land use change scenarios: A sparrow-informed analysis*, JAWRA Journal of the American Water Resources Association, 56 (2020), pp. 100–112.

[312] F. J. Millero and A. Poisson, *International one-atmosphere equation of state of seawater*, Deep Sea Research Part A. Oceanographic Research Papers, 28 (1981), pp. 625–629.

[313] R. C. Miranda, *Nitrogen biogeochemical cycle modeling in the North Atlantic Ocean*, 1999.

[314] Y. Mohamoud, R. Parmar, and K. Wolfe, *Modeling best management practices (bmps) with hspf*, in Watershed Management 2010: Innovations in Watershed Management under Land Use and Climate Change, 2010, pp. 892–898.

[315] Y. Mohamoud and H. Zhang, *Applications of linked and nonlinked complex models for tmdl development: approaches and challenges*, Journal of Hydrologic Engineering, 24 (2019), p. 04018055.

[316] P. Mongeon and A. Paul-Hus, *The journal coverage of web of science and scopus: a comparative analysis*, Scientometrics, 106 (2016), pp. 213–228.

[317] A. Mooser, G. Anfuso, A. T. Williams, R. Molina, and P. P. Aucelli, *An innovative approach to determine coastal scenic beauty and sensitivity in a scenario of increasing human pressure and natural impacts due to climate change*, Water, 13 (2021), p. 49.

[318] D. N. Moriasi, N. Pai, J. L. Steiner, P. H. Gowda, M. Winchell, H. Rathjens, P. J. Starks, and J. A. Verser, *Swat-lut: A desktop graphical user interface for updating land use in swat*, JAWRA Journal of the American Water Resources Association, 55 (2019), pp. 1102–1115.

[319] L. M. Mosley, R. Daly, D. Palmer, P. Yeates, C. Dallimore, T. Biswas, and S. L. Simpson, *Predictive modelling of ph and dissolved metal concentrations and speciation following mixing of acid drainage with river water*, Applied Geochemistry, 59 (2015), pp. 1–10.

[320] L. MOUAKKIR AND S. MORDANE, *Numerical modeling of the tide in the coast area casablanca-mohammedia (morocco)*.

[321] A. MOUJANE, A. BENTAMY, M. CHAGDALI, AND S. MORDANE, *Analysis of high spatial and temporal surface winds from aladin model and from remotely sensed data over the canarian upwelling region*, Teledetection, 10 (2011), pp. 11–22.

[322] M. R. MULHOLLAND, R. MORSE, T. EGERTON, P. W. BERNHARDT, AND K. FILIPPINO, *Blooms of dinoflagellate mixotrophs in a lower chesapeake bay tributary: carbon and nitrogen uptake over diurnal, seasonal, and interannual timescales*, Estuaries and coasts, 41 (2018), pp. 1744–1765.

[323] B. NA, S. SON, AND J.-C. CHOI, *Modeling of accidental oil spills at different phases of lng terminal construction*, Journal of Marine Science and Engineering, 9 (2021), p. 392.

[324] M. NADIR, M. AGNAOU, Z. IDARDARE, A. CHAHID, T. BOUZID, AND A. MOUKRIM, *Impact study of m'zar submarine emissary (agadir bay, morocco): Trace metals accumulation (cd, pb and hg) and biochemical response of marine mollusk donax trunculus (linnaeus, 1758)*, J. Mater. Environ. Sci, 6 (2015), pp. 2292–2300.

[325] B. R. NAIK, M. GAUNS, K. BEPARI, H. USKAIKAR, AND D. M. SHENOY, *Variation in phytoplankton community and its implication to dimethylsulphide production at a coastal station off goa, india*, Marine environmental research, 157 (2020), p. 104926.

[326] S. NASIRI, H. ANSARI, AND A. N. ZIAEI, *Simulation of water balance equation components using swat model in samalqan watershed (iran)*, Arabian Journal of Geosciences, 13 (2020), pp. 1–15.

[327] L. NATIJ, Z. DAMSIRI, K. KHALIL, M. LOUDIKI, O. ETTAHIRI, AND K. ELKALAY, *Phytoplankton abundance and diversity in the coastal waters of oualidia lagoon, south moroccan atlantic in relation to environmental variables*, International Journal of Advanced Research, 2 (2014), pp. 1022–1032.

[328] F. NCHE-FAMBO, U. SCHARLER, AND K. TIROK, *Resilience of estuarine phytoplankton and their temporal variability along salinity gradients during drought and hypersalinity*, Estuarine, Coastal and Shelf Science, 158 (2015), pp. 40–52.

[329] S. P. NERUR, A. A. RASHEED, AND V. NATARAJAN, *The intellectual structure of the strategic management field: An author co-citation analysis*, Strategic Management Journal, 29 (2008), pp. 319–336.

[330] F. D. S. NEVES, *Dynamics and hydrology of the tagus estuary: results from in situ observations*, (2010).

[331] R. NEVES, *Étude experimentale et modélisation des circulations trasitoire et résiduelle dans l'estuaire du sado*, PhD thesis, Ph. D. Thesis, Univ. Liège, 1985.

[332] K. NIETO, H. DEMARCQ, AND S. MCCLATCHIE, *Mesoscale frontal structures in the canary upwelling system: New front and filament detection algorithms applied to spatial and temporal patterns*, Remote Sensing of Environment, 123 (2012), pp. 339–346.

[333] D. NONG, C. WANG, AND A. Q. AL-AMIN, *A critical review of energy resources, policies and scientific studies towards a cleaner and more sustainable economy in vietnam*, Renewable and Sustainable Energy Reviews, 134 (2020), p. 110117.

[334] B. NOTTER, H. HURNI, U. WIESMANN, AND J. O. NGANA, *Evaluating watershed service availability under future management and climate change scenarios in the pangani basin*, Physics and Chemistry of the Earth, Parts A/B/C, 61 (2013), pp. 1–11.

[335] L. NYKJÆR AND L. VAN CAMP, *Seasonal and interannual variability of coastal upwelling along northwest africa and portugal from 1981 to 1991*, Journal of Geophysical Research: Oceans, 99 (1994), pp. 14197–14207.

[336] W. S. OF WASHINGTON DEPARTMENT OF ENVIRONMENT), *Comprehensive circulation and water quality study at budd inlet, southern puget sound water quality assessment study*, 1984.

[337] K. O. OLOWE ET AL., *Assessment of some existing water quality models.*, Nature Environment & Pollution Technology, 17 (2018).

[338] P. OSKARSSON, K. B. NIELSEN, K. LAHIRI-DUTT, AND B. ROY, *India's new coal geography: Coastal transformations, imported fuel and state-business collaboration in the transition to more fossil fuel energy*, Energy Research & Social Science, 73 (2021), p. 101903.

[339] A. OSTFELD AND S. SALOMONS, *A hybrid genetic—instance based learning algorithm for ce-qual-w2 calibration*, Journal of Hydrology, 310 (2005), pp. 122–142.

[340] R. A. OTEKE, *Assessment of gender barriers to marine resources access: A case study of inhaca island, mozambique*, Master's thesis, 2018.

[341] H. PAERL AND R. FULTON, *Ecology of harmful cyanobacteria*, in Ecology of harmful algae, Springer, 2006, pp. 95–109.

[342] H. W. PAERL, *Mitigating harmful cyanobacterial blooms in a human-and climatically-impacted world*, Life, 4 (2014), pp. 988–1012.

[343] ——, *Why does n-limitation persist in the world's marine waters?*, Marine Chemistry, 206 (2018), pp. 1–6.

[344] R. PARK AND J. CLOUGH, *Aquatox (release 3.1 plus), modeling environmental fate and ecological effects in aquatic ecosystems*, in Volume 2: Technical Documentation, 2014.

[345] R. A. PARK, *A generalized model for simulating lake ecosystems*, Simulation, 23 (1974), pp. 33–50.

[346] R. A. PARK, C. I. CONNOLLY, J. R. ALBANESE, L. S. CLESCERI, AND G. W. HEITZMAN, *Modeling the fate of toxic organic materials in aquatic environments*, US Environmental Protection Agency, Environmental Research Laboratory, 1982.

[347] S. PARK, K. KIM, C. SHIN, J.-H. MIN, E. H. NA, AND L. J. PARK, *Variable update strategy to improve water quality forecast accuracy in multivariate data assimilation using the ensemble kalman filter*, Water research, 176 (2020), p. 115711.

[348] D. Pataki, C. Boone, T. Hogue, G. Jenerette, J. McFadden, and S. Pincetl, *Socio-ecohydrology and the urban water challenge*, Ecohydrology, 4 (2011), pp. 341–347.

[349] J. T. Paul, N. Ramaiah, and S. Sardessai, *Nutrient regimes and their effect on distribution of phytoplankton in the bay of bengal*, Marine Environmental Research, 66 (2008), pp. 337–344.

[350] R. Pawlowicz, B. Beardsley, and S. Lentz, *Classical tidal harmonic analysis including error estimates in matlab using t_tide*, Computers & Geosciences, 28 (2002), pp. 929–937.

[351] F. Pearce, *When the rivers run dry, fully revised and updated edition: water-the defining crisis of the twenty-first century*, Beacon Press, 2018.

[352] J. Pelegrí, A. Marrero-Díaz, A. Ratsimandresy, A. Antoranz, J. Cisneros-Aguirre, C. Gordo, D. Grisolía, A. Hernández-Guerra, I. Láiz, A. Martínez, et al., *Hydrographic cruises off northwest africa: the canary current and the cape ghir region*, Journal of Marine Systems, 54 (2005), pp. 39–63.

[353] C. Peng, M. He, S. L. Cutrona, C. I. Kiefe, F. Liu, and Z. Wang, *Theme trends and knowledge structure on mobile health apps: Bibliometric analysis*, JMIR mHealth and uHealth, 8 (2020), p. e18212.

[354] Z. Peng, W. Hu, G. Liu, H. Zhang, R. Gao, and W. Wei, *Development and evaluation of a real-time forecasting framework for daily water quality forecasts for lake chaohu to lead time of six days*, Science of the total environment, 687 (2019), pp. 218–231.

[355] D. Pereiro, C. Souto, and J. Gago, *Dynamics of floating marine debris in the northern iberian waters: A model approach*, Journal of Sea Research, 144 (2019), pp. 57–66.

[356] M. Pesce, A. Critto, S. Torresan, E. Giubilato, L. Pizzol, and A. Marcomini, *Assessing uncertainty of hydrological and ecological parameters originating from the application of an ensemble of ten global-regional climate model projections in a coastal ecosystem of the lagoon of venice, italy*, Ecological Engineering, 133 (2019), pp. 121–136.

[357] A. Pfeiffer-Herbert, C. Kincaid, D. Bergondo, and R. Pockalny, *Dynamics of wind-driven estuarine-shelf exchange in the narragansett bay estuary*, Continental Shelf Research, 105 (2015), pp. 42–59.

[358] M.-T. Phan, V. C. Tran, H. L. Bui, T. A. Nguyen, P. T. P. Thao, H. D. Duan, et al., *Estimation of residence time in coastal waters of vietnam: A comparison of radioactivity, hydrodynamics, and loicz approach*, Journal of Marine Science and Technology, 28 (2020), p. 6.

[359] E. B. Phelps and H. Streeter, *A study of the pollution and natural purification of the ohio river*, tech. rep., US Department of Health, Education, & Welfare, 1958.

[360] J. O. Pierini, F. J. Campuzano, P. C. Leitão, E. A. Gómez, and R. J. Neves, *Atmospheric influence over the residence time in the bahia blanca estuary, argentina*, Thalassas: An International Journal of Marine Sciences, 35 (2019), pp. 275–286.

[361] C. Piroddi, H. Teixeira, C. P. Lynam, C. Smith, M. C. Alvarez, K. Mazik, E. Andonegi, T. Churilova, L. Tedesco, M. Chifflet, et al., *Using ecological models to assess ecosystem status in support of the european marine strategy framework directive*, Ecological Indicators, 58 (2015), pp. 175–191.

[362] L. Portela, *Mathematical modeling of hydrodynamic processes and water quality in the Tagus estuary.PhD Dissertation.Environmental Engineering, Technical University of Lisbon, Portugal*, PhD thesis, 1996.

[363] D. T. Pugh, *Tides, surges and mean sea level*, (1987).

[364] J. Pyo, L. J. Park, Y. Pachepsky, S.-S. Baek, K. Kim, and K. H. Cho, *Using convolutional neural network for predicting cyanobacteria concentrations in river water*, Water Research, 186 (2020), p. 116349.

[365] J. Qi, S. Li, Q. Li, Z. Xing, C. P.-A. Bourque, and F.-R. Meng, *A new soil-temperature module for swat application in regions with seasonal snow cover*, Journal of Hydrology, 538 (2016), pp. 863–877.

[366] M. C. C. Quesada, J. García-Lafuente, E. Garel, J. D. Cabello, F. Martins, and J. Moreno-Navas, *Effects of tidal and river discharge forcings on tidal propagation along the guadiana estuary*, Journal of Sea Research, 146 (2019), pp. 1–13.

[367] D. E. Radcliffe, D. K. Reid, K. Blombäck, C. H. Bolster, A. S. Collick, Z. M. Easton, W. Francesconi, D. R. Fuka, H. Johnsson, K. King, et al., *Applicability of models to predict phosphorus losses in drained fields: A review*, Journal of environmental quality, 44 (2015), pp. 614–628.

[368] P. Rameshwaran, P. Naden, C. A. Wilson, R. Malki, D. R. Shukla, and K. Shiono, *Inter-comparison and validation of computational fluid dynamics codes in two-stage meandering channel flows*, Applied Mathematical Modelling, 37 (2013), pp. 8652–8672.

[369] T. Ramírez, D. Cortés, J. Mercado, M. Vargas-Yañez, M. Sebastián, and E. Liger, *Seasonal dynamics of inorganic nutrients and phytoplankton biomass in the nw alboran sea*, Estuarine, Coastal and Shelf Science, 65 (2005), pp. 654–670.

[370] L. Á. Ramos-Ramírez, M. A. Guevara-Luna, J. S. Chiriví-Salomón, and D. M. Muñoz-Nieto, *Simulation of cr-iii dispersion in the high bogotá river basin using the wasp model*, Revista Facultad de Ingeniería Universidad de Antioquia, (2020), pp. 30–40.

[371] A.-R. Ramos-Rodríguez and J. Ruíz-Navarro, *Changes in the intellectual structure of strategic management research: A bibliometric study of the strategic management journal, 1980–2000*, Strategic management journal, 25 (2004), pp. 981–1004.

[372] F. M. Rana, M. Adamo, R. Lucas, and P. Blonda, *Sea surface wind retrieval in coastal areas by means of sentinel-1 and numerical weather prediction model data*, Remote Sensing of Environment, 225 (2019), pp. 379–391.

[373] M. H. Ranjbar, A. Etemad-Shahidi, and B. Kamranzad, *Modeling the combined impact of climate change and sea-level rise on general circulation and residence time in a semi-enclosed sea*, Science of The Total Environment, 740 (2020), p. 140073.

[374] S. RANJITH, A. V. SHIVAPUR, P. S. K. KUMAR, C. G. HIREMATH, AND S. DHUNGANA, *Water quality model for streams: a review*, Journal of Environmental Protection, 10 (2019), pp. 1612–1648.

[375] B. RATTER AND C. LEYSHON, *Perceptions of and resilience to coastal climate risks*, in Oxford Research Encyclopedia of Climate Science, 2021.

[376] B. RAZDAR, K. MOHAMMADI, J. SAMANI, AND B. PIROOZ, *Determining the best water quality model for the rivers in north of iran (case study: Pasikhan river)*, Computational Methods in Civil Engineering, 2 (2011), pp. 105–116.

[377] M. REQUIER-DESJARDINS, B. ADHIKARI, AND S. SPERLICH, *Some notes on the economic assessment of land degradation*, Land Degradation & Development, 22 (2011), pp. 285–298.

[378] T. REUTERS, *The thomson reuters impact factor available at: http://wokinfo.com/essays/impact-factor*, 2016.

[379] H. RHOMAD, K. KHALIL, R. NEVES, B. BOUGADIR, AND K. ELKALAY, *Modeling investigation of the nutrients and phytoplankton dynamics in the moroccan atlantic coast: A case study of agadir coast*, Ecological Modelling, 447 (2021), p. 109510.

[380] A. RIGOSI, R. MARCÉ, C. ESCOT, AND F. J. RUEDA, *A calibration strategy for dynamic succession models including several phytoplankton groups*, Environmental Modelling & Software, 26 (2011), pp. 697–710.

[381] P. RIOU, J.-C. LE SAUX, F. DUMAS, M.-P. CAPRAIS, S. LE GUYADER, AND M. POMMEPUY, *Microbial impact of small tributaries on water and shellfish quality in shallow coastal areas*, Water research, 41 (2007), pp. 2774–2786.

[382] M. RODRIGUES, A. OLIVEIRA, H. QUEIROGA, V. BROTAS, AND A. B. FORTUNATO, *Modelling the effects of climate change in estuarine ecosystems with coupled hydrodynamic and biogeochemical models*, in Developments in Environmental Modelling, vol. 27, Elsevier, 2015, pp. 271–288.

[383] J. ROMERO, J. ANTENUCCI, AND J. IMBERGER, *One-and three-dimensional biogeochemical simulations of two differing reservoirs*, Ecological Modelling, 174 (2004), pp. 143–160.

[384] B. Z. ROUSSO, E. BERTONE, R. STEWART, AND D. P. HAMILTON, *A systematic literature review of forecasting and predictive models for cyanobacteria blooms in freshwater lakes*, Water Research, 182 (2020), p. 115959.

[385] M. A. RUDD AND R. N. LAWTON, *Scientists' prioritization of global coastal research questions*, Marine Policy, 39 (2013), pp. 101–111.

[386] D. RUDNICK, R. PASTOROK, D. PREZIOSI, Y. BRAMLEY, E. FARRELLY, D. HUGGETT, ET AL., *Design and calibration of an aquatox ecosystem model for assessing effects of the herbicide prosulfocarb on aquatic food webs*, in SETAC North America annual meeting, 2012, pp. 11–15.

[387] P. Rynne, A. Reniers, J. van de Kreeke, and J. MacMahan, *The effect of tidal exchange on residence time in a coastal embayment*, Estuarine, Coastal and Shelf Science, 172 (2016), pp. 108–120.

[388] A. Sadeghian, S. C. Chapra, J. Hudson, H. Wheater, and K.-E. Lindenschmidt, *Improving in-lake water quality modeling using variable chlorophyll a/algal biomass ratios*, Environmental Modelling & Software, 101 (2018), pp. 73–85.

[389] N. Salvação and C. G. Soares, *Wind resource assessment offshore the atlantic iberian coast with the wrf model*, Energy, 145 (2018), pp. 276–287.

[390] Y. Santana-Falcón, M. Benavides, P. Sangrà, E. Mason, E. D. Barton, A. Orbi, and J. Arístegui, *Coastal–offshore exchange of organic matter across the cape ghir filament (nw africa) during moderate upwelling*, Journal of Marine Systems, 154 (2016), pp. 233–242.

[391] Y. Santana-Falcon, E. Mason, and J. Arístegui, *Offshore transport of organic carbon by upwelling filaments in the canary current system*, Progress in Oceanography, 186 (2020), p. 102322.

[392] P. Santoro, M. Fernández, M. Fossati, G. Cazes, R. Terra, and I. Piedra-Cueva, *Pre-operational forecasting of sea level height for the río de la plata*, Applied Mathematical Modelling, 35 (2011), pp. 2462–2478.

[393] P. Santoro, M. Fossati, P. Tassi, N. Huybrechts, D. P. Van Bang, and J. I. Piedra-Cueva, *A coupled wave–current–sediment transport model for an estuarine system: Application to the río de la plata and montevideo bay*, Applied Mathematical Modelling, 52 (2017), pp. 107–130.

[394] S. Saraiva, L. Fernandes, J. van der Meer, R. Neves, and S. Kooijman, *The role of bivalves in the balgzand: First steps on an integrated modelling approach*, Ecological Modelling, 359 (2017), pp. 34–48.

[395] S. Saraiva, P. Pina, F. Martins, M. Santos, F. Braunschweig, and R. Neves, *Modelling the influence of nutrient loads on portuguese estuaries*, Hydrobiologia, 587 (2007), pp. 5–18.

[396] J. L. Sarmiento, R. Slater, M. Fasham, H. Ducklow, J. Toggweiler, and G. Evans, *A seasonal three-dimensional ecosystem model of nitrogen cycling in the north atlantic euphotic zone*, Global biogeochemical cycles, 7 (1993), pp. 417–450.

[397] N. Sava and G. Marusic, *Digital techniques for water pollution control*, Journal of Engineering Sciences, (2021), pp. 138–148.

[398] M. Savina, M. Lunghi, B. Archambault, L. Baulier, M. Huret, and O. Le Pape, *Sole larval supply to coastal nurseries: Interannual variability and connectivity at interregional and interpopulation scales*, Journal of Sea Research, 111 (2016), pp. 1–10.

[399] D. W. Schindler, *Eutrophication and recovery in experimental lakes: implications for lake management*, Science, 184 (1974), pp. 897–899.

[400] G. Schwarz, A. B. Hoos, R. Alexander, and R. Smith, *Section 3. the sparrow surface water-quality model—theory, application and user documentation*, tech. rep., US Geological Survey, 2006.

[401] A. F. Semadeni-Davies, C. M. Jones-Todd, M. Srinivasan, R. W. Muirhead, A. H. Elliott, U. Shankar, and C. C. Tanner, *Clues model calibration: residual analysis to investigate potential sources of model error*, New Zealand Journal of Agricultural Research, (2019), pp. 1–24.

[402] M. Sgroi, F. G. Vagliasindi, and P. Roccaro, *Feasibility, sustainability and circular economy concepts in water reuse*, Current opinion in environmental Science & Health, 2 (2018), pp. 20–25.

[403] A. Shabani, X. Zhang, and M. Ell, *Modeling water quantity and sulfate concentrations in the devils lake watershed using coupled swat and ce-qual-w2*, JAWRA Journal of the American Water Resources Association, 53 (2017), pp. 748–760.

[404] A. Shalby, M. Elshemy, and B. Zeidan, *Modeling of climate change impacts on lake burullus, coastal lagoon (egypt)*, International Journal of Sediment Research, 36 (2021), pp. 756–769.

[405] D. Sharma and A. Kansal, *Assessment of river quality models: a review*, Reviews in Environmental Science and Bio/Technology, 12 (2013), pp. 285–311.

[406] X. Shen, B. J. Lee, M. Fettweis, and E. A. Toorman, *A tri-modal flocculation model coupled with telemac for estuarine muds both in the laboratory and in the field*, Water research, 145 (2018), pp. 473–486.

[407] Z. Shen, Y. Zhong, Q. Huang, and L. Chen, *Identifying non-point source priority management areas in watersheds with multiple functional zones*, Water research, 68 (2015), pp. 563–571.

[408] L. Shoemaker, *Compendium of tools for watershed assessment and tmdl development*, (1997).

[409] R. Sinha, L. A. Pearson, T. W. Davis, M. A. Burford, P. T. Orr, and B. A. Neilan, *Increased incidence of cylindrospermopsis raciborskii in temperate zones–is climate change responsible?*, Water research, 46 (2012), pp. 1408–1419.

[410] J. Skákala, D. Ford, J. Bruggeman, T. Hull, J. Kaiser, R. R. King, B. Loveday, M. R. Palmer, T. Smyth, C. A. Williams, et al., *Towards a multi-platform assimilative system for north sea biogeochemistry*, Journal of Geophysical Research: Oceans, 126 (2021), p. e2020JC016649.

[411] J. Skakala, D. A. Ford, J. Bruggeman, T. Hull, J. Kaiser, R. R. King, B. R. Loveday, M. R. Palmer, T. J. Smyth, C. A. J. Williams, et al., *Towards a multi-platform assimilative system for ocean biogeochemistry*, Earth and Space Science Open Archive ESSOAr, (2020).

[412] S. SKEJIĆ, A. CAR, I. MARASOVIĆ, S. JOZIĆ, M. BUŽANČIĆ, J. ARAPOV, Ž. NINČEVIĆ GLADAN, A. BAKRAČ, G. KUŠPILIĆ, O. VIDJAK, ET AL., *Morphology and ecology of the poorly known dinoflagellate prorocentrum arcuatum (dinophyceae) from the medulin bay (eastern adriatic sea)*, Acta Adriatica: International journal of Marine Sciences, 58 (2017), pp. 41–50.

[413] A. SLAUGHTER, D. HUGHES, D. RETIEF, AND S. MANTEL, *A management-oriented water quality model for data scarce catchments*, Environmental modelling & software, 97 (2017), pp. 93–111.

[414] H. SMALL, *Co-citation in the scientific literature: A new measure of the relationship between two documents*, Journal of the American Society for information Science, 24 (1973), pp. 265–269.

[415] T. J. SMAYDA AND C. S. REYNOLDS, *Strategies of marine dinoflagellate survival and some rules of assembly*, Journal of Sea Research, 49 (2003), pp. 95–106.

[416] J. G. SMITS AND J. K. VAN BEEK, *Eco: a generic eutrophication model including comprehensive sediment-water interaction*, PLoS One, 8 (2013), p. e68104.

[417] L. SOMOUE, *Structure des communautés planctoniques de lécosystème pélagique de lAtlantique sud marocain entre cap Boujdor et cap Blanc (26°30-21°N)*, PhD thesis, 2004.

[418] S. SOROURIAN, H. HUANG, C. LI, D. JUSTIC, AND A. R. PAYANDEH, *Wave dynamics near barataria bay tidal inlets during spring–summer time*, Ocean Modelling, 147 (2020), p. 101553.

[419] F. SOULIGNAC, P.-A. DANIS, D. BOUFFARD, V. CHANUDET, E. DAMBRINE, Y. GUÉNAND, T. HARMEL, B. W. IBELINGS, D. TREVISAN, R. UITTENBOGAARD, ET AL., *Using 3d modeling and remote sensing capabilities for a better understanding of spatio-temporal heterogeneities of phytoplankton abundance in large lakes*, Journal of Great Lakes Research, 44 (2018), pp. 756–764.

[420] M. C. SOUSA, N. VAZ, I. ALVAREZ, AND J. M. DIAS, *Effect of minho estuarine plume on rias baixas: numerical modeling approach*, Journal of Coastal Research, (2013), pp. 2059–2064.

[421] K. SPILLING, K. OLLI, J. LEHTORANTA, A. KREMP, L. TEDESCO, T. TAMELANDER, R. KLAIS, H. PELTONEN, AND T. TAMMINEN, *Shifting diatom—dinoflagellate dominance during spring bloom in the baltic sea and its potential effects on biogeochemical cycling*, Frontiers in Marine Science, 5 (2018), p. 327.

[422] S. SRICHANDAN, J. Y. KIM, A. KUMAR, D. R. MISHRA, P. BHADURY, P. R. MUDULI, A. K. PATTNAIK, AND G. RASTOGI, *Interannual and cyclone-driven variability in phytoplankton communities of a tropical coastal lagoon*, Marine pollution bulletin, 101 (2015), pp. 39–52.

[423] J. STANSFIELD, B. MOSS, AND K. IRVINE, *The loss of submerged plants with eutrophication iii. potential role of organochlorine pesticides: a palaeoecological study*, Freshwater Biology, 22 (1989), pp. 109–132.

[424] P. J. STATHAM, *Nutrients in estuaries—an overview and the potential impacts of climate change*, Science of the total environment, 434 (2012), pp. 213–227.

[425] I. STEVENS AND J. JOHNSON, *A numerical modelling study of upwelling filaments off the nw african coast*, Oceanologica acta, 26 (2003), pp. 549–564.

[426] L. C. STRINGER AND A. J. DOUGILL, *Channelling science into policy: enabling best practices from research on land degradation and sustainable land management in dryland africa*, Journal of Environmental Management, 114 (2013), pp. 328–335.

[427] A. STROTMANN AND D. ZHAO, *Author name disambiguation: What difference does it make in author-based citation analysis?*, Journal of the American Society for Information Science and Technology, 63 (2012), pp. 1820–1833.

[428] Y. SU, Y. YU, AND N. ZHANG, *Carbon emissions and environmental management based on big data and streaming data: A bibliometric analysis*, Science of The Total Environment, 733 (2020), p. 138984.

[429] J. C. SULLIVAN, Y. WAN, AND R. A. WILLIS, *Modeling floodplain inundation, circulation, and residence time under changing tide and sea levels*, Estuaries and Coasts, (2020), pp. 1–15.

[430] Z. SUN, W. SUN, C. TONG, C. ZENG, X. YU, AND X. MOU, *China's coastal wetlands: conservation history, implementation efforts, existing issues and strategies for future improvement*, Environment International, 79 (2015), pp. 25–41.

[431] Y. SUZUKI AND M. TAKAHASHI, *Growth responses of several diatom species isolated from various environments to temperature*, Journal of Phycology, 31 (1995), pp. 880–888.

[432] W. M. SWEILEH, *Bibliometric analysis of peer-reviewed literature on food security in the context of climate change from 1980 to 2019*, Agriculture & Food Security, 9 (2020), pp. 1–15.

[433] S. TAHIR, T. STEICHEN, AND M. SHOULER, *Water and circular economy: A white paper*, Ellen MacArthur Foundation, Arup, Antea Group, (2018).

[434] Y. TANG, M. ZHANG, J. ZHANG, T. LYU, M. COOPER, AND G. PAN, *Reducing arsenic toxicity using the interfacial oxygen nanobubble technology for sediment remediation*, Water Research, 205 (2021), p. 117657.

[435] J. TAO, D. QIU, F. YANG, AND Z. DUAN, *A bibliometric analysis of human reliability research*, Journal of Cleaner Production, 260 (2020), p. 121041.

[436] K. E. TAYLOR, *Summarizing multiple aspects of model performance in a single diagram*, Journal of Geophysical Research: Atmospheres, 106 (2001), pp. 7183–7192.

[437] M. J. TEHRANI, F. HELFER, AND G. JENKINS, *Impacts of climate change and sea level rise on catchment management: A multi-model ensemble analysis of the nerang river catchment, australia*, Science of The Total Environment, 777 (2021), p. 146223.

[438] J. A. TERRY, A. SADEGHIAN, H. M. BAULCH, S. C. CHAPRA, AND K.-E. LINDENSCHMIDT, *Challenges of modelling water quality in a shallow prairie lake with seasonal ice cover*, Ecological modelling, 384 (2018), pp. 43–52.

[439] S. THATJE, J. LAUDIEN, O. HEILMAYER, AND C. E. NAUEN, *Understanding el niño—the importance of grey literature in coastal ecosystem research and management*, Marine Policy, 31 (2007), pp. 85–93.

[440] P. THUPAKI, M. S. PHANIKUMAR, D. J. SCHWAB, M. B. NEVERS, AND R. L. WHITMAN, *Evaluating the role of sediment-bacteria interactions on escherichia coli concentrations at beaches in southern lake michigan*, Journal of geophysical research: oceans, 118 (2013), pp. 7049–7065.

[441] K. TODO AND K. SATO, *Directive 2000/60/ec of the european parliament and of the council of 23 october 2000 establishing a framework for community action in the field of water policy*, Environmental Research Quarterly, (2002), pp. 66–106.

[442] M. TOSIC, F. MARTINS, S. LONIN, A. IZQUIERDO, AND J. D. RESTREPO, *Hydrodynamic modelling of a polluted tropical bay: Assessment of anthropogenic impacts on freshwater runoff and estuarine water renewal*, Journal of environmental management, 236 (2019), pp. 695–714.

[443] P. TRAMBAUER, S. MASKEY, H. WINSEMIUS, M. WERNER, AND S. UHLENBROOK, *A review of continental scale hydrological models and their suitability for drought forecasting in (sub-saharan) africa*, Physics and Chemistry of the Earth, Parts A/B/C, 66 (2013), pp. 16–26.

[444] A. TRANCOSO, *Modelling macroalgae in estuaries*, Trabalho Final de Curso da Licenciatura em Engenharia do Ambiente. Instituto Superior Tecnico, Universidade Tecnica de Lisboa. Lisboa, (2002).

[445] A. TRANCOSO, *Operational modelling as a tool in wind power forecast and meteorological warnings*, PhD in Environmental Engineering, Instituto Superior Técnico, Technical University of Lisbon, (2012).

[446] A. TRANCOSO, S. SARAIVA, L. FERNANDES, P. PINA, P. LEITÃO, AND R. NEVES, *Modelling macroalgae using a 3d hydrodynamic-ecological model in a shallow, temperate estuary*, Ecological Modelling, 187 (2005), pp. 232–246.

[447] G. TRIANTAFYLLOU, G. KORRES, I. HOTEIT, G. PETIHAKIS, AND A. BANKS, *Assimilation of ocean colour data into a biogeochemical flux model of the eastern mediterranean sea*, Ocean Science, 3 (2007), pp. 397–410.

[448] G. TSAKIRIS AND D. ALEXAKIS, *Water quality models: An overview*, European Water, 37 (2012), pp. 33–46.

[449] D. L. TUFFORD AND H. N. MCKELLAR, *Spatial and temporal hydrodynamic and water quality modeling analysis of a large reservoir on the south carolina (usa) coastal plain*, Ecological modelling, 114 (1999), pp. 137–173.

[450] A. D. UDOMSAP AND P. HALLINGER, *A bibliometric review of research on sustainable construction, 1994–2018*, Journal of Cleaner Production, 254 (2020), p. 120073.

[451] R. ULAŃCZYK, C. KLIŚ, B. ŁOZOWSKI, A. BABCZYŃSKA, A. WOŹNICA, J. DŁUGOSZ, AND E. WILK-WOŹNIAK, *Phytoplankton production in relation to simulated hydro-and thermodynamics during a hydrological wet year–goczałkowice reservoir (poland) case study*, Ecological Indicators, 121 (2021), p. 106991.

[452] F. M. UNDERWOOD, R. W. BURN, AND T. MILLIKEN, *Dissecting the illegal ivory trade: an analysis of ivory seizures data*, PloS one, 8 (2013), p. e76539.

[453] F. UNDUCHE, H. TOLOSSA, D. SENBETA, AND E. ZHU, *Evaluation of four hydrological models for operational flood forecasting in a canadian prairie watershed*, Hydrological Sciences Journal, 63 (2018), pp. 1133–1149.

[454] U. N. E. P. (UNEP), *Water security and ecosystem services: The critical connection*, A contribution to the United Nations World Water Assessment Program, (2009).

[455] J. VALENTIM, N. VAZ, H. SILVA, B. DUARTE, I. CAÇADOR, AND J. DIAS, *Tagus estuary and ria de aveiro salt marsh dynamics and the impact of sea level rise*, Estuarine, Coastal and Shelf Science, 130 (2013), pp. 138–151.

[456] I. VALIELA AND I. VALIELA, *Marine ecological processes*, vol. 686, Springer, 1995.

[457] N. J. VAN ECK, *Methodological advances in bibliometric mapping of science*, no. EPS-2011-247-LIS, 2011.

[458] N. J. VAN ECK AND L. WALTMAN, *Software survey: Vosviewer, a computer program for bibliometric mapping*, scientometrics, 84 (2010), pp. 523–538.

[459] ——, *Text mining and visualization using vosviewer*, arXiv preprint arXiv:1109.2058, (2011).

[460] N. VAZ, M. MATEUS, S. PLECHA, M. SOUSA, P. LEITÃO, R. NEVES, AND J. DIAS, *Modeling sst and chlorophyll patterns in a coupled estuary-coastal system of portugal: The tagus case study*, Journal of Marine Systems, 147 (2015), pp. 123–137.

[461] N. VELEZ, K. R. NICASTRO, C. D. MCQUAID, AND G. I. ZARDI, *Small scale habitat effects on anthropogenic litter material and sources in a coastal lagoon system*, Marine Pollution Bulletin, 160 (2020), p. 111689.

[462] R. VICEN-BUENO AND D. ELEFTHERAKIS, *Isr sensors to increase the security of underwater communication cables: Case study for coastal and shallow water areas*, in OCEANS 2019 MTS/IEEE SEATTLE, IEEE, 2019, pp. 1–11.

[463] N. VOULVOULIS, *Water reuse from a circular economy perspective and potential risks from an unregulated approach*, Current Opinion in Environmental Science & Health, 2 (2018), pp. 32–45.

[464] D. VU, T. YAMADA, AND H. ISHIDAIRA, *Assessing the impact of sea level rise due to climate change on seawater intrusion in mekong delta, vietnam*, Water Science and Technology, 77 (2018), pp. 1632–1639.

[465] S. Vydra and J. Kantorowicz, *Tracing policy-relevant information in social media: The case of twitter before and during the covid-19 crisis*, Statistics, Politics and Policy, (2021).

[466] M. Wahl, V. Saderne, and Y. Sawall, *How good are we at assessing the impact of ocean acidification in coastal systems? limitations, omissions and strengths of commonly used experimental approaches with special emphasis on the neglected role of fluctuations*, Marine and Freshwater Research, 67 (2015), pp. 25–36.

[467] M. Waithaka, G. C. Nelson, T. S. Thomas, and M. Kyotalimye, *East african agriculture and climate change: A comprehensive analysis*, (2013).

[468] S. Waldman, S. Baston, R. Nemalidinne, A. Chatzirodou, V. Venugopal, and J. Side, *Implementation of tidal turbines in mike 3 and delft3d models of pentland firth & orkney waters*, Ocean & Coastal Management, 147 (2017), pp. 21–36.

[469] F. Wang, C. J. Sanders, I. R. Santos, J. Tang, M. Schuerch, M. L. Kirwan, R. E. Kopp, K. Zhu, X. Li, J. Yuan, et al., *Global blue carbon accumulation in tidal wetlands increases with climate change*, National Science Review, (2021).

[470] Q. Wang, S. Li, P. Jia, C. Qi, and F. Ding, *A review of surface water quality models*, The Scientific World Journal, 2013 (2013).

[471] X. Wang, J. Zhang, V. Babovic, and K. Y. Gin, *A comprehensive integrated catchment-scale monitoring and modelling approach for facilitating management of water quality*, Environmental Modelling & Software, 120 (2019), p. 104489.

[472] Y. Wang, R. M. Castelao, and D. Di Iorio, *Salinity variability and water exchange in interconnected estuaries*, Estuaries and Coasts, 40 (2017), pp. 917–929.

[473] Y. Wang, X. Mao, and W. Jiang, *Long-term hazard analysis of destructive storm surges using the adcirc-swan model: A case study of bohai sea, china*, International journal of applied earth observation and geoinformation, 73 (2018), pp. 52–62.

[474] F. Wariaghli, *Etude écotoxicologique et parasitologique chez l'Anguille (Anguilla anguilla L.) dans les estuaires marocains: Sebou et Loukkos (Atlantique)*, PhD thesis, 2013.

[475] S. C. Watson, F. G. Grandfield, R. J. Herbert, and A. C. Newton, *Detecting ecological thresholds and tipping points in the natural capital assets of a protected coastal ecosystem*, Estuarine, Coastal and Shelf Science, 215 (2018), pp. 112–123.

[476] X. Y. Wei, C. Wang, P. F. Wang, and C. J. Qian, *Applying aquatox to simulate the response of eutrophic state to nutrient input in yincun port river*, in Applied Mechanics and Materials, vol. 737, Trans Tech Publ, 2015, pp. 481–486.

[477] C. Wellen, G. B. Arhonditsis, T. Labencki, and D. Boyd, *A bayesian methodological framework for accommodating interannual variability of nutrient loading with the sparrow model*, Water Resources Research, 48 (2012).

[478] H. D. White and K. W. McCain, *Visualizing a discipline: An author co-citation analysis of information science, 1972–1995*, Journal of the American society for information science, 49 (1998), pp. 327–355.

[479] D. WICHELNS, *Advising morocco: adopting recommendations of a water footprint assessment would increase risk and impair food security for the country and its farmers*, Water International, 43 (2018), pp. 762–784.

[480] T. WINTGENS, A. NATTORP, L. ELANGO, AND S. R. ASOLEKAR, *Natural water treatment systems for safe and sustainable water supply in the indian context: Saph Pani*, IWA Publishing, 2016.

[481] V. WOLFS, M. F. VILLAZON, AND P. WILLEMS, *Development of a semi-automated model identification and calibration tool for conceptual modelling of sewer systems*, Water science and technology, 68 (2013), pp. 167–175.

[482] T. WOOL, R. B. AMBROSE, J. L. MARTIN, AND A. COMER, *Wasp 8: The next generation in the 50-year evolution of usepa's water quality model*, Water, 12 (2020), p. 1398.

[483] T. A. WOOL, *Wasp8 stream transport-model theory and user's guide*, (2017).

[484] W. S. WOOSTER, A. BAKUN, AND D. R. MCLAIN, *Seasonal upwelling cycle along the eastern boundary of the north atlantic.*, Journal of Marine Research, 34 (1976), pp. 131–141.

[485] S. WU, Y. ZHOU, AND W. YAN, *Coastal service industry, industrial structure optimization and environmental governance: An empirical analysis based on chinese coastal cities*, Journal of Coastal Research, 109 (2020), pp. 114–120.

[486] U. WWAP, *The united nations world water development report 2014: water and energy*, United Nations, Paris, (2014).

[487] W. XIAO, X. LIU, A. J. IRWIN, E. A. LAWS, L. WANG, B. CHEN, Y. ZENG, AND B. HUANG, *Warming and eutrophication combine to restructure diatoms and dinoflagellates*, Water research, 128 (2018), pp. 206–216.

[488] L. XINGPO, L. MUZI, C. YAOZHI, T. JUE, AND G. JINYAN, *A comprehensive framework for hspf hydrological parameter sensitivity, optimization and uncertainty evaluation based on svm surrogate model-a case study in qinglong river watershed, china*, Environmental Modelling & Software, 143 (2021), p. 105126.

[489] N. XU, S. DUAN, A. LI, C. ZHANG, Z. CAI, AND Z. HU, *Effects of temperature, salinity and irradiance on the growth of the harmful dinoflagellate prorocentrum donghaiense lu*, Harmful Algae, 9 (2010), pp. 13–17.

[490] W. XU, *Development of a steady-state river hydrodynamic and temperature model based on ce-qual-w2*, (2014).

[491] B. XUE, H. ZHANG, Y. WANG, Z. TAN, Y. ZHU, AND S. SHRESTHA, *Modeling water quantity and quality for a typical agricultural plain basin of northern china by a coupled model*, Science of The Total Environment, (2021), p. 148139.

[492] Y. YANG, G. CHEN, G. RENIERS, AND F. GOERLANDT, *A bibliometric analysis of process safety research in china: Understanding safety research progress as a basis for making china's chemical industry more sustainable*, Journal of Cleaner Production, 263 (2020), p. 121433.

[493] M. N. YAZDI, M. KETABCHY, D. J. SAMPLE, D. SCOTT, AND H. LIAO, *An evaluation of hspf and swmm for simulating streamflow regimes in an urban watershed*, Environmental Modelling & Software, 118 (2019), pp. 211–225.

[494] H. M. YESUF, M. ASSEN, T. ALAMIREW, AND A. M. MELESSE, *Modeling of sediment yield in maybar gauged watershed using swat, northeast ethiopia*, Catena, 127 (2015), pp. 191–205.

[495] Y. YIN, H. KARUNARATHNA, AND D. E. REEVE, *Numerical modelling of hydrodynamic and morphodynamic response of a meso-tidal estuary inlet to the impacts of global climate variabilities*, Marine Geology, 407 (2019), pp. 229–247.

[496] C. G. YOON, H.-P. RHEE, Y. SON, ET AL., *Applicability study of ecological impact assessment using aquatox model in paldang reservoir, south korea*, DESALINATION Water Treat, 60 (2017), pp. 39–47.

[497] K. YOUNG AND R. J. VAN AARDE, *Science and elephant management decisions in south africa*, Biological Conservation, 144 (2011), pp. 876–885.

[498] S. J. YU, J. Y. LEE, AND S. R. HA, *Effect of a seasonal diffuse pollution migration on natural organic matter behavior in a stratified dam reservoir*, Journal of Environmental Sciences, 22 (2010), pp. 908–914.

[499] J. YUAN AND Y. LIU, *Evaluation of tourism efficiency in the coastal areas of china in the context of the happiness industry*, Journal of Coastal Research, 99 (2020), pp. 144–150.

[500] F. ZARE, S. ELSAWAH, T. IWANAGA, A. J. JAKEMAN, AND S. A. PIERCE, *Integrated water assessment and modelling: A bibliometric analysis of trends in the water resource sector*, Journal of Hydrology, 552 (2017), pp. 765–778.

[501] H. ZHANG, W. CHENG, Y. CHEN, Z. SHI, W. GONG, AND S. LIU, *Importance of large-scale coastal circulation on bay-shelf exchange and residence time in a subtropical embayment, the northern south china sea*, Ocean & Coastal Management, 168 (2019), pp. 72–89.

[502] R. ZHANG, X. QIAN, H. LI, X. YUAN, AND R. YE, *Selection of optimal river water quality improvement programs using qual2k: A case study of taihu lake basin, china*, Science of the Total Environment, 431 (2012), pp. 278–285.

[503] W. ZHANG, J. M. MORIARTY, H. WU, AND Y. FENG, *Response of bottom hypoxia off the changjiang river estuary to multiple factors: A numerical study*, Ocean Modelling, 159 (2021), p. 101751.

[504] X. ZHANG, L. CHEN, AND Z. SHEN, *Impacts of rapid urbanization on characteristics, sources and variation of fecal coliform at watershed scale*, Journal of Environmental Management, 286 (2021), p. 112195.

[505] Y. J. ZHANG, F. YE, E. V. STANEV, AND S. GRASHORN, *Seamless cross-scale modeling with schism*, Ocean Modelling, 102 (2016), pp. 64–81.

[506] Z. ZHANG, B. SUN, AND B. E. JOHNSON, *Integration of a benthic sediment diagenesis module into the two dimensional hydrodynamic and water quality model–ce-qual-w2*, Ecological modelling, 297 (2015), pp. 213–231.

[507] L. Zheng, H. Wang, C. Liu, S. Zhang, A. Ding, E. Xie, J. Li, and S. Wang, *Prediction of harmful algal blooms in large water bodies using the combined efdc and lstm models*, Journal of Environmental Management, 295 (2021), p. 113060.

[508] Y. Zhong, M. Notaro, and S. J. Vavrus, *Spatially variable warming of the laurentian great lakes: an interaction of bathymetry and climate*, Climate Dynamics, 52 (2019), pp. 5833–5848.

[509] Y. Zhou, Y. Zhang, F. Li, L. Tan, and J. Wang, *Nutrients structure changes impact the competition and succession between diatom and dinoflagellate in the east china sea*, Science of the Total Environment, 574 (2017), pp. 499–508.

[510] Y. Zhou, Y. Zhang, T. Liang, and L. Wang, *Shifting of phytoplankton assemblages in a regulated chinese river basin after streamflow and water quality changes*, Science of the Total Environment, 654 (2019), pp. 948–959.

[511] W. Zhu, Q. Niu, R. Zhang, R. Ye, X. Qian, and Y. Qian, *Application of qual2k model to assess ecological purification technology for a polluted river*, International journal of environmental research and public health, 12 (2015), pp. 2215–2229.

[512] A. Zieminska-Stolarska and J. Skrzypski, *Review of mathematical models of water quality*, Ecological Chemistry and Engineering, 19 (2012), p. 197.

[513] S. W. Zison, *Rates, constants, and kinetics formulations in surface water quality modeling*, Environmental Protection Agency, Office of Research and Development ..., 1978.

[514] B. Zouabi-Aloui, S. M. Adelana, and M. Gueddari, *Effects of selective withdrawal on hydrodynamics and water quality of a thermally stratified reservoir in the southern side of the mediterranean sea: a simulation approach*, Environmental monitoring and assessment, 187 (2015), pp. 1–19.

[515] H. Zouiten, C. Á. Díaz, A. G. Gómez, J. A. R. Cortezón, and J. G. Alba, *An advanced tool for eutrophication modeling in coastal lagoons: Application to the victoria lagoon in the north of spain*, Ecological modelling, 265 (2013), pp. 99–113.

[516] I. Zupic and T. Čater, *Bibliometric methods in management and organization*, Organizational research methods, 18 (2015), pp. 429–472.